

UFRRJ

INSTITUTO DE TECNOLOGIA

**PROGRAMA DE PÓS-GRADUAÇÃO EM CIÊNCIA E
TECNOLOGIA DE ALIMENTOS**

TESE

**Construção e avaliação de um nariz eletrônico (e-nose) de
baixo custo para uso no controle de qualidade de produtos
agrícolas**

Marcus Vinicius Da Silva Ferreira

2023



**UNIVERSIDADE FEDERAL RURAL DO RIO DE JANEIRO
INSTITUTO DE TECNOLOGIA
PROGRAMA DE PÓS-GRADUAÇÃO EM CIÊNCIA E TECNOLOGIA
DE ALIMENTOS**

**CONSTRUÇÃO DE UM NARIZ ELETRÔNICO (E-NOSE) DE BAIXO
CUSTO PARA USO NO CONTROLE DE QUALIDADE DE PRODUTOS
AGRÍCOLAS**

MARCUS VINICIUS DA SILVA FERREIRA

Sob orientação do Professor

Jose Lucena Barbosa Junior

Co orientação do Professor

Douglas Fernandes Barbin

Tese submetida como requisito parcial para obtenção do grau de **Doutor em Ciência e Tecnologia de Alimentos**, no curso de Pós-Graduação em Ciência e Tecnologia de Alimentos, Área de concentração em Ciência de Alimentos.

Seropédica, RJ
Dezembro de 2023

Universidade Federal Rural do Rio de Janeiro
Biblioteca Central / Seção de Processamento Técnico

Ficha catalográfica elaborada
com os dados fornecidos pelo(a) autor(a)

F383c Ferreira, Marcus Vinicius Da Silva , 1989-
Construção e avaliação de um nariz eletrônico (e
nose) de baixo custo para uso no controle de
qualidade de produtos agrícolas / Marcus Vinicius Da
Silva Ferreira. - Rio de Janeiro, 2023.
147 f.

Orientador: Jose Lucena Barbosa Junior.
Coorientador: Douglas Fernandes Barbin .
Tese(Doutorado). -- Universidade Federal Rural do
Rio de Janeiro, Programa De Pós-Graduação Em Ciência E
Tecnologia De Alimentos, 2023.

1. Sensores olfativos. 2. sensores ópticos. 3.
Machine learning. 4. produtos agrícola. I. Barbosa
Junior, Jose Lucena , 1975-, orient. II. Fernandes
Barbin , Douglas, 1980-, coorient. III Universidade
Federal Rural do Rio de Janeiro. Programa De Pós
Graduação Em Ciência E Tecnologia De Alimentos. IV.
Título.



MINISTÉRIO DA EDUCAÇÃO
UNIVERSIDADE FEDERAL RURAL DO RIO DE JANEIRO
PROGRAMA DE PÓS-GRADUAÇÃO EM CIÊNCIA E TECNOLOGIA DE
ALIMENTOS



TERMO Nº 1476/2023 - PPGCTA (12.28.01.00.00.00.41)

Nº do Protocolo: 23083.085486/2023-75

Seropédica-RJ, 27 de dezembro de 2023.

MARCUS VINICIUS DA SILVA FERREIRA

Tese submetida como requisito parcial para obtenção do grau de Doutor em Ciência e Tecnologia de Alimentos, no Curso de Pós-Graduação em Ciência e Tecnologia de Alimentos, área de Concentração em Ciência de Alimentos.
TESE APROVADA EM 19/12/2023

JOSE LUCENA BARBOSA JUNIOR (Dr.) UFRRJ (orientador)

ANTONIO RENATO BIGANSOLLI (Dr) UFRRJ

JOAO VICTOR NICOLINI (Dr) UFRRJ

CLEITON ANTÔNIO NUNES (Dr) UFV

FLAVIO NAPOLE RODRIGUES (Dr) IFRJ

Documento não acessível publicamente

(Assinado digitalmente em 30/12/2023 10:38)

ANTONIO RENATO BIGANSOLLI

PROFESSOR DO MAGISTERIO SUPERIOR

DEQ (12.28.01.00.00.00.45)

Matricula: ###231#2

(Assinado digitalmente em 03/01/2024 16:37)

JOAO VICTOR NICOLINI

PROFESSOR DO MAGISTERIO SUPERIOR

CoordCGEngM (12.28.01.00.00.00.39)

Matricula: ###033#6

(Assinado digitalmente em 27/12/2023 22:13)

JOSE LUCENA BARBOSA JUNIOR

COORDENADOR CURS/POS-GRADUACAO - TITULAR

PPGCTA (12.28.01.00.00.00.41)

Matricula: ###550#9

(Assinado digitalmente em 10/01/2024 21:49)

CLEITON ANTONIO NUNES

ASSINANTE EXTERNO

CPF: ###.###.016-##

(Assinado digitalmente em 29/12/2023 16:26)

FLAVIO NAPOLE RODRIGUES

ASSINANTE EXTERNO

CPF: ###.###.327-##

Visualize o documento original em <https://sipac.ufrrj.br/public/documentos/index.jsp> informando seu número: 1476, ano: 2023, tipo: TERMO, data de emissão: 27/12/2023 e o código de verificação: eff13faa79

AGRADECIMENTOS

Agradeço ao meu orientador Dr. José Lucena Barbosa Junior e coorientador Dr. Douglas Fernandes Barbin e membros da banca, pelas preciosas contribuições prestadas para este trabalho. De igual modo, agradeço ao Departamento de Tecnologia de Alimentos da Universidade Federal Rural do Rio de Janeiro, à Capes E CNPq, pela concessão da bolsa de estudos, e por ter financiado meu estágio no exterior por meio do PDSE. À todos, que direta ou indiretamente auxiliaram na execução deste projeto, meu agradecimento.

“O presente trabalho foi realizado com apoio da Coordenação de Aperfeiçoamento de Pessoal de Nível Superior - Brasil (CAPES) - Código de Financiamento 001”

RESUMO

DA SILVA FERREIRA, Marcus Vinicius. **Construção De Um Nariz Eletrônico (E-Nose) De Baixo Custo Para Uso No Controle De Qualidade De Produtos Agrícolas**. 2023. 147p. Tese (Programa de Pós-graduação em Ciência e Tecnologia de Alimentos). Instituto de Tecnologia, Universidade Federal Rural do Rio de Janeiro, Seropédica, RJ, 2023.

O nariz eletrônico (e-nose) é um dispositivo cujo intuito é otimizar o sistema olfativo das células dos mamíferos e é projetado para identificar odores. Esse equipamento é baseado na capacidade dos sensores em detectar a presença de odores (compostos voláteis) nos alimentos e transformá-los em sinal elétrico (tensão). Na indústria de alimentos, o nariz eletrônico tem sido amplamente utilizado para avaliação de produtos agrícolas, especialmente em frutas e commodities vegetais, onde seu uso aumentou nos últimos anos. Outras técnicas baseadas em sensores, como os ópticos tais como infra vermelho próximo (NIR) e imagem RGB (dentro da visão computacional) também são técnicas empregadas em análises de alimentos no intuito de se obter informação química. O funcionamento do NIR envolve a interação da radiação luminosa com uma amostra, onde suas propriedades físicas e químicas são refletidas nos espectros NIR resultantes. Já o sistema de sensores RGB é uma tecnologia que usa computadores para extrair dados úteis de entradas visuais (ex., imagens), uma vez que os métodos para determinação de fitoquímicos (ex., compostos fenólicos) nessas culturas são onerosas e demoradas, como cromatografia gasosa (CG-MS), além desse método requer a destruição do analito. O objetivo do trabalho foi investigar o efeito de parâmetros do nariz eletrônico de baixo custo (NEBC) (ex., temperatura dos sensores, espaço da câmara, fluxo de ar e tempo de aquisição) aplicando análise multivariada, *principal component analysis* PCA, *partial least square regression* PLSR, PLS-DA *partial least square discriminant Analysis* para avaliação de produtos agrícolas, além de investigar a performance do nariz eletrônico de baixo custo frente a outras tecnologias (NIR e camera RGB dentro do conceito de computer vision). O NEBC mostrou-se uma poderosa ferramenta analítica na classificação de estágios de maturação na pitaya além de potencial de predição de parâmetros como acidez e sólidos solúveis RPD>2 para acidez titulável e pH. Também de chás preto com base na origem (Brasil, Índia e Estados Unidos). Desempenho este compatível com outros sensores ópticos, como o infravermelho próximo (NIR) (para pitaya e chá) e Imagem RGB comparada à análise da pitaya. A otimização do tempo de aquisição da amostra em 2 minutos tanto para a pitaya quanto para os chás foram suficientes para obtenção dos dados bem como a implementação das condições de temperatura e umidade em 25 °C e 40% respectivamente foram bem sucedidas. O nariz eletrônico de baixo custo se mostrou como uma alternativa para a indústria de alimentos e pode ser considerado para o controle de qualidade, como vida de prateleira em frutas e autenticação em chá preto.

Palavras-chave: Sensores olfativos. sensores ópticos. Machine learning. produtos agrícola

ABSTRACT

DA SILVA FERREIRA, Marcus Vinicius. **Construction of a Low-Cost Electronic Nose (E-Nose) for Use in the Quality Control of Agricultural Products**. 2023. 147p. Thesis (PhD in Food Science and Technology). Instituto de Tecnologia, Universidade Federal Rural do Rio de Janeiro, Seropédica, RJ, 2023.

The electronic nose (e-nose) is a device designed to optimize the olfactory system of mammalian cells and is intended to identify odors. This equipment is based on the ability of sensors to detect the presence of odors (volatile compounds) in food and convert them into an electrical signal (voltage). In the food industry, the electronic nose has been widely used for the evaluation of agricultural products, especially in fruits and vegetable commodities, where its use has increased in recent years. Other sensor-based techniques, such as optical ones like near-infrared (NIR) and RGB imaging (inside of computer vision), are also employed in food analysis to obtain chemical information. The operation of NIR involves the interaction of light radiation with a sample, where its physical and chemical properties are reflected in the resulting NIR spectra. On the other hand, the RGB sensor system is a technology that uses computers to extract useful data from visual inputs (e.g., images), as methods for determining phytochemicals (e.g., phenolic compounds) in these crops are costly and time-consuming, such as gas chromatography (GC-MS), and this method requires the destruction of the analyte. The aim of the study was to investigate the effect of low-cost electronic nose parameters (LCEC) (e.g., sensor temperature, chamber space, air flow, and acquisition time) by applying multivariate analysis such as principal component analysis (PCA), partial least square regression (PLSR), and PLS-DA (partial least square discriminant analysis) for the evaluation of agricultural products. Additionally, the study aimed to investigate the performance of the low-cost electronic nose compared to other technologies (NIR and RGB camera within the concept of computer vision). The LCEC proved to be a powerful analytical tool in the classification of ripening stages in pitaya, as well as the prediction potential of parameters such as acidity and soluble solids with $RPD > 2$ for titratable acidity and pH. It also demonstrated effectiveness in distinguishing black teas based on origin (Brazil, India, and the United States). This performance was comparable to other optical sensors, such as near-infrared (NIR) (for pitaya and tea) and RGB imaging compared to pitaya analysis. Optimizing the sample acquisition time to 2 minutes for both pitaya and teas was sufficient for obtaining data, as well as successfully implementing temperature and humidity conditions at 25°C and 40%, respectively. The low-cost electronic nose proves to be an alternative for the food industry and can be considered for quality control, shelf-life assessment in fruits, and authentication in black tea.

Keywords: Olfactive sensors. optical sensors. agricultural products. machine learning.

LISTA DE TABELAS

CAPÍTULO I

Table 1.1: Low-cost-e-noses used to evaluate fruits	24
Table 1.2: Commonly compounds in fruits detected by LC-e-noses noses.....	26
Table 1.3: Low-cost-e-noses used to evaluate tea.....	31
Table 1.4: LC-e-noses used to evaluate coffee	34
Table 1.5: Commonly compounds (VOCs) in coffee detected by LC-e-noses	39
Table 1.6: LC-e-noses used to evaluate cocoa	39
Table 1.7: Commonly compounds (VOCs) in cocoa detected by LC-e-noses	43

CAPÍTULO II

Table 1.1: Physicochemical parameters for pitaya during different shelf-life indexes	60
Table 1.2: Pearson correlation for physicochemical parameters of pitaya.....	61
Table 1.3: Confusion matrix for LDA and PLS-DA classification of pitaya using NIR spectra and e-nose data	63
Table 1.4: Sensitivity, specificity, accuracy, and error rate values for classification of pitaya according to shelf-life index by using NIR spectra and e-nose.....	64
Table 1.5: Tukey test ANOVA for combined temperatures for of Pitaya fruit using NIR.....	70
Table 1.6: Tukey test ANOVA for combined temperatures for of Pitaya fruit using e-nose	70
Table 1.7: Parameters for the calibration and prediction sets for reference analysis in Pitaya using portable NIR and e-nose with PLSR	71

CAPÍTULO III

Table 1.1: Selected spectra intervals found in tea PCA loadings data, adapted from Chen et al. (2018)	78
Table 1.2: Sensitivity, specificity, accuracy, and error rate values for classification of tea origin	87

LISTA DE FIGURAS

CAPÍTULO I

Figure 1.1: Electrochemical equipment set up and sensor, adapted from Ma et al. (2016).....	21
Figure 1.2: MOS sensor setup and circuit connections, adapted from Ma et al. (2016).....	22
Figure 1.3: Most common e-nose design for evaluation of fruits (a)-(p).....	29
Figure 1.4: Sensors response for LC-e-nose sensors adapted from Ralisnawati et al. (2018)..	32
Figure 1.5: Most common LC-e-nose designs for the evaluation of tea (a)-(f).....	34
Figure 1.6: Most common LC-e-nose designs for the evaluation of coffee (a)-(j).....	37
Figure 1.7: Most common LC-e-nose designs for the evaluation of cocoa (a)-(h).....	41

CAPÍTULO II

Figure 1.1: NIR and e-nose set up	57
Figure 1.2: PCA (a) scores and (b) loadings for NIR spectra absorbance mode; PCA (c) scores and (d) loadings for e-nose data	61
Figure 1.3: PLSR models with the best performance for the total of soluble solids (TSS), pH, total titratable acidity (TTA), moisture and total phenolics from NIR data	67
Figure 1.4: PLSR models with the best performance for total titratable acidity (TTA), total of soluble solids (TSS), pH, moisture, and total phenolics from e-nose system data	68

CAPÍTULO III

Figure 1.1: Low-cost-e-nose.	79
Figure 1.2: Spectra for BNIR (a) and PNIR (b) for each type of sample (red, green, blue, insert which sample they are).....	81
Figure 1.3: Average Spectra for BNIR (a) and PNIR (b). Red, Brazil, green, India, Blue, USA.....	81
Figure 1.4: PCA (a) scores and (b) loadings for NIR spectra for PNIR	82
Figure 1.5: PCA (a) scores and (b) loadings for BNIR spectra reflectance mode for BNIR	83
Figure 1.6: LC-e-nose Acquisition data (a) and temperature and humidity reading (b)	83
Figure 1.7: PCA (a) scores and (b) loadings for LC-e-nose	84
Figure 1.8: The major VOCs structure in black tea: Catechins (a), Caffeine (b) and Theaflavin (c)	84
Figure 1.9: HPLC chromatogram for Caffeine in the tree tested tea origins (BR, IND and USA	85
Figure 1.10: Confusion matrix of LDA (A) PNIR (B) BNIR and (C) LC-e-nose	87
Figure 1.11: Confusion matrix of PLS-DA (a) PNIR (b) BNIR and (c) LC-e-nose	88

LISTA DE ABREVIACOES E SIGLAS

ADC	Analogic digital converter
ANN	Artificial neural networks
AS-MLV-P2	(Austria, Europe- 20 ppm DR 3.0V)
BNIR	Benchtop NIR
BOP	Flower broken Orange Pekoe
CNN	Convolutional neural network
DAQ	Data acquisition card
DHT11	Digital temperature and humidity sensor
DR	Detection range
DTC	Decision tree classifier
EC	Electrochemical sensor
ELM	Extreme Learning Machine
FBOP	Flower broken Orange Pekoe
KDM	Kernel distribution model
KNN	K-nearest neighbors' algorithm
KW	Kilo Ohm
LDA	Linear discriminant analysis
LS-SVM	Least-squares support-vector machines
LV	Latent variables
MC	Mean centering
ML	Machine Learning
MOS	Metal oxide sensor
MP-xxx	Metal oxide type sensor – Winsen, Zhengzhou, China– 10 – 1,000 ppm DR, 5V
MQ-xxx	Metal oxide type sensor – Winsen, Zhengzhou, China– 300 – 10,000 ppm DR, 5V
MSE	Mean square error
MS-xxxx	Metal oxide type sensor – Ogam, Jeollanam-do, Korea – 10 – 1,000 ppm DR, 5V
mV	Milli volts
MW	Mega Ohm
(o)	Polynomial order
PCA	Principal component analysis

PKNN	Principal component analysis with K-nearest neighbor
PLS-DA	Partial least square discriminant analysis
PLS-R	Partial least squares regression
PNIR	Portable NIR
PNN	Probabilistic neural network
PSMVM	Principal component analysis with support vector machine
QDA	Quadratic discriminant analysis
R2C	Coefficient of determination of calibration
R2CV	Coefficient of determination of cross-validation
R2P	Coefficient of determination of prediction
REN	Recurrent Elman network
RER	Ratio error
RF	Random Forest
RMSEC	Root mean square error of calibration
RMSECV	Root mean square error of cross-validation
RMSEP	Root mean square error of prediction
RPD	Ratio of standard deviation
SB-xxx	Figaro, Osaka, Japan – 20 – 150 ppm DR, 5V
S-G	Savitzky–Golay
SNV	Standard normal variate
SOMs	Self-organizing maps
SVM	Support machine vector machine
TGS-xxxx	Figaro, Osaka, Japan– 50– 5,000 ppm DR, 3.3V
V	Volts
VOCs	Volatile organic compounds
(w)	Windows size
WSP-xxxx	Metal oxide type sensor – Winsen, Zhengzhou, China – 1 – 50 ppm DR, 5V

SUMÁRIO

1	INTRODUÇÃO GERAL	1
2	OBJETIVOS	6
2.1	Objetivo Geral.....	6
2.2	Objetivos Específicos	6
3.	JUSTIFICATIVA DO TRABALHO	7
4.	REFERÊNCIAS BIBLIOGRÁFICAS	7
	CAPÍTULO I	16
	Low-cost electronic-nose (LC-e-nose) systems for the evaluation of plantation and fruit crops: recent advances and future trends	17
1.1	Abstract.....	17
1.2	Introduction.....	18
1.3	Most common of LC-e-nose sensors used for fruit and plantation crops	19
1.3.1	LC-e-noses based on electrochemical (EC) sensors	20
1.3.2	LC-e-noses based on MOS sensors	21
1.4	Application of LC-e-nose in fruits	23
1.4.1	LC-e- in climacteric fruits.....	25
1.4.2	LC-e-nose used for non-climacteric fruits.....	27
1.5	Application of LC-e-nose to evaluate plantation crops	30
1.5.1	LC-e-nose applications for tea.....	30
1.5.2	LC-e-nose applied for coffee.....	33
1.5.3	LC-e-nose applied for cocoa	38
1.6	Common data treatment methods used with LC-e-nose systems in plantation and	44
1.6.1	Data treatment used for LC-e-nose based on chemometrics.....	45
1.6.2	Data treatment used for LC-e-nose based on machine learning	45
1.7	Conclusion and future trends.....	46
1.8	References.....	47
	CAPÍTULO II	54
	Determination of pitaya quality using portable NIR spectroscopy and innovative low-cost electronic nose	55
1.1	Abstract.....	55
1.2	Introduction.....	55
1.3	Materials and Methods	56
1.3.1	Acquisition of the fruits.....	56
1.3.2	Reference Analysis.....	56
1.3.3	Data acquisition using NIR spectra	57
1.3.4	E-nose set up and fruit acquisition	57
1.3.5	Multivariate analysis	57
1.3.5.1	NIR (Spectra) and e-nose data pre-processing.....	57
1.3.5.2	Principal Component Analysis (PCA).....	58
1.3.5.3	Linear Discriminant Analysis (LDA)	58
1.3.5.4	Partial Least Square Discriminant Analysis (PLS-DA)	58
1.3.5.5	Partial Least Square Regression (PLSR)	59
1.4	Result and Discussion	60
1.4.1	Reference Analysis.....	60

1.4.2	Principal Components Analysis (PCA)	61
1.4.3	Classification model using LDA	62
1.4.4	Classification model using PLS-DA.....	64
1.4.5	Prediction of reference analyzes using PLSR.....	65
1.5	Conclusions.....	69
1.6	References.....	72
CAPÍTULO III		75
Machine learning-based classification performance of black tea from three origins (BR, IND and US) using NIR devices (portable and benchtop) and a Low-cost-e-nose.....		76
1.1	Abstract.....	76
1.2	Introduction.....	76
1.3	Materials and Methods	77
1.3.1	Sample acquisition and preparation.....	77
1.3.4	NIR spectra acquisition	78
1.3.5	Olfactive Sensors	78
1.3.6	Multivariate analysis	79
1.3.6.1	Data labeling	79
1.3.6.2	Data	79
1.3.6.3	Principal Component Analysis (PCA).....	79
1.3.6.4	Linear Discriminant Analysis (LDA)	80
1.4	Results and Discussion.....	80
1.4.1	Principal Components Analysis (PCA).....	80
1.4.1.1	Raw for NIR systems.....	80
1.4.1.2	PNIR results.....	82
1.4.1.3	BNIR results	82
1.4.2	PCA for LC-e-nose system	83
1.4.4	Classification model using LDA	86
1.4.4.1	LDA for NIR Systems	86
1.4.4.2	LDA for LC-enose.....	87
1.4.5	Classification model using PLS-DA.....	87
1.4.5.1	PLSDA for NIR Systems.....	87
1.4.5.2	PLS-DA for LC-enose.....	88
1.5	Conclusions.....	89
1.6	Acknowledgments.....	89
1.7	References.....	89
CONCLUSÕES GERAIS.....		92
PERSPECTIVAS FUTURAS		92
APÊNDICE.....		93
Deep computer vision system and image explanation for dragon fruit.....		111
1.5	Abstract.....	111
1.6	Introduction.....	111
1.7	Material and Methods	113
1.7.1	Deep Computer Vision System	113
1.7.2	Explainable Deep Computer Vision.....	115
1.7.3	Fruit acquisition and RGB imaging setup	116
1.7.4	Deep Learning and Explainable Methods	117
1.7.5	Model Performance Criteria.....	118

1.8	Results and Discussion.....	119
1.8.1	Overall accuracy	119
1.8.2	Visualisation methods performance.....	121
1.8.3	Approach Limitations.....	127
1.8.4	Explainability remarks	127
1.9	Conclusion	129
1.10	Acknowledgement	129
1.11	Declaration of Interest.....	129
1.10	References.....	130

ESTRUTURA DA TESE

A tese está estruturada em capítulos, contendo a introdução geral, objetivos, justificativa e um capítulo dedicado a elucidar técnicas que não foram abordadas no artigo de revisão, além dos seguintes capítulos:

No capítulo I, apresenta-se uma revisão da literatura onde são discutidos os mais recentes trabalhos envolvendo o uso de narizes eletrônicos de baixo custo para classificação dos mesmos materiais do capítulo I.

No capítulo II, o nariz eletrônico adaptado a frutas é utilizado para classificar pitayas em diferentes estágios de maturação e prever alguns parâmetros de interesse no fruto (sólidos totais, acidez, compostos fenólicos e umidade). Também é utilizado o sensor ótico infravermelho próximo (NIR) para testar o potencial classificatório da tecnologia de baixo custo.

No capítulo III, é proposta outra comparação de desempenho, desta vez utilizando melhorias na aquisição de dados em relação ao controle de umidade e temperatura. O chá preto é utilizado para representar o grupo das commodities agrícolas, finalizando a ideia inicial da tese em propor um nariz de baixo custo para frutas e commodities agrícolas estudadas (chá, café e cacau). Para testar a validação dos dados, modelos de classificação (LDA e PLS-DA) são propostos. Da mesma forma, dois dispositivos NIR são utilizados para comparação (portátil e de bancada) com o nariz eletrônico.

Por fim, as considerações finais são expostas, e são apresentadas sugestões para estudos futuros. Cada capítulo está apresentado na forma de artigo e segue com formatação própria para cada revista à qual foi submetido. Em anexo, apresento um quarto artigo no qual a mesma fruta utilizada no capítulo II (pitaya) é empregada com outro sensor ótico RGB (visão computacional) para também testar o potencial do nariz frente à capacidade de gerar resultados reprodutíveis diante de outros sensores de baixo custo. Foi utilizado inteligência artificial em imagens digitais (RGB) do fruto com as mesmas divisões de classes propostas anteriormente (capítulo II). Para performance F1 scores utilizando *ResNet* e *Vit transformer* como *feature extraction* das regiões de interesse da imagem.

INTRODUÇÃO GERAL

O Brasil é o maior produtor de frutas tropicais do mundo e está na lista dos grandes produtores de chá preto (PINTO; JACOMINO, 2013). Pitaya (*Selenicereus undatus*) é uma fruta cujo consumo tem sido destacado no mercado brasileiro (ATTAR et al., 2022). A Pitaya tem sido consumida em larga escala devido à presença de antocianinas, que apresentam propriedades antioxidantes e também pelo potencial da fruta em controlar o crescimento dos microrganismos em alimentos (conservantes) (CHEAH et al., 2016). Já o chá preto é caracterizado como chá (oxidadas, fermentadas e secas, usado para infusão), e seus constituintes mais prevalentes são polifenóis, cafeína, aminoácidos e flavonoides. Esses componentes também têm propriedades e benefícios significativos para a saúde humana, incluindo um mecanismo anti-inflamatório que reduz o risco de doenças cardiovasculares e previne o câncer (XIAO et al., 2022). Depois da água, é a bebida mais popular em todo o mundo e muito embora, no Brasil, a produção e consumo de chá preto ainda seja pequena se comparada a outros países, esta vem crescendo ao longo dos últimos anos e se mostra uma área promissora (XIAO et al., 2022).

O pós-colheita e processamento de frutas, bem como *commodities* agrícolas (chá preto), exigem produtos seguros e de alta qualidade, necessitando de medidas de controle de qualidade completas. A economia global tem visto um crescimento significativo na indústria de frutas e *commodities* agrícolas (CHOPRA; KRISHNAKUMAR; PETER, 2016).

A escolha adequada sensores (óticos e olfativos) é crítica na detecção de pequenas mudanças na concentração de gases odoríferos relacionados a transformações de alimentos durante seu armazenamento ou processamento. Tyagi et al. (2023) associaram a identificação de compostos voláteis VOCs aos estágios de maturação da fruta e *commodities* agrícolas e condições de armazenamento no pós-colheita. Além disso, sensores no infravermelho, luz visível e nariz eletrônico são valiosos para classificar frutas em estágios de maturação e determinar origem de *commodities* agrícolas como chá, café e cacau, em função das perdas anuais alarmantes de US\$ 10 bilhões devido a fraudes na indústria global de alimentos (TSENG et al., 2021).

No âmbito de sensores óticos, a espectroscopia de infravermelho próximo (NIR) é uma poderosa técnica analítica utilizada na faixa de comprimento de onda de 780 a 2500 nm, enquadrada na categoria de espectroscopia vibracional de alta energia. Este método não destrutivo envolve a interação da radiação eletromagnética com uma amostra, em que suas propriedades físicas e químicas são refletidas nos espectros NIR resultantes (FAN et al., 2016; OLIVEIRA et al., 2014). As interações químicas leves ocorrem com grupos moleculares associados a ligações químicas C–H, O–H e N–H. A maioria das bandas de absorção NIR associadas a esses grupos são harmônicas ou combinações de bandas de absorção fundamental na região do infravermelho, que por sua vez são devidas a transições vibracionais e rotacionais (NICOLAI et al., 2007). Quando a radiação NIR penetra em um produto, suas características espectrais mudam por meio de processos de absorção e espalhamento dependentes do comprimento de onda. Essas mudanças espectrais são influenciadas por variações na composição química interna do produto (por exemplo, teor de umidade) e pelas propriedades de dispersão de luz (por exemplo, tamanho de partícula). NIR tem sido muito utilizado para estágios de maturação em frutas e *commodities* agrícolas (chá, café e cacau) (PANDISELVAM et al., 2022; SHAH et al., 2020) e chá (DING et al., 2022).

Ainda sobre sensores óticos métodos baseados na análise de imagens digitais, geralmente conhecidos como métodos de visão computacional (CV), é uma ferramenta potente que usa computadores para extrair dados úteis de entradas visuais, como imagens ou vídeos.

Este campo inclui uma variedade de técnicas para coletar dados de sensores de imagem, como câmeras digitais. A CV permite a extração, análise e compreensão rápida e automática de informações importantes de imagens únicas ou coleções de imagens. O método procura identificar, rastrear ou descobrir informações reconhecendo características externas. A imagem digital tem sido usada na preparação de alimentos para rastrear variáveis de qualidade externa, como tamanho e mudanças na estrutura da superfície, mudanças de cor causadas pelo processamento e mudanças no tamanho e na estrutura da superfície (XIAO et al., 2022). A tecnologia de imagem digital também tem sido empregada e na avaliação do grau da maturação em fruto (JIANG et al., 2022; SALUNKHE; PATIL, 2015) como também grau de fermentação em chá (DONG et al., 2018). Tanto NIR e CV possuem um grande potencial para testar qualidade de alimentos e têm sido amplamente empregados, porém esses dispositivos não conseguem gerar uma leitura direta dos compostos voláteis que são liberados por alimentos, exemplo, frutas e *commodities* agrícolas.

A importância de detectar VOCs em alimentos em geral está em entender como eles se relacionam com alterações físicoquímicas e sensoriais nesses produtos, o que é de extrema importância para a indústria de alimentos (BROOKS et al., 2021). Nos últimos anos, o uso de narizes eletrônicos teve um crescimento significativo, principalmente devido à natureza onerosa e demorada dos métodos convencionais de avaliação de qualidade para essas culturas. Entre os métodos atuais para determinar os VOCs nesses frutos estão a espectroscopia e os métodos cromatográficos (VIEIRA et al., 2017), que demandam mais tempo como a cromatografia gasosa (CG-EM), cromatografia líquida de alto desempenho (HPLC) (Hammel Sobreira, Da Silva Ferreira, and Kamruzzaman 2023), a espectroscopia de infravermelho com transformada de Fourier (FT-IR). Contudo, estes métodos requerem a aquisição de equipamentos mais caros, uso de produtos químicos e a destruição das amostras em sua grande maioria (BURATTI ET AL. 2011; JIN ET AL. 2021).

Portanto, a adoção de narizes eletrônicos oferece uma alternativa mais rápida e não destrutiva para avaliação de qualidade. Em contraste, os dispositivos de nariz eletrônico experimentaram um aumento nas aplicações nos últimos anos. Eles oferecem uma alternativa não destrutiva e eficiente para avaliar a qualidade das culturas, tornando-os altamente valiosos na indústria. Ao eliminar a necessidade de métodos complexos e com uso intensivo de recursos, os narizes eletrônicos fornecem uma solução mais rápida e econômica para garantir a segurança, qualidade e autenticidade de frutas e *commodities* agrícolas (BURATTI et al., 2011; SANAEIFAR et al., 2017; VIEIRA et al., 2017; WILSON, 2018; WILSON, 2018).

Os sistemas de *e-nose* têm sido aplicados em muitos produtos agrícolas, como por exemplo em produtos à base de carne, cereais e grãos, frutas, sementes e vegetais. O equipamento tem sido usado para identificar amostras fraudulentas e prever adulteração, bem como outros atributos agrícolas como contaminação de trigo (LIPPOLIS et al., 2014), envelhecimento do arroz (RAHIMZADEH et al., 2019), detectando odores em bananas, limão e lichia (PAN; HSIEH; TANG, 2013; TANG et al., 2010), amadurecimento em uvas (ALEIXANDRE et al., 2015), aroma em café (GONZALEZ VIEJO et al., 2020), sólidos solúveis em caqui e laranjas (XU et al., 2019; ZHANG et al., 2016). Também em produtos de origem animal como frescor, qualidade sensorial e microbiológica da carne vermelha (LI et al., 2014; PAPADOPOULOU et al., 2013; TIMSORN et al., 2014), frescor da carne, frango e peixe (LIU et al., 2020), compostos voláteis em leite desnatado (CHI et al., 2021), identificação de deterioração em produtos lácteos (PHUKKAPHAN et al., 2021).

Muitos autores têm proposto novos aparatos físicos para o *e-nose* (CHEN et al., 2021; CHENG et al., 2021; CHILO et al., 2016; GONZALEZ VIEJO; FUENTES, 2020; MACÍAS et al., 2013; SPINELLE et al., 2017). Na maioria desses trabalhos, o desenvolvimento da câmara e

na escolha de sensores são descritos como um desafio (JULIAN et al., 2020; WOJNOWSKI et al., 2017). No geral, o projeto proposto para um sistema de nariz eletrônico é geralmente retangular e composto por muitas câmaras e dispositivos para bombear o ar para a câmara de reação (microcontrolador, microbombas e câmara de sensores) (MACÍAS et al., 2013). O sistema *e-nose* é composto basicamente por um conjunto de sensores, uma placa-mãe para aquisição de dados e um *software* para traduzir os dados. Um nariz eletrônico detecta os VOCs das amostras em questão através de uma matriz de sensores monitorados por *software* e sistemas de reconhecimento de padrões.

Dentre os aparatos físicos disponíveis, como os sensores de polímero condutor (CP) (CHOWDHURY et al., 2019), eletroquímico (EC) (HARUN; COVINGTON; GARDNER, 2009), Microbalança de cristal de quartzo (QCM), onda acústica superficial (SAW) (MATATAGUI et al., 2019), óptica (THEPUDOM; SRICHAROENCHAI; KERDCHAROEN, 2013) e óxido de metal (MOS) (CHARUMPORN et al., 2006; NAKE et al., 2005), este último é conhecido por sua tecnologia consolidada de baixo custo, circuito de hardware simples e boa durabilidade, além de possuir sensibilidade em um amplo espectro (CHENG et al., 2021). Muitos pesquisadores têm usado MOS para compor seus sistemas de nariz eletrônico, e eles os têm usado para estudar muitos produtos agrícolas como: farinha, arroz, frango e suco de tomate (LI et al., 2014; LIPPOLIS et al., 2014; RAHIMZADEH et al., 2019; TIMSORN et al., 2014). Dentre as opções acima, os sensores mais comumente encontrados em *e-noses* são os sensores EC (eletroquímicos), que são especialistas em detectar gases ou compostos químicos específicos por meio de eletrodos. Notavelmente, os sensores EC são frequentemente empregados para detectar gases como CO₂, H₂S e NH₃. Por outro lado, os sensores MOS (Metal Oxide Semiconductor) representam outro tipo de sensor ainda mais usado em narizes eletrônicos devido ao preço reduzido. Esses sensores detectam mudanças nas características elétricas dentro de um revestimento de óxido de metal colocado em um substrato semiconductor (EMERSON, 2019; TAN; XU, 2020).

Para compreender melhor o funcionamento, as vantagens e a disponibilidade desses dois tipos de sensores, foi realizada uma investigação sobre narizes eletrônicos baseados em EC e MOS no contexto de frutas e *commodities* agrícolas (chá, café e cacau). Os sensores de detecção de gás semicondutores são uma boa escolha ao construir um dispositivo portátil e acessível. Os sensores contêm um eletrodo do sensor de gás MOS a camada de dióxido de estanho, bem como o fluxo do circuito elétrico. No eletrodo, enquanto em modo IDLE, o O₂ presente no ar liga os elétrons na camada de dióxido de estanho que bloqueia a passagem de corrente no sistema. Posteriormente, quando os gases redutores interagem com o revestimento de óxido metálico e a característica elétrica do filme muda, a corrente é desbloqueada gerando o sinal do equipamento (EMERSON, 2019; TAN; XU, 2020). A placa mãe de um dispositivo de nariz eletrônico é baseada no “AD Board”, que é uma controladora que serve de interface entre o dispositivo e o PC para aquisição de dados. Vários modelos têm sido usados em sistemas olfativos, como placa microcontroladora baseada em Arduino, como o Uno Rev3 ATmega 328P (BINSON; SUBRAMONIAM, 2021), MCP3208 12bit AD (BOROWIK et al., 2021) 32F10 (CHEN et al., 2021) USB-6218 16 bits (CHILO et al., 2016), sendo as diferenças entre eles basicamente a robustez referente ao seu hardware (material) e também da capacidade de controlar periféricos (entradas) no sistema. Esta parte do equipamento é responsável por fornecer energia aos sensores, bem como para criar uma configuração de tensão do analógico para a unidade digital.

A placa-mãe baseada em Arduino parece uma escolha confiável (BINSON; SUBRAMONIAM, 2021), e é uma plataforma de código aberto que usa hardware com configuração simples aos usuários. O equipamento permite entradas de leitura (resposta ao sensor) e se transformará em uma saída (sinal de tensão). O dispositivo faz isso usando a linguagem de programação Arduino baseada em *mirring* e no *software* Arduino (IDE). O design do *software* é

apresentado em diversos formatos, alguns são escritos em linguagem C/C++ (MACÍAS et al., 2013) e não precisam de recursos especiais. Outros programas são baseados em Arduino (CHENG et al., 2021), que geralmente é dividido em duas partes. A primeira parte é baseada no computador *host* (hospedeiro) que apresenta a interface gráfica para traçar o gráfico de tensão gerado pela aquisição de dados (ou seja, resposta de sensores a gases).

Além de outros componentes, como sensores, sistemas de aquisição de dados e métodos de reconhecimento de padrões, alguns parâmetros físicos são muito importantes para o perfeito funcionamento do *e-nose*. Os fatores físicos influenciam a análise e a qualidade dos dados obtidos. Portanto, existem algumas propostas na literatura nesse sentido para resolver esses problemas (YIN et al., 2016). Alguns parâmetros de aquisição de dados importantes para o sistema de nariz eletrônico incluem: *headspace* estático e dinâmico no qual afeta a maneira que os voláteis interagem com o sensor (JULIAN et al., 2020; RALISNAWATI et al., 2018; RODRÍGUEZMÉNDEZ et al., 2016), controle da temperatura, afeta o movimento dos elétrons pela mídia (sensor) (LI et al., 2015; ZHAO et al., 2016) e controle da umidade altera a afinidade dos sítios de ligação dos sensores (HOMER et al., 1999; LI et al., 2015; YAN et al., 2021; ZHAO et al., 2016).

Os pré-tratamentos são transformações importantes que dizem respeito as correções feitas aos sinais registrados por um determinado instrumento, levando-se em conta a contribuição determinística (sinal verdadeiro) e estocástica (variações indesejadas). Para o sistema do nariz eletrônico já foram testados transformações e pré-processamentos como a razão sinal/ruído que proporciona maior acurácia no tratamento de dados (LIU et al., 2019; YAN et al., 2015), autoescalamento (*Steady-state response feature extraction optimization*) tem se mostrado eficaz >94% a acurácia das análises no *e-nose* (AGUSTIKA et al., 2020).

A análise exploratória ajuda a tomar um grande volume de dados, interpretá-los e representar suas informações químicas de uma forma que possam ser aplicadas técnicas como métodos de classificação e também para prever amostras em questão. Entre esses métodos, os de reconhecimento de padrões análise de componentes principais (PCA) são os mais utilizados, onde se pode encontrar padrões e reconhecer tendências de agrupamento (JIMÉNEZ-CARVELO et al., 2019). A Análise de Componentes Principais (PCA) é uma ferramenta estatística não supervisionada que reconhece padrões a partir de informações observáveis em um grupo amostral. Seu objetivo é manter o máximo de variação possível enquanto projeta os pontos de dados nos componentes principais. Para atingir esse fim, o método identifica as informações singulares presentes no conjunto de dados do grupo amostral. (AGUSTIKA et al., 2020; TANG; LIN; SHYU, 2010). PCA é muito utilizado como análise exploratória em vários trabalhos envolvendo análise multivariada para tratar dados de *e-noses* em produtos alimentícios como por exemplo em frutas como as myricas (CHENG et al., 2015) e as nozes de cacau (TAN; KERR, 2018). Existem vários métodos de classificação sendo utilizados recentemente, no entanto, os mais utilizados são os vizinhos k-mais próximos (KNN), a *partial lest square discriminant regression* (PLSD-DA) e o método *soft independent modeling of class analogy* (SIMCA). São métodos supervisionados (dados rotulados) para qualificação e classificação (JIMÉNEZ-CARVELO et al., 2019).

A análise discriminatória opera estabelecendo limites entre classes distintas estabelecidas por objetos de treinamento (JIMÉNEZ-CARVELO et al., 2019). PLS-DA é um método de classificação supervisionado que utiliza uma base quantitativa. O método atribui um valor numérico usando um algoritmo de regressão multivariada, então esses valores são classificados em suas classes (JIMÉNEZ-CARVELO et al., 2019). Muitos estudos têm usado o PLS-DA como método de classificação para tratar dados de nariz eletrônico como por exemplo: classificar arroz (FENG et al., 2013) e chá (NI et al., 2018) de acordo com origem geográfica e autenticação no vinho (SPRINGER, 2019).

O método de regressão por quadrados mínimos parciais PLS-R, que é um método de previsão também é usado para modelos de determinação de dados de nariz eletrônico. PLSR é um

método supervisionado que usa uma abordagem de quantificação e calibração, e é usado para construir modelos de previsão a partir da análise de referência e dos dados do sistema de nariz eletrônico. Muitos estudos têm usado PLS para tratar dados do *e-nose* (JIMÉNEZ-CARVELO et al., 2019; ZHANG et al., 2021). Algumas das análises de referência mais utilizadas incluem cromatografia gasosa (CG) (Tan and Kerr 2018) e métodos físico-químicos padrão (WEI; WANG; ZHANG, 2015).

Equipamentos de baixo custo têm sido utilizados para detecção de aroma em alimentos (MACÍAS et al., 2013; CANO MARCHAL et al., 2021), como qualidade da cerveja (GONZALEZ VI-EJO; FUENTES, 2020) e aroma de café (GONZALEZ VIEJO; TONGSON; FUENTES, 2021) porém ainda não existem muitos trabalhos com narizes de baixo custo nesta categoria (*Low-cost-e-nose*) em frutas e *commodities* agrícolas (chá preto). Embora o *e-nose* de baixo custo tenha sido recentemente proposto (CHENG et al., 2021; JIA et al., 2019; ALI et al., 2020) a maioria das pesquisas ainda usam formatos comerciais caros (CHENG et al., 2015; JIA et al., 2019; LI et al., 2014; LIPPOLIS et al., 2014; QIU; WANG; GAO, 2015; RUSSO et al., 2013; WEI; SHAO et al., 2018; WEI; ZHANG et al., 2018; ZHANG et al., 2016), o que torna o processo inviável para muitas empresas. Assim essa possível lacuna viabiliza a proposta que vise melhorar a integração de componentes eletrônicos e processamento de dados, na construção de um e-nariz de baixo custo projetado para ser utilizado em produtos agrícolas.

OBJETIVOS

2.1 Objetivo Geral

Confecção de um nariz eletrônico de baixo custo (LC-*e-nose*) que seja capaz de identificar os compostos voláteis presentes nas amostras estudadas e que a partir destes compostos seja possível prever o estágio de maturação dos frutos analisados, e origem de chá, viabilizando seu uso na indústria de alimentos. Além de aprimorar a medição e a predição de parâmetros importantes no pós colheita de frutas e produção de chá preto entre outros possíveis produtos agropecuários na classe frutas e *commodities* agrícolas.

2.2 Objetivos Específicos

Fornecer uma visão geral da função do sensor, comparando EC e MOS, e apresentar relatórios ao longo dos últimos 13 anos de dispositivos Low-cost-*e-nose* totalmente definidos com base em MOS aplicados em frutas, chá, cacau e café, incluindo seus designs, *e-noses* e tratamentos comuns de dados. Além dos métodos mais comuns para análise de dados também são discutidos.

Propor o uso de duas técnicas (NIR e *e-nose*) para prever a vida útil da pitaya com bases no conteúdo total de sólidos solúveis, pH, acidez titulável, umidade e compostos fenólicos usando modelos PLSR, bem como para discriminar a fruta em 5 estágios (dias) usando modelos LDA e PLS-DA.

Investigar o uso de LC-*e-nose* e dois NIR de bancada (PNIR e BNIR) para classificar folhas de chá de três origens diferentes (Brasil, Estados Unidos e Índia) usando modelos LDA e PLS-DA. Além de fazer o uso da cromatografia gasosa como confirmação dos voláteis presentes.

3. JUSTIFICATIVA DO TRABALHO

O Brasil é o maior produtor de frutas tropicais do mundo e está na lista dos grandes produtores de chá preto (PINTO; JACOMINO, 2013). A pitaya (*Selenicereus undatus*) é uma fruta cujo consumo tem sido destacado no mercado brasileiro (ATTAR et al., 2022). Encontrar meios econômicos para monitoramento da produção e garantir parâmetros de qualidades para estes produtos é de grande importância.

Existem várias explicações e benefícios para o uso de narizes eletrônicos de baixo custo (e-nose) e simples de se utilizar em países em desenvolvimento para detectar diferentes estágios de maturação de frutas e chás (CHENG et al., 2021; JIA et al., 2019; ALI et al., 2020). Os métodos tradicionais para determinar os estágios de maturação frequentemente exigem aparelhos de laboratório de custo elevado e trabalhadores qualificados, o que pode não ser prático em ambientes com poucos recursos (BURATTI et al., 2011; SANAEIFAR et al., 2017; VIEIRA et al., 2017; WILSON, 2018). Narizes eletrônicos de baixo custo podem oferecer uma opção mais econômica, sendo ferramentas de teste não destrutivas, portanto, não danificam as frutas ou as folhas de chá durante a análise. Ao utilizarem a tecnologia, os agricultores podem acompanhar as fases de amadurecimento sem abrir mão de uma parte de sua colheita, o que ajuda a reduzir o desperdício e maximizar a produtividade (XU et al., 2019; ZHANG et al., 2016). Outra vantagem é o monitoramento em tempo real, visto que o nariz eletrônico pode oferecer dados sobre a maturidade de frutas e folhas de chá em tempo real e como resultado, a qualidade do produto aumenta e as perdas por amadurecimento excessivo ou insuficiente são reduzidas. Isso permite que agricultores e produtores tomem decisões oportunas sobre colher ou processar as safras (LIPPOLIS et al., 2014; WEI; SHAO et al., 2018; WEI; ZHANG et al., 2018). Além disso, esses dispositivos favorecem a portabilidade e alcance a vários ambientes, pois geralmente têm designs portáteis e fáceis de usar. Eles podem ser levados direto para o campo, permitindo que os agricultores avaliem os vários estágios de amadurecimento sem ter que enviar amostras para um laboratório distante. Agricultores de pequena escala como a grande maioria das pequenas propriedades familiares, que muitas vezes são a base do setor agrícola em países subdesenvolvidos, não têm acesso a tecnologias mais avançadas. Ao fornecer a esses agricultores uma ferramenta para ajudá-los a tomar melhores decisões e serem mais produtivos em geral, a introdução de narizes eletrônicos de baixo custo pode fortalecê-los. O uso de narizes eletrônicos de baixo custo em nações subdesenvolvidas também pode produzir informações úteis sobre variações regionais, padrões de amadurecimento de safras e outros detalhes pertinentes. Esta informação pode ser utilizada para gerar soluções focadas para melhorar a agricultura e para pesquisas futuras e desenvolvimentos de políticas públicas que agreguem a economia circular frente a demandas da agricultura 5.0.

E por último, o projeto justifica-se por aprimorar o processo de amadurecimento, os produtores podem diminuir sua dependência de agentes químicos de amadurecimento ou conservantes, resultando em uma prática agrícola mais ecológica e sustentável, além de tornar possível identificação de origem auxiliando na autenticidade de produtos agrícolas (ex. chás) Embora os narizes eletrônicos de baixo custo tenham muitos benefícios, é importante levar em conta coisas como calibração para variedades de culturas regionais e dar aos agricultores e produtores o treinamento para aproveitá-los ao máximo. No entanto, o uso dessa tecnologia tem o potencial de melhorar os métodos agrícolas e apoiar o crescimento econômico das nações subdesenvolvidas.

4. REFERÊNCIAS BIBLIOGRÁFICAS

- AGUSTIKA, D. K. et al. Steady-state response feature extraction optimization to enhance electronic nose performance. In: IEEE. 2020 7th International Conference on Electrical Engineering, **Computer Sciences and Informatics (EECSI)**. [S.l.: s.n.], 2020. p. 144–149.
- ALEIXANDRE, M. et al. A wireless and portable electronic nose to differentiate musts of different ripeness degree and grape varieties. **Sensors**, MDPI, v. 15, n. 4, p. 8429–8443, 2015.
- ALI, M. M. et al. Principles and recent advances in electronic nose for quality inspection of agricultural and food products. **Trends in Food Science & Technology**, 2020 Elsevier, v. 99, p. 1–10.
- ATTAR, Ş. H. et al. Nutritional analysis of red-purple and white-fleshed pitaya (*Hylocereus*) species. **Molecules**, 2022, MDPI, v. 27, n. 3, p. 80..
- BINSON, V. A.; SUBRAMONIAM, M. Design and development of an e-nose system for the diagnosis of pulmonary diseases. **Acta of Bioengineering & Biomechanics**, v. 23, n. 1, 2021.
- BOROWIK, P. et al. Application of a low-cost electronic nose for differentiation between pathogenic oomycetes pythium intermedium and phytophthora plurivora. **Sensors**, MDPI, 2021 v. 21, n. 4, p. 1326.
- BROOKS, C. et al. A review of food fraud and food authenticity across the food supply chain, with an examination of the impact of the COVID-19 pandemic and Brexit on food industry, 2021 v. 130, p. 108171.
- BURATTI, S. et al. Monitoring of alcoholic fermentation using near infrared and mid infrared spectroscopies combined with electronic nose and electronic tongue. **Analytica chimica acta** 2021, Elsevier, v. 697, n. 1-2, p. 67–74.
- CANO MARCHAL, P. et al. Prediction of fruity aroma intensity and defect presence in virgin olive oil using an electronic nose. **Sensors**, 2021 MDPI, v. 21, n. 7, p. 2298.
- CHARUMPORN, B. et al. Compact electronic nose systems using metal oxide gas sensors for fire detection systems. In: IEEE. THE 2006 IEEE International Joint Conference on Neural Network Proceedings. [S.l.: s.n.], 2006. p. 2214–2217.
- CHEAH, L. K. et al. Phytochemical properties and health benefits of *Hylocereus undatus*. . 2016), v. 1, p. 100-120
- CHEN, K. et al. Recognizing lung cancer and stages using a self-developed electronic nose system. **Computers in Biology and Medicine**, 2021 Elsevier, v. 131, p. 104294,
- CHENG, H. et al. Characterization of aroma-active volatiles in three Chinese bayberry (*Myrica rubra*) cultivars using GC–MS–olfactometry and an electronic nose combined with principal component analysis. **Food Research International**, 2015, Elsevier, v. 72, p. 8–15, 2015.
- CHENG, L. et al. Development of compact electronic noses: A review. **Measurement Science and Technology**, 2021 IOP Publishing, v. 32, n. 6, p. 062002, 2021.
- CHI, X. et al. Distinction of volatile flavor profiles in various skim milk products via HS-SPME–GC–MS and E-nose. **European Food Research and Technology**, 2021, Springer, v. 247, p. 1539–1551.
- CHILO, J. et al. E-nose application to food industry production. **IEEE Instrumentation & Measurement Magazine**, 2016 IEEE, v. 19, n. 1, p. 27–33, 2016
- CHOPRA, V. L.; KRISHNAKUMAR, V.; PETER, K. V. **Plantation Crops and Plantations**. , 2016, v. 3, p 230-270.

- CHOWDHURY, S. R. et al. Analysis of a data acquisition system for a compact electronic nose. In: SPRINGER. PROCEEDINGS of the **2nd International Conference on Communication, Devices and Computing: ICCDC**, 2019. [S.l.: s.n.],. p. 615–628.
- DING, Y. et al. Classification of tea quality levels using near-infrared spectroscopy based on CLPSO-SVM. **Foods**, 2022 MDPI, v. 11, n. 11, p. 1658.
- DONG, C. et al. Prediction of congou black tea fermentation quality indices from color features using non-linear regression methods. **Scientific reports**, 2018, Nature Publishing Group UK London, v. 8, n. 1, p. 10535.
- EMERSON. **Electrochemical vs. Semiconductor Gas Detection – a Critical Choice.**, 2019, [S.l.]: Emerson. p. 1–6. Disponível em: <<<https://www.emerson.com/documents/automation/white-paper-electrochemical-vs-semiconductor-gas-detection-en-5351906.pdf>>>. Acesso em: 21 jun. 2022.
- FAN, S. et al. Effect of spectrum measurement position variation on the robustness of NIR spectroscopy models for soluble solids content of apple. **Biosystems Engineering**, 2016 Elsevier, v. 143, p. 9–19.
- FENG, X. et al. Preliminary study on classification of rice and detection of paraffin in the adulterated samples by Raman spectroscopy combined with multivariate analysis. **Talanta**, 2013 Elsevier, v. 115, p. 548–555.
- GONZALEZ VIEJO, C. et al. Development of a low-cost e-nose to assess aroma profiles: An artificial intelligence application to assess beer quality. **Sensors and Actuators B: Chemical**, 2020. Elsevier, v. 308, p. 127688,
- GONZALEZ VIEJO, C. FUENTES, S. Low-cost methods to assess beer quality using artificial intelligence involving robotics, an electronic nose, and machine learning, 2021. v. 21, n. 6, p. 2016
- GONZALEZ VIEJO, C.; TONGSON, E.; FUENTES, S. Integrating a low-cost electronic nose and machine learning modelling to assess coffee aroma profile and intensity. **Sensors**, 2021. MDPI, v. 308, p. 127688
- HARUN, F. K. C.; COVINGTON, J. A.; GARDNER, J. W. Portable e-Mucosa System: Mimicking the biological olfactory. *Procedia Chemistry*, 2009 Elsevier, v. 1, n. 1, p. 991–994
- HOMER, M. L. et al. Compensating for relative humidity changes while monitoring air quality using an electronic nose. **Jet Propulsion Laboratory Report**, 2002, p. 209
- JIA, W. et al. Advances in electronic nose development for application to agricultural products. **Food Analytical Methods**, 2029, Springer, v. 12, p. 2226–2240.
- JIANG, H. et al. Maturity Stage Discrimination of *Camellia oleifera* fruit using visible and near-infrared hyperspectral imaging. **Molecules**, 2022 MDPI, v. 27, n. 19, p. 6318.
- JIMÉNEZ-CARVELO, A. M. et al. Alternative data mining/machine learning methods for the analytical evaluation of food quality and authenticity—A review. **Food Research International**, , 2019, Elsevier, v. 122, p. 25–39
- JULIAN, T. et al. Intelligent mobile electronic nose system comprising a hybrid polymer-functionalized quartz crystal microbalance sensor array. **ACS omega**, , ACS Publications, 2020. v. 5, n. 45, p. 29492–29503.
- LI, D. et al. A novel headspace integrated E-nose and its application in discrimination of Chinese medical herbs. **Sensors and Actuators B: Chemical**, 2015, Elsevier, v. 221, p. 556–563.

- LI, H. et al. Non-destructive evaluation of pork freshness using a portable electronic nose (E-nose) based on a colorimetric sensor array. **Analytical Methods**, 2014 Royal Society of Chemistry, v. 6, n. 16, p. 6271–6277.
- LIPPOLIS, V. et al. Screening of deoxynivalenol contamination in durum wheat by MOS-based electronic nose and identification of the relevant pattern of volatile compounds. *Food Control*, 2014, Elsevier, v. 37, p. 263–271.
- LIU, T. et al. A data-driven meat freshness monitoring and evaluation method using rapid centroid estimation and hidden Markov models. **Sensors and Actuators B: Chemical**, 2020 Elsevier, v. 311, p. 127868.
- LIU, T. et al. A novel multi-odour identification by electronic nose using non-parametric modelling-based feature extraction and time-series classification. **Sensors and Actuators B: Chemical**, 2019 Elsevier, v. 298, p. 126690.
- MA, L. et al. A low-cost compact measurement system constructed using a smart electrochemical sensor for the real-time discrimination of fruit ripening. **Sensors**, MDPI, v. 16,
- MACÍAS, M. M. et al. A compact and low cost electronic nose for aroma detection. **Sensors**, Molecular Diversity Preservation International (MDPI), 2013 v. 13, n. 5, p. 5528–5541.
- MATATAGUI, D. et al. Portable low-cost electronic nose based on surface acoustic wave sensors for the detection of BTX vapors in air. **Sensors**, MDPI, 2019 v. 19, n. 24, p. 5406.
- Mimicking the biological olfactory. **Procedia Chemistry**, Elsevier, v. 1, n. 1, p. 991–994, 2009.
- MOS-based electronic nose and identification of the relevant pattern of volatile compounds. 2016, n. 4, p. 501.
- NAKE, A. et al. Outdoor in situ monitoring of volatile emissions from wastewater treatment plants with two portable technologies of electronic noses. **Sensors and Actuators B: Chemical**, 2005 Elsevier, v. 106, n. 1, p. 36–39.
- NI, K. et al. Multi-element composition and isotopic signatures for the geographical origin discrimination of green tea in China: A case study of Xihu Longjing. **Journal of Food Composition and Analysis**, 2018 Elsevier, v. 67, p. 104–109.
- NICOLAI, B. M. et al. Nondestructive measurement of fruit and vegetable quality by means of NIR spectroscopy: A review. **Postharvest biology and technology**, 2007 Elsevier, v. 46, n. 2, p. 99–118
- OLIVEIRA, G. A. et al. Comparison of NIRS approach for prediction of internal quality traits in three fruit species. **Food Chemistry**, 2014. Elsevier, v. 143, p. 223–230.
- PAN, C.-H.; HSIEH, H.-Y.; TANG, K.-T. An analog multilayer perceptron neural network for a portable electronic nose. **Sensors**, 2013. MDPI, v. 13, n. 1, p. 193–207.
- PANDISELVAM, R. et al. Recent advancements in NIR spectroscopy for assessing the quality and safety of horticultural products: A comprehensive review. **Frontiers in Nutrition**, , 2022. Frontiers, v. 9, p. 973457.
- PAPADOPOULOU, O. S. et al. Sensory and microbiological quality assessment of beef fillets using a portable electronic nose in tandem with support vector machine analysis. **Food Research International**, 2013 Elsevier, v. 50, n. 1, p. 241–249.
- PHUKKAPHAN, N. et al. The application of gas sensor array based electronic nose for milk spoilage detection. In: IEEE. 2021 7th International Conference on Engineering, Applied Sciences and Technology (ICEAST), 2021 [S.l.: s.n.]. p. 273–276.
- FOOD Quality, Safety and Technology. [S.l.: s.n.], 2013. p. 77–87.

- QIU, S.; WANG, J.; GAO, L. Qualification and quantisation of processed strawberry juice based on electronic nose and tongue. **LWT-Food Science and Technology**, 2015. Elsevier, v. 60,n. 1, p. 115–123.
- RAHIMZADEH, H. et al. On the feasibility of metal oxide gas sensor based electronic nose software modification to characterize rice ageing during storage. **Journal of Food Engineering**, 2019. Elsevier, v. 245, p. 1–10.
- RALISNAWATI, D. et al. Detecting aroma changes of local flavored green tea (*Camellia sinensis*) using electronic nose. In: IOP PUBLISHING, 1. IOP Conference Series: Earth and Environmental Science. 2018. v. 131, p. 012004.
- RODRÍGUEZ-MÉNDEZ, M. L. et al. Electronic noses and tongues in wine industry. **Frontiers in Bioengineering and Biotechnology**, 2016. Frontiers Media SA, v. 4, p. 81
- RUSSO, M. et al. Non-destructive flavour evaluation of red onion (*Allium cepa* L.) Ecotypes: An electronic-nose-based approach. **Food Chemistry**, 2013 v. 141, n. 2, p. 896–899. I
- SALUNKHE, R. P.; PATIL, A. A. Image processing for mango ripening stage detection: RGB and HSV method. In: IEEE, 2015 Third International Conference on Image Information Processing (ICIIP). [S.l.: s.n.], 2015. p. 362–365.
- SANAEIFAR, A. et al. Early detection of contamination and defect in foodstuffs by electronic nose: A review. **TrAC Trends in Analytical Chemistry**, 2017 v. 97, p. 257–271.
- SHAH, S. S. A. et al. Towards fruit maturity estimation using NIR spectroscopy. **Infrared Physics & Technology**, 2020 Elsevier, v. 111, p. 103479.
- SPINELLE, L. et al. Review of Portable and Low-Cost Sensors for the Ambient Air Monitoring of Benzene and Other Volatile Organic Compounds. **Sensors**,2017 v. 17, n. 7, p.100-110.
- SPRINGER, A. E. Wine authentication: a fingerprinting multiclass strategy to classify red varieties through profound chemometric analysis of volatiles. **European Food Research and Technology**,2019 v. 245, p. 179–190.
- TAN, J.; KERR, W. L. Determining degree of roasting in cocoa beans by artificial neural network (ANN)-based electronic nose system and gas chromatography/mass spectrometry (GC/MS). **Journal of the Science of Food and Agriculture**,2018 Wiley Online Library, v. 98, n. 10, p. 3851–3859.
- TAN, J.; XU, J. Applications of Electronic Nose (e-Nose) and Electronic Tongue (e-Tongue) in Food Quality-Related Properties Determination: A Review. **Artificial Intelligence in Agriculture**, 2020, v. 4, p. 104–115.
- TANG, K.-T.; LIN, Y. S.; SHYU, J. M. A Local Weighted Nearest Neighbor Algorithm and a Weighted and Constrained Least-Squared Method for Mixed Odor Analysis by Electronic Nose Systems. **Sensors**, 2010 v. 10, n. 11, p. 10467–10483.

- TANG, K.-T. et al. Development of a portable electronic nose system for the detection and classification of fruity odors. **Sensors**, 2010 v. 10, n. 10, p. 9179–9193.
- THEPUDOM, T.; SRICHAROENCHAI, N.; KERDCHAROEN, T. Classification of instant coffee odors by electronic nose toward quality control of production. In: 2013 10th International Conference on Electrical Engineering/Electronics, Computer, Telecommunications and Information Technology. [S.l.: s.n.], 2013. p. 1–4.
- TIMSORN, K. et al. Discrimination of chicken freshness using electronic nose combined with PCA and ANN. In: IEEE. 2014 11th International Conference on Electrical Engineering/Electronics, Computer, Telecommunications and Information Technology (ECTI-CON). [S.l.: s.n.], 2014. p. 1–4.
- TSENG, T.-S. et al. Utilization of a gas-sensing system to discriminate smell and to monitor fermentation during the manufacture of oolong tea leaves. **Micromachines**, , 2021. MDPI, v. 12, n. 1, p. 93
- TYAGI, P. et al. E-nose: a low-cost fruit ripeness monitoring system. **Journal of Agricultural Engineering**, , 2023. v. 54, n. 1, p. 100.
- VIEIRA, G. S. et al. Determination of anthocyanins and non-anthocyanin polyphenols by ultra performance liquid chromatography/electrospray ionization mass spectrometry (UPLC/ESI-MS) in jussara (*Euterpe edulis*) extracts. **Journal of Food Science and Technology**, 2017. Springer, v. 54, p. 2135–2144.
- WEI, X.; SHAO, X. et al. Rapid detection of adulterated peony seed oil by electronic nose. **Journal of Food Science and Technology**, 2018. Springer, v. 55, p. 2152–2159.
- WEI, X.; ZHANG, Y. et al. Rapid and non-destructive detection of decay in peach fruit at the cold environment using a self-developed handheld electronic-nose system. **Food Analytical Methods**, , 2018. Springer, v. 11, p. 2990–3004
- WEI, Z.; WANG, J.; ZHANG, W. Detecting internal quality of peanuts during storage using electronic nose responses combined with physicochemical methods. **Food Chemistry**, , 2015. Elsevier, v. 177, p. 89–96.
- WILSON, A. D. Applications of electronic-nose technologies for noninvasive early detection of plant, animal and human diseases. **Chemosensors**, 2018. MDPI, v. 6, n. 4, p. 45.
- WILSON, A. D. Application of electronic-nose technologies and VOC-biomarkers for the noninvasive early diagnosis of gastrointestinal diseases. **Sensors**, MDPI, v. 18, n. 8, p. 2613.
- WOJNOWSKI, W. et al. Portable electronic nose based on electrochemical sensors for food quality assessment. **Sensors**, 2017 MDPI, v. 17, n. 12, p. 2715.
- WU, Z. et al. Development of a low-cost portable electronic nose for cigarette brands identification. **Sensors**, 2020, MDPI, v. 20, n. 15, p. 4239.
- XIAO, Z. et al. Application of machine vision system in food detection. **Frontiers in Nutrition, Frontiers**, 2022, v. 9, p. 888245.
- XU, S. et al. Study of the similarity and recognition between volatiles of brown rice plant hoppers and rice stem based on the electronic nose. **Computers and Electronics in Agriculture**, 2018 Elsevier, v. 152, p. 19–25, 2018.

- XU, S. et al. Visible/near infrared reflection spectrometer and electronic nose data fusion as an accuracy improvement method for portable total soluble solid content detection of orange. **Applied Sciences**, MDPI, v. 9, n. 18, p. 3761, 2019.
- YAN, J. et al. Electronic nose feature extraction methods: A review. **Sensors**, MDPI, v. 15, n. 11, p. 27804–27831, 2015.
- YAN, M. et al. Humidity compensation based on power-law response for MOS sensors to VOCs. **Sensors and Actuators B: Chemical**, Elsevier, v. 334, p. 129601, 2021.
- YIN, X. et al. Temperature modulated gas sensing E-nose system for low-cost and fast detection. **IEEE Sensors Journal**, IEEE, v. 16, n. 2, p. 464–474, 2016.
- ZHANG, W. et al. A study on soluble solids content assessment using electronic nose: persimmon fruit picked on different dates. **International Journal of Food Properties**, Taylor & Francis, v. 19, n. 1, p. 53–62, 2016.
- ZHANG, X. et al. The qualitative and quantitative assessment of xiaochaihu granules based on e-eye, e-nose, e-tongue and chemometrics. **Journal of Pharmaceutical and Biomedical Analysis**, Elsevier, v. 205, p. 114298, 2021.
- ZHAO, Z. et al. A novel spectrum analysis technique for odor sensing in optical electronic nose. **Sensors and Actuators B: Chemical**, Elsevier, v. 222, p. 769–779, 2016.
- WANG,B.,CHEN,Z.,GAO,J.,FU,L.,SU,B.,CUI,Y., The acquisition of kiwifruit feature point coordinates imabased on the spatial coordinates of ge. **IFIPAdv. Inf** 2016 p. 12-16,
- TU,S.,XUE,Y.,ZHENG,C.,QI,Y.,WAN,H.,MAO,L., Detection of passion fruit sand maturity classification using Red-Green-Blue Depthimages.**Biosyst.Eng.** 2018 v.175, p.156–167.
- WANG,Z.,WALSH,K.B.,VERMA,B., On-tree mango fruit size estimation usingRGB-D images.**Sensors** 2017 v.17,p. 2738,
- GENÉ-MOLA,J.,VILAPLANA,V.,ROSELL-POLO,J.R.,MORROS,J.R.,RUIZ-HIDALGO,J.,GREGORIO, E..Multi-modal deep learning for Fuji apple detection using RGB-Dcameras andtheirradiometriccapabilities.**Comput.Electron.Agric.** 2019 v. 162,p. 689–698. ,
- MILELLA,A.,MARANI,R.,PETITTI,A.,REINA,GIn-field high through put grapevine phenotyping withaconsumer-gradedepthcamera.**Comput.Electron.Agric.** .,2019. v. 156, p. 293–306
- ARAD,B.,BALENDONCK,J.,BARTH,R.,BEM.,SHAHAR,O.,EDAN,Y.,HELLSTRÖM,T.,HEMMING,J., KURTSE,P.,RINGDAHL,O.,TIELEN,T.,VANTUIJL,B. .Development of a sweet Pepper harvesting robot.**J.F.Robot.** 2010. p.1–13
- LIU, ZHIZHE, LUO SUN, AND QIAN ZHANG.. “High Similarity Image Recognition a Classification Algorithm Based on Convolutional Neural Network.” **Computational Intelligence and Neuroscience** 2022.
- YAHUI, L.; XIAOBO, Z.; TINGTING, S.; JIYONG, S.; JIEWEN, Z.; HOLMES, M. Determination of geographical origin and anthocyanin content of black Goji berry (*Lycium ruthenicum* Murr.) using near-infrared spectroscopy and chemometrics. **Food Anal. Methods** 2017, v. 10, p. 1034–1044. [CrossRef]

STUPPNER, S.; MAYR, S.; BEGANOVIC, A.; BEĆ, K.; GRABSKA, J.; AUFSCHNAITER, U.; GROENEVELD, M.; RAINER, M.; JAKSCHITZ, T.; BONN, G.K.; ET AL. Near-infrared spectroscopy as a rapid screening method for the determination of total anthocyanin content in sambucus fructus. **Sensors** 2020, v. 20,p. 4983. [CrossRef]

CUQ, S.; LEMETTER, V.; KLEIBER, D.; LEVASSEUR-GARCIA, C. Assessing macro- (P, K, Ca, Mg) and micronutrient (Mn, Fe, Cu, Zn, B) concentration in vine leaves and grape berries of *Vitis vinifera* by using near-infrared spectroscopy and chemometrics. **Comput. Electron. Agric.** 2020, v. 179,p. 105841. [CrossRef]

SUMMERSON, V.; VIEJO, C.G.; SZETO, C.; WILKINSON, K.L.; TORRICO, D.D.; PANG, A.; DE BEI, R.; FUENTES, S. Classification of smoke contaminated cabernet sauvignon berries and leaves based on chemical fingerprinting and machine learning algorithms. **Sensors** 2020, v. 20, p. 5099. [CrossRef]

ARSLAN, M.; XIAOBO, Z.; XUETAO, H.; ELRASHEID TAHIR, H.; SHI, J.; KHAN, M.R.; ZAREEF, M. NEAR infrared spectroscopy coupled with chemometric algorithms for predicting chemical components in black goji berries (*Lycium ruthenicum* Murr.). **J. Near Infrared Spectrosc.** 2018, v. 26,p. 275–286. [CrossRef]

MUSINGARABWI, D.M.; NIEUWOUDT, H.H.; YOUNG, P.R.; EYÉGHÈ-BICKONG, H.A.; VIVIER, M.A. A rapid qualitative and quantitative evaluation of grape berries at various stages of development using Fourier-transform infrared spectroscopy and multivariate data analysis. **Food Chem.** 2016, V. 190, p. 253–262 [CrossRef] [PubMed]

TINGTING, S.; XIAOBO, Z.; JIYONG, S.; ZHIHUA, L.; XIAOWEI, H.; YIWEI, X.; WU, C. Determination Geographical Origin and Flavonoids Content of Goji Berry Using Near-Infrared Spectroscopy and Chemometrics. **Food Anal. Methods** 2016, v. 9, p. 68–79. [CrossRef]

REICH, G. Near-infrared spectroscopy and imaging: Basic principles and pharmaceutical applications. *Adv. Drug Deliv. Rev.* 57, p. 1109–1143, [CrossRef] [PubMed]

TEIXEIRA DOS SANTOS, C.A.; LOPO, M.; PÁSCOA, R.N.M.J.; LOPES, J.A. A review on the applications of portable near-infrared spectrometers in the agro-food industry. **Appl. Spectrosc.** 2013, v. 6.(7), p. 1215–1233. [CrossRef] Ozaki, Y., T.

GENKAWA, FUTAMI Y. *Encyclopedia of Spectroscopy and Spectrometry Near-Infrared Spectroscopy*. 3rd ed. Elsevier Ltd. 2016.

BROWN, STEVEN, TAULER, R, BEATA WALCZAK, R.. “*Comprehensive Chemometrics.*” *Comprehensive Chemometrics* p. 1–4, 2010.

FAN J., LEE J. AND Y. LEE, "Image Classification Using Fusion of Multiple Neural Networks," 2021 36th International Technical Conference on Circuits/Systems, **Computers and Communications** (ITC-CSCC), Jeju, Korea (South), 2021, p. 1-4, doi: 10.1109/ITC-CSCC52171.2021.9501468.

Yan, X.; Xie, Y.; Chen, J.; Yuan, T.; Leng, T.; Chen, Y.; Xie, J.; Yu, Q. NIR Spectrometric Approach for Geographical Origin Identification and Taste Related Compounds Content Prediction of Lushan Yunwu Tea. *Foods* **2022**, v. *11*, p. 2976.

WANG J, Xiaohong WU Jun ZHENG, Bin WU, Rapid identification of green tea varieties based on FT-NIR spectroscopy and LDA/QR, *Food Science and Technology*, 2022,v 42.

CAPÍTULO I

LOW-COST ELECTRONIC-NOSE (LC-E-NOSE) SYSTEMS FOR THE EVALUATION OF PLANTATION AND FRUIT CROPS: RECENT ADVANCES AND FUTURE TRENDS

Artigo publicado na Revista Analytical Methods, da Royal Society of Chemistry.

Low-cost electronic-nose (LC-e-nose) systems for the evaluation of plantation and fruit crops: recent advances and future trends

Marcus Vinicius da Silva Ferreira¹ - Jose Lucena Barbosa Jr.^{1,*} - Mohammed Kamruzzaman² - Douglas Fernandes Barbin³

¹Federal Rural University of Rio de Janeiro (UFRRJ), Department of Food Technology, Seropédica, RJ, Brazil

²Department of Agricultural and Biological Engineering, University of Illinois at Urbana-Champaign, Urbana, IL 61801, United States

³Department of Food Engineering and Technology, School of Food Engineering, University of Campinas, Campinas, SP, Brazil

* Correspondence e-mail: lucena@ufrj.br

1.1 Abstract

An electronic nose (e-nose) is a device designed to recognize and classify odors by mimicking the olfactory cells of humans. The equipment is built around a series of sensors that detect the presence of odors, especially volatile compounds (VOCs), and generate an electric signal (voltage), known as e-nose data, which contains chemical information. In the food business, the use of e-noses for analyses and quality control of fruits and plantation crops has increased in recent years. Their use is particularly relevant due to the lack of non-invasive and inexpensive methods to detect VOCs in these crops. However, the majority of reports in the literature involve commercial e-noses, with only a few studies addressing low-cost e-nose (LC-e-nose) devices or providing a data-designed orientated description to assist researchers decide their setup and appropriate statistical methods to analyze these crops' data. Therefore, the objective of this study is to discuss the hardware of the two most common e-nose sensors: (Electrochemical EC and Metal oxide Sensors - MOS) as well as a critical review of the literature reporting MOS based low-cost e-nose devices used for investigating of plantation and fruit crops, including and main features of such devices. Miniaturization of equipment from lab-scale to portable and convenient gear, allowing producers to take it to the field, as shown in many appraised systems, is one of the future advancements in this area. By utilizing the low-cost designs provided in this review, researchers can develop their own devices based on practical demands such as quality control and compare results with devices reported in the literature. Overall, this review thoroughly discusses the applications of low-cost e-noses based on MOS for fruits, tea, and coffee, as well as the key features of their equipment (i.e., advantages and disadvantages) based on their technical parameters (i.e., electronic and physical parts). As a final remark, LC-e-nose technology deserves significant attention at it has the potential to be a valuable quality control tool for emerging countries.

Keywords: multi-sensor devices. chemometrics. quality control. Machine learning.

1.2 Introduction

E-nose is a multi-sensor device designed to identify volatile compounds similar to the olfactive sense of humans and then classify the material based on variation in its aroma. The equipment is based on a set of sensors capable of detecting the presence of odors from samples (volatile compounds) and transforming them into an electric signal (voltage, e-nose data) (PEARCE et al., 2003). This signal can be compared to chemical data used or categorical variables as a reference to assess sample quality, composition, or any other variations.

E-noses are applied in agriculture, cosmetics and pharmaceutical, environmental, military, and food analyses (CARON et al., 2016; CHENG et al., 2021; FANG; ZHANG; WEI, 2014; GOBBI et al., 2015; HERRERO et al., 2016; PENG et al., 2015; PERIS; ESCUDERGILABERT, 2009; RODRIGUEZ-LUJAN et al., 2014). In the food industry, e-nose has been used for beer aroma evaluation (GONZALEZ VIEJO; FUENTES, 2020), sensory attributes of food (ZHONG, 2019), rice aging (RAHIMZADEH et al., 2019), freshness in chicken (TIM- SORN et al., 2014), drying of cocoa (TAN; KERR, 2018) among other agricultural products, especially in fruits and plantation crops.

Fruits post-harvesting and processing require safe and high-quality products, thus demanding thorough quality control (TYLEWICZ et al., 2019), as well as the plantation crops industry (e.g., cocoa, tea, and coffee) that have recently grown in a global economy (CHOPRA; KRISHNAKUMAR; PETER, 2016). E-noses are applied to these crops targeting VOCs such as bromodichloromethane ethyl benzene, butyl benzene, and n- ethylene dichloride (FLEMING-JONES; SMITH, 2003), related to ripening and other chemical changes of interest. In these products, each sensor choice is crucial to detect the small changes in concentration of odor gases related to some of these food transformations due to storage or processing. Identification of VOCs has been related to fruit ripeness stage and post-harvest storage condition (TYAGI et al., 2023) and determination of origin for plantation crops such as tea, coffee, and cocoa, where fraud alone accounts for more than USD 10 billion loss per year in the global food industry (TSENG et al., 2021). Detecting VOCs in these products is crucial to understand how they are related to the alteration within these crops, which is in demand in the growing food industry (BROOKS et al., 2021).

Applications of e-nose devices have grown over the past few years since the methods for quality evaluation of these crops are onerous and time-consuming. Some of these methods include gas or liquid chromatography (CG) and Fourier-transform Infrared Spectroscopy (FT-IR) spectroscopy; which require expensive equipment or the use of chemicals, in addition to the destruction of the sample being analyzed (BURATTI et al., 2011; SANAEIFAR et al., 2017; VIEIRA et al., 2017; WILSON, 2018).

Some e-nose devices have been developed in the laboratory (DAI et al., 2019; TIAN; CAI; ZHANG, 2012; WEI et al., 2018), and even though lab setups have been established, there is still a threshold that needs to be overcome to disseminate the use of e-nose systems (CUI et al., 2017; ZHANG; LIU; DENG, 2017). Additionally, e-nose systems have been evaluated by many studies focusing on the improvement of sensors and data acquisition (FONOLLOSA et al., 2016; YIN et al., 2019; ZHANG et al., 2016), as well as sensor types such as metal oxide and electrochemical in which the former outnumber the latter. Other improvements focus on the overall stability within the system (LOUTFI et al., 2015; WILSON, 2018), since some parameters are crucial for the industries when working with odors sensors, such as variation in temperature and humidity (KIANI; MINAEI; GHASEMI-VARNAMKHASTI, 2016; LOUTFI et al., 2015).

The current demand and trend of e-nose development have grown over the past few years with new design concepts and set-ups to fulfill the demand. Many applications in quality inspection of food can be performed to solve issues in the supply chain due to quality inspection deficiency being a serious matter in the food industry. Likewise, reducing common electronic components, such as analog-digital converter (ADC), as well as reducing other part sizes such as pumps, are investigated to achieve smaller devices (ALI et al., 2020; CHENG et al., 2021; JIA et al., 2019). Even though compact e-noses in food have been recently attested for portability as the main focus of their design while improving real-time performance (CHENG et al., 2021), LC-e-nose built to assess fruits and plantation crops have not yet been compiled.

LC-device is defined as a piece of equipment whose cost is below the typical cost for a category, which for e-noses would price far behind the average (25,000 dollars). However, in the literature, many authors have used more expensive commercial formats (CHENG et al., 2015; WEI et al., 2018; ZAKARIA et al., 2012; ZHANG et al., 2016). The price will be mainly derived from the structure of the proposed devices, such as the motherboard and sensors, rather than other peripherals. However, the sensor array is decisive in determining the final price of the e-nose system. For that, the most common ones used for low-cost equipment are electrochemical (EC) and metal oxide sensors (MOS) (CHENG et al., 2021); others, such as colorimetric are not easily described in papers as low cost and only a few can be found in the literature using this terminology (KIM et al., 2022), therefore for the scope of this review only EC and MOS due to their similarity will be carried out in the investigation as best options to mount LC-e-nose devices. Another major research focus is algorithms to treat the acquired data, e.g. data processing and pattern recognition (JIANG et al., 2017; JING et al., 2016; LIU et al., 2019; QU; CHAI; YANG, 2009; RODRIGUEZ-LUJAN et al., 2014; TANG; LIN; SHYU, 2010; YAN et al., 2015; ZHANG; ZHANG, 2014; ZHANG et al., 2014; ZHAO et al., 2016). Multivariate data analysis has been applied to interpret the signal from e-noses, which may allow the combination of several sensors with a vast amount of data from samples. Some of the main statistical methods include principal components analysis (PCA) and hierarchical clustering analysis (HCA), along with supervised regression methods, such as partial least square (PLS), and classification (i.e., partial least square discriminant analysis (PLS-DA) and soft independent modeling by class analogy (SIMCA)). Machine learning (ML) methods have also been used to explore e-nose data, including support vector machine (SVM) and artificial neural network (ANN) with extreme learning machine (ELM) (VOSS; AYUB; STEVAN, 2020).

However, most studies found in the literature cover commercial e-noses and there is no compilation focused on Low-cost-e-nose devices (LC-e-nose). Additionally, only a few studies use electrical chemical on fruit and plantation crops. Therefore, the aim of this review is to provide an overview of sensor function, comparing EC and MOS, and present reports over the past 13 years of fully defined Low-cost-e-nose devices based on MOS applied in fruits, tea, cocoa and coffee, their designs, e-nose, and common data treatments. Furthermore, the most common methods for data analysis are also discussed.

1.3 Most common of LC-e-nose sensors used for fruit and plantation crops

E-nose is often utilized in e-noses is the MOS sensor, in which changes in the electrical characteristics of a metal oxide coating placed on a semiconductor substrate are detected by these sensors (EMERSON, 2019; TAN; XU, 2020). To understand the function, advantages and availability of these two sensors, the investigation of EC and MOS based e-noses in fruits and plantation crops was conducted as a brief comparison between these two sensors.

1.3.1 LC-e-noses based on electrochemical (EC) sensors

Many authors used Low-cost-e-nose systems to investigate plantation crops and fruits, more specifically to determine the ripeness stage of fruits (QIAO et al., 2022; TYAGI et al., 2023). The device described by MA et al. (2016) will be used to demonstrate an EC e-nose system. The device consisted of a single sensor for ethylene (Figure 1.1a) attached to a simple motherboard mounted on an LCD (a1), circuit board (a2), micropump (a3), sample chamber (a4), smart EC sensor (a5), gas chamber (a6), triple valve (a7). Regarding the sensing unit (b1), it includes a gas diffusion layer (b2), a hydrophobic membrane-upper gas diffusion layer (3), a gas sensing layer (b4), a sensing electrode (b5), electrolyte and counter electrolyte (b6). The electrical circuit and respective electrons flow is shown in Figure 1.1b (b7- b9). The concentration range that the device was able to measure ranged from 0 to 10 ppm. During the application to ripeness detection on apples, kiwi, and pears, 0.413 ppm was obtained as the detection limit of ethylene, which is reasonably good for trace detection to help fruit harvesting and marketing. The chemical reaction that happens in the sensor is described below in the reference electrode (Equations 4.1-4.3).



While the counter electrode is the reaction that promotes the equilibrium by transforming the oxygen in the air into water



The functioning of the sensor follows Butler-Volmer Equation.

$$I_{lim} = \frac{(n.F.D.CC_{2H_4})}{\delta} \quad (4.3)$$

Where I_{lim} stands for limiting current density; n is the number of transferred electrons; F is Faraday's constant; D the diffusion coefficient for C_2H_4 ; $C_{C_2H_4}$ stands for the concentration of C_2H_4 gas in the dimension of the electrolyte and the δ represents the thickness of the diffusive layer. The result is that the current within the sensor would be proportional to the C_2H_4 gas in concentration. EC has been used either for portable devices, as demonstrated by WOJNOWSKI et al. (2017). They proposed what, 2023; SILVA FERREIRA et al., 2023). Yet competitive MOS can still beat EC in price in most applications (EMERSON, 2019).

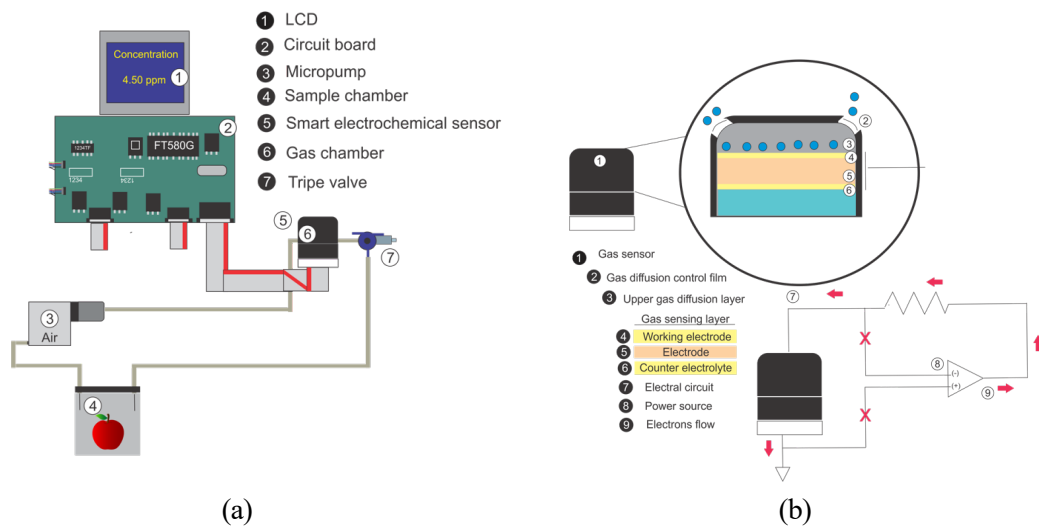


Figure 1.1: Electrochemical equipment set up and sensor, adapted from Ma et al. (2016).

1.3.2 LC-e-noses based on MOS sensors

Semiconductor gas detection sensors are then a good choice when building a portable and affordable device (Figure 1.1). The common setup comprises an air pump (a1), valve (a2), sensor array (a3), escape valve (a4), sample chamber (a5), motherboard (a6), and MOS connection in (a7). Figure 1.2b shows the gas sensor itself (b1), the MOS gas sensor electrode (b2) the tin dioxide layer (b4-b6) as well as the electric circuit flow (b7- b9). In the electrode, while in IDLE mode, the O₂ present in the air binds electrons in the tin dioxide layer and blocks the passage of current in the system. Later, when reducing gases interact with the metal oxide coating and the electrical characteristic of the film changes, the current is unblocked (EMERSON, 2019; TAN; XU, 2020).

A piece of low-cost equipment has recently been compared to mass-spectroscopy chromatography and succeeded in identifying 45 compounds e.g., 3-Methylfuran, Methyl furfuryl disulfide, and 3-Furaldehyde for coffee intensity (GONZALEZ VIEJO; TONGSON; FUEN- TES, 2021). Prediction models for these same compounds had high calibration, validation, and prediction accuracy, showing a correlation coefficient of 0.99, 0.98, and 0.99, respectively, and a low mean square error (MSE) ($\sim 10^{-10}$). The evaluated MOS sensors were MQ (3 - ethanol, 4 - methane (CH₄), 7 - carbon monoxide (CO), 8 - hydrogen (H), 135 - ammonia/alcohol/benzene, 136 - hydrogen sulfide (H₂S), 137 - ammonia (NH₃), 138 - benzene alcohol and ammonia and 811 - carbon dioxide (CO₂)).

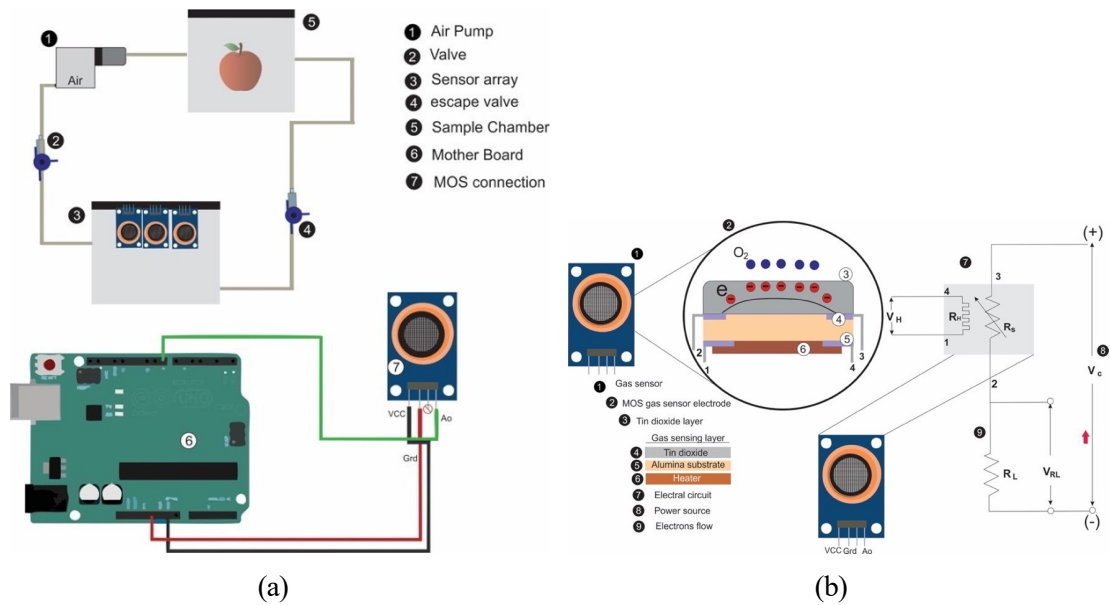


Figure 1.2: MOS sensor setup and circuit connections, adapted from Ma et al. (2016).

* ⁽¹⁾ Least-squares support-vector machines - LS-SVM; ⁽²⁾ Extreme Learning Machine (ELM); ⁽³⁾ K-nearest neighbors (KNN); ⁽⁴⁾ Support vector machine (SVM); ⁽⁵⁾ Random Forest (RF); ⁽⁶⁾ Convolutional Neural Network (CNN); Linear Discriminant Analysis (LDA); ⁽⁷⁾ Principal component analysis with support vector machine (PSMVM); ⁽⁸⁾ Nearest neighbor (NN); ⁽⁹⁾ Probabilistic neural network (PNN); ⁽¹⁰⁾ K-nearest neighbor (KNN); ⁽¹¹⁾ Principal component analysis with K-nearest neighbor (PKNN); ⁽¹²⁾ Quadratic discriminant analysis (QDA); metal oxide sensors (MOS).

Another study on coffee regarding alcohol. MICS from SGX (Sensor-tech, China) were also used to compose this device: MICS 5524 can sense carbon monoxide, ethanol, hydrogen, ammonia, and methane. The analog-digital converter (ADC), which is an electronic circuit to measure signal values and data acquisition time of one minute to complete the acquisition, is one of the features of this lab-made device.

MOS sensors have been used to determine ripening stages in fruits using some previous sensors (e.g., MQ - 135, 2, 3, 4) added MQ-5, which accounts for natural gas alcohol and hydrogen. They showed the differences between the measurement circuit of both sensors type TGS 26-xxxx (Figaro, Osaka, Japan– 50– 5,000 ppm DR, 3.3V) and MQ-xxx (Winsen, Zhengzhou, China– 300 – 10,000 ppm DR, 5V). Other manufacture models such as WSP-xxxx Metal oxide type sensor – Winsen, Zhengzhou, China– 1 – 50 ppm DR, 5V, MP-xxx Metal oxide type sensor – Winsen, Zhengzhou, China– 10 – 1,000 ppm DR, 5V and MS-xxxx Metal oxide type sensor – Ogam, Jeollanamdo, Korea – 10 – 1,000 ppm DR, 5V are also seen in a few LC-e-nose applications for soil-based gases (SHI et al., 2022). Even the combination of them sometimes may improve equipment performance (VOSS; AYUB; STEVAN, 2020).

Even though there are similarities between EC and MOS sensors, such as the possibility of low-cost devices (GONZALEZ VIEJO; FUENTES, 2020; KOSCINSKI, 2016), some advantages of the MOS are available in the market, and the fact that they do not present some irreversibly inhibit sensitivity with some silicon vapors and alkaline metal. MOS sensors' longevity is over 10 years, and their sensitivity is 50-5000 ppm average, which gives this type of sensor the greatest life expectancy out of the other technologies available (EMERSON, 2019).

Overall, both sensors (EC and MOS) offer include the temperature range, which is limited for EC devices, for example, and affected by alkaline metals, which might be the reason why the use of MOS for agricultural products (e.g., fruits and plantation crops) (RAHIMZADEH et al., 2019) outnumbers EC devices. Therefore, all LC-e-nose setups presented will then follow MOS-based equipment.

1.4 Application of LC-e-nose in fruits

Fruits are abundant sources of fiber, phytochemicals, and micronutrients (vitamins, minerals) that, either alone or in combination, are beneficial to human health (YAHIA; GARCÍA- SOLÍS; CELIS, 2019). The demand for high-quality foods that preserve their flavors and tastes devoid of additives and preservatives has increased among consumers in recent years. The difficulty for the fruit sector is to create such goods while considering consumer acceptance based on quality control and safety (TYLEWICZ et al., 2019). In this regard, LC-e-noses have been used in fruits to guarantee food quality control and safety (ANTICUANDO; DIRECTO; PADILLA, 2022). They are usually divided into two groups where fruits are categorized: climacteric or non-climacteric. The difference is that for the former, the fruit reaches a ripening stage and once attaining that stage, continues to develop to full physiological maturity, even when harvested. On the other hand, non-climacteric fruit needs to stay on the plant to reach full physiological maturity since when harvested, the ripening process stops, and the fruit no longer gains flavor or sugar, having its highest eating quality at harvest (FAN et al., 2022).

Climacteric fruit such as peaches, plums, cantaloupe, bananas, pears, and tomatoes continue to gain flavor and get sweeter by changing starch into sugar after being harvested. E-nose systems have been widely applied to detect odors in bananas, lemons, and lychee (PAN; HSIEH; TANG, 2013; TANG et al., 2010) as well as other fruits. Also, many studies used fruit odors and correlated them with ripening in grapes (ALEIXANDRE et al., 2015), coffee aroma profile (GONZALEZ VIEJO et al., 2020), solids content in persimmon fruit (ZHANG et al., 2016) and decay in peach fruit (WEI et al., 2018). All these approaches have been conducted to climacteric fruit that can be left at room temperature until consumed or mature and then stored at refrigerated condition. Since many climacteric fruits soften as they ripen, they are harvested crisp and physiologically immature to reduce damage during transportation and increase shelf life. However, if the fruit is left at ambient temperature for a few days, it develops more taste and sweetness, which is how sensors detect alteration within the fruit based on ethylene production (GOLDY, 2019).

Non-climacteric fruits are less investigated in LC-e-nose systems due to not changing drastically after harvesting. However, systems have been developed for this fruit category and some examples of LC-e-nose devices being used for fruits are shown in Table 1.1, which shows systems for climacteric and non-climacteric and the most common chemicals senses are presented in Table 1.2. Some examples of non-climacteric fruits presented are cherries, grapes, oranges, and raspberries. Some investigation with non-climacteric fruit using e-nose includes the evaluation of odor sensing (SRIVASTAVA; SADISATP, 2016) and total soluble solid content in oranges (XU et al., 2019).

Table 1.1: Low-cost-e-noses used to evaluate fruits.

Ripeness Type	Application	Data Treatment (*)	e-nose name / sensors	References
			Lab-developed	
	Fruit ripening (Apples)	Kinetic models	Ethylene gas sensor /	Ma et al. (2016)
	Peaches	PLSR ⁽¹⁾ LSSVM ⁽²⁾	Electrochemical Self-developed (e-nose I) / MOS (TGS-xxxx) Self-developed /	Wei et al. (2018)
	Banana fruit	ANN	MOS (TGS-xxxx/ MQ-xxx)	Hendrick et al. (2022)
	Peach growth monitoring	ELM ⁽²⁾ KNN ⁽³⁾ SVM ⁽⁴⁾	Self-developed / MOS (TGS/MQ)	Voss, Ayub e Stevan (2020)
	Ripening	PCA LDA	Self-developed - Lab scale /	
	Cab Apples	PLSR SVM ⁽⁴⁾ RF ⁽⁵⁾	MOS(TGS-xxxx/ MP-xxx/MS-xxx)	Qiao et al. (2022)
Climateric	Oil Palm fresh fruits	Trapezoidal integration method	Self-developed - Lab Scale / MOS (MQ-xxx)	Husein et al. (2022)
	Tomato (<i>Lycopersicum esculentum</i> L.) Fruit odor	SVM ⁽⁴⁾ CNN ⁽⁶⁾ LDA ⁽⁷⁾	TOMATO designed enose / MOS (MQ-xxx)	Anticuando, Directo e Padilla (2022)
	(Bananas, Lemons and Lychees)	ANN ⁽⁶⁾	MLPNN chip	Pan, Hsieh e Tang (2013)
	Fruit odor	SVM ⁽⁴⁾ PPSMVM ⁽⁷⁾	Self-developed -	
	(Banana, Lemon, Litchi and Longan)	NN ⁽⁸⁾ PNN ⁽⁹⁾ KNN ⁽¹⁰⁾ PKNN ⁽¹¹⁾	Lab Scale / MOS (TGS-xxxx)	Tang, Lin e Shyu (2010)
Non-climateric	Apples, bananas, oranges, grapes and pomegranates	ANN ⁽⁶⁾	Self-developed / MOS (TGS-xxxx- MQ-xxx)	Tyagi et al. (2023)
	Maturation stages of Dragon Fruit (<i>Hylocereus polyrhizus</i>)	PCA LDA ⁽⁷⁾ PLSR	Self-Developed e-nose / MOS (MQ-xxx)	Silva Ferreira et al. (2023)
Non-climateric	Ripeness of oranges	LDA ⁽⁷⁾ QDA ⁽¹²⁾ KNN ⁽³⁾	Low-cost optimized handheld (TGS-xxxx)	Srivastava e Sadisatp (2016)

* ⁽¹⁾ Least-squares support-vector machines - LS-SVM; ⁽²⁾ Extreme Learning Machine (ELM); ⁽³⁾ K-nearest neighbors (KNN); ⁽⁴⁾ Support vector machine (SVM); ⁽⁵⁾ Random Forest (RF); ⁽⁶⁾ Convolutional Neural Network (CNN); Linear Discriminant Analysis (LDA); ⁽⁷⁾ Principal component analysis with support vector machine (PSMVM); ⁽⁸⁾ Nearest neighbor (NN); ⁽⁹⁾ Probabilistic neural network (PNN); ⁽¹⁰⁾ K-nearest neighbor (KNN); ⁽¹¹⁾ Principal component analysis with K-nearest neighbor (PKNN); ⁽¹²⁾ Quadratic discriminant analysis (QDA); metal oxide sensors (MOS).

1.4.1 LC-e- in climacteric fruits

LC-e-nose labeled as lab-made devices have been usefully employed to analyze peaches in a cold environment, where classification and prediction models reached 95% accuracy and residual prediction deviation (RPD) of 9.30 (WEI et al., 2018). It is important to highlight that RPD values higher than 3.00 are considered excellent for attribute prediction (SAEYS; MOUAZEN; RAMON, 2005).

Low-cost-e- sensors (B) mounted and attached to the chamber (C) and computer (E) for data treatment (F). It used a sensor-paired array with a microcontroller, and data obtained were used as predictors for deep learning, convolutional neural network (CNN) models. The results achieved 86% accuracy for their classification models of tomatoes' ripening stages with their device. One of the problems reported includes data acquisition since multiple factors may affect the system, such as sensor sensitivity and other equipment features, as a drawback of low-cost devices when compared with well-established e-nose brands in the market (BERNAL; MELO; DÍAZ MORENO, 2014).

Despite some equipment issues previously mentioned, such as data acquisition, another e-lab-made e-nose system (Figure 1.3c) was used to detect banana ripeness levels using Artificial Neural Network (ANN) (HENDRICK et al., 2022). The equipment was composed of a separate sample chamber (A), an air pump (B), a set of sensors (C) that was specially designed in a relatively large format, a motherboard (D), and a computer for data treatment (E and F). Since e-noses rely on temperature and humidity control, the number of sensors may impact the ability to control the dissipated heat which may lead to overheating that may affect measurements. The lab-made device consisted of thirteen sensors and had an accuracy of 100% using thirteen inputs nodes (i.e., the transfer function of weighted input connection), one hidden layer (i.e., artificial neurons take in a set of weighted inputs and produce an output through) and three outputs and the training process was set to two thousand epochs (i.e., iterations) for their classification model for ripeness levels (HENDRICK et al., 2022). In this work, it was developed user-friendly software to screen the fruit condition and their respective prediction with three possible outcomes to be displayed on the screen (unripe, ripe, and rotten) (Figure 1.3c).

The ripeness stages of apples, bananas, oranges, grapes, and pomegranates were also analyzed with a simple device composed of six MOS sensors (Figure 1.3e) compared to sensory analysis of ripeness Tyagi et al. (2023). The equipment was composed of a compressor (A), a sensor chamber (B), which was literally a hard plastic container with a sealed lid, a computer for data acquisition (C), and a motherboard (E). The results demonstrated that it was possible to classify the fruits according to their ripeness stages (unripe, ripe, overripe non-fruit) designated by human assessment, with an F- score that the device cost USD 65 and the prototype has been validated in the lab, therefore being classified as level 4 according to technology readiness level (4 - technology validated in lab, 5 - technology validated in a relevant environment-, 6- technology demonstrated in a relevant environment, and 7 - system model or prototype demonstration in an operational environment). An interesting observation is that some MQ-xxx sensors presented the same response as TGS-xxxx ones, considering that sensor choice is a challenging part of an e-nose project, thus being useful to have different options with comparative performance.

The equipment shown in Figure 1.3g was composed of an air circulation system (A), and signal conditioning (B), which is used to used either concentrate as well as standardize the input gases, the set of sensors (TGS-26xx models and 9 from MQ-xxx (C), an analog data multiplex (i.e., combines multiple signals into one), a microcontroller (i.e., an integrated circuit designed to command a specific operation), in this case, control the response of the sensor) and transmit the

signal to the SD card (F) and computer (G). Peaches were divided according to each blooming class and correlated the samples with the most abundant volatiles identified, such as alcohols, esters, ketones and aldehydes, terpenoids, and lactones. A classifier and data reducer LDA-RF was able to reduce the number of sensors used from thirteen to six. The data acquisition graph is shown in Figure 1.3h, and it is composed of data from the two sensor types used, and it is clear to observe the difference in voltage operation baseline, that phenomenon can be explained not only due to the different sensor construction but also by their sensitivity (VOSS; AYUB; STEVAN, 2020). Overall, their equipment showed good sensitivity for detecting VOCs released by peaches in the agriculture field. However, minor improvements and compensations can be made using drift correction so they can match as described in previous studies (DI CARLO; FALASCONI, 2012).

Table 1.2: Commonly compounds in fruits detected by LC-e-noses.

Application	Class	Compound	Reference
Peach growth monitoring	Aldehydes	Hexanal	Voss, Ayub e Stevan (2020)
		Benzaldehyde	
	Alcohols	(E)-2-Hexenal	
		(E)-2-Hexenol	
		(Z)-3-Hezenol	
		Hexanol	
	Esters	Hexyl acetate	
		(E)-2-Hexenyl	
	Ketones	Acetoin	
	Terpenoids	μ -terpinene	
g-terpinene			
Lactones	g-lactone		
	derived compounds		
	d-lactone		
	derived compounds		
Ripeness stages of dragon fruit (/Hylocereus} /polyr	Hydroxyl acid	Malic Acid Other organic compounds	Silva Ferreira et al. (2023)

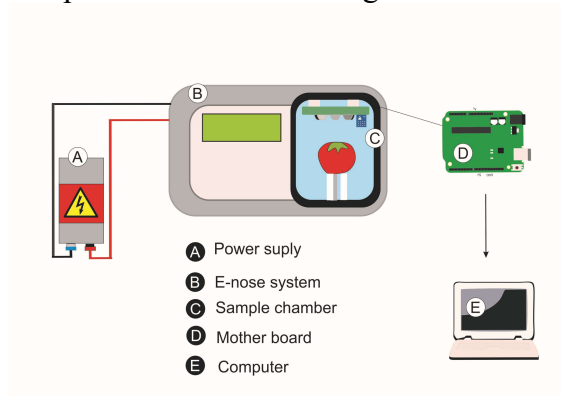
* All compounds are based most common volatiles present in fruits.

A different e-nose design (Figure 1.3i) was applied to detect three odors related to ripening stages in bananas, lemon, and lychee (TANG et al., 2010). The system had an accurate gas pump (A), four neck bottle chamber for separate gas injection (B), and logic parts such as a hub for connectivity (C), a logic board, and a display (D-E). Despite the unusual assembly and design, the system achieved an accuracy of over 70% for identifying ripeness in bananas, in which the authors demonstrated that the equipment was suitable for odor discrimination in that fruit.

1.4.2 LC-e-nose used for non-climacteric fruits

The previously described equipment used for climacteric fruits (Figure 1.3i) was used for longan, a non-climacteric fruit. The idea was to validate the LC-e-nose for its functionality for one class (climacteric fruits) and then further analysis so that further analysis could be conducted using the other class. Results demonstrated that the equipment could be used for non-climacteric fruits again to distinguish between their distinctive odors variation through ripeness stages, and the possibility of application of this type of sensor for other odors aside from ethylene was considered in other studies with non-climacteric fruit (SILVA FERREIRA et al., 2023; SRIVASTAVA; SADISATP, 2016).

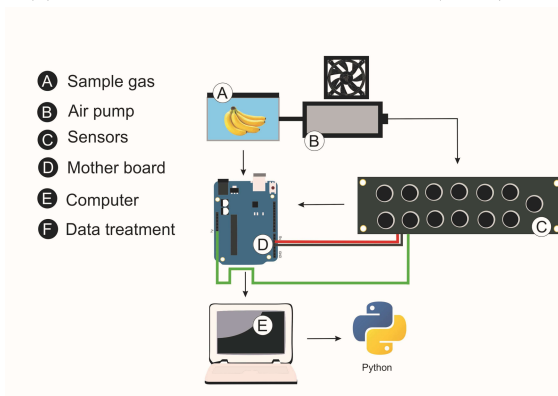
An LC-enose device (the description, that price or cost was not mentioned in the work. Apart from the computer (A), another interesting aspect of this device is the sensor array, which, instead of multiple individual units (single unit or printed circuit board (PCB) - mounted sensors), consisted of four thin nanocrystalline tin oxide layers (Figure 1.3) deposited over a micro mechanized silicon hot plate (B), in which temperature ranged from 200 °C to 350 °C (C) controlled by a Peltier cooler in which the sample was placed (D). The system among other components has a digital Loire Valley in France (ALEIXANDRE et al.)



(a) Anticuando, Directo e Padilla (2022)

NA*

(b)



(c) Hendrick et al. (2022)

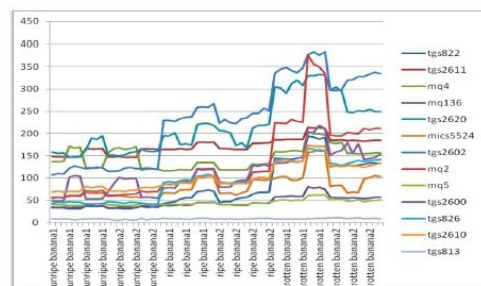
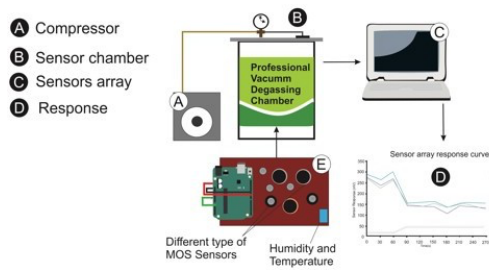
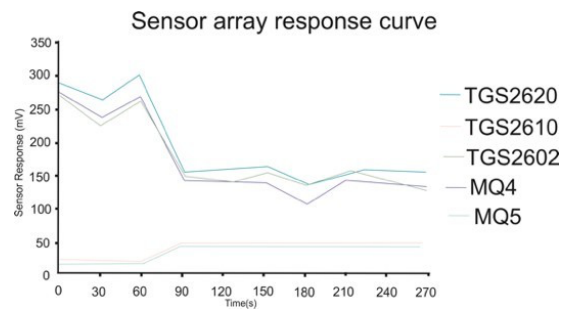


Figure 13. Comparison graph of all gas sensor tests

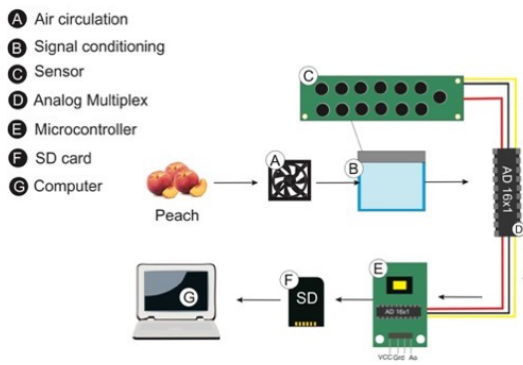
(d)



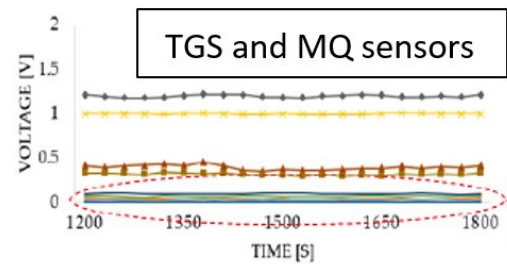
(e) Tyagi et al. (2023)



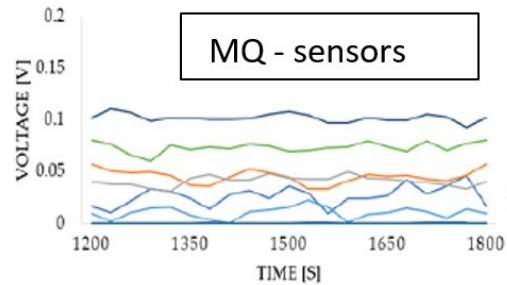
(f)



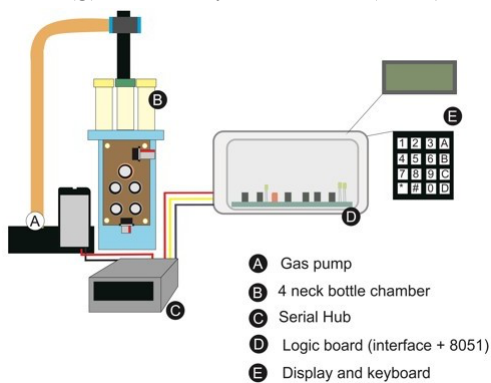
(g) Voss, Ayub e Stevan (2020)



(a)

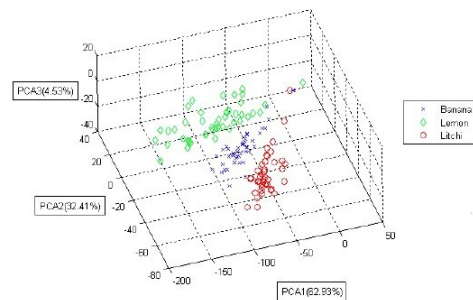


(h)

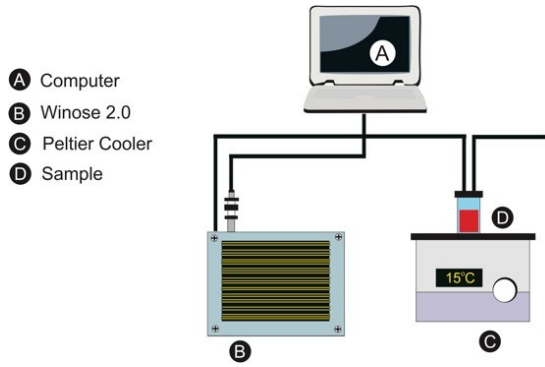


(i) Tang et al. (2010)

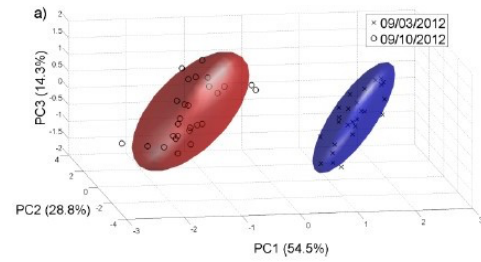
Figure 7. The PCA result of lemon, banana, and litchi.



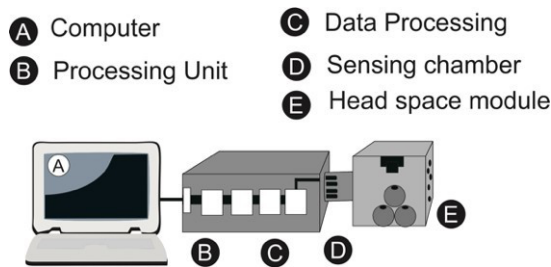
(j)



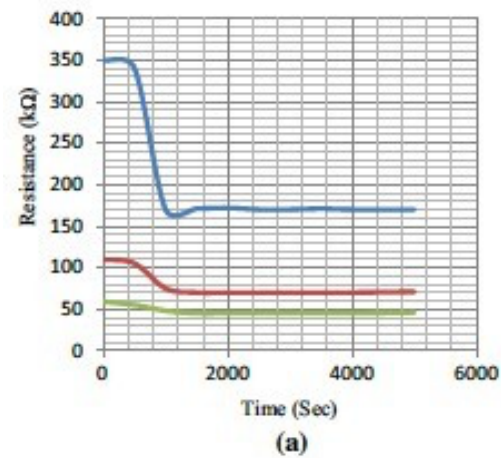
(k) Alexandre et al. (2015)



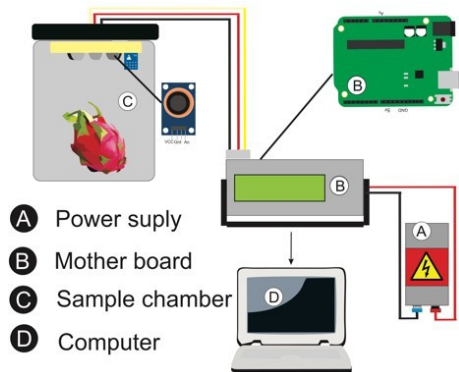
(l)



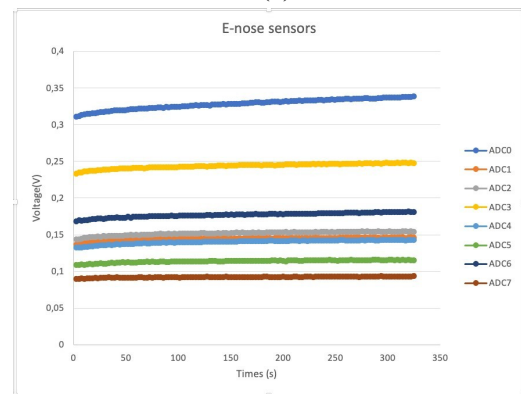
(m) Srivastava e Sadiatp (2016)



(n)



(o) Silva Ferreira et al. (2023)



(p)

Figure 1.3: Most common e-nose design for evaluation of fruits (a)-(p).

* In alphabetical order, each letter represents a part of the equipment immediately followed by each signal acquisition / data treatment. NA* indicates the signal was not provided by the Author. All set up were redesigned following the same principle as the original.

Oranges were also classified R2 of 94 ± 0.5 when comparing this two equipment for harvesting dates. The set-up is composed of Figure 1.3m computer (A), a processing unit, to connect sensors followed by the data processing unit, to process the input data (C), a sensing chamber (D), and a headspace module €. The headspace chamber was a crucial part where the authors selectively tested some TGS-xx series to be used in the equipment to develop models for humidity and temperature correction to finally propose the 4 sensors that were used to sort

their samples. Their response graph in kilohm ($K\Omega$) is shown in Figure 1.3n. The authors claim that their system is easily adjustable to other types of fruits, such as mango and grapes, with minor modifications, such as data training and temperature compensation, to accommodate new material (SRIVASTAVA; SADISATP, 2016).

A portable lab-made e-nose device, Figure 1.3o, was proposed to assess the maturity stages of pitaya (dragon fruit). The equipment was composed of a power supply (A), e-nose system (B), sample chamber (C), motherboard, and computer (D-E). Pitaya is rich in fiber and vitamins, and its quality is often related to attributes such as total soluble solids (TSS), moisture content, and titratable acidity (TA). Due to the lack of ethylene variation, the classification was proposed based on a shelf-life index (SLI), being the ratio between TSS and TA, which assigned fruits to 4 different stages, namely SLI30 (day 0), SLI 50 (day 7), SLI 80 (days 14 and 21) and SLI 100 (day 25) (SILVA FERREIRA et al., 2023).

Sample acquisition can be seen in Figure 1.3p, where the responses for each one of the 8 MOS sensors were plotted as voltage (V) versus time (s) and each digital data converter (ADC) (0-7) corresponds to MQ-2, MQ-3, MQ-4, MQ-6, MQ-8, MQ-9, MQ-135 and MQ-138.

From the data, all sensors responded to the VOCs released during sample measurement. The results reported accuracy over 95% for PLS-DA models that classified samples according to the SLI and could rightfully be used to distinguish between early storage days and late stages. Also, PLSR models achieved good prediction of the parameters: pH (root mean square error of prediction (RMSEP) = 0.22, R^2 = 0.86) and TA (RMSEP = 0.04, R^2 = 0.85). The cost of assembling the device was lower than USD 200.

1.5 Application of LC-e-nose to evaluate plantation crops

Plantation crops are valued commercial crops which play an important role in the agricultural economy and export trade of several developing and developed countries including China, India, Brazil, and the US. As the World Trade Organization (WTO) emphasizes agriculture more, the commercial aspects of cultivating and growing these crops gather remarkable economic significance. Some of the most important crops on a plantation scale include cardamom, cashew, cocoa, coconut, coffee, oil palm, rubber, and tea (CHOPRA; KRISHNAKUMAR; PE- TER, 2016; HUSEIN et al., 2022). This review will focus on the use of LC-e-noses on the three most relevant plantation crops accessed by e-noses: tea, coffee, and cocoa.

1.5.1 LC-e-nose applications for tea

In the final production of tea, six steps are considered such as harvesting, 1- withering, 2- leaf distortion/rolling, 3-fermentation, 4-firing, 5-grading, and lastly 6-sorting (TURGUT; KÜÇÜKÖNER; KARACABEY, 2021). Fermentation level is related to catechins oxidation (flavan-3-ols), as in black tea, for example, is labeled as oxidized or fully-fermented; oolong tea is semi or fully fermented as well as puerh (a variety of fermented tea traditionally produced in Yunnan Province). Bioactive compounds such as flavonoid glycosides are compounds of major importance in tea (HU et al., 2021). Tea also has four epimers that come from major catechins (around 80% in black tea) that include catechin (C), catechin gallate (CG), galliccatechin (GC), and galliccatechin gallate (GCG) being abundant in epicatechin (EC), epicatechin gallate (ECG), epigallocatechin (EGC), and epigallocatechin gallate (EGCG), that are greatly affected during tea fermentation (LIU et al., 2022).

Lab-made -noses have been used to detect several aspects of tea (Table 1.4), such as the aroma of locally flavored green tea (*Camellia sinensis*) (RALISNAWATI et al., 2018). The prototype e-nose used specific (G2 Delphi) software to control the inputs and other peripherals, as well as analog data from the sensor that will be converted to digital data using an ADC. The sensor response and the maximum value are represented in Figure 1.4. The sensors used were from TGS-26xx model. From the eight sensors used, TGS 826 and 2600 had a signal amplitude of over 350mV on ginger and lime leaves (427 and 392 mV), respectively. All sensors had a weak response to lemongrass (average 157 mV), which suggested that ginger-flavored tea samples had a stronger aroma when compared to other varieties of tea. Overall, ginger, lemongrass, and lime flavor can be detected by the device with a percentage of variation of 99.6, 99.3, and 99.4% respectively (RALISNAWATI et al., 2018). Other attempts to discriminate green tea against black tea using commercial systems had very similar outcomes, which suggest lab-made devices are reliable.

Table 1.3: Low-cost-e-noses used to evaluate tea.

Application	Data Treatment (*)	e-nose name / sensors	Reference
Tea - ginger Lemongrass flavor	PCA PLS-DA PLSR	Laboratory of Material Physics and Instrumentation Universitas Gadjah Mada/ MOS (TGS-xxxx)	Ralisnawati et al. (2018)
Black Tea (Singbulli) classification	Wavelet energy Feature Dunn Index KNN(1) PLS-DA	Self-developed – e-nose Set-up/ MOS (TGS-xxxx)	 Banerjee et al. (2019)
Black Tea Classification	PCA BP-MLP (3) RBF(4) PNN (5)	Customized e-nose for tea/ MOS Sensors (TGS-xxx)	Bhattacharyya et al. (2008)
Fermentation of Black Tea Green Tea	Reccurent Elman network	Customized e-nose for tea/ MOS Sensors (TGS-xxxx) Customized e-nose for tea/	Ghosh et al. (2019)
Quality level Oolong tea leaves Fermentation	RF(6) MLP(7) SVM LDA	MOS Sensors (TGS-xxxx, MQ-xxx) Gs-sensing system (Lab-made equipment) MOS (TGS-xxxx) Lu et al. (2019)	 Tseng et al. (2021)

* (1) K-nearest neighbors (KNN); (2) Support vector machine (SVM); (3) Black propagation-multilayer perception (BP-MLP); (4) Radial basis function (RBF); (5) Probabilistic neural network (PNN); (6) Random Forest (RF); (7) multi-Layer perception (MLP); metal oxide sensors (MOS).

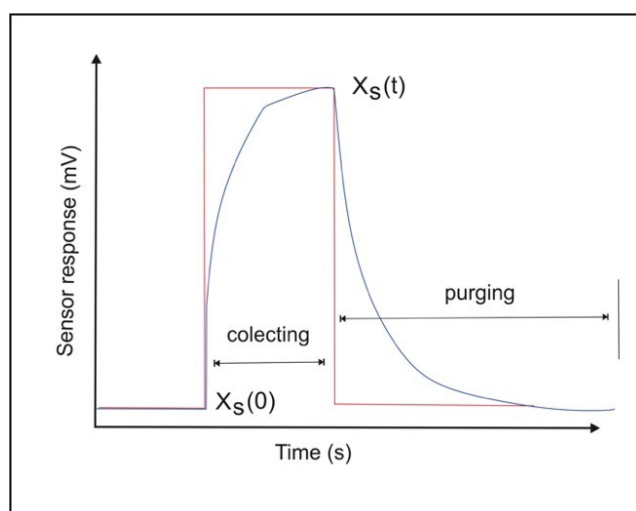


Figure 1.4: Sensors response for LC-e-nose sensors adapted from Ralisnawati et al. (2018).

Black tea from different origins and grades (Singbulli, MinFTGFOP, Sungama, and Chamong) have also been identified by e-nose devices. Four hundred samples were divided into each class and evaluated with five sensors TGS-26xx and 832, sensitive to some chemicals, such as Terpeniol, and Geraniol and other compounds (Table 5) that are present in tea, with sixty-six data points (acquired data) along time obtained by each sensor. A KNN classifier achieved an accuracy of 84.25%, which showed a good potential for grade classification power when compared to other traditional feature extraction methods (BANERJEE et al., 2019). Another customized LC-e-nose using MOS TGS-xx sensors was also used to detect volatiles in black tea during fermentation stages (GHOSH et al., 2019). The variation observed in the emanated volatile concentration was interpreted from the impedance of the semiconductor material (Figure 1.5a). It used heating from lamps driven by an air pump (A) to accelerate the release of the volatile compounds, and multiple valves (B) secured the air sent to the right compartment as well as the sensors chamber (D) by monitoring the variation in volatile concentration emitted from black tea samples. The voltage (V) was acquired along the Time (s) (Figure 1.5b).

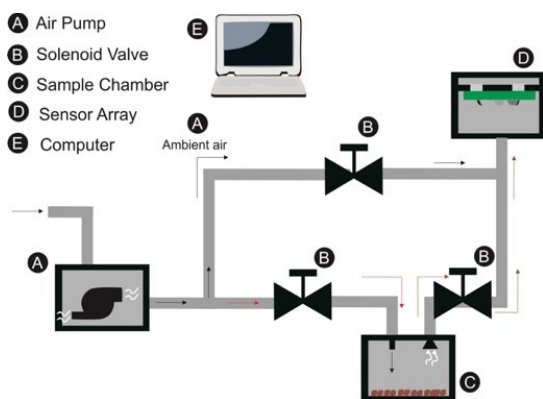
Another design (Figure 1.5c) was proposed using TGS26-xxxx and MQ-xxx sensor array to evaluate West Lake Longjing green tea (LU et al., 2019). The system was composed of the sample chamber (A), electromagnetic directional valve (B) used to switch the air channels (clean and sample) enhanced by air pumps (C), with data processing unit Arduino (D). Drying pipes were used, composed of the desiccant system connected to two air pumps where the moisture could be removed from the air guarantying humidity control. This feature makes the equipment looks bigger than it should, however, it is a well-designed device that was able to accurately spot different brands of green tea (> 95%), with application to the tea industry. The system's data interface (data acquisition graph) specific for tea is shown in Figure 1.5d.

Oolong tea fermentation was evaluated using another lab-made equipment mixing TGS-26xx sensors with SB-xx-xx (Japanese– 20 – 150 ppm DR, 5V) ones. It was developed a DAQ system mounted to an electric circuit that sends data to a computer so it can be seen the fermentation process (changes) that accounts for many transformations in tea composition and therefore altering the VOCs profile. Shaking rounds before firing (fixation) improves chemical

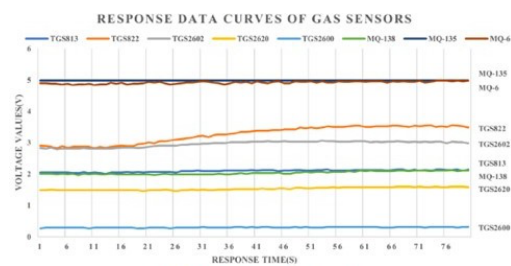
variation, which represents changes in volatile organic compounds (VOCs) for each shaking cycle. E-nose was then proposed for detecting grassy smell during each shaking step out of four cycles. Figure 1.5e shows the set-up where the tea samples would be fermented in a chamber (A) and directed by valves (B) and pumps (C) to the 14 sensors chamber (D), where adsorbent was used for cleaning purposes (E). Their signal is plotted in voltage (V) vs time (h) Figure 1.5f shows the drift in the shaking process for all sensors used, where each red arrow represents one of four shake processes. The results showed strong similarity with the response obtained by perception practitioners in the capability of sensing the grassy smell characteristic for this type of tea, as well as its feasibility of using a lab-made device in an online experiment to replace human sensory perception that has been currently used in the tea industry (TSENG et al., 2021).

1.5.2 LC-e-nose applied for coffee

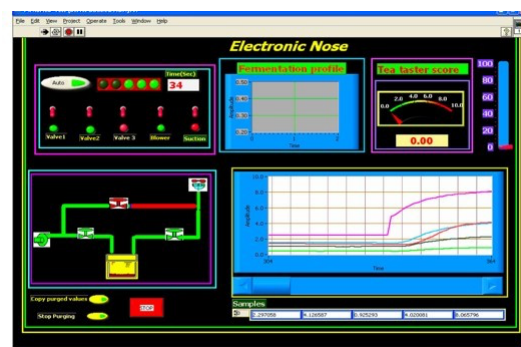
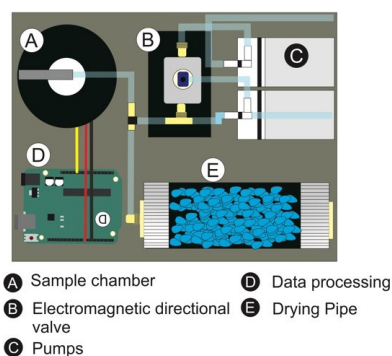
Coffee is made from ground-roasted beans, which grants a unique aroma and taste. These characteristics make it one of the most famous drinks in the world. Some studies have shown that coffee's volatile concentrations are very complex due to huge diverse sensory characteristics and one of the most important attributes for consumers' choice (SENINDE; CHAMBERS IV, 2020). E-nose has been used to evaluate coffee aroma in different applications, mostly to eliminate the need for empirical observation by well-trained operators. The vast use of brand-name equipment using embedded MOS sensors has been used to analyze the roasting process of coffee in automated systems to boost system performance for coffee bean quality characterization (ROMANI et al., 2012). Table 1.5 shows the LC-e-nose papers used to evaluate coffee during most common practices in the industry.



(a) Ghosh et al. (2019)



(b)



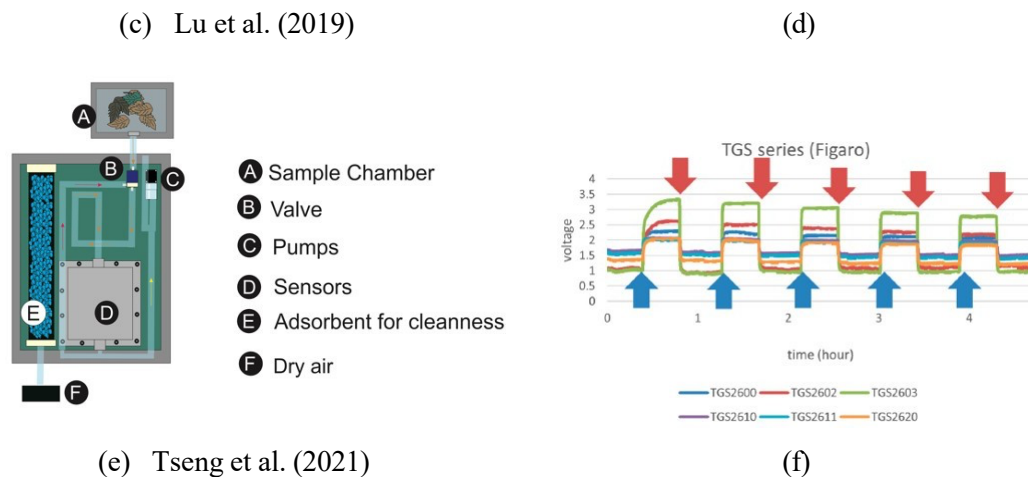


Figure 1.5: Most common LC-e-nose designs for the evaluation of tea (a)-(f).

* In alphabetical order, each subsequential letter represents the equipment immediately followed by each signal acquisition / data treatment. All the setup was redesigned following the same principle as the original ones.

Fermentation is a crucial step in the processing of coffee beans, and it can have a significant impact on the final quality of the coffee. During wet fermentation, the coffee cherries are soaked in water, and the fruit pulp surrounding the beans is broken down by natural microorganisms, such as bacteria and yeast, which can significantly influence the flavor and aroma of coffee. Wet fermentation can help to remove any undesirable flavors or odors from the coffee, while also enhancing the desirable ones, like bringing out fruity or floral notes in coffee (SEESAARD; WONGCHOOSUK, 2022) that come from coffee’s VOCs. This aspect was investigated using electronic noses for quality control of Colombian coffee (RODRÍGUEZ; DURÁN; REYES, 2010). It was developed a system of ST-xxxx and TGS-xxxx sensors (Fig. 5a and b), that included the e-nose (A), a concentration chamber (B) to collect and concentrate VOCs, and the computer (C). Results demonstrate that PCA and neural networks allowed the classification of the samples, separating defective coffee from regular ones.

Table 1.4: LC-e-noses used to evaluate coffee.

Application	Data Treatment (*)	e-nose name / sensors	Reference
Coffee aroma	ANN (1)	e-nose Food and Wine Group from The University of Melbourne (DAFW; UoM) / MOS (MQ-xxx)	Gonzalez Viejo, Tongson e Fuentes (2021)
Civet and Non-Civet Coffee	Logistic regression SVM (2) DTC (3) Naïve Bayes.	Self-developed / MOS (MQ-xxx)	Wakhid et al. (2020)
Recognition of Coffee Coffee	PCA SVM(2)	Lab-designed sensor array (TGS-xxxx) A-nose - Lab-designed	Brudzewski, Osowski e Dwulit (2012) Thepudom, Sricharoen-
classification	PCA	Enose System/ (TGS-xxx)	chai e Kerdcharoen (2013)

Coffee Quality control “cup test”	PCA MLP (4)	A-nose - Lab-designed e-nose / MOS (TGS-xxxx,SP-xx)	Rodríguez, Durán e Reyes (2010)
---	----------------	---	---------------------------------

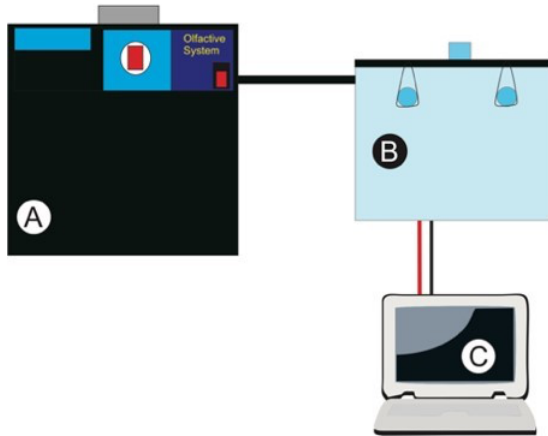
* (1) Artificial Neural Network (ANN); (2) Support vector machine (SVM); (3) Decision tree classifier (DTC); (4) multi-Layer perception (MLP); (5) kernel discrimination models (KDM); metal oxide sensors (MOS).

Results demonstrate that PCA and neural networks allowed the classification of the samples, separating defective coffee from regular ones. Regarding taste, Arabica beans have a more complex and nuanced flavor profile with notes of fruit, berries, and chocolate. Robusta beans have a stronger, more bitter taste with notes of earthy and woody flavors. As per price, Arabica beans are generally more expensive than Robusta beans due to their higher quality, more complex flavor, and the fact that they are difficult to grow. However, there is a market for both types of beans depending on the intended use and desired taste.

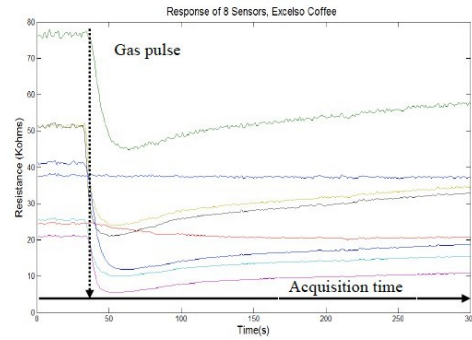
A differential e-nose based on MOS sensors (6c) was used to recognize two types of coffee (Arabica and Robusta) by using a special procedure for their signal acquisition (BRUDZEWSKI; OSOWSKI; DWULIT, 2012). After ambient air (A) is pumped into the chamber (B), they used the differential signals of all pairs of sensors (C) as a function of time. The work included a mixture of varieties Arabica and Robusta from 10 - 90%. Two sensors array were used for data acquisition so that the differential nose system could account for interferents in the environment during data analysis (6d). PCA was used to explore data and signal pre-treatment (e.g., the ratio of signal and air) removed the baseline calibration, which is a common practice in e-nose devices (MAREK et al., 2020).

Similar equipment using TGS-xxx sensors was applied to identify variations in bran brewing temperatures and concentration (THEPUDOM; SRICHAROENCHAI; KERDCHAROEN, 2013). To promote a more homogenized flow direction of gas (A) in the way the gas was injected (B), a centrifuge was designed so that the gas would go straight to the sensors (C) in a cylindric chamber (D), then to the data analog (D) (6e). PCA provided five clusters from five different brands and their results also showed that concentration and temperatures may affect coffee bean quality. The signals for each of the 6 sensors are presented in 6f.

- (A) A - nose
- (B) Concentration chamber
- (C) Computer

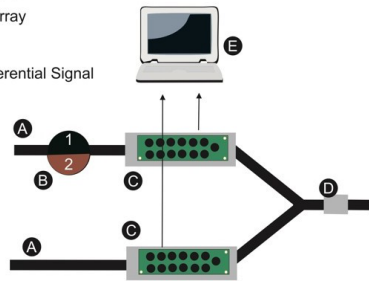


(a) Rodríguez, Durán e Reyes (2010)

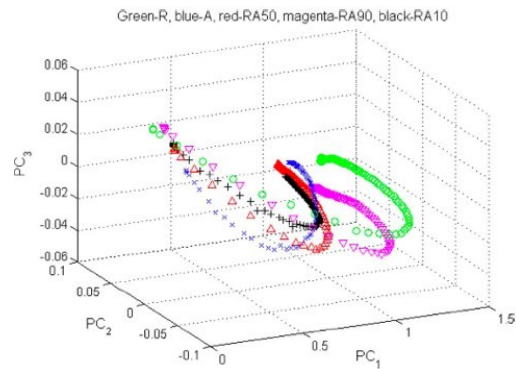


(b)

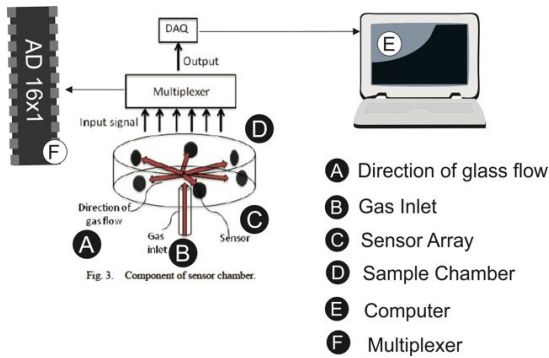
- (A) Ambient air
- (B) Sample Chamber
- (C) Dual Sensor Array
- (D) Outlet
- (E) Computer Differential Signal



(c) Brudzewski, Osowski e Dwulit (2012)



(d)



(e) Thepudom (2013)

(f)

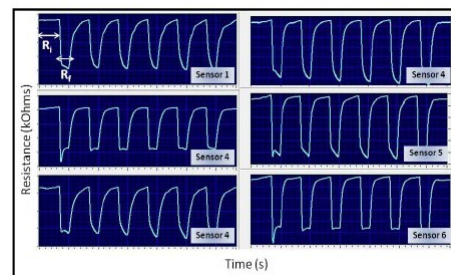
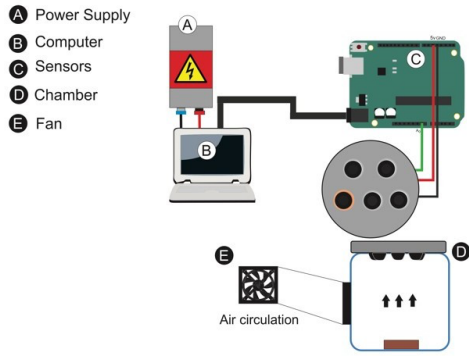


Figure 1.6: Most common LC-e-nose designs for the evaluation of coffee (a)-(j).

* In alphabetical order, each letter represents the equipment immediately followed by each signal acquisition / data treatment. All the setup was redesigned following the same principle as the original ones.



(g) Wakhid et al. (2020)

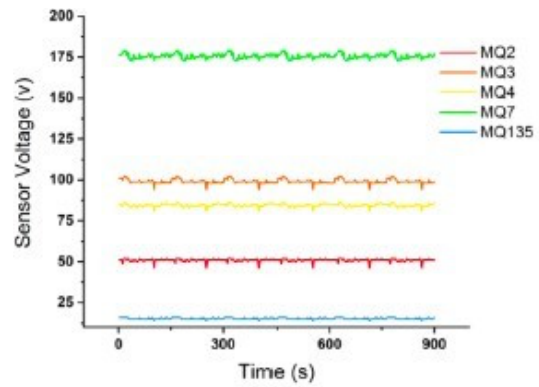
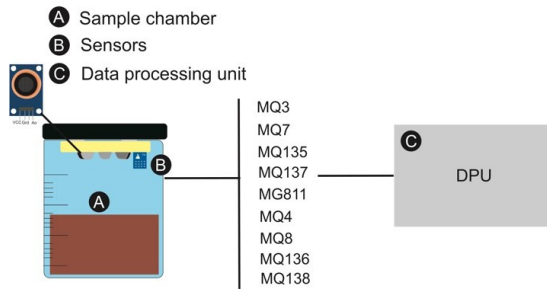
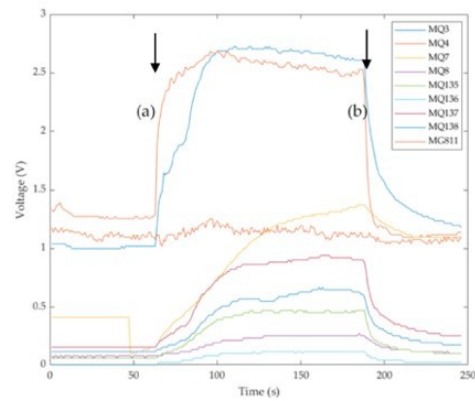


Figure. 6 Result of raw signal LA

(h)



(i) Gonzalez Viejo, Tongson e Fuentes (2021)



(j)

Figure 1.6: Most common LC-e-nose designs for the evaluation of coffee (a)-(j).

* In alphabetical order, each letter represents the equipment immediately followed by each signal acquisition / data treatment. All the setup was redesigned following the same principle as the original ones.

An experiment was carried out for each batch of from different countries (Costa Rica, Ethiopia, Brazil, Peru, and Guatemala). The results demonstrated that the degree of roasting used did not change every single aromatic property of the tested coffees, concluding that VOCs were specific to each coffee, related to growth, harvesting, and storage.

A simple LC-e-nose using reusable food glass as a chamber was used to identify coffee with civet and non-civet aromas. These two classes of coffee have different authentic scents and are the beans separated manually by trained people. The equipment used is a practical setup (Figure 1.6g), with a power supply (A) and computer (B) connected to the mounted five sensors (C) to measure the targeted volatiles. The cheap recycled glass-made setup and chamber (D) proposed by this group were ready for sensors for carbon dioxide, methane, propane, LPG, I-butane, alcohol, H₂, smoke CO, benzene, hexane, and natural gas with airflow controlled by a fan on the bottle (E), the VOCs used were typical gases targets found in MQ-xxx sensors in the market. The results Data were collected 50 times for each type of coffee and temperature data collection was carried out at room temperature (between 20 °C and 25 °C). Each measurement was carried out for 15 minutes and 15 grams of coffee, and the model achieved an accuracy of 96% for six classes or 100% when having two classes only for civet and non-civet coffee. It was observed a variation in the baseline for voltages for each sensor (6h), which suggests further investigation would be necessary to check if the increment of coffee from two types from different regions would have an impact on the models' response (WAKHID et al., 2020)

Coffee intensity and aroma using a wireless LC-e-nose (Figure .6i) and machine learning. The design is very simple and mainly comprises three compartments: (A) sample chamber (B) sensors, and (C) data processing unit. The results were compared with GC/MS output that was used as a reference. The data extraction from the e-nose can be seen in 6j where the initial and final signals were automatically divided into 10 signal intervals so that 10 averages could be obtained. This approach reduces noise and increases the input number for machine learning models. The correlations indicated that the phenols, aldehydes, furans, and pyrroles (Table 5) were identified by MQ-3, MQ-135, 136, 137, and 138 sensors. Adding this device to coffee machines during the brewing process would allow coffee producers to diminish problems with unwanted variables such as temperature, water quality, and other problems during the brewing process (GONZALEZ VIEJO; TONGSON; FUENTES, 2021).

1.5.3 LC-e-nose applied for cocoa

Cocoa is a commonly used ingredient in the food industry, and, similar to coffee, has a complex aroma profile that can be challenging to determine using traditional tools and sensory methods. E-nose emerges as a powerful solution in this scenario (GIACOMETTI; JOLIĆ; JOSIĆ, 2015). Several studies have explored the use of low-cost electronic noses for cocoa aroma analysis (OLUNLOYO; IBIDAPO; DINRIFO, 2011; TAN et al., 2019; TAN; KERR, 2019) (Table 5). A multi-chamber piece of equipment based on a TGS 26XX metal oxide sensor array, with an artificial neural network (ANN) to assess data obtained by the electronic nose to assess the aroma of cocoa beans (OLUNLOYO; IBIDAPO; DINRIFO, 2011). The equipment set-up (Figure 1.7a) presented multiple compartments to refine and quantitatively inject the sample gases to be measured by sensors. Their system contains a computer (A), a data logger (B), and a vacuum pump (C) connected by solenoid valves (D and F) and finally, the sensors array (E) that is then connected to the sample chamber (G) that has a heater (H) on its base to serve the purpose of the work of heating the beans. They found that the electronic nose was able to

distinguish between two classes unacceptable (moldy or showing insect infestation) or acceptable (well fermented, good chocolate flavor), based on their aroma profiles, and the results showed 95% of the classification score when choosing between these two classes.

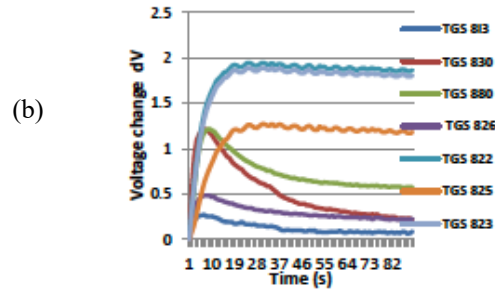
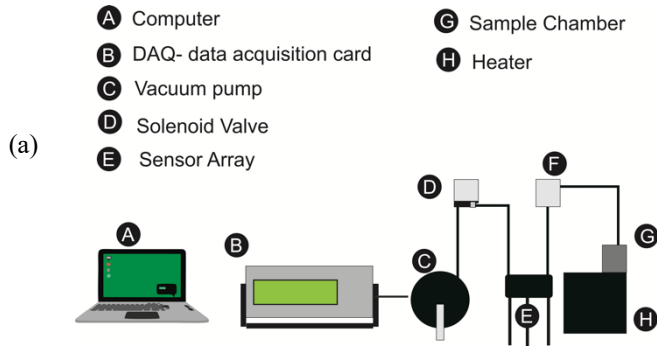
Table 1.5: Commonly compounds (VOCs) in coffee detected by LC-e-noses.

Application	Class	Compound	Reference
Coffee aroma	Furans	3 – Methylruran	Gonzalez Viejo, Tongson e Fuentes (2021)
		2,5 - Dimethylfuran	
		2- Vinylfuran	
		2-Butylfuran	
		2-Propanoyl furan	
	Pyrazines	2-Acetyl-5-methylfuran	
		Linalool oxide	
		2- methylpyrazine	
	Aldehydes	2-Ethylpyrazine	
		Nutty pyrazine	
Pyrazine, 2,3-diethyl-5-methyl- Pyrazine, 2-ethyl-6-methyl- 3-Aldehydes			
		Benzaldehyde	
		Benzeneacetaldehyde	
	1- Furfuryl pyrrole		
	Terpenes / Alcohol	1-Methyl-2-pyrrole carboxaldehyde	
	Others	Furfuryl acetate Methyl salicylate	

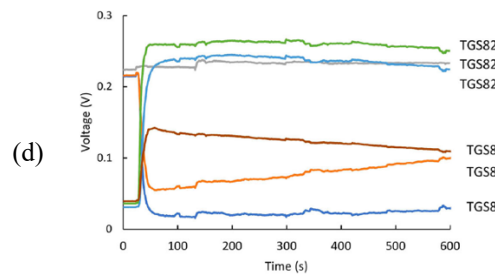
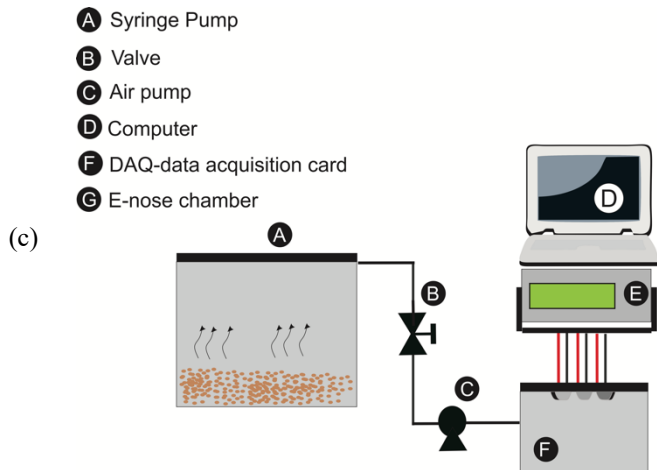
* All compounds are based most common volatiles present in coffee.

Table 1.6: LC-e-noses used to evaluate cocoa.

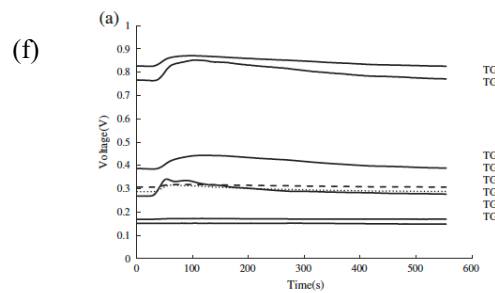
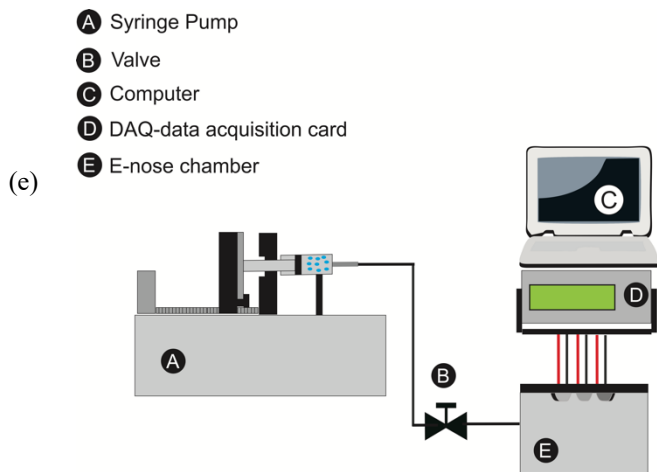
Cocoa beans	PCA ANN (1)	Lab-made e-nose / MOS(TGS-xxxx)	Olunloyo, Ibadapo e Dinrifo (2011)
Cocoa beans		Lab-made e-nose	
fermentation and roasting	ANN	Software / MOS(TGS-xxxx)	Tan e Kerr (2019)
Cocoa refining	KDM (5)	Lab-made e-nose / MOS(TGS-xxxx)	Tan et al. (2019)
Cocoa beans roasting	ANN (1)	Lab-made e-nose Software / MOS(TGS-xxxx)	Tan e Kerr (2018)



Olunloyo
, Ibidapo,
and
Dinrifo
(2011)



Tan et al.
(2019)



Tan and
Kerr
(2018)

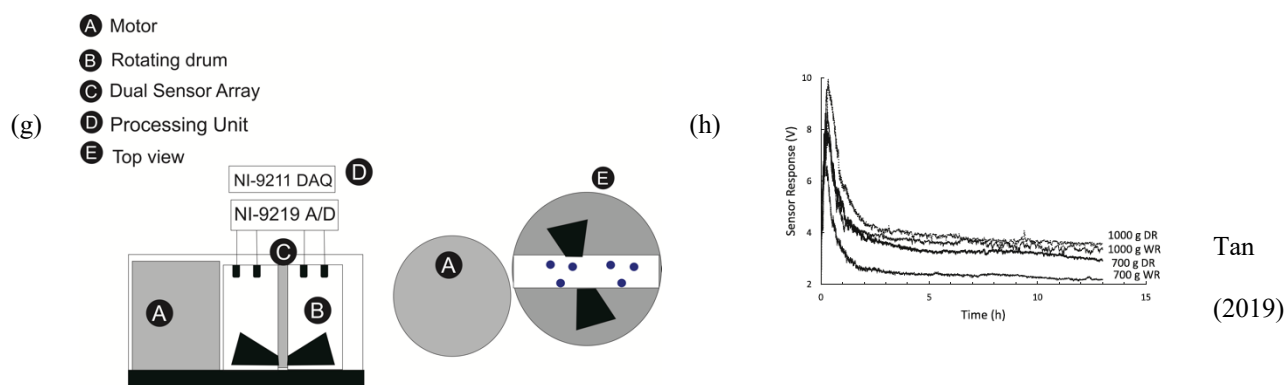


Figure 1.7: Most common LC-e-nose designs for the evaluation of cocoa (a)-(h).

In alphabetical order, each subsequential letter represents the equipment immediately followed by each signal acquisition / data treatment. All the setup was redesigned following the same principle as the original ones.

Another study investigated the use of a low-cost electronic nose to assess the VOCs fingerprint of cocoa bean shells (CBS) (BARBOSA-PEREIRA et al., 2019). Cocoa shells from two different continents (America and Africa) and 18 Countries (Brazil, Cameroon, Colombia, Congo, Dominican Republic, Ecuador, Ghana, Ivory Coast, Jamaica, Madagascar, Mexico, Peru, São Tomé, Togo, Uganda, Venezuela) were analyzed. To test their hypothesis of being able to determine the fingerprint in CBS, they used solid-phase microextraction coupled with gas chromatography-mass spectrometry (HS-SPME/GC-MS) methodology analysis and chemometrics to data treatment PCA and Pairwise Sperman's non-parametric-correlation that was used to explain the relationship between variables (sensors responses) and their acquisition (VOCs concentration). The authors established for the first-time strong evidence for the fingerprint in CBS and were even able to spot aroma markers such as 2-methyl propanal, 3-methyl butanal, phenylacetaldehyde, dimethyl trisulfide, 2-phenyl ethyl acetate, 2,3,5-trimethylpyrazine, 2-ethyl-3,5-dimethyl pyrazine, 2-heptanol, 2-phenyl ethanol, 2-methyl propanoic acid, and 3-methyl butanoic acid changes within CBS.

Fermentation is the process where cocoa beans are transformed by the action of microorganisms and some metabolites are due to chemical changes in the bean (GIA-COMETTI; JOLIĆ; JOSIĆ, 2015), thus monitoring this process may help achieve high-quality beans. A new way of sensing the degree of fermentation of cocoa (*Theobroma cacao* L) using an LC-e-nose (Figure 1.7c) was used to compared six different machine learning models for sample classification: bootstrap forest, boosted tree, decision tree, artificial neural network (ANN), Naïve Bayes and K-nearest neighbors (KNN). An interesting part of the device is a chamber (A) to accommodate the cocoa beans for controlled fermentation. The sensors used were from TGS26xx and TG8xx series, and others for most common VOCs, such as hydrogen, ammonia, ethanol, propane, and organic solvents, followed by a valve (B) to direct the flow of volatile compounds, an air pump (C), a computer (D), and data acquisition card (DAQ) to the sensor array (E). Sensors that presented the highest sensitivity were TG822, 23, 26, and TG2610 and 20 for the first 4 days of fermentation. One drawback of the experiment is that the temperature varied between 28 and 50 °C during this long period; therefore, air pumped to the sensor chamber should be controlled. Although it is mentioned some factors that might have influenced results

including environmental temperature fluctuation, the machine learning models granted good results where only 9.4% of misclassification was observed by the bootstrap model. The results demonstrated that the e-nose device rightfully classified cocoa beans based on the roasting stage, being competitive when compared to GC-MS for identification of the sample's VOCs (TAN et al., 2019).

The fermentation process is followed by drying and roasting, which grants cocoa its final aroma for chocolate production. In this process, the beans are heated from 250 °F (120 °C) to 300 °F (150 °C), approximately, to eliminate the undesirable odor and taste. The volatile acids present in the beans promote the final product's bitterness and total acidity (TAN; KERR, 2018). E-noses can then be easily applicable to this type of process at an industry level.

A lab-made equipment (Figure 1.7e) was used to adapt an injection system that used a syringe pump since it needed to identify a refined aroma profile characterized by the roasting step. It used 600 seconds of e-nose evaluation Figure 1.7f, and the sensors that most responded were TGS26xx and TGS8xx, which account for organic volatiles (e.g., alcohol, methane, and propane) (TAN et al., 2019), which are presented in Table 5.

Refining is also an important step in chocolate production. It involves grinding the roasted cocoa nibs (i.e., the inner part of the cocoa bean) into chocolate liquor. The refining process helps to break down the cocoa solids into tiny particles, which makes the chocolate smoother, in addition to removing any residual compounds from the chocolate (TAN;KERR, 2019).

Table 1.7: Commonly compounds (VOCs) in cocoa detected by LC-e-noses.

Application	Class	Compound	Reference
Fruits	Aldehydes	Hexanal Benzaldehyde (E)-2-Hexenal	Voss, Ayub, and Stevan (2020)
		Alcohols	
	Esters		
	Ketones	Acetoin	
	Terpenoids	α -terpinene γ -terpinene	
	Lactones	γ -lactone derived compounds δ -lactone derived compounds	
	Hydroxyl acid	Malic Acid Other organic compounds	Da Silva Ferreira et al. (2023)
Application	Class	Compound *	Reference
	Furans	3 – Methylruran 2,5 - Dimethylfuran 2- Vinylfuran 3-Furanmethanol 2-Butylfuran 2-Propanoyl furan 2-Acetyl-5- methylfuran	
	Pyrazines	2- methylpyrazine 2-Ethylpyrazine Nutty pyrazine Pyrazine, 2,3-diethyl- 5-methyl-	

Plantation Crops (Cocoa and Coffee)	Pyrazine, 2-ethyl-6-methyl-	Viejo et al (2021); Tan and Kerr (2018)
Aldehydes	3-Aldehydes Benzaldehyde Benzeneacetaldehyde	
Pyrroles	1-Methyl-2-pyrrole carboxaldehyde 1-Furfuryl pyrrole	
Organic Acids	Acetic acid Octanoic acid	
Others	Furfuryl acetate Methyl salicylate	

* All compounds are based most common volatiles present in fruits and plantation crops (coffee and cocoa).

In a follow-up from previous research, Tan e Kerr (2019) adapted a melanger (Figure 1.7g), which is a grinder used to grind cocoa bean nibs into chocolate liquor, that mounted with an e-nose to characterize the cocoa refining process. Since the process takes a very long time, data acquisition was performed for 15 hours (Figure 1.7h). The research concluded that their low-cost device would be able to continuously monitor VOCs emanating from cocoa powder and liquor during the refining step.

Conching is a process that follows refining and involves mixing and kneading the chocolate liquor with other ingredients (e.g., sugar, milk powder, and cocoa butter), which may involve several hours. This process accounts for chocolate flavor and aroma and improves its texture and mouthfeel, reducing bitterness or astringency by breaking down tannins in cocoa solids (GIACOMETTI; JOLIĆ; JOSIĆ, 2015).

1.6 Common data treatment methods used with LC-e-nose systems in plantation and fruits crops

E-nose response data is complex, involving many variables that carry some chemical information. Hence, choosing the best methods to work with this specific data is challenging, and either chemometrics or machine learning (ML) can be extremely helpful when dealing with e-nose datasets. Chemometrics is useful when dealing with complex chemical data sets that have a large number of variables, while machine learning, on the other hand, is applied especially when the relationship within a variable is non-linear. A combination of both techniques has also been investigated (NICOLAS; ROMAIN; MATERNOVA, 2001).

1.6.1 Data treatment used for LC-e-nose based on chemometrics

The most common methods in plantation and fruit crops include principal component analysis (PCA), linear discriminant analysis (LDA), and partial least square discriminant analysis (PLS-DA). From the chemometrics perspective, PCA is explored useful tool to explore the information of samples contained in the e-nose data as a first screening performance (QIAO et al., 2022; TSENG et al., 2021). Further analysis using supervised classification LDA, has been used for fruits (QIAO et al., 2022) and plantation crops (TSENG et al., 2021), achieving reasonable results. However, many studies propose regression models using PLSR models, which are useful for e-nose applications, measuring the relationship between the sensor readings (predictor variables) and the concentration of the gas being detected (response variable). PLSR is particularly well-suited for e-nose data analysis since it can handle the high-dimensional data generated by these devices and can identify the most important features (i.e., sensors) that contribute to odor or gas detection (RALISNAWATI et al., 2018; SILVA FERREIRA et al., 2023). Despite chemometrics being suitable for most LC-e-nose purposes, many authors take advantage of ML due to its ability to handle non-linear relationships. ML algorithms can capture non-linear relationships between variables and can be then used when traditional chemometric techniques do not achieve satisfactory results.

1.6.2 Data treatment used for LC-e-nose based on machine learning

Support vector machines (SVM), and artificial neural networks (ANN) are the most common methods employed for e-nose systems. SVM is a supervised method that finds the best boundary to separate two or more classes, and it can also be used for regression. It has been used in several LC-e-nose studies (GONZALEZ VIEJO; TONGSON; FUENTES, 2021; HEN-DRICK et al., 2022; TYAGI et al., 2023).

SVM has been used for sensing the aroma of Longgjing green tea. Results reported nearly 95% accuracy and can be used to standardize Longgjing tea in the market (LU et al., 2019).

A probabilistic neural network (PNN) is a group of artificial neural networks that includes probabilistic concepts and techniques for modeling uncertainty and producing predictions that have been applied for classification and pattern recognition applications (MOHEBALI et al., 2020). PNN model was applied for black tea classification (BHATTACHARYYA et al., 2008), achieving 90% accuracy. PNN performance sometimes stands out, since it uses probability, and any unsigned data is evaluated based on previous data, this approach reduces variation when having reduced data set. This feature grants the model a better performance over others, such as backpropagation multilayered perception (BP-MLP).

Reinforcement learning systems can now be fueled by BP-powered neural networks that effectively compute the gradients of the weights and biases concerning the loss function. The backpropagation method employs many computational iterations by taking the gradient of weight. MLP continuously learns to produce increasingly accurate predictions by repeatedly modifying the weights depending on the computed gradients (KUBO; CHALMERS; LUCZAK, 2022). BP-MLP has also achieved 81% accuracy for their prediction model for four tasters' parameters (leaf quality, infusion, liquor, and aroma) used for their black tea samples to correlate with sensory analysis responses, which was lower than the 90% obtained with PNN (BHATTACHARYYA et al., 2008). According to the authors, greater PNN values might be linked to their dataset size and also the idea that PNN is derived from a probability base that uses a previous sample to move forward the model output, which depending on the variations in your sample

size favors more accurate values.

ANN is based on a neural network that mimics the human brain and therefore is used for more complex models (i.e., data) (GONZALEZ VIEJO; TONGSON; FUENTES, 2021; GURESEN; KAYAKUTLU, 2011; TAN; KERR, 2018; TYAGI et al., 2023).

Another study (GONZALEZ VIEJO; TONGSON; FUENTES, 2021) used ANN to assess coffee aroma profile and obtained 100 and 94% accuracy for training and testing models, respectively, from e-nose data. Also used ANN to train the model using a back-propagation algorithm and was able to spot differences in fruit and nonfruit odors with 100% accuracy. Similarly, it was possible to differentiate overripe fruits from other ripeness stages with slightly lower accuracy (> 90%).

Alternatively, other methods have been used such as extreme learning machine (ELM), which is an ML algorithm method derived from neural networks. The primary principle underlying ELM is to assign weights across the input and hidden layers randomly and then solve the output weights in a single step. ELM has several advantages over traditional neural networks, including fast training times, good generalization ability, and the potential to handle large datasets. ELM was used by Voss, Ayub e Stevan (2020) to monitor the maturation of peaches in their natural habitat, their pre-processing stages accounted for the application of the average filter, compensation gas sensor, data normalization and feature selection finalizing in the dimensionality reduction. Results obtained for the ELM model reached 88.90% ($R^2 = 0.852$) and 90.38% ($R^2 = 0.872$) accuracy for their validation models.

Another neural network approach used with LC-e-nose while using recurrent Elman network (REN) for the tea fermentation process, which is a type of artificial neural network for prediction. The network's architecture is straightforward, with an input layer, a hidden layer, and an output layer. The hidden layer has a feedback connection to itself in an Elman network; thus, the prior state of the hidden layer is fed back into the network as an additional input for the current time step. This feedback connection enables the network to retain previous time step information and use it to anticipate the current one. The Authors applied REN to their fermentation time models and were able to predict the oxidation process using their electronic nose to record variations in VOCs. The novelty of their work came from this used model and its identification of a suitable method for treating data from the tea fermentation process (GHOSH et al., 2019).

1.7 Conclusion and future trends

LC-e-nose systems are reliable equipment that can be employed for multiple agricultural products, including the assessment of the quality and freshness of products in plantation crops such as tea, coffee, and fruits. Each work reported in this review was meticulously designed for a specific purpose. Therefore, all physical parameters, such as headspace, chamber size, shape, temperature, and humidity involving thermodynamics and fluid mechanics when transporting gases as well as chemistry in all the chemicals have peculiar attention for each food group. Additionally, the chemical characteristic of each sample within those groups are vital variables that must be included in an e-nose project.

Data acquisition and treatment, as well as the design, are essential to a successful project; many aspects have to be carefully analyzed for retrieving data from e-nose devices from a sensor perspective, such as acquisition time, signal type, from a computer interface (i.e., code and data logger). The noise generated in these steps can be a pitfall and, therefore, must be considered

when building this type of device, where integrated systems and the right motherboard, PCB, and other microcontrollers play an important role. Data treatment approach must be included in the project when thinking about LC-e- board PCBs have evolved and helps many users at a lower price, still choosing the correct data treatment method will save time and money. Overall, fruits, tea, and coffee have been extensively covered, and most aspects of their equipment (i.e., pros and cons) were exposed. LC-e-noses offer many advantages over other devices. Future trends in this field include miniaturization, with equipment evolving from lab-scale to portable and practical gear, allowing manufacturers to take it to the field, as seen in many evaluated systems. Along with customization, the use of specific sensors will enable the equipment to be accurate while being affordable.

Internet of Things, which is the connectivity of the Internet of PCs in every piece of equipment leading to automation, is also a future development to be studied. Low-cost, portable, wi-fi integrated solutions were mentioned (LEE et al., 2023). Agroindustry has been employing integrated odor sensors to identify fluctuations in volatiles before harvest, as well as provide strong insights into the resources that they have used, such as water and fertilizer. So far, e-nose sensors were reported for monitoring the quality of fruits and plantation crops (i.e., freshness), allowing growers to determine their pricing and profitability, and further applications in this area are in the near future. Low-cost devices may be used as useful and accessible quality control tools for small producers and food processors.

1.8 Author Contributions

The authors confirm contribution to the paper as follows: study conception and design: Marcus Vinicius da Silva Ferreira; for writing the original draft and and Jose Lucena Barbosa Jr Mohammed Kamruzzamanb and Douglas Fernandes Barbin for writing-review and editing. All authors reviewed the and approved final version of the manuscript.

1.9 Conflicts of interest

“There are no conflicts to declare”.

1.10 Acknowledgments

This Research was financed partially by the Coordenação de Aperfeiçoamento de Pessoal de Nível Superior - Brasil (CAPES) - Finance Code 001 and São Paulo Research Foundation (FAPESP) (project number 2015/24351-2). Marcus V S Ferreira and Prof. Douglas Fernandes Barbin, CNPq research fellow project (308260/2021-0).

1.11 References

- ALEIXANDRE, M. et al. A wireless and portable electronic nose to differentiate musts of different ripeness degree and grape varieties. **Sensors**, MDPI, v. 15, n. 4, p. 8429–8443, 2015.
- ALI, M. M. et al. Principles and recent advances in electronic nose for quality inspection of agricultural and food products. **Trends in Food Science & Technology**, Elsevier, v. 99, p. 1–10, 2020.
- ANTICUANDO, M. K. D.; DIRECTO, C. K. R.; PADILLA, D. A. Electronic Nose and Deep Learning Approach in Identifying Ripe *Lycopersicon esculentum* L. TomatoFruit. In: IEEE.

2022 13th International Conference on Computing Communication and Networking Technologies (ICCCNT). [S.l.: s.n.], 2022. p. 1–6

BANERJEE, M. B. et al. Black tea classification employing feature fusion of E-Nose and E-Tongue responses. **Journal of Food Engineering**, Elsevier, v. 244, p. 55–63, 2019.

BARBOSA-PEREIRA, L. et al. Assessment of volatile fingerprint by HS-SPME/GC-qMS and E-nose for the classification of cocoa bean shells using chemometrics. **Food Research International**, Elsevier, v. 123, p. 684–696, 2019.

BERNAL, L. J.; MELO, L. A.; DÍAZ MORENO, C. Evaluation of the antioxidant properties and aromatic profile during maturation of the blackberry (*Rubus glaucus* Benth) and the bilberry (*Vaccinium meridionale* Swartz). **Revista Facultad Nacional de Agronomía Medellín**, Facultad de Ciencias Agrarias - Universidad Nacional de Colombia, v. 67, n. 1, p. 7209–7218, 2014.

FAN, D. et al. Do Non-climacteric Fruits Share a Common Ripening Mechanism of Hormonal Regulation? **Frontiers in Plant Science**, Frontiers, v. 13, p. 923484, 2022.

FANG, Y.; ZHANG, B.; WEI, Y. Effects of the specific mechanical energy on the physicochemical properties of texturized soy protein during high-moisture extrusion cooking. **Journal of Food Engineering**, Elsevier, v. 121, p. 32–38, 2014.

FLEMING-JONES, M. E.; SMITH, R. E. Volatile organic compounds in foods: a five year study. **Journal of Agricultural and Food Chemistry**, ACS Publications, v. 51, n. 27, p. 8120–8127, 2003.

FONOLLOSA, J. et al. Calibration transfer and drift counteraction in chemical sensor arrays using Direct Standardization. **Sensors and Actuators B: Chemical**, Elsevier, v. 236, p. 1044–1053, 2016.

GHOSH, S. et al. A recurrent Elman network in conjunction with an electronic nose for fast prediction of optimum fermentation time of black tea. **Neural Computing and Applications**, Springer, v. 31, p. 1165–1171, 2019.

GIACOMETTI, J.; JOLIĆ, S. M.; JOSIĆ, D. Cocoa processing and impact on composition. In: **PROCESSING and impact on active components in food**. [S.l.]: Elsevier, 2015. p. 605–612.

GOBBI, E. et al. Rapid diagnosis of *Enterobacteriaceae* in vegetable soups by a metal oxide sensor based electronic nose. **Sensors and Actuators B: Chemical**, Elsevier, v. 207, p. 1104–1113, 2015.

GOLDY, R. **All fruit and vegetables are not created equal when it comes to proper storage conditions**. Michigan: Michigan State University Extension – Food Preservation, 2019. Disponível em: <<<https://www.canr.msu.edu/news/all-fruit-and-vegetables-are-not-created-equal-when-it-comes-to-proper-storage-conditions>>>. Acesso em: 2 mai. 2023.

GONZALEZ VIEJO, C.; FUENTES, S. Low-cost methods to assess beer quality using artificial intelligence involving robotics, an electronic nose, and machine learning. **Fermentation**, MDPI, v. 6, n. 4, p. 104, 2020.

GONZALEZ VIEJO, C.; TONGSON, E.; FUENTES, S. Integrating a low-cost electronic nose and machine learning modelling to assess coffee aroma profile and intensity. **Sensors**, MDPI, v. 21, n. 6, p. 2016, 2021.

GONZALEZ VIEJO, C. et al. Development of a low-cost e-nose to assess aroma profiles: An

- artificial intelligence application to assess beer quality. **Sensors and Actuators B: Chemical**, Elsevier, v. 308, p. 127688, 2020.
- GURESEN, E.; KAYAKUTLU, G. Definition of artificial neural networks with comparison to other networks. **Procedia Computer Science**, Elsevier, v. 3, p. 426–433, 2011.
- HARUN, F. K. C.; COVINGTON, J. A.; GARDNER, J. W. Portable e-Mucosa System: Mimicking the biological olfactory. **Procedia Chemistry**, Elsevier, v. 1, n. 1, p. 991–994, 2009.
- HENDRICK et al. E-Nose Application for Detecting Banana Fruit Ripe Levels Using Artificial Neural Network Backpropagation Method. **International Journal of Data Science**, v. 3, n. 1, p. 11–18, 2022.
- HERRERO, J. L. et al. On-line classification of pollutants in water using wireless portable electronic noses. **Chemosphere**, Elsevier, v. 152, p. 107–116, 2016.
- U, S. et al. Changes of fungal community and non-volatile metabolites during pile-fermentation of dark green tea. **Food Research International**, Elsevier, v. 147, p. 110472, 2021.
- HUSEIN, I. R. et al. Wavelength Dependence of Optical Electronic Nose for Ripeness Detection of Oil Palm Fresh Fruits. **Science, Technology and Communication Journal**, v. 2, n. 3, p. 73–80, 2022.
- JASINSKI, G.; STRZELCZYK, A.; KOSCINSKI, P. Low cost electrochemical sensor module for measurement of gas concentration. In: IOP PUBLISHING, 1. IOP Conference Series: Materials Science and Engineering. [S.l.: s.n.], 2016. v. 104, p. 012034.
- JIA, W. et al. Advances in electronic nose development for application to agricultural products. **Food Analytical Methods**, Springer, v. 12, p. 2226–2240, 2019.
- JIANG, X. et al. A novel electronic nose learning technique based on active learning: EQBC-RBFNN. **Sensors and Actuators B: Chemical**, Elsevier, v. 249, p. 533–541, 2017.
- JING, Y.-Q. et al. A bioinspired neural network for data processing in an electronic nose. **IEEE Transactions on Instrumentation and Measurement**, IEEE, v. 65, n. 10, p. 2369–2380, 2016.
- KIANI, S.; MINAEI, S.; GHASEMI-VARNAMKHASTI, M. Application of electronic nose systems for assessing quality of medicinal and aromatic plant products: A review. **Journal of Applied Research on Medicinal and Aromatic Plants**, Elsevier, v. 3, n. 1, p. 1–9, 2016.
- KIM, C. et al. A phage- and colorimetric sensor-based artificial nose model for banana ripening analysis. **Sensors and Actuators B: Chemical**, Elsevier, v. 362, p. 131763, 2022.
- KUBO, Y.; CHALMERS, E.; LUCZAK, A. Combining backpropagation with Equilibrium Propagation to improve an Actor-Critic reinforcement learning framework. **Frontiers in Computational Neuroscience**, Frontiers, v. 16, p. 980613, 2022.
- LEE, K. et al. Ultra-low-power e-nose system based on multi-micro-led-integrated, nanostructured gas sensors and deep learning. **ACS nano**, ACS Publications, v. 17, n. 1, p. 539–551, 2023.
- LIU, T. et al. A novel multi-odour identification by electronic nose using non-parametric modelling-based feature extraction and time-series classification. **Sensors and Actuators B: Chemical**, Elsevier, v. 298, p. 126690, 2019.

- LIU, Z. et al. Dynamic changes of volatile and phenolic components during the whole manufacturing process of Wuyi Rock tea (Rougui). **Food Chemistry**, Elsevier, v. 367, p. 130624, 2022.
- LOUTFI, A. et al. Electronic noses for food quality: A review. **Journal of Food Engineering**, Elsevier, v. 144, p. 103–111, 2015.
- LU, X. et al. Quality level identification of West Lake Longjing green tea using electronic nose. **Sensors and Actuators B: Chemical**, Elsevier, v. 301, p. 127056, 2019.
- MA, L. et al. A low cost compact measurement system constructed using a smart electrochemical sensor for the real-time discrimination of fruit ripening. **Sensors**, MDPI, v. 16, n. 4, p. 501, 2016.
- MAREK, G. et al. Detection and differentiation of volatile compound profiles in roasted coffee arabica beans from different countries using an electronic nose and GC-MS. **Sensors**, MDPI, v. 20, n. 7, p. 2124, 2020.
- MOHEBALI, B. et al. Probabilistic neural networks: a brief overview of theory, implementation, and application. **Handbook of probabilistic models**, Elsevier, p. 347–367, 2020.
- NICOLAS, J.; ROMAIN, A.-C.; MATERNOVA, J. Chemometrics methods for the identification and the monitoring of an odour in the environment with an electronic nose. In: **SENSORS and Chemometrics**. [S.l.]: Research Signpost, 2001.
- OLUNLOYO, V. O.; IBIDAPO, T. A.; DINRIFO, R. R. Neural network-based electronic nose for cocoa beans quality assessment. **Agricultural Engineering International: CIGR Journal**, v. 13, n. 4, 2011.
- PAN, C.-H.; HSIEH, H.-Y.; TANG, K.-T. An analog multilayer perceptron neural network for a portable electronic nose. **Sensors**, MDPI, v. 13, n. 1, p. 193–207, 2013.
- PEARCE, T. C. et al. **Handbook of Machine Olfaction: Electronic Nose Technology**. [S.l.]: John Wiley & Sons, 2003.
- PENG, X. et al. A novel sensor feature extraction based on kernel entropy component analysis for discrimination of indoor air contaminants. **Sensors and Actuators A: Physical**, Elsevier, v. 234, p. 143–149, 2015.
- PERIS, M.; ESCUDER-GILABERT, L. A 21st century technique for food control: Electronic noses. **Analytica chimica acta**, Elsevier, v. 638, n. 1, p. 1–15, 2009.
- QIAO, J. et al. Study on the Application of Electronic Nose Technology in the Detection for the Artificial Ripening of Crab Apples. **Horticulturae**, v. 8, n. 5, 2022. ISSN 2311-7524. DOI: <10.3390/horticulturae8050386>. Disponível em: <<<https://www.mdpi.com/2311-7524/8/5/386>>>.
- QU, J.; CHAI, Y.; YANG, S. X. A real-time de-noising algorithm for e-noses in a wireless sensor network. **Sensors**, Molecular Diversity Preservation International (MDPI), v. 9, n. 02, p. 895–908, 2009.
- RAHIMZADEH, H. et al. On the feasibility of metal oxide gas sensor based electronic nose software modification to characterize rice ageing during storage. **Journal of Food Engineering**, Elsevier, v. 245, p. 1–10, 2019.
- RALISNAWATI, D. et al. Detecting aroma changes of local flavored green tea (*Camellia sinensis*) using electronic nose. In: IOP PUBLISHING, 1. IOP Conference Series: Earth and

- Environmental Science. [S.l.: s.n.], 2018. v. 131, p. 012004.
- RODRIGUEZ-LUJAN, I. et al. On the calibration of sensor arrays for pattern recognition using the minimal number of experiments. **Chemometrics and Intelligent Laboratory Systems**, Elsevier, v. 130, p. 123–134, 2014.
- RODRÍGUEZ, J.; DURÁN, C.; REYES, A. Electronic nose for quality control of Colombian coffee through the detection of defects in “Cup Tests”. **Sensors**, Molecular Diversity Preservation International (MDPI), v. 10, n. 1, p. 36–46, 2010.
- ROMANI, S. et al. Evaluation of coffee roasting degree by using electronic nose and artificial neural network for off-line quality control. **Journal of Food Science**, Wiley Online Library, v. 77, n. 9, p. c960–c965, 2012.
- SAEYS, W.; MOUAZEN, A. M.; RAMON, H. Potential for onsite and online analysis of pig manure using visible and near infrared reflectance spectroscopy. **Biosystems Engineering**, Elsevier, v. 91, n. 4, p. 393–402, 2005.
- SANAEIFAR, A. et al. Early detection of contamination and defect in foodstuffs by electronic nose: A review. **TrAC Trends in Analytical Chemistry**, v. 97, p. 257–271, 2017. ISSN 0165-9936. DOI: <<https://doi.org/10.1016/j.trac.2017.09.014>>. Disponível em: <<<https://www.sciencedirect.com/science/article/pii/S0165993617302005>>>. Acesso em: 7 jan. 2023.
- SEESAARD, T.; WONGCHOOSUK, C. Recent Progress in Electronic Noses for Fermented Foods and Beverages Applications. **Fermentation**, MDPI, v. 8, n. 7, p. 302, 2022.
- SENINDE, D. R.; CHAMBERS IV, E. Coffee flavor: A review. **Beverages**, MDPI, v. 6, n. 3, p. 44, 2020.
- SHI, X.-H. et al. A two-stage framework for detection of pesticide residues in soil based on gas sensors. **Chinese Journal of Analytical Chemistry**, v. 50, n. 11, p. 100124, 2022. ISSN 1872-2040. DOI: <<https://doi.org/10.1016/j.cjac.2022.100124>>. Disponível em: <<<https://www.sciencedirect.com/science/article/pii/S1872204022000792>>>.
- SILVA FERREIRA, M. V. da et al. Determination of pitaya quality using portable NIR spectroscopy and innovative low-cost electronic nose. **Scientia Horticulturae**, Elsevier, v. 310, p. 111784, 2023.
- SRIVASTAVA, S.; SADISATP, S. Development of a low cost optimized handheld embedded odor sensing system (HE-Nose) to assess ripeness of oranges. **Journal of Food Measurement and Characterization**, Springer, v. 10, p. 1–15, 2016.
- TAN, J.; KERR, W. L. Characterizing cocoa refining by electronic nose using a Kernel distribution model. **LWT**, Elsevier, v. 104, p. 1–7, 2019.
- _____. Determining degree of roasting in cocoa beans by artificial neural network (ANN)-based electronic nose system and gas chromatography/mass spectrometry (GC/MS). **Journal of the Science of Food and Agriculture**, Wiley Online Library, v. 98, n. 10, p. 3851–3859, 2018.
- TAN, J.; XU, J. Applications of Electronic Nose (e-Nose) and Electronic Tongue (e-Tongue) in Food Quality-Related Properties Determination: A Review. **Artificial Intelligence in Agriculture**, v. 4, p. 104–115, 2020.
- TAN, J. et al. Sensing fermentation degree of cocoa (*Theobroma cacao* L.) beans by machine learning classification models based electronic nose system. **Journal of Food Process Engineering**, Wiley Online Library, v. 42, n. 6, e13175, 2019.

- TANG, K.-T.; LIN, Y. S.; SHYU, J. M. A Local Weighted Nearest Neighbor Algorithm and a Weighted and Constrained Least-Squared Method for Mixed Odor Analysis by Electronic Nose Systems. **Sensors**, v. 10, n. 11, p. 10467–10483, 2010.
- TANG, K.-T. et al. Development of a portable electronic nose system for the detection and classification of fruity odors. **Sensors**, v. 10, n. 10, p. 9179–9193, 2010.
- THEPUDOM, T.; SRICHAROENCHAI, N.; KERDCHAROEN, T. Classification of instant coffee odors by electronic nose toward quality control of production. In: 2013 10th International Conference on Electrical Engineering/Electronics, Computer, Telecommunications and Information Technology. [S.l.: s.n.], 2013. p. 1–4. DOI: <10.1109/ECTICon.2013.6559482>.
- TIAN, X.-Y.; CAI, Q.; ZHANG, Y.-M. Rapid classification of hairtail fish and pork freshness using an electronic nose based on the PCA method. **Sensors**, Molecular Diversity Preservation International (MDPI), v. 12, n. 1, p. 260–277, 2012.
- TIMSORN, K. et al. Discrimination of chicken freshness using electronic nose combined with PCA and ANN. In: IEEE. 2014 11th International Conference on Electrical Engineering/Electronics, Computer, Telecommunications and Information Technology (ECTI-CON). [S.l.: s.n.], 2014. p. 1–4.
- TSENG, T.-S. et al. Utilization of a gas-sensing system to discriminate smell and to monitor fermentation during the manufacture of oolong tea leaves. **Micromachines**, MDPI, v. 12, n. 1, p. 93, 2021.
- TURGUT, S. S.; KÜÇÜKÖNER, E.; KARACABEY, E. TeaPot: A chemometric tool for tea blend recipe estimation. **Applied Food Research**, Elsevier, v. 1, n. 1, p. 100006, 2021.
- TYAGI, P. et al. E-nose: a low-cost fruit ripeness monitoring system. **Journal of Agricultural Engineering**, v. 54, n. 1, 2023.
- TYLEWICZ, U. et al. **Safety, quality, and processing of fruits and vegetables**. v. 8. [S.l.]: MDPI, 2019. p. 569.
- VIEIRA, G. S. et al. Determination of anthocyanins and non-anthocyanin polyphenols by ultra performance liquid chromatography/electrospray ionization mass spectrometry (UPLC/ESI–MS) in jussara (*Euterpe edulis*) extracts. **Journal of Food Science and Technology**, Springer, v. 54, p. 2135–2144, 2017.
- VOSS, H. G. J.; AYUB, R. A.; STEVAN, S. L. E-nose Prototype to Monitoring the Growth and Maturation of Peaches in the Orchard. **IEEE Sensors Journal**, IEEE, v. 20, n. 20, p. 11741–11750, 2020.
- WAKHID, S. et al. Detection and Classification of Indonesian Civet and Non-Civet Coffee Based on Statistical Analysis Comparison Using E-Nose. **International Journal of Intelligent Engineering and Systems**, v. 13, p. 56–65, ago. 2020. DOI: <10.22266/ijies2020.0831.06>.
- WEI, X. et al. Rapid and non-destructive detection of decay in peach fruit at the cold environment using a self-developed handheld electronic-nose system. **Food Analytical Methods**, Springer, v. 11, p. 2990–3004, 2018.
- WILSON, A. D. Applications of electronic-nose technologies for noninvasive early detection of plant, animal and human diseases. **Chemosensors**, MDPI, v. 6, n. 4, p. 45, 2018.
- WOJNOWSKI, W. et al. Portable electronic nose based on electrochemical sensors for food quality assessment. **Sensors**, MDPI, v. 17, n. 12, p. 2715, 2017.

- XU, S. et al. Visible/near infrared reflection spectrometer and electronic nose data fusion as an accuracy improvement method for portable total soluble solid content detection of orange. **Applied Sciences**, MDPI, v. 9, n. 18, p. 3761, 2019.
- YAHIA, E. M.; GARCÍA-SOLÍS, P.; CELIS, M. E. M. Contribution of fruits and vegetables to human nutrition and health. In: *POSTHARVEST physiology and biochemistry of fruits and vegetables*. [S.l.]: Elsevier, 2019. p. 19–45.
- YAN, J. et al. Electronic nose feature extraction methods: A review. **Sensors**, MDPI, v. 15, n. 11, p. 27804–27831, 2015.
- YIN, Y. et al. Long-term robust identification potential of a wavelet packet decomposition based recursive drift correction of E-nose data for Chinese spirits. **Measurement**, Elsevier, v. 139, p. 284–292, 2019.
- ZAKARIA, A. et al. Improved maturity and ripeness classifications of magnifera indica cv. harumanis mangoes through sensor fusion of an electronic nose and acoustic sensor. **Sensors**, Molecular Diversity Preservation International (MDPI), v. 12, n. 5, p. 6023–6048, 2012.
- ZHANG, L.; LIU, Y.; DENG, P. Odor recognition in multiple E-nose systems with cross-domain discriminative subspace learning. **IEEE Transactions on Instrumentation and Measurement**, IEEE, v. 66, n. 7, p. 1679–1692, 2017.
- ZHANG, L.; ZHANG, D. Domain adaptation extreme learning machines for drift compensation in E-nose systems. **IEEE Transactions on instrumentation and measurement**, IEEE, v. 64, n. 7, p. 1790–1801, 2014.
- ZHANG, L. et al. A rapid discreteness correction scheme for reproducibility enhancement among a batch of MOS gas sensors. **Sensors and Actuators A: Physical**, Elsevier, v. 205, p. 170–176, 2014.
- ZHANG, W. et al. A study on soluble solids content assessment using electronic nose: persimmon fruit picked on different dates. **International Journal of Food Properties**, Taylor & Francis, v. 19, n. 1, p. 53–62, 2016.
- ZHAO, Z. et al. A novel spectrum analysis technique for odor sensing in optical electronic nose. **Sensors and Actuators B: Chemical**, Elsevier, v. 222, p. 769–779, 2016.
- ZHONG, Y. Electronic nose for food sensory evaluation. In: *EVALUATION technologies for food quality*. [S.l.]: Elsevier, 2019. p. 7–22.

CAPÍTULO II

DETERMINATION OF PITAYA QUALITY USING PORTABLE NIR SPECTROSCOPY AND INNOVATIVE LOW-COST ELECTRONIC NOSE

Artigo publicado na Revista Scientia Horticulturae, da Elsevier.

Determination of pitaya quality using portable NIR spectroscopy and innovative low-cost electronic nose

Marcus Vinicius da Silva Ferreira¹ - Ingrid Alves de Moraes² - Rafael Valsani Leme Passos² - Douglas Fernandes Barbin^{2,*} - Jose Lucena Barbosa Jr¹

¹Federal Rural University of Rio de Janeiro (UFRRJ), Department of Food Technology, Seropédica, RJ, Brazil

²Department of Food Engineering and Technology, School of Food Engineering, University of Campinas, Campinas, SP, Brazil

* Correspondence e-mail: dfbarbin@unicamp.br

1.1 Abstract

Pitaya (*Hylocereus polyrhizus*), also known as dragon fruit, is an exotic and highly valued fruit with a high amount of fiber and vitamins, and its quality is often related to attributes such as soluble solids, moisture content, and acidity. Traditional analytical techniques (e.g., gas chromatograph-mass spectrometry – GC-MS) for physicochemical quantification are costly and not environmentally friendly. This work proposes a quick and non-destructive evaluation of pitaya quality using low-cost Near-Infrared Spectroscopy (NIRS) and electronic nose (e-nose) devices. Classification models for either NIR spectra or e-nose data as predictors presented accuracy higher than 90% when classifying samples according to their shelf-life index stage (SLI30, 50, 80, and 100). Total titratable acidity (TA) and pH could be predicted using partial least squares regression (PLSR) and NIR spectra as predictors with coefficients of determination (R^2_p) of 0.89 and 0.83, respectively, and root means square error (RMSEP) of 0.03 and 0.23, respectively. Similarly, PLSR models for the prediction of TA and pH using e-nose data achieved R^2_p of 0.85 and 0.86, and RMSEP of 0.04 and 0.22 respectively. RPD and RER values for NIRS show that all predictors can be used to at least distinguish between low and high values. The results demonstrate that inexpensive devices based on NIRS, and a novel Low-cost-e-nose could be used in combination for the prediction of TSS, pH, TA, moisture, and phenolics, as well as to classify pitaya according to their shelf-life stages.

Keywords: chemometrics. optic sensors. MOS sensors. dragon fruit. pitahaya.

1.2 Introduction

Food production in Brazil stands out among the agricultural products commercialized in the Country, where Brazil is the biggest producer of tropical fruits globally (PINTO; JACO-MINO, 2013). Pitaya (*Hylocereus polyrhizus*) is a fruit, which consumption has been increased in the Brazilian market. This fruit, known as dragon fruit in the American market, is consumed on a large scale due to anthocyanins, which are molecules that show antioxidant properties. Besides that, the fruit has the potential of controlling the growth of microorganisms in food (acting as a preservative) (CHEAH et al., 2016). Among the current methods to determine the phytochemicals in these fruits are the chromatographic methods (VIEIRA et al., 2017), which are time-consuming and costly and sometimes require the fruit's violation. This equipment includes gas chromatography (GC-MS) and high-performance liquid chromatography (HPLC) (BU-RATTI et al., 2011; SANAEIFAR et al., 2017; WILSON, 2018; WILSON, 2018). However, the fruit's short shelf life is a common

problem that restricts its use (WU et al., 2019). Therefore, finding methods to evaluate shelf life and target compounds present in these fruits is extremely important. However, among the common methods today, are chromatography and physical-chemical analysis, which most of the time is laborious and may require an invasive approach. NIR spectroscopy is a non-invasive technique that in combination with chemometrics tools (predictive models) can show great potential for the food industry in measuring agricultural features, such as total solids (TSS) acidity (TTA), moisture, and phenolic compounds. Some of the equipment used includes Hyperspectral imaging (HIS-HIR) and Near-Infrared Spectroscopy (NIR). where the latter presents a lower price. Allow a predictive model to be transferred to another device and yet correct differences in the spectrum by that equipment is difficult in modeling.

Electronic nose (e-nose) is a piece of equipment that mimics the olfactive cells of mammals, and it was projected to identify and classify odors (PEARCE et al., 2003). Following the same trend of non-destructive techniques. Near-Infrared Spectroscopy – NIRS is based on the vibrational forces of organic chemical molecules and their interaction with the radiation of the infrared spectrum (BASANTIA; NOLLET; KAMRUZZAMAN, 2018). Both analyses have been shown to substitute consolidated techniques in the industry. such as gas chromatography- mass spectroscopy (GC-MS) and titratable acidity (LOUTFI et al., 2015). These custom analytical techniques used to determine physicochemical properties related to the ripening of fruits are onerous and need the use of chemicals (Alander et al., 2013). Therefore, these two techniques (NIR and e-nose) have been proposed to predict the shelf-life of pitaya based on total soluble solids content (TSS), pH and titratable acidity (TTA) moisture and phenolics using PLSR models as well as discriminate the fruit for 5 stages (days) using LDA and PLS-DA models.

1.3 Materials and Methods

1.3.1 Acquisition of the fruits

A total of 140 pitayas (red-fleshed variety) were obtained immediately after harvest from a local producer and 30 samples were analyzed for total phenolic compounds, total soluble solids (TSS), pH, titratable acidity (TA), and moisture content. Also, NIR spectra and e-nose data were acquired. The remaining samples were stored at two temperatures (15 oC and 25 oC), and the same analyses were performed after 7, 14, 21, and 25 days of storage.

1.3.2 Reference Analysis

Total Phenolics was performed using the Folin-Ciocalteu method proposed by Ferreira et al. (2019). Total soluble solids content (TSS), pH and titratable acidity (TTA) moisture and phenolics were analyzed. The content of total soluble solids was determined using a manual refractometer model (KASVI, K52-032), on a scale from 0 to 32%, and calibrated with distilled water AOAC 932.12. The moisture content of the samples was obtained by the gravimetric method after drying 4 g of sample in a vacuum oven at 60 °C until constant weight (AOAC, 2006). The pH was determined using a pH meter (model MB-10; Marte, São Paulo, Brazil), titratable acidity was measured from the juice of the fruit (NIELSEN et al., 2003) as well as phenolics according to Ferreira et al. (2019).

1.3.3 Data acquisition using NIR spectra

The range used for NIR measurements was 902 – 1700 nm using a 4 nm interval applied around the entire fruit using absorbance mode. The measuring was performed straight to fruit (peel) using a portable device (DLPR NIRscan™ Nano, Texas Instruments, USA), equipped with a 10 W halogen lamp and the Software NIRscan™. As per the replicates, for each sample, 60 scans were taken for each analyzed part of the fruit so that it could statistically represent the samples.

1.3.4 E-nose set up and fruit acquisition

The e-nose system is described as shown in Figure 1.1 and it is composed of the sample chamber and the computer for data acquisition. The e-nose has a set of 8 sensors: MQ2, MQ3, MQ4, MQ6, MQ8, MQ9, MQ135 and MQ138 (Zhengzhou Winsen Electronics Technology, China). Each of them is responsible for propane, alcohol, methane (CH₄), propane, inflammable gases, carbon monoxide (CO), ammonium (NH₄⁺), toluene (C₇H₈), and hydrogen and volatile compounds, respectively. The equipment also presents two controlling sensors, one for temperature and another one for humidity.

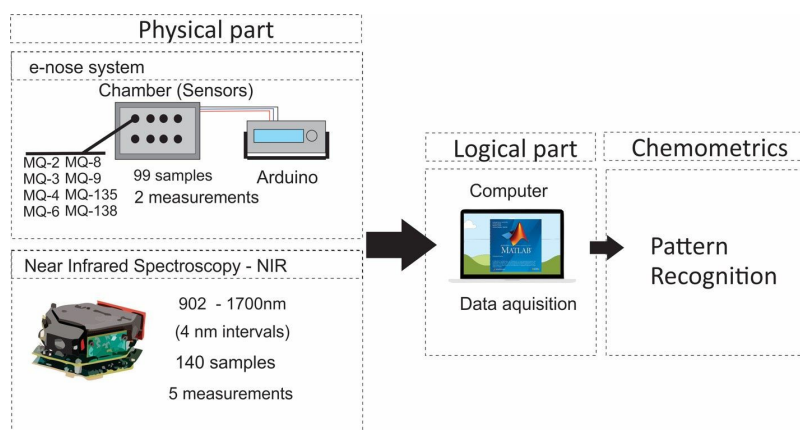


Figure 1.1: NIR and e-nose set up.

Each fruit was placed in the sensors chamber, where the volatiles was driven to each one of them. The time of each measurement was 2 min. Between each class, clean air was used to wash the volatiles compounds out as well as 2 min air is performed within each class so that the ratio signal(sample)/air was obtained.

1.3.5 Multivariate analysis

1.3.5.1 NIR (Spectra) and e-nose data pre-processing

The data used for the classification model (PLS-DA) and prediction model (PLSR) were randomly divided into a subset composed of 70% for the calibration and 30% for the prediction model respectively. For NIR system the data sets were calibration (99) and prediction (41), whereas for the e-nose system the data was calibration (67) and prediction (32). For NIR spectra, mean center was used (MC), and then pre-processing approaches were applied such as first (1st) and second (2nd) derivatives to correct the baseline; the derivatives were calculated using the Savitzky-Golay algorithm, with window size (w) of 9 to 11. The standard normal variate (SNV)

were applied to correct the effects of light scattering (BARNES; DHANOA; LISTER, 1989; MARTENS; GELADI, 1983). As per the e-nose, the voltage matrix data was pre-processed using only autoscaling (AS). For both NIR and e-nose the cross-validation method used was venetian blinds with 10 splits and blind thickness of 1.

1.3.5.2 Principal Component Analysis (PCA)

To simplify the size of data and obtain an overview of the variation between samples principal component analysis (PCA) was used as an unsupervised method. In addition, the information was used to identify whether or not the sensors were sensitive to pitaya's shelf life. This chemometric technique relies on linear transformation from the original variables, that were once initially correlated to each other in a smaller group of non-correlated variable nominated principal components (PCs). PCA models were designed with the complete data range, using the singular value decomposition algorithm (SVD) (95% confidence level) for the computation of the eigen generic sequence and a further cluster of the data. For the construction of the models, outliers (anomalous measuring) were identified and excluded using the amount of Q residuals and Hotelling T² plots.

1.3.5.3 Linear Discriminant Analysis (LDA)

Linear Discriminant Analysis was applied as a supervised method for data feature extraction and variable selection. For that, the mean covariance accounting for Gaussian distribution is calculated for each class while performing classification training. The model was developed by using the loadings from PCA of the most responsive peaks (1010, 1130, 1320, 1400, 1480, and 1660 nm) from the 140 samples used as predictors, divided into 5 storage days previously displayed. The software used to treat the data was MINITAB® Release 14.12.0 (SANAEIFAR et al., 2014).

1.3.5.4 Partial Least Square Discriminant Analysis (PLS-DA)

Partial least squares discriminant analysis was used to classify pitaya's fruit to its shelf-life stage within 5 studied categories (days 0, 7, 14, 21, and 25). The choice of the number of the latent variables (LVs) that should be included in the PLS-DA models was calculated based on the lowest root mean squared error for cross-validation (RMSECV) (BARBIN et al., 2013). The performance of the classification models was evaluated by sensitivity (Eq. 6.1) and Specificity (Eq. 6.2), which can be related to the model's ability to correctly classify positive and negative samples. respectively. The error rate (Eq. 6.3) and accuracy (Eq. 6.4) account for the error and the global value of the model's performance respectively.

$$\text{Sensitivity (\%)} = \frac{TP}{(TP+FN)} \times 100 \quad (6.1)$$

$$\text{Accuracy (\%)} = \frac{(TP+TN)}{TOTAL} \times 100 \quad (6.2)$$

$$\text{Specificity (\%)} = \frac{TN}{(TN+FP)} \times 100. \quad (6.3)$$

$$\text{Error rate (\%)} = \frac{(FP+FN)}{TOTAL} \times 100 \quad (6.4)$$

Where, TP = true positive; FN = false negative; TN = true negative; and FP = false positive.

1.3.5.5 Partial Least Square Regression (PLSR)

Partial Least-squares Regression (PLSR) was applied using both NIR spectra and e-nose dataset as predictors for each characteristic analyzed. The spectral region from 902 – 10701 nm was used for NIR, while for e-nose the entire dataset was used. The performance of the regression models was assessed by the coefficient of determination (R^2), the number of latent variables (LV), and root mean squared error (RMSE) for calibration (RMSEC), cross-validation (RMSECV), and prediction (RMSEP) (SKIBSTED et al., 2004), residual predictive deviation (RPD) and the range error ratio (RER) (BARBIN et al., 2015). Where RPD tell how model is (unusable) $RPD < 1.5$, (able to distinguish between high and low values) $1.5 < RPD < 2.0$, (quantitative prediction) $2.0 < RPD < 2.5$, (indication of a good prediction) $2.5 < RPD < 3.0$ and (excellent prediction) $RPD > 3$ (SAEYS; MOUAZEN; RAMON, 2005). While, $RER \geq 4$ means that the model is qualified for screening calibration, $RER \geq 10$ the model is acceptable for quality control and $RER \geq 15$ the model is very good for quantification (RAMBO; AMORIM; FERREIRA, 2013).

$$RMSEP = \sqrt{\frac{\sum_{p=1}^P (y_p - \hat{y}_p)^2}{P}} \quad (6.5)$$

$$RMSECV = \sqrt{\frac{\sum_{i=1}^I (y_i - \hat{y}_i)^2}{I}} \quad (6.6)$$

$$RPD = \frac{SD}{RMSEP \text{ ou } RMSECV} \quad (6.7)$$

$$RER = \frac{Range}{RMSEP \text{ ou } RMSECV} \quad (6.8)$$

1.4 Result and Discussion

1.4.1 Reference Analysis

Results for physical and chemical analysis of pitaya (Table 1.1), and Pearson correlation (Table 1.2) among features, demonstrated that changes in TSS, pH, TA, and phenolic compounds occurred during storage. Moisture did not have significant variation within the tested days ($p < 0.05$). A recent study suggested that TSS content does not change significantly within the maturity stages. On the other hand, TA decreased during maturation (shelf-life) (Freitas and Mitcham 2013). However, it was observed that TSS decreased continuously until the latest stage SLI100 10.54 ± 1.26 .

Acidity decreased during storage, and pH values increased, which may explain the spoilage in some fruits after two weeks. This degradation might be linked to the oxidation process that consumes some of the organic acids present in the fruit. As a result, an increase in SLI (TSS/TA) occurred during the period. Previous work reported an abrupt increase in pH after three weeks of storage, although in a different variety of pitaya (Franco, Esguerra, Tababa, & Castro, 2022). In this work, it was also observed a decrease in total phenolics in the late shelf-life stages, which is following previous studies (Angonese et al., 2021; Franco et al., 2022).

Table 1.1. Physicochemical parameters for pitaya during different shelf-life indexes

Analyzes	SLI30 (0)		SLI50 (7)		SLI80 (14 and 21)		SLI100 (25)	
	Min - Max	Mean \pm SD	Min - Max	Mean \pm SD	Min - Max	Mean \pm SD	Min - Max	Mean \pm SD
TSS	10.10 - 12.95	11.74 ^A \pm 0.72	8.95 - 13.20	11.29 ^{AB} \pm 1.32	8.45 - 14.70	10.97 ^B \pm 1.209	8.50 - 12.80	10.54 ^B \pm 1.26
pH	3.62 - 4.37	3.96 ^D \pm 0.20	3.88 - 4.79	4.44 ^C \pm 0.21	4.77 - 5.60	5.10 ^B \pm 0.17	5.17 - 5.57	5.35 ^A \pm 0.13
TA	0.24 - 0.47	0.35 ^A \pm 0.06	0.15 - 0.32	0.22 ^B \pm 0.04	0.20 - 0.82	0.15 ^C \pm 0.02	0.09 - 0.14	0.11 ^D \pm 0.02
Moisture	78.61 - 89.24	86.64 ^A \pm 1.43	84.16 - 92.65	87.31 ^A \pm 1.78	78.93 - 90.01	86.58 ^A \pm 2.23	84.15 - 90.42	86.81 ^A \pm 1.56
Phenolics	0.57 - 0.87	0.70 ^B \pm 0.08	0.64 - 0.84	0.73 ^{AB} \pm 0.05	0.59 - 0.87	0.75 ^A \pm 0.08	0.49 - 0.71	0.62 ^C \pm 0.07
TSS/TA		33.43 ^D \pm 2.9		50.25 ^C \pm 4.54		81.73 ^B \pm 4.74		104.32 ^A \pm 9.22

* The data correspond to the mean \pm SE of two repetitions. Different letters for the same parameter analyzed indicate significant differences. between the storage days. by ANOVA ($P < 0.05$). (TSS) content of total soluble solids. (TA) titratable acidity. (SLI ,30,50, 80 and 100) shelf-life index for pitaya fruit for each day group 0, 7, 14 and 21, 25, respectively.

Table 1.2. Pearson correlation for physicochemical parameters of pitaya.

	<i>TSS</i>	<i>pH</i>	<i>Moisture</i>	<i>Phenolics</i>	<i>TA</i>
TSS	1.00				
pH	-0.39	1.00			
Moisture	-0.46	0.35	1.00		
Phenolics	-0.24	0.49*	0.28	1.00	
TA	0.31	-0.90**	-0.28	-0.38	1.00

*Values in modulus are equal to 0.5, **values in modulus are > 0.5

1.4.2 Principal Components Analysis (PCA)

For the e-nose system, PCA was performed using data from the whole data set for all 8 sensors. Figure 1.2 shows the PCA scores plot on the PC1 vs PC2 for the e-nose device and PC1 vs PC2 for portable NIR.

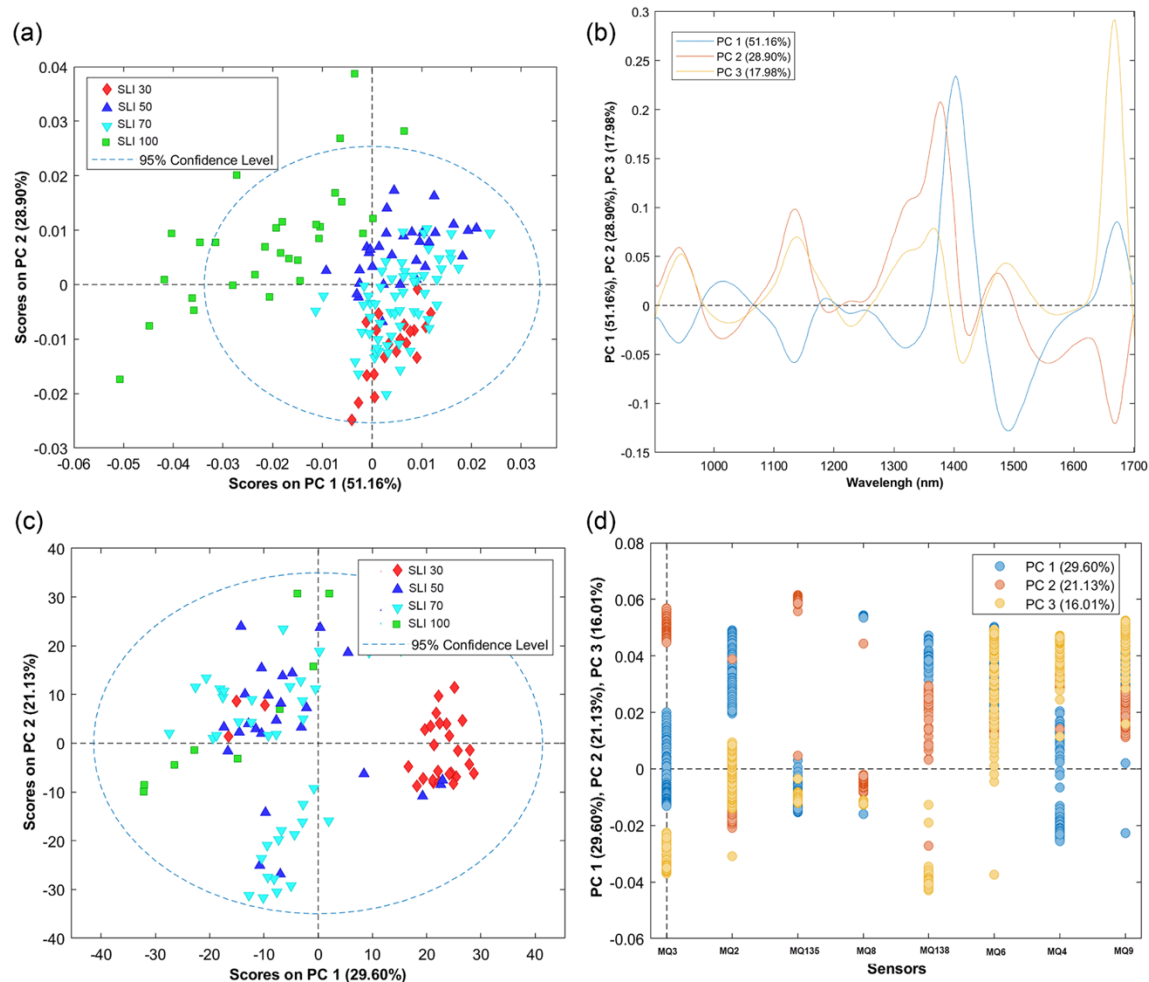


Figure 1.2: PCA (a) scores and (b) loadings for NIR spectra absorbance mode; PCA (c) scores and (d) loadings for e-nose data.

PC1 and PC2 explain more than 80% of the total variance (Figure 1.2a). It is also possible to observe a trend to split samples stored for long periods (SLI 100) on the negative side of PC1, to

fresher samples (SLI 50, 70) on the positive side of PC1. The loadings (Figure 1.2b) show that the wavelengths 905, 1010, 1130, 1320, 1400, 1480, and 1660 are responsible for the variation in the PC1. The wavelengths at 905, 1010, and 1130 nm are related to hydrogen and oxygen (H-O) (Osborne, 1986), and carbon and hydrogen interaction, second and first vibration of O-H related to aromatic compounds (Magwaza et al., 2012); 1320 and 1400 nm might be related to organic acids (Weyer & Lo, 2006). From those, 1010 and 1400 nm overlap with water which is correlated to the moisture present in the fruit. The peaks at 1480 and 1660 nm are associated with glucose (Osborne, 1986), and some authors have reported this wavelength to be related to lignin, starch, and cellulose (Ertlen, Schwartz, Trautmann, Webster, & Brunet, 2010). The variations observed during the storage period of the fruit as well as the response for phenolic compounds may be attributed to acid compound degradation, such as ascorbic acid, gallic acid, and malic acid (Cheah et al., 2016). The region responsible for the picks in the spectra at 1000 and 1440 nm could be related to organic acids, which for pitaya is represented by malic acid (C₄H₆O₅) since it is the major component in the fruit (Angonese et al., 2021).

For the e-nose system, it is possible to observe that samples from SLI 30 were on the positive side for PC1 scores (Figure 1.2c) while SLI 50, 70, and 100 were on the negative side. PC1, PC2, and PC3 together, explained 66.64% of the total variation. It can be seen in Figure 1.2c that the e-nose system can differentiate the storage days of pitaya in the aforementioned groups. The loadings for the PCA with e-nose data (Figure 2d) show the contribution of each sensor to the separation of the fruits. All sensors identified some type of compounds; however, the biggest peaks were presented by sensors MQ138 and MQ3, which are responsible for the volatile compounds present in fruit and alcohols derived molecules, respectively. Some of the compounds previously reported in pitayas include alcohols, 1-hexadecanol, and 2-ethyl-hexanol, aldehydes - octenal and octanal, and ketones – diphenyl-1- (2-furanyl)-ethanone (Attar et al., 2022), related to most of the volatile compounds. While MQ3 sensitivity to alcohol may explain the sensor's selectivity towards the molecule of malic acid and other organic acids due to its OH group, others, such as MQ8 did not respond considerably well to pitaya, yet it still might be relevant to PCA separation. A reason for that may be linked to hydrogen sulfide (H₂S) in the fruit respiration process in the postharvest (Hu et al., 2012). Previous work has demonstrated a correlation between the presence of this gas and the delay in senescence of the fruit, which helps to prolong the fruit's shelf-life (Hu et al., 2012). Likewise, carbon monoxide (CO) plays a role in fruit respiration (Young, Romani, & Biale, 1962) and are related to food quality (Krupa & Tomala, 2021), therefore MQ9 was an important sensor to monitor this gas level that increases over time during storage. MQ4 and MQ6 responses for methane and propane might be related to the release of these gases during storage since they are related to the rotten process in fruit waste (Gunaseelan, 2004). Even though pitaya is classified as non-climacteric fruit, the mechanisms involving ethylene production in fruits are still unknown (Aizat, Able, Stangoulis, & Able, 2013), and perhaps small variations in this hormone levels may be enough to obtain a response in MQ138 and MQ4 sensors.

1.4.3 Classification model using LDA

LDA classification of pitaya according to SLI using NIR spectra provided good results, using a few selected wavelengths. The wavelengths of 930, 950, 1010, 1020, 1140, 1190, 1320, 1400, 1480, 1660, 1670 nm were used in the models. Mainly, misclassification of samples observed for neighboring classes (Table 1.3). FT-NIR in combination with LDA has been successfully used to detect variation in morphological and chemical properties of lemon (Ruggiero, Amalfitano, Di Vaio, & Adamo, 2022), where the major component was attributed to polysaccharide content. This finding could be related to sugar and phenolic compounds since

Jamila et al. (2020) also obtained a perfect classification rate using NIR spectroscopy and chemometrics for garcinia fruit.

The LDA results for e-nose showed lower overall accuracy (95%) when compared to portable NIR spectrometer (97%). These results could be related to the transformations of volatile compounds compared to other chemical changes related to water and solid contents since NIR spectra are influenced by vibrational bonds in molecules related to major components such as water content, which may lead to a better classification, whereas the generated volatiles might not be sufficiently sensitive to MOS sensors in e-nose. From that, all classes had misclassified samples, where SLI100 presented the highest accuracy (99%). The SLI50 accuracy (91%) for e-nose was the lowest among classes, similar to the result obtained using NIR spectra (94%). All parameters sensitivity, selectivity, accuracy, and error rate are presented in Table 1.4.

Table 1.3: Confusion matrix for LDA and PLS-DA classification of pitaya using NIR spectra and e-nose data.

Classification method	Equipment					
		SLI30	SLI50	SLI80	SLI100	
LDA	NIR spectrometer	SLI30	25	2	0	0
		SLI50	2	21	3	0
		SLI70	0	1	58	0
		SLI100	0	0	1	27
	e-nose	SLI30	26	3	0	0
		SLI50	2	18	0	0
		SLI70	0	4	37	1
		SLI100	0	0	1	10
PLS-DA	NIR spectrometer	SLI30	10	2	0	0
		SLI50	0	8	5	0
		SLI70	0	1	9	1
		SLI100	0	0	0	7
	e-nose	SLI30	11	0	0	0
		SLI50	0	6	0	0
		SLI70	0	1	8	0
		SLI100	0	0	3	4

Table 1.4. Sensitivity, specificity, accuracy, and error rate values for classification of pitaya according to shelf-life index by using NIR spectra and e-nose.

Statistical method	Equipment	Shelf-life index	Sensitivity	Specificity	Accuracy	Error rate
LDA	NIR spectrometer	SLI30	0.93	0.98	0.97	0.02
		SLI50	0.88	0.96	0.94	0.06
		SLI70	0.94	0.99	0.96	0.04
		SLI100	1	0.99	0.99	0.01
	e-nose	SLI30	0.93	0.96	0.95	0.05
		SLI50	0.72	0.97	0.91	0.09
		SLI70	0.97	0.92	0.94	0.06
		SLI100	0.91	0.99	0.98	0.02
PLS-DA	NIR spectrometer	SLI30	1.00	0.94	0.95	0.05
		SLI50	0.73	0.84	0.81	0.19
		SLI70	0.64	0.93	0.84	0.16
		SLI100	0.88	1.00	0.98	0.02
	e-nose	SLI30	1.00	1.00	1.00	0.00
		SLI50	0.86	1.00	0.97	0.03
		SLI70	0.73	0.95	0.88	0.12
		SLI100	1.00	0.90	0.91	0.09

LDA has been used together with a low-cost electronic nose to classify oranges in different ripening stages, shelf life, and storage time as well as, early stages of contamination (Srivastava & Sadiatp, 2016). Other authors tested multiple e-nose systems for recognition of different odors (i.e., C₇H₈ C₆H₆ NH₃ CO, NO₂ and CH₂O) with LDA and obtained an average accuracy of 70.06% (Zhang, Liu and Deng 2017). Some of these components are equal to the ones attested in the equipment presented in this work, explaining the high classification rate found for pitaya. This gain in performance may be associated with the equipment robustness, sensor choice, and meticulous data treatment, despite the fact that the device used in this work is a low-cost one.

1.4.4 Classification model using PLS-DA

The confusion matrix of PLS-DA models for pitaya using NIR spectra is shown in Table 3, while sensitivity, selectivity, accuracy, and error rate are presented in Table 6 4. The four classes (SLI30, 50, 70, and 100) represent the storage indexes and the numbers on the diagonal of the matrix represent the samples correctly classified according to their respective classes, on the other hand, values that do not fall in that position are misplaced values. The transformations performed in the data were mean center, smoothing S-G order (o) 0, (w) 11 in combination with 1st S-G derivative (o 2, w 9), since they showed the best results. Regarding the best model for PLS-DA using NIR spectra, it showed 95%, 81%, 84%, and 98% for SLI30, 50, 70, and 100, respectively, where the overall accuracy for the prediction model was 90%.

NIR has been used to discriminate nectarine's shelf-life over 21 days using different irrigation strategies. They build models varying from 57 to 84% of accuracy (Pérez-Marín et al. 2011), it should be pointed out that the spectra acquisition was performed using different equipment. A similar approach was performed for kiwi, this time using NIR-HSI used PLS-DA for the classification of ripeness evaluation reached good accuracy, classifying the fruit during ripening with a sensitivity of over 73.3% (Benelli et al. 2021). Therefore, the results found in this work are promising compared to the ones found in the literature, considering the low-cost device that was used.

E-nose results (Table 1.3) showed better classification performance when compared to NIR. The overall accuracy was > 94% whereas the accuracy for SLI30 and SLI50 were 100 and 97%, respectively. Sensitivity, selectivity, accuracy, and error rate are presented in Table 1.4. The accuracy of the calibration model for each equipment was similar to those of the prediction model, which attests to the absence of over and underfitting. The data suggest e-nose equipment is suitable for the classification of pitaya in the presented shelf-life indexes with excellent accuracy (>93%), higher than (91.7%) found by Zhang (2019) when discriminating the content of *aspergillus carbonarius* in grapes based on their volatile compounds. Both NIR and e-nose presented accuracy over (91%). The results found in this research are promising for the classification of fruits according to the shelf-life stages.

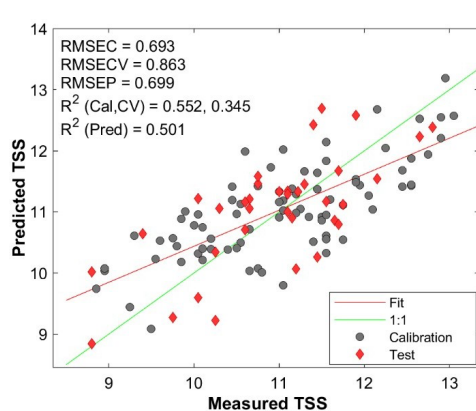
1.4.5 Prediction of reference analyzes using PLSR

Partial Least Squares Regression (PLSR) was used to model the relationship for each of the analyses (NIR and E-nose) with the physicochemical features TSS, pH, TA, moisture, and total phenolics of pitaya. RMSEC and RMSEP as well as the coefficient of determination (R^2) for both techniques are presented in Figure 1.3 and Figure 1.4. The spectral region from 900 to 1700 nm was used for the NIR spectra acquisition and various pre-treatments were tested, where mean center, smoothing (o) 0 (w) 9, and SNV presented the best results, while, for e-nose, autoscaling was used for all models.

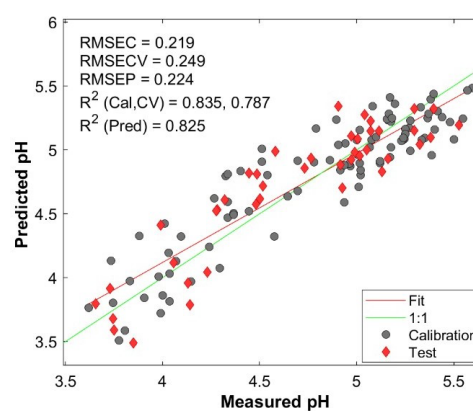
Regarding the PLSR models using NIR spectra (Table 5), pH and TA presented higher values of R^2 for calibration and prediction models compared to moisture and phenolics. Xu et al. (2019) found good models for TSS in oranges. They used NIR and e-nose in a fusion system to improve the prediction of the total sugar content. In the postharvest of fruits using NIR the prediction of direct correlation (e.g., TSS and water absorption) and secondary ones (e.g., TA and pH), where the latter are predicted indirectly from maturity stages or a compound such as chlorophyll, can be made to the stages of the fruit, as long as, the relationship is robust based on the variation that they may have (e.g., environmental and seasonal). The drawback is to assure the robustness of the correlation between these measured variables and the compound of interest in the fruit or vegetable (i.e., TA with chlorophyll content) to make such assumptions (Walsh, McGlone, & Han, 2020). This challenge reinforces the difficulty in obtaining a good correlation between the analyzed features (i.e., TSS, TA, pH, moisture, and phenolics) for pitaya as observed in the Pearson correlation table (Table 6.2). The good responses for pH and TA rely on the fact that pitaya presents many organic acids, whereas malic acid (451 mg/100g) is the main one in the red-fleshed variety (Angonese et al., 2021), therefore O-H bonds that are absorbed on the overtone by NIR in some wavelengths (i.e., 970 and 990 nm) is present in the structure of this molecule.

For the PLSR models using the full spectra, NIR models for TSS and moisture showed RPD values of 1.73 and 1.98, which fell into the $1.5 < RPD < 2$ range suggesting that TSS and moisture models can distinguish between high and low values (Saeys et al., 2005). pH and TA

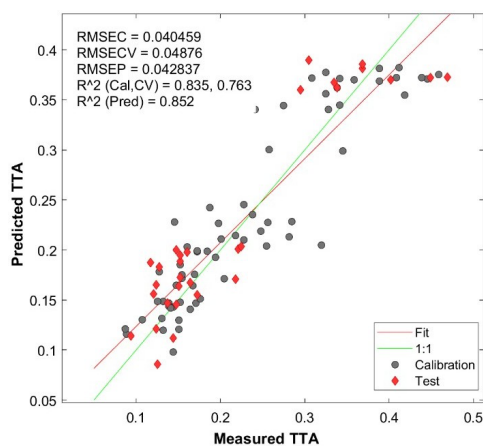
showed RPD 2.40, 2.78, falling into $2.0 < \text{RPD} < 2.5$ and $2.5 < \text{RPD} < 3.0$, respectively, which suggests a model for quantitative predictions (Saeys et al., 2005). On the other hand, phenolics presented 1.55 for RPD which is the threshold for the group that includes TSS and moisture. Even though it shows a moderate correlation with pH (Table 2), it did not present good prediction values, at least using the total phenolics method, as proposed in this work. A study on phenolics in red wine grapes found models with an RPD of 1.2 (Rouxinol, Martins, Murta, Barroso, & Rato, 2022), which may indicate the difficulty of working with these compounds. A reason for that lies on the complexity of the molecules that also have a hydroxyl functional group (-OH) since they are a group of aromatic carbon compounds derived from alcohols. As per RER for NIR equipment, TSS, pH, and moisture presented values 8.94, 8.81, and 8.82 making them fall into the $\text{RER} \geq 8$ thresholds, which means they are qualified for screening calibration. While TA RER was 11.57, which attests that the model is acceptable for quality control.



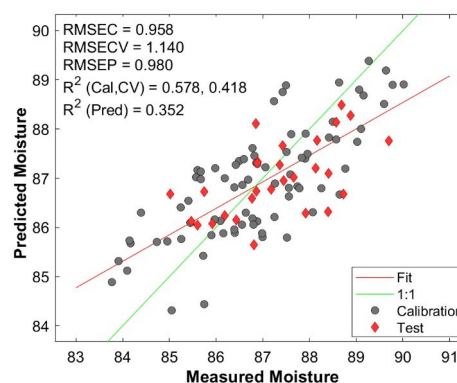
(a)



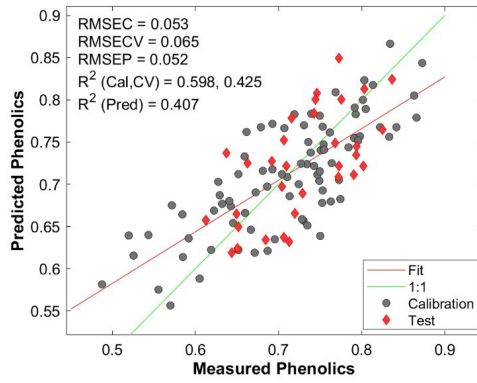
(b)



(c)

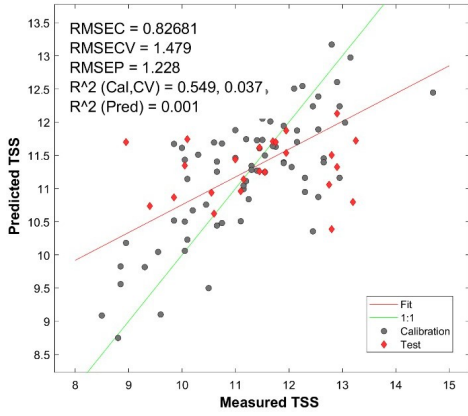


(d)

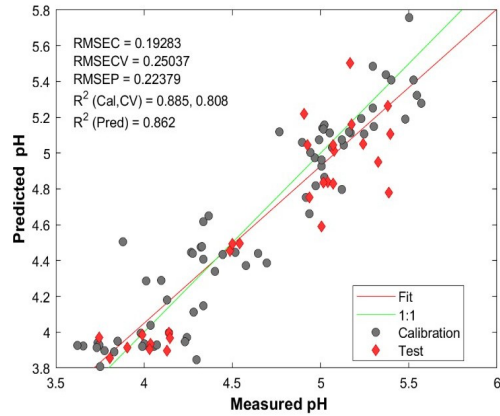


(e)

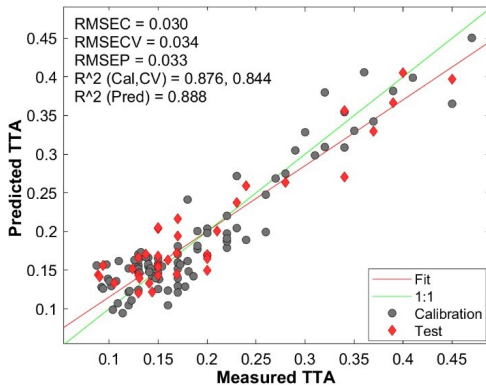
Figure 1.3: PLSR models with the best performance for the total of soluble solids (TSS), pH, total titratable acidity (TTA), moisture and total phenolics from NIR data.



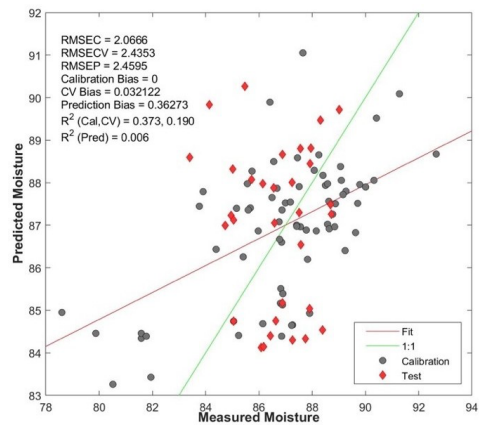
(a)



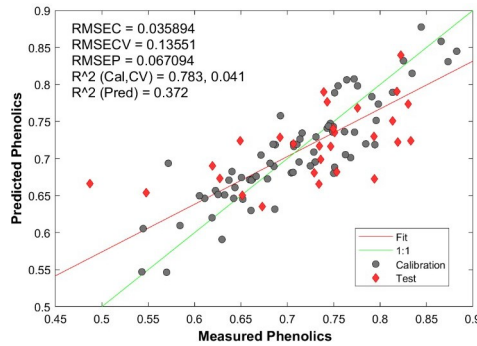
(b)



(c)



(d)



(e)

Figure 1.4: PLSR models with the best performance for total titratable acidity (TTA), total of soluble solids (TSS), pH, moisture, and total phenolics from e-nose system data.

As per e-nose, PLSR models for e-nose (Table 1.5 – Supplementary material) presented similar results. However, models for pH and TA generated high R^2 for calibration and prediction models. A possible reason for that may be linked to the presence of organic acids (Angonese et al., 2021; Balois-Morales, Peña-Valdivia, & Arroyo-Peña, 2013) and its degradation during the evaluated time confirmed by the increase in pH. TSS and moisture presented low R^2 values since it was not possible to build good models for those parameters, as these parameters are not related to any feature that would be captured by MOS sensors; therefore, it is not a surprise these two models did not present a good fit. Although the models for phenolics presented an R^2 of 0.78 for calibration, the prediction models were not so good, thus not suitable for prediction in the current work. The poor correlation may rely on the fact that the measurements were performed in the non-violated fruit; therefore, the volatile compounds that were being released from the peel might not be enough to be captured by the sensors. The evaluation of odor in fruit peel using e-nose is usually performed by grinding the peel and resuspending in solvent (Li et al., 2022), which was not the scope of this paper.

E-nose RPD values for TSS, moisture, and phenolics were below 1.5 which indicates an unusable model; however, pH fell into $2.5 < RPD < 3.0$, which indicates a good prediction model, and TA RPD > 2 indicates a model for quantitative predictions. Regarding RER for e-nose models, only TA and pH fell into the $RER \geq 8$ thresholds, which means they are qualified for screening calibration. Some of the unsatisfactory prediction models obtained could be because measurements were performed again with intact fruits. Pitaya has a thick peel that obstructs the penetration of the light from NIRS sensors, thus affecting the model for attributes such as TSS and moisture content, for example.

There are only a few studies on pitaya regarding fruit quality, yet volatile compounds and primary metabolites (e.g., sugar) appears as urgent indicators of fruit quality and flavor that will ensure the acceptability by consumers (García-Cruz, Dueñas, Santos-Buelgas, Valle-Guadarrama, & Salinas-Moreno, 2017; Walsh et al., 2020). However, variability within them can affect prediction models regarding their robustness when using NIR sensors (Walsh et al., 2020). Likewise, moisture and TSS, for example, affect fruits (e.g., strawberries) abruptly, in which small variation in intracellular structure may lead to an interference in model performance when using NIR spectroscopy (Xie, Liu, & Guo, 2021). Similarly, even though e-nose MOS sensors are well-established in determining and identifying a vast number of gases, such as ethanol, toluene, and benzene, allowing them to be used with LDA and PLS models, a drawback in this technology is the difficulty of the sensor to detect small concentrations (i.e., ppb) (Spinelle, Gerboles, Kok, Persijn, & Sauerwald, 2017). The fact that the release of phenolic compounds from the peel might be low combined with the high detection limit (100-1000 ppm) by the sensors may explain the poor response for e-nose TPC PLS mode.

1.5 Conclusions

Delivering high-quality fruits is essential to please consumers and has always been a concern in food safety and health. Likewise, agriculture 5.0 is around the corner determining a new resolution to consumers and producers in how they perceive food. This scenario facilitates the use of clean and smart technologies, such as smart sensors systems to assure good quality food for the growing population. When evaluating NIR and e-nose as possible equipment to evaluate pitaya shelf-life, LDA showed excellent classification for both NIR and e-nose, even though the former presented lower accuracy ($> 85\%$) compared to the latter ($> 98\%$). PLS-DA showed excellent accuracy in classifying pitaya in the 5 classes (days) in combined temperatures (15 and 25 °C) 92% and 96%, respectively. The analyzed PLS regression methods for the NIR system showed good prediction models with reasonable R^2_p and RMSEP for TSS and phenolics and good ones for TTA and pH. These two predictors showed RPD 2.40, and 2.18 $RPD > 2$, which suggests a model for quantitative predictions. For e-nose, TTA and pH showed good R^2_p and RMSEP. In addition, the pH model fell into $2.5 < RPD < 3.0$ indicates a good prediction model while TTA showed $RPD > 3$, which indicates an excellent model, therefore, both techniques could be used to predict the shelf-life stages of pitaya fruit for TTA, pH for both e-nose and NIR with a good prediction model and distinguishing between high and low values for TSS, moisture and phenolics for NIR. Yet, e-nose and NIR systems presented as good equipment for the prediction and classification of pitaya. The major chemical constituent for classification and prediction may be the volatile compounds associated with malic acid. The use of NIR and e-nose system combined with chemometrics can be used in the industry to distinguish the different stages of pitaya, which would facilitate the selection of these fruits for specific use and products, which includes their sorting for the marketplace as well as processed products such as ice cream jelly, and juice.

Table 1.5: Tukey test ANOVA for combined temperatures for of Pitaya fruit using NIR.

Analyzes	Storage Days									
	0		7		14		21		25	
	Min - Max	Mean \pm SD	Min - Max	Mean \pm SD	Min - Max	Mean \pm SD	Min - Max	Mean \pm SD	Min - Max	Mean \pm SD
TSS	10.10 - 12.95	11.74A \pm 0.72	8.95 - 13.20	11.29AB \pm 1.32	8.45 - 14.70	10.92B \pm 1.38	9.25 - 12.45	11.08AB \pm 0.78	8.50 - 12.80	10.54B \pm 1.26
pH	3.62 - 4.37	3.96D \pm 0.20	3.88 - 4.79	4.44C \pm 0.21	4.77 - 5.60	5.13B \pm 0.19	4.86 - 5.37	5.05B \pm 0.11	5.17 - 5.57	5.35A \pm 0.13
TTA	0.24 - 0.47	0.35A \pm 0.06	0.15 - 0.32	0.22B \pm 0.04	0.20 - 0.11	0.15C \pm 0.02	0.64 - 0.82	0.15C \pm 0.02	0.09 - 0.14	0.11D \pm 0.01
Moisture	78.61 - 89.24	86.46A \pm 2.12	84.16 - 92.65	87.31A \pm 1.78	78.93 - 90.01	86.55A \pm 2.62	84.39 - 88.42	86.63A \pm 1.31	84.15 - 90.42	86.81A \pm 1.56
Phenolics	0.57 - 0.87	0.70B \pm 0.08	0.64 - 0.84	0.73AB \pm 0.05	0.59 - 0.87	0.75A \pm 0.08	0.64 - 0.82	0.75AB \pm 0.06	0.49 - 0.71	0.62C \pm 0.07

* The data correspond to the mean \pm SE of two repetitions. Different letters for the same parameter analyzed indicate significant differences. between the storage days. by ANOVA ($P < 0.05$). (TSS) content of total soluble solids. (TTA) titratable acidity.

Table 1.6: Tukey test ANOVA for combined temperatures for of Pitaya fruit using e-nose.

Analyzes	Storage Days									
	0		7		14		21		25	
	Min - Max	Mean \pm SD	Min - Max	Mean \pm SD	Min - Max	Mean \pm SD	Min - Max	Mean \pm SD	Min - Max	Mean \pm SD
TSS	10.10-12.95	11.77A \pm 0.67	8.95-13.20	11.32AB \pm 1.33	8.85 -14.45	11.02AB \pm 1.43	10.75 - 12.45	11.35AB \pm 0.53	8.50 - 12.80	10.4B \pm 1.54
pH	3.62 - 4.37	3.97D \pm 0.20	3.88 - 5.39	4.44C \pm 0.29	4.77 - 5.50	5.09B \pm 0.18	4.91 - 5.55	5.05B \pm 0.08	5.17 - 5.57	5.37A \pm 0.14
TTA	0.19 - 0.47	0.36A \pm 0.06	0.127 - 0.320	0.20B \pm 0.05	0.12 - 0.204	0.15C \pm 0.02	0.09 - 0.15	0.14CD \pm 0.01	0.09 - 0.14	0.11D \pm 0.01
Moisture	78.61 - 89.78	85.48B \pm 2.80	84.95 - 92.65	87.73A \pm 2.68	83.76 - 90.01	87.57A \pm 1.86	84.40 - 88.41	86.87AB \pm 1.23	83.40 - 91.27	86.73AB \pm 2.35
Phenolics	0.19 - 0.47	0.70B \pm 0.08	0.63 - 0.83	0.73AB \pm 0.05	0.63 - 0.89	0.73AB \pm 0.08	0.54 - 0.84	0.78A \pm 0.05	0.49 - 0.70	0.61C \pm 0.07

* The data correspond to the mean \pm SE of two repetitions. Different letters for the same parameter analysed indicate significant differences. between the storage days. by ANOVA ($P < 0.05$). (TSS) content of total soluble solids. (TTA) titratable acidity.

Table 1.7: Parameters for the calibration and prediction sets for reference analysis in Pitaya using portable NIR and e-nose with PLSR.

Reference Analyzes	Equipment	Pre- Processing	Model	Variable number	LV	R ² C	RMSEC	R ² Cv	RMSECV	R ² P	RMSEP	RPD	RER
TSS	NIR	MC. SM S-G (o) 0 (w) 11. 1st S-G (o)2. (w) 9. SNV	full	228	9	0.55	0.693	0.345	0.863	0.501	0.699	1.73	8.94
	e-nose	Autoscaling		928	4	0.55	0.83	0.037	1.48	0.00	1.23	0.98	5.04
pH	NIR	MC. SM S-G (o) 0 (w) 11. 1st S-G (o)2. (w) 9 2nd (o) 2 (w) 9.SNV	full	228	6	0.83	0.220	0.249	0.825	0.224	2.40	8.81	
	e-nose	Autoscaling. smoothing S-G o (0) (w) 9		928	7	0.89	0.19	0.808	0.25	0.862	0.224	2.50	8.71
TTA	NIR	MC. SM S-G (o) 0 (w) 11. 1st S-G (o)2. (w) 9 2nd (o)2. (w) 9.SNV	full	228	5	0.84	0.040	0.763	0.005	0.852	0.04	2.18	9.09
	e-nose	AS. SM S-G (o) 0 (w) 9		928	7	0.88	0.03	0.844	0.034	0.888	0.033	3.11	11.57
Moisture	NIR	MC. SM S-G (o) 0 (w) 11. 1st S-G (o)2. (w) 9 2nd (o)2. (w) 9.SNV	full	228	8	0.58	0.958	1.14	0.352	1.98	8.82		
	e-nose	Autoscaling		928	5	0.37	2.06	0.190	2.46	0.00	2.46	0.96	5.86
Phenolics	NIR	MC. SM S-G (o) 0 (w) 11. 1st S-G (o)2. (w) 9 2nd (o)2. (w) 9.SNV	full	228	9	0.60	0.05	0.425	0.065	0.407	0.05	1,55	7,41
	e-nose	Autoscaling smoothing S-G (o) 0 (w) 9		928	20	0.78	0.20	0.810	0.24	0.699	0.334	1.02	5.86

1.6 References

- AIZAT, W. M. et al. Characterisation of ethylene pathway components in non-climacteric capsicum. **BMC Plant Biology**, Springer, v. 13, p. 1–14, 2013.
- ANGONESE, M. et al. Organic dragon fruits (*Hylocereus undatus* and *Hylocereus polyrhizus*) grown at the same edaphoclimatic conditions: Comparison of phenolic and organic acids profiles and antioxidant activities. **LWT**, Elsevier, v. 149, p. 111924, 2021.
- ATTAR, Ş. H. et al. Nutritional analysis of red-purple and white-fleshed pitaya (*Hylocereus*) species. **Molecules**, MDPI, v. 27, n. 3, p. 808, 2022.
- BALOIS-MORALES, R.; PEÑA-VALDIVIA, C. B.; ARROYO-PEÑA, V. B. Symptoms and sensitivity to chilling injury of pitahaya (*Hylocereus undatus* (Haw.) Britton & Rose) fruits during postharvest. **Agrociencia**, Colegio de Postgraduados, v. 47, n. 8, p. 795–813, 2013.
- BARBIN, D. F. et al. Non-destructive determination of chemical composition in intact and minced pork using near-infrared hyperspectral imaging. **Food Chemistry**, Elsevier, v. 138, n. 2-3, p. 1162–1171, 2013.
- BARBIN, D. F. et al. Prediction of chicken quality attributes by near infrared spectroscopy. **Food Chemistry**, Elsevier, v. 168, p. 554–560, 2015.
- BARNES, R. J.; DHANOA, M. S.; LISTER, S. J. Standard normal variate transformation and de-trending of near-infrared diffuse reflectance spectra. **Applied Spectroscopy**, SAGE Publications, London, England, v. 43, n. 5, p. 772–777, 1989.
- BASANTIA, N. C.; NOLLET, L. M. L.; KAMRUZZAMAN, M. **Hyperspectral Imaging Analysis and Applications for Food Quality**. [S.l.]: CRC Press, 2018.
- BENELLI, A. et al. Ripeness evaluation of kiwifruit by hyperspectral imaging. **Biosystems Engineering**, Elsevier, v. 223, p. 42–52, 2022.
- BURATTI, S. et al. Monitoring of alcoholic fermentation using near infrared and mid infrared spectroscopies combined with electronic nose and electronic tongue. **Analytica chimica acta**, Elsevier, v. 697, n. 1-2, p. 67–74, 2011.
- CHEAH, L. K. et al. Phytochemical properties and health benefits of *Hylocereus undatus*. **Nanomedicine & Nanotechnology**, v. 1, n. 1, 2016. DOI: <<https://doi.org/10.23880/nnoa-16000103>>.
- ERTLEN, D. et al. Discriminating between organic matter in soil from grass and forest by near-infrared spectroscopy. **European Journal of Soil Science**, Wiley Online Library, v. 61, n. 2, p. 207–216, 2010.
- FERREIRA, M. V. S. et al. Ohmic heating for processing of whey-raspberry flavored beverage. **Food Chemistry**, Elsevier, v. 297, p. 125018, 2019.
- FRANCO, R. K.; CASTRO, A.; ESGUERRA, E. Harvest maturity affects the quality and storage behavior of white-fleshed dragon fruit [*Hylocereus undatus* (Haworth) Britton and Rose]. **Food Research**, Rynnye Lyan Resources, v. 6, n. 2, 2022.
- GARCÍA-CRUZ, L. et al. Betalains and phenolic compounds profiling and antioxidant capacity of pitaya (*Stenocereus* spp.) fruit from two species (*S. Pruinosis* and *S. stellatus*). **Food Chemistry**, Elsevier, v. 234, p. 111–118, 2017.
- JAMILA, N. et al. Application of phytochemical and elemental profiling, chemometric multivariate analyses, and biological activities for characterization and discrimination of fruits of four *Garcinia* species. **Analytical Letters**, Taylor & Francis, v. 53, n. 1, p. 122–139, 2020.

- LOUTFI, A. et al. Electronic noses for food quality: A review. **Journal of Food Engineering**, Elsevier, v. 144, p. 103–111, 2015.
- MAGWAZA, L. S. et al. NIR spectroscopy applications for internal and external quality analysis of citrus fruit—a review. **Food and Bioprocess Technology**, Springer, v. 5, p. 425–444, 2012.
- MARTENS, J. H. S.; GELADI, P. Multivariate Linearity Transformations for Near-Infrared Reflectance Spectrometry. In: PROCEEDINGS of Nordic Symposium for Applied Statistics. [S.l.: s.n.], 1983. p. 205–234.
- MISHRA, P. et al. Sequential fusion of information from two portable spectrometers for improved prediction of moisture and soluble solids content in pear fruit. **Talanta**, Elsevier, v. 223, p. 121733, 2021.
- NIELSEN, S. S. et al. **Food Analysis Laboratory Manual**. 3. ed. [S.l.]: Springer, 2003.
- OSBORNE, B. G. Theory of Near Infrared Spectrophotometry. In: [s.l.]: John Wiley & Sons, Ltd Chichester, UK, 1986. p. 212.
- PEARCE, T. C. et al. **Handbook of Machine Olfaction: Electronic Nose Technology**. [S.l.]: John Wiley & Sons, 2003.
- PÉREZ-MARÍN, D. et al. Postharvest shelf-life discrimination of nectarines produced under different irrigation strategies using NIR-spectroscopy. **LWT-Food Science and Technology**, Elsevier, v. 44, n. 6, p. 1405–1414, 2011.
- PINTO, P. M.; JACOMINO, A. P. The postharvest of tropical fruits in Brazil. In: SPRINGER. **Food Quality, Safety and Technology**. [S.l.: s.n.], 2013. p. 77–87.
- RAGAZOU, K. et al. Agriculture 5.0: A new strategic management mode for a cut cost and an energy efficient agriculture sector. **Energies**, MDPI, v. 15, n. 9, p. 3113, 2022.
- RAMBO, M. K. D.; AMORIM, E. P.; FERREIRA, M. M. C. Potential of visible-near infrared spectroscopy combined with chemometrics for analysis of some constituents of coffee and banana residues. **Analytica Chimica Acta**, Elsevier, v. 775, p. 41–49, 2013.
- ROUXINOL, M. I. et al. Quality Assessment of Red Wine Grapes through NIR Spectroscopy. **Agronomy**, MDPI, v. 12, n. 3, p. 637, 2022.
- RUGGIERO, L. et al. Use of near-infrared spectroscopy combined with chemometrics for authentication and traceability of intact lemon fruits. **Food Chemistry**, Elsevier, v. 375, p. 131822, 2022.
- SAEYS, W.; MOUAZEN, A. M.; RAMON, H. Potential for onsite and online analysis of pig manure using visible and near infrared reflectance spectroscopy. **Biosystems Engineering**, Elsevier, v. 91, n. 4, p. 393–402, 2005.
- SANAEIFAR, A. et al. Early detection of contamination and defect in foodstuffs by electronic nose: A review. **TrAC Trends in Analytical Chemistry**, v. 97, p. 257–271, 2017. ISSN 0165-9936. DOI: <<https://doi.org/10.1016/j.trac.2017.09.014>>. Disponível em: <<<https://www.sciencedirect.com/science/article/pii/S0165993617302005>>>. Acesso em: 7 jan. 2023.
- SANAEIFAR, A. et al. Development and application of a new low cost electronic nose for the ripeness monitoring of banana using computational techniques (PCA, LDA, SIMCA, and SVM). Czech Academy of Agricultural Sciences, 2014.

- SKIBSTED, E. T. S. et al. New indicator for optimal preprocessing and wavelength selection of near-infrared spectra. **Applied Spectroscopy**, Society for Applied Spectroscopy, v. 58, n. 3, p. 264–271, 2004.
- SPINELLE, L. et al. Review of Portable and Low-Cost Sensors for the Ambient Air Monitoring of Benzene and Other Volatile Organic Compounds. **Sensors**, v. 17, n. 7, 2017. Disponível em: <<<https://www.mdpi.com/1424-8220/17/7/1520>>>. Acesso em: 10 dez. 2022.
- SRIVASTAVA, S.; SADISATP, S. Development of a low cost optimized handheld embedded odor sensing system (HE-Nose) to assess ripeness of oranges. **Journal of Food Measurement and Characterization**, Springer, v. 10, p. 1–15, 2016.
- VIEIRA, G. S. et al. Determination of anthocyanins and non-anthocyanin polyphenols by ultra performance liquid chromatography/electrospray ionization mass spectrometry (UPLC/ESI–MS) in jussara (*Euterpe edulis*) extracts. **Journal of Food Science and Technology**, Springer, v. 54, p. 2135–2144, 2017.
- WALSH, K. B.; MCGLONE, V. A.; HAN, D. H. The uses of near infra-red spectroscopy in postharvest decision support: A review. **Postharvest Biology and Technology**, Elsevier, v. 163, p. 111139, 2020.
- WEYER, L. G.; LO, S.-C. Spectra–structure correlations in the near-infrared. In: **HANDBOOK of Vibrational Spectroscopy**. [S.l.]: Wiley Online Library, 2006.
- WILSON, A. D. Applications of electronic-nose technologies for noninvasive early detection of plant, animal and human diseases. **Chemosensors**, MDPI, v. 6, n. 4, p. 45, 2018.
- WILSON, A. D. Application of electronic-nose technologies and VOC-biomarkers for the noninvasive early diagnosis of gastrointestinal diseases. **Sensors**, MDPI, v. 18, n. 8, p. 2613, 2018.
- WU, Q. et al. Comparative volatile compounds and primary metabolites profiling of pitaya fruit peel after ozone treatment. **Journal of the Science of Food and Agriculture**, Wiley Online Library, v. 99, n. 5, p. 2610–2621, 2019.
- XIE, D.; LIU, D.; GUO, W. Relationship of the optical properties with soluble solids content and moisture content of strawberry during ripening. **Postharvest Biology and Technology**, Elsevier, v. 179, p. 111569, 2021.
- XU, S. et al. Visible/near infrared reflection spectrometer and electronic nose data fusion as an accuracy improvement method for portable total soluble solid content detection of orange. **Applied Sciences**, MDPI, v. 9, n. 18, p. 3761, 2019.
- ZHANG, L.; LIU, Y.; DENG, P. Odor recognition in multiple E-nose systems with cross-domain discriminative subspace learning. **IEEE Transactions on Instrumentation and Measurement**, IEEE, v. 66, n. 7, p. 1679–1692, 2017.

CAPÍTULO III

MACHINE LEARNING-BASED CLASSIFICATION PERFORMANCE OF BLACK TEA FROM THREE ORIGINS (BR, IND AND US) USING NIR DEVICES (PORTABLE AND BENCHTOP) AND A LOW-COST-E-NOSE

Artigo submetido à Revista Journal of Food Engineering, da Elsevier.

Machine learning-based classification performance of black tea from three origins (BR, IND and US) using NIR devices (portable and benchtop) and a Low-cost-e-nose

Marcus Vinicius da Silva Ferreira¹ - Mohammed Kamruzzaman² - Douglas Fernandes Barbin^{2,*} - Jose Lucena Barbosa Jr¹

¹Federal Rural University of Rio de Janeiro (UFRRJ), Department of Food Technology, Seropédica, RJ, Brazil

²Department of Food Engineering and Technology, School of Food Engineering, University of Campinas, Campinas, SP, Brazil

* Correspondence e-mail: dfbarbin@unicamp.br

1.1 Abstract

Black tea adulteration is a widespread practice, involving the mixing or substituting leaves from lower quality in place of high-quality samples. The authentication of black tea regarding its composition and origin is crucial to ensure its quality and consumer trust. However, usual methods for tea analysis are expensive, demand chemicals and generate waste. To address this gap, this study proposes an investigation of two NIR instruments (portable (PNIR) and a benchtop (BNIR)), and a low-cost multi-sensor device (electronic nose (LCe-nose)), for characterization and classification of tea leaves from three different origins (Brazil, United States, and India). The methods employed in this study including data analyses were performed by Principal Component Analysis (PCA), Linear Discriminant Analysis (LDA), and Partial Least Squares Discriminant Analysis (PLS-DA). Results for the e-nose exhibited F1 scores above 99% for all models, indicating its potential alternative to NIR spectroscopy for investigation of tea quality and origin. Overall, this research demonstrates the potential of using NIR spectroscopy and LC-e-nose as reliable tools for tea quality assessment, which could significantly contribute to guaranteeing the quality and authenticity of tea in the market.

Keywords: adulteration, black tea, machine learning, beverage, Infra-red spectroscopy.

1.2 Introduction

Black tea is the most consumed beverage in the world, after water and is characterized as oxidized tea (LIN; SUN, 2020) where (REN et al., 2023), which suggests the use of more feasible procedures and different options for tea analysis. Near infrared (NIR) is a non-destructive analysis used in many types of food. The different chemical bonds present in a given food can emit or absorb spectra, providing vibrations that give information on the composition of the product (POREP; KAMMERER; CARLE, 2015). The equipment used for spectrometry analysis is presented as benchtop or portable equipment. The former generally has better resolutions yet is more expensive. On the other hand, the latter as a portable device is a more affordable option, however with lower spectral resolution. Electronic nose (e-nose), a tool designed to recognize and categorize volatile substances, is a way of trying to improve olfactory cells found in animals (PEARCE et al., 2003). At a reduced cost and without the use of chemicals, e-nose and NIRS analyses have both been employed to replace established approaches in the industry. These

specialized analytical methods have been utilized to identify physicochemical characteristics associated with fruit ripening (LOUTFI et al., 2015). NIR spectroscopy and e-nose stands out as a better alternative than laborious and expensive methods mentioned above, both are found in a wide range of price where portable NIR vary from two thousand to twenty-five thousand USD.

E-noses on the other hand, since are still filling the market range from eleven thousand to a hundred and fifty thousand USD, that is why more research should be conducted offering Low-cost-e-nose option to evaluate food stuff (i.e., tea). Together with NIR and e-nose analysis, chemometrics and multivariate analysis enhance equipment performance, in which both techniques are used to treat device's chemical data such as linear discriminant analysis (LDA) and Partial least square discriminant analysis (PLS-DA) (VISCARRA ROSSEL, 2008). It is generally used with equipment that does not result in direct data, obtaining mathematically and statistically important chemical information from the studied material. In this regard there is no research evaluating tea checking the performance of tea classification using NIR and e-nose. Thus, this work proposed an investigation in the use of LC-e-nose and two benchtop NIR (PNIR and BNIR) to classify tea leaves from three different origins (Brazil, United States and India).

1.3 Materials and Methods

1.3.1 Sample acquisition and preparation

Approximately 120 tea samples from Brazil (BR), United States (USA) and India (IND) were used totaling 360 samples all divided in two variety (broken orange pekoe - BOP and Flower broken Orange Pekoe - FBOP) of teas (Table 7.1). The two different NIR spectrometers used for data acquisition were a portable (PNIR) and a benchtop (BNIR) device and LC-e-nose.

1.3.2 Extraction

Tea extract was performed as described by the International Organization for Standardization (ISO) 14502-1. An amount of 0.20 grams of each sample was weighed and taken in a volumetric flask. Then, 5 mL of 70% methanol at 70 °C was added and the extract was mixed and heated using a vortex at 70 °C for 10 minutes followed by cooling at room temperature. The extract was centrifuged at 200 g for 10 minutes and the supernatant was collected in a centrifuge tube. The extraction step was repeated twice and both extracts were combined to fill a 10 mL flask (Sanches et al., 2022).

1.3.3 HPLC

The High-performance liquid chromatography (HPLC) analysis for the caffeine content will be performed as described by (Sanches et al., 2022) with slight modifications. The modifications consisted in replacing the phase A & B with 1% formic acid and acetonitrile respectively. The gradient variation was as follows: 97% to 94% A (3 minutes), 94% to 90% A (3 minutes), 90% to 87% A (8 minutes), 87% to 85% A (2 minutes), 85% to 80% A (2 minutes), 80% to 75% A (1 minute), 75% to 70% A (2 minutes), 70% to 50% A (5 minutes), 50% to 70% A (3 minutes), 70% to 97% A (4 minutes) at a flow rate of 1 mL/min. Before each injection, the system will be re-equilibrated for 2 minutes (97% A). The column oven temperature was set to 29° C. The selected chromatograms for the analysis will be 350 nm, 325 nm and 260 nm. The experiment will be performed in duplicates. Caffeine will be predominantly absorbed in UV at 260 nm, which is considered a common wavelength for that compound.

1.3.4 NIR spectra acquisition

Two different Near-Infrared (NIR) spectrometers were used for data acquisition: a portable NIR spectrometer (PNIRS) (NIRscan™ Nano Digital Light Processing (DLPR), Texas Instrument, USA), and a benchtop NIR spectrometer (BNIRS) (Bruker Tango FT-NIR, Bruker Optik, Germany).

The BNIRS collected one spectrum for each sample by rotating cups, and each spectrum was an average of sixty-four (64) scans taken from 867-2535 nm with a resolution of 2 nm. The PNIRS collected one spectrum for each sample, as the average of ten (10) spectra, in the wavelength range of 900–1700 nm with intervals of 4 nm, using a 10 W halogen bulb as a light source and an InGaAs detector. The acquired spectra for both devices were set as reflectance mode, corrected using white/dark references, and later transformed into absorbance units through logarithmic transformation to allow for direct evaluation between the equipment.

Table 1.1: Selected spectra intervals found in tea PCA loadings data, adapted from Chen et al. (2018).

Elements	Wavelengths (nm)	Bonds
Theaflavins	926 - 956	Water absorption
Total catechins	1099 - 1172	C – H second overtone
Theaflavin-3 gallate	1173 - 1256	C – H = second overtone First overtone of C – H
Free amino acids	1256 - 1352	combinations
Caffeine	1353 - 1464	N – H first overtone
Water extracts	1465 - 1597	C – H first overtone
Total catechins	1598 - 1756	C – H first overtone and S – H first overtone
Catechins	1904 – 2500	C=O stretching second overtones, C-H and C-H combinations

Adapted from (Chen et al. 2018)

1.3.5 Olfactive Sensors

A low-cost prototype, e-nose type multi-sensor device (LC- e-nose) was used assembled (Figure 1). For each sample, information from ten (10) replicates were acquired during a 2 min period, with fresh air puffed into the sample chamber to clean the sensors after each acquisition. The e-nose device has a set of 6 metal oxidative semiconductor (MOS) sensors, with respective codes and sensitiveness: MQ2 (smoke and propane), MQ3 (alcohol), MQ4 (methane (CH₄)), MQ5 (propane), MQ8 (inflammable gasses (Hydrogen gas) and MQ135 (volatile compounds such as NH₃, NO_x, alcohol, Benzene, smoke, CO₂). (Bonatech Electronics Technology, China and Zhengzhou Winsen Electronics Technology, China). The equipment also presented one sensor (DHT11) for temperature and another sensor for humidity measurements.

1.3.6 Multivariate analysis

1.3.6.1 Data labeling

Tea samples were classified based on their origin (Brazil, India and US) and processing class (BOP and FBOP). Also, BOP and FBOP samples were mixed for each origin to create variation for classification purposes.

1.3.6.2 Data

NIR spectra were pre-processed using mean center (MC), smoothing Savitzky-Golay algorithm (S-G), with window size (w) of 9 to 13 by polynomial regression order (o) 0 and first (1st) and second (2nd) derivatives using S-G, with window size (w) of 9 to 1, where a window size of (9) was chosen since it showed the best performance. Standard normal variate (SNV) was applied to correct the effects of light scattering (Barnes, Dhanoa, and Lister 1989; Martens and Geladi 1983). Voltage matrix data obtained by the e-nose device were pre-processed using only autoscaling (AS). For both NIR and e-nose data, Venetian blinds with 10 splits and blind thickness of 1 were used for cross-validation. For the classification model (PLS-DA) samples were randomly divided into a subset composed of 70% of samples for calibration and 30% for validation (external test set). For LDA cross-validation and discriminant function was used using the same dataset used for PLS-DA.

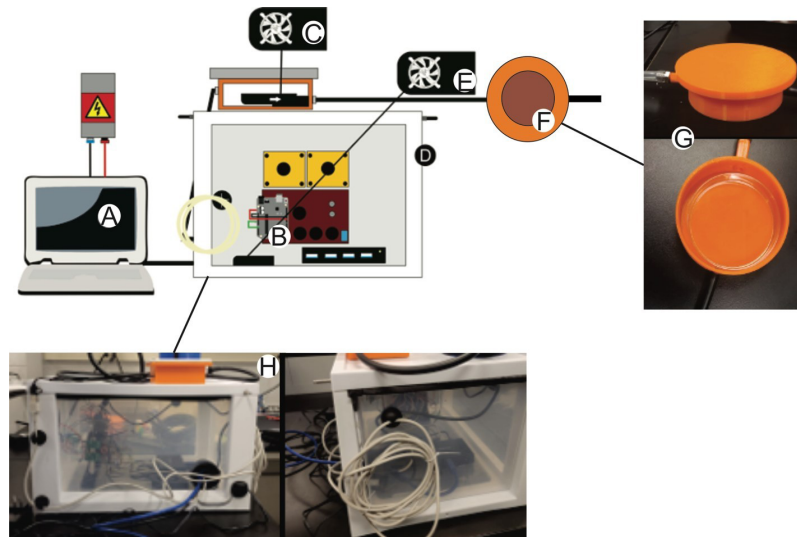


Figure 1.1: Low-cost-e-nose.

* (A) computer, (B) motherboard + sensors, (C) air pump, (D) sensor chamber, (E) fan for air convection, (F and G) sample chamber, (H) sensors chamber.

1.3.6.3 Principal Component Analysis (PCA)

Principal component analysis (PCA) is an exploratory analysis that works by projecting the data points onto principal components and simultaneously keeping the most variation as possible. This method was used as an unsupervised screening method for an overview of the variation between samples, and to identify the most important wavelengths for NIR spectra and the importance of each e-nose sensor to tea volatiles variation. PCA plots were designed with the

complete data range using the singular value decomposition algorithm (SVD) (95% confidence level) for the computation of the eigen generic sequence and a further cluster of the data. To build a PCA plot, outliers (anomalous measuring) were identified and excluded using the amount of Q residuals and Hotelling T² plots.

1.3.6.4 Linear Discriminant Analysis (LDA)

Linear Discriminant Analysis is a method derived from Fisher's linear discriminant analysis and operates by finding linear combinations from sample's features that will further characterize and classify them into different classes. LDA was applied as a supervised classification method using the most important wavelengths identified in the loadings from PCA using MINITAB® (Release 14.12.0). The performance of the classification models was evaluated by sensitivity (Eq. 8.1) and specificity (Eq. 8.2), accuracy (Eq. 8.3), F1 score (Eq. 7.4) and error rate (Eq. 7.5).

$$\text{Sensitivity (\%)} = \frac{TP}{(TP+FN)} \times 100 \quad (8.1)$$

$$\text{Specificity (\%)} = \frac{TN}{(TN+FP)} \times 100 \quad (8.2)$$

$$\text{Accuracy (\%)} = \frac{(TP+TN)}{TOTAL} \times 100 \quad (8.3)$$

$$\text{F1 score (\%)} = \frac{(TP+TN)}{TOTAL} \times 100 \quad (8.4)$$

$$\text{Error rate (\%)} = \frac{(FP+FN)}{TOTAL} \times 100. \quad (8.5)$$

Where, TP = true positive; FN = false negative; TN = true negative; and FP = false positive.

1.4 Results and Discussion

1.4.1 Principal Components Analysis (PCA)

1.4.1.1 Raw for NIR systems

Raw spectra for bow BNIR and PNIR equipment, for three tea origins (Brazil - red, India - green and US - blue) is presented in Figure 1.2 a and b respectively. For both device's the whole spectra was used for the purpose of the study which was discriminate the origin of black tea. As well as the average spectra that is presented in Figure 1.3 a and b, respectively.

It is possible to effectively assign the spectral stretching and bending of chemical bonds (O-H, N-H, and C-H) between 700 and 2505 nm utilizing different NIR equipment measurement modes. Therefore, the precise absorption of organic molecules in the NIR range can offer useful information on their chemical composition. Since NIR absorption bands frequently overlap, they reduce the sensitivity of conventional spectroscopy. For tea most of the absorption are related to polyphenols and caffeine for example in the range of 1100 - 1450 while from 1900 - 2500 catechins play an important role in tea chemical composition (Wang et al. 2018).

The removal of noise, variability, uncertainties, and undetected features using pattern recognition techniques is frequently used to accurately evaluate the original spectral data of NIR spectroscopy. NIR spectroscopy allows direct absorption of highly scattering substances, without the need for lengthy pre-treatments (Ni et al. 2018; Zhu et al. 2019). On the spectra data in this research, we used a 9-window first and second derivative approach. This method enabled us to improve the spectral characteristics and extract useful data for future investigation and interpretation.

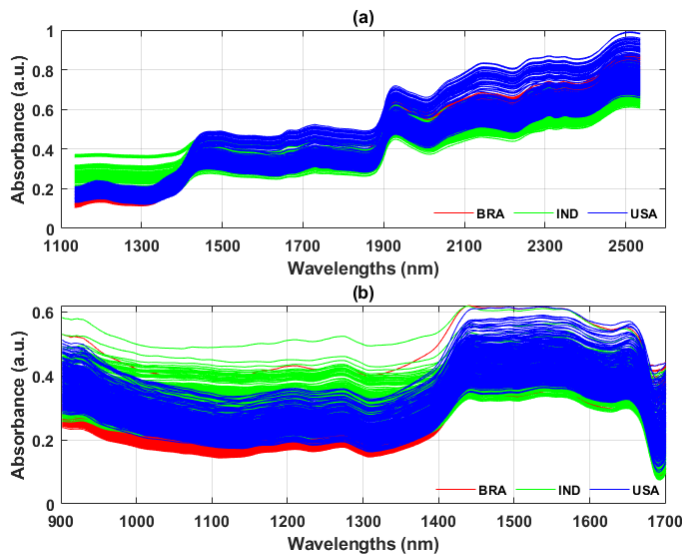


Figure 1.2 Raw Spectra for BNIR (a) and PNIR (b) for each type of sample (red, green, blue, insert which sample they are).

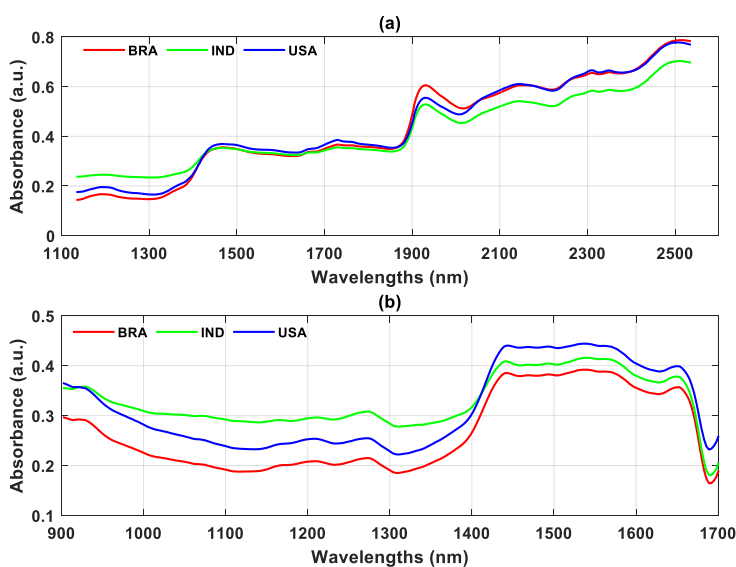


Figure 1.3 Average Spectra for BNIR (a) and PNIR (b). Red, Brazil, green, India, Blue, USA.

1.4.1.2 PNIR results

For PNIR, PC1 and PC2 explain more than 90.3% of the total variance (Figure 1.4). United States samples are positioned in negative scores for PC2, while India samples are mainly positioned in positive scores of PC2, with samples from Brazil in between them. The loadings (Figure 1.4b) show that the wavelengths 980, 1204, 1302, 1400, 1450 and 1660 are responsible for the variation in both PC1 and PC2, as PC2 was mostly responsible for sample discrimination according to their origin. The wavelength at 980 nm is related to hydrogen and oxygen (H-O) (Osborne 1986) which is also related to total catechins (Chen et al. 2018), and carbon and hydrogen interaction related to aromatic compounds (Magwaza et al. 2012). Wavelengths 1302 and 1400 nm might be related to organic acids (Weyer and Lo 2006) and free amino acids (Chen et al. 2018). From those, 1400 nm overlap with water which is correlated to the moisture present in the leaves. The peaks at 1400 and 1700 nm are associated with caffeine and catechins respectively (Chen et al. 2018; Osborne 1986).

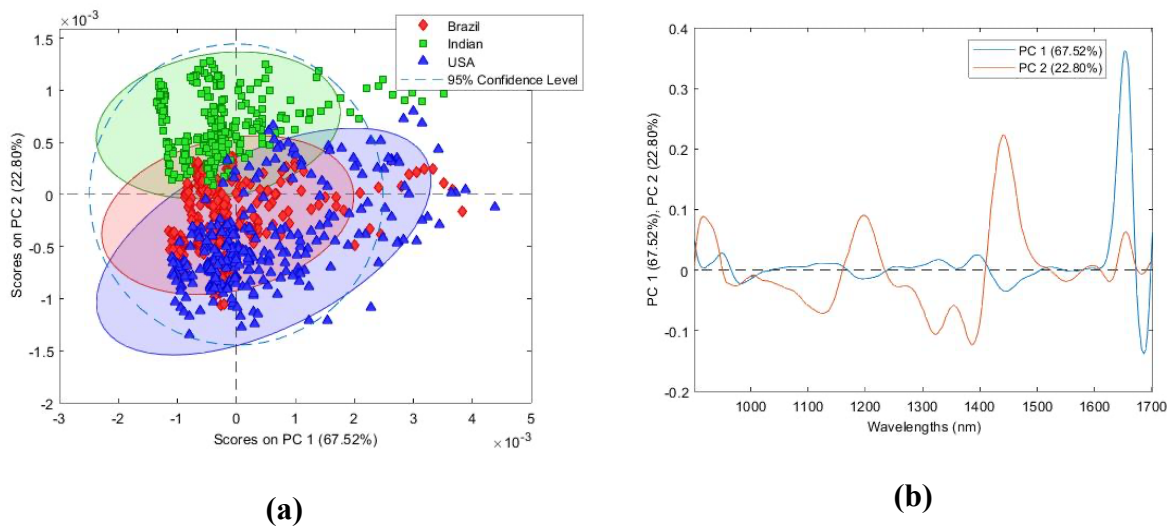


Figure 1.4. PCA (a) scores and (b) loadings for NIR spectra for PNIR

1.4.1.3 BNIR results

As per BNIR, PC1 and PC2 explain more than 85.35% of the total variance (Figure 1.5), where from PC1, Brazil and India samples fall in positive and negative values, respectively showing an excellent separation. PC2 shows a separation between USA samples, which are on positive scores, and Brazil and India samples, located in the negative scores. The loadings (Figure 1.5b) show, in addition to the wavelengths for BNIR PCA, the wavelengths 1900, 2000, 2101, 2200 and 2404 nm. The absorption peak observed at 1920–1940 nm might correspond to the combination of stretching and bending of the O-H bond of water and 1940–2404 nm to total catechins C - H first overtone and S - H first overtone and catechins that involves C=O stretching second overtones, C-H and C-H combinations (Chen et al. 2018). The separation in the PCA scores plot, in addition to the peaks in the PCA loadings, demonstrates the importance of the wavelength range between 1700nm and 2500nm to differentiate the tea samples.

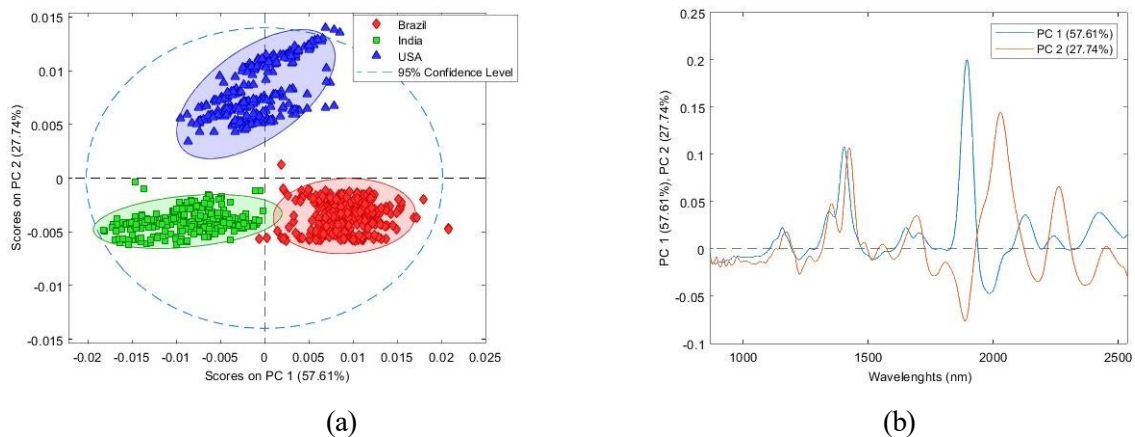


Figure 1.5: PCA (a) scores and (b) loadings for BNIR spectra reflectance mode for BNIR

1.4.2 PCA for LC-e-nose system

The general signal response collected for 2 minutes is shown in (Figure 1.5) for the concentration versus time for the six MQ sensors. Humidity and temperature were kept constant at $40 \pm 2\%$ and $25 \pm 2^\circ\text{C}$ for the same period. The variables for PCA plot were accounted as the sensors (MQ2, MQ3, MQ4, MQ5, MQ8 and MQ135), where each value corresponded to each sensor and was assigned for that specific sensor.

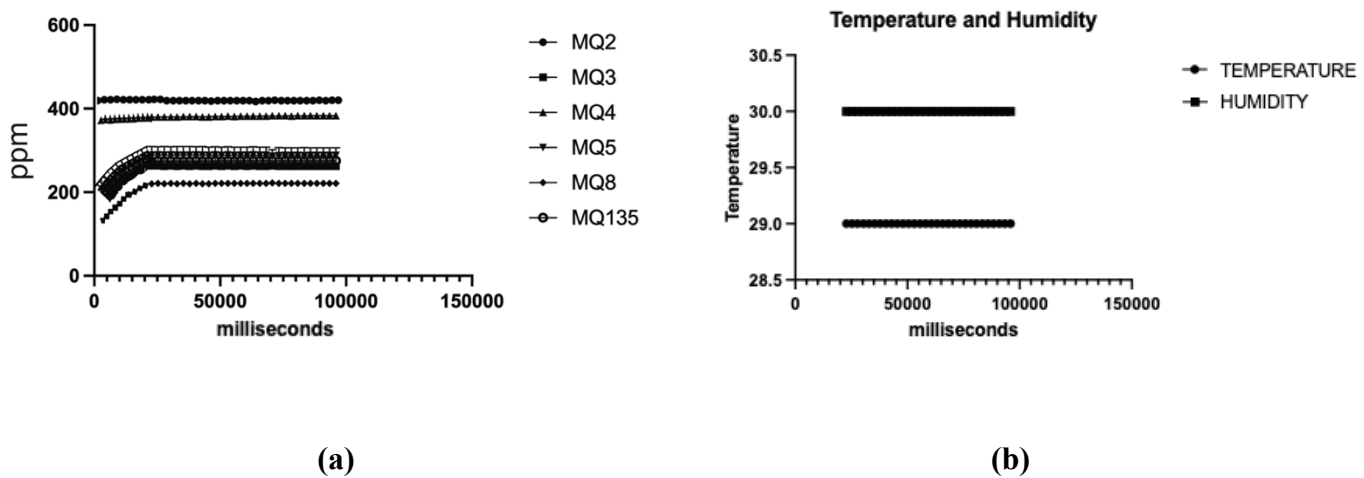


Figure 1.6: LC-e-nose Acquisition data (a) and temperature and humidity reading (b).

PCA was performed using data from the whole data set for all 6 sensors used in the e-nose (Figure 7.8) shows the PCA scores (PC1 vs PC2), where USA samples were on the negative side for both PC1 and PC2 scores, while India samples were in the positive side of PC2. Samples from Brazil were located in between samples from USA and India. It can be observed that India and Brazil samples were divided in two clusters within each origin; these two groups might be due to the BOP and FBOP varieties used in the assay. Together, PC1 and PC2 explained 85.83% of the total variation, demonstrating that LC-e-nose can differentiate samples according to their origin.

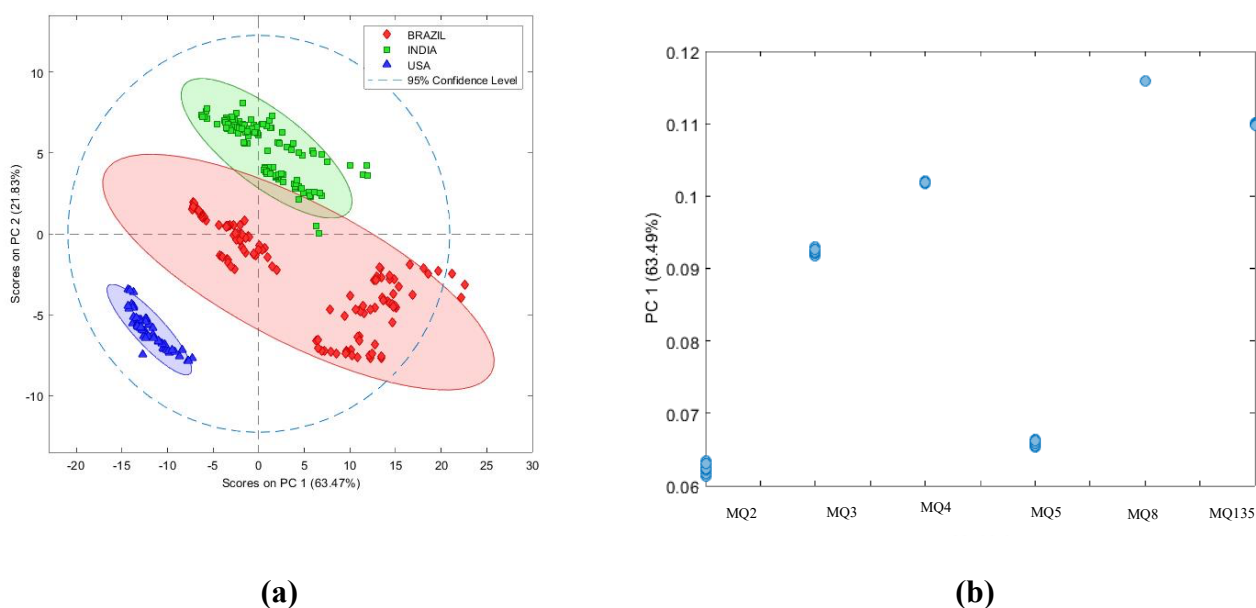


Figure 1.7: PCA (a) scores and (b) loadings for LC-e-nose

The loadings Figure 7.9 shows the most responsive sensors were MQ3, MQ4, MQ8 and MQ135. Black tea is rich in four epimers derived from major catechins (comprising approximately 80% of black tea), which include epicatechin (EC), epicatechin gallate (ECG), epigallocatechin (EGC), and epigallocatechin gallate (EGCG). It is noteworthy that approximately 80% of these epimers may undergo changes during the fermentation process and can be identified in VOCs profile (Liu et al., 2022). These volatile organic compounds (Figure 1.8), such as catechins caffeine and theaflavins structure, are identified by MQ3 (alcohol), MQ135 (volatile compounds such as NH₃, NO_x, alcohol, Benzene, smoke, CO₂), MQ4 (methane (CH₄), MQ8 (inflammable gasses (Hydrogen gas), that account for these and other VOCs (Ghosh et al. 2019; Tseng et al. 2021).

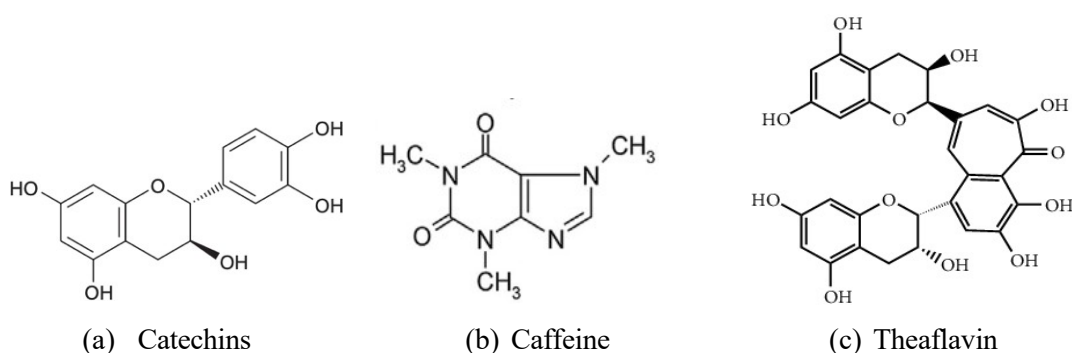


Figure 1.8: The major VOCs structure in black tea: Catechins (a), Caffeine (b) and Theaflavin (c).

Theaflavin, caffeine, and catechins are not normally gaseous substances in and of themselves. Nevertheless, they might be parts of chemicals that, in some circumstances, result in gaseous byproducts. For instance, volatile organic compounds (VOCs) can be released during the heat breakdown of organic materials containing these substances and can be catch by MOS sensors. One example is the following compounds: benzeneacetaldehyde, (Z)-3-hexenol,1,3-

dimethyl-benzene, dimethyl sulfide, (Z)-3-hexenyl butyrate, ethylbenzene, 1-penten-3-ol, (E) - 4,8-dimethylnona-1,3,7-triene, 3 - heptanone, (Z)-3-hexenyl- α -methylbutyrate, 2-decanone, and 2-butylfuran which are produced through the Strecker degradation reaction of phenylalanine and has a distinct rose-like aroma as well as Additionally, dimethyl sulfide, known for its cabbage like odor is considered a beneficial component contributing to the aroma of oolong tea (Xue et al. 2022).

1.4.3 HPLC Analysis

Data for GC-MS is shown in figure 7.11. The peak for caffeine (the most relevant for aroma in tea) are shown in the chromatogram. Peaks 1.40 has been attributed to caffeine in all three origins variants while other registered peaks 1.39, 1.43 and 1.52 different were observed USA samples. Similarity has been found for Brazilian and Indian samples, which can explain their proximity in PCA plot. Other studies evaluating caffeine as major VOCs in tea that contributes to aroma corresponding to 3-5 % measured using HPLS, which is a versatile and efficient technique that can greatly improve the separation of caffeine from other substances such as tannic acid and caffeic acid. The development of specialized techniques suited to the separation of these particular substances is made possible by the optimization of chromatographic conditions, including the selection of stationary and mobile phases (Shrestha 2016). Teas derived from *Camellia sinensis* exhibit higher caffeine levels compared to mate tea, with notable variations observed among different types of tea, brands, and batches. An intriguing aspect of the study reveals that a significant portion of caffeine present in tea leaves is transferred to the infusion during the preparation process. The research, as outlined in Table 2, highlights the average daily intake of 263 mL of tea contributing to a potential ingestion of up to 47.6 mg day⁻¹ of caffeine HPLC data identified caffeine content in many tea samples including black (TFOUNI, 2018). Since caffeine forms are almost important as tea VOCs, the identification and classification of tea might rely on this compound.

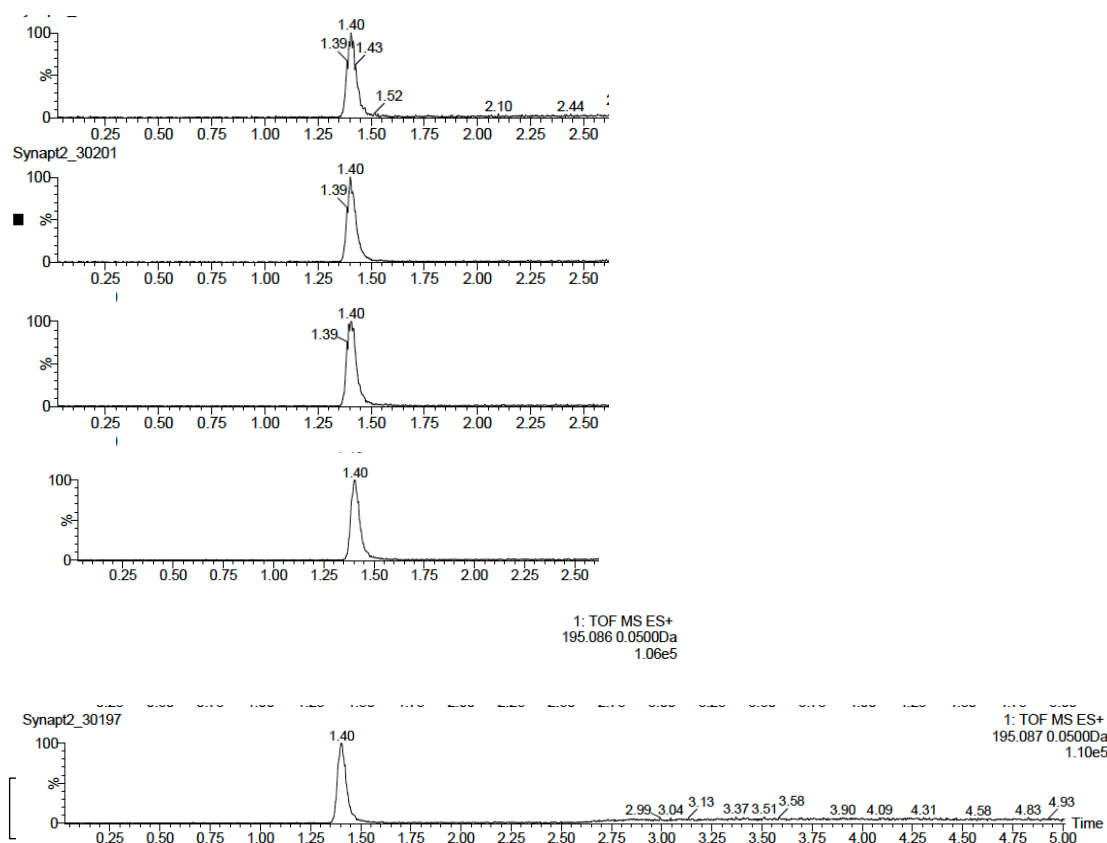


Figure 1.9 HPLC chromatogram for Caffeine in the tree tested tea origins (BR, IND and USA)

1.4.4 Classification model using LDA

1.4.4.1 LDA for NIR Systems

LDA were performed using only few selected wavelengths for PNIR (1103, 1204,1302, 1400, 1450 and 1660) and BNIR (1100,1400, 1701, 1900, 2000, 2101, 2201, 2404). Results for LDA using spectra acquired by PNIR showed one misclassifications of sample from Brazil (classified as USA) and six samples for USA (classified as Brazil) (Figure.11a); while for BNIR there was Brazil sample misclassified as USA (Figure 11b). Both PNIR and BNIR models showed overall F1-scores over 99%. All values for F1-scores, sensitivity, specificity, accuracy and error rate are presented in Table 2.

A previous study reported the discrimination of black tea samples using LDA applied to NIR spectra to find the linear combination of variables that optimally separate tea classes according to the fermentation, tea polyphenols and catechins that are oxidized and polymerized by polyphenol oxidase, in which unique flavor compounds of black tea are formed. The interval tested was from 950 to 2400 (1140–1160, 1430–1450 and 1920–1940 nm), and the classification rate (%) ranged from 58.33 using Competitive adaptive reweighted sampling (CARS), to 75% using PCA (Zhang et al. 2023). Tea types dark, black, green, white, oolong, yellow from different countries (China, India, Japan, Kenya and Taiwan) were classified using LDA (Egger and Yu 2022) Similar problem in performance was also spot when discriminating eleven Sri Lankan tea using spectroscopy methods (e.g., Raman) that present a sharp focused signal when compared to NIR (Seetohul et al. 2013), which is the problem with high collinearity issues (Egger and Yu 2022).

Statistical Methods	Equipment	Origin	Sensitivity	Specificity	Accuracy	F1-score	Error rate	
LDA	PNIR	BR	0,997	0,989	0,992	0,988	0,008	
		USD	1,000	1,000	1,000	1,000	0,000	
		USA	0,979	0,998	0,992	0,987	0,008	
	BNIR	BR	0,997	1,000	0,999	0,998	0,001	
		USD	1,000	1,000	1,000	1,000	0,000	
		USA	1,000	0,998	0,999	0,998	0,001	
	LC-e-nose	BR	0,993	0,995	0,994	0,993	0,006	
		USD	1,000	1,000	1,000	1,000	0,000	
		USA	0,985	0,996	0,994	0,985	0,006	
	PLSDA	PNIR	BR	0,989	0,994	0,992	0,989	0,080
			USD	1,000	1,000	1,000	1,000	0,000
			USA	0,988	0,994	0,992	0,988	0,008
BNIR		BR	1,000	1,000	1,000	1,000	0,000	
		USD	1,000	1,000	1,000	1,000	0,000	
		USA	1,000	1,000	1,000	1,000	0,000	
LC-e-nose		BR	1,000	0,982	0,990	0,989	0,010	
		USD	1,000	1,000	1,000	1,000	0,000	
		USA	0,947	1,000	0,990	0,973	0,010	

Table 1.2 Sensitivity, specificity, accuracy, and error rate values for classification of tea origin

		True Class				
		Brazil	India	US		
Predicted Class	Brazil	299	0	6	Predicted Class	
	India	0	280	0		
	US	1	0	274		

(a)

		True Class				
		Brazil	India	US		
Predicted Class	Brazil	299	0	0	Predicted Class	
	India	0	280	0		
	US	1	0	280		

(b)

		True Class				
		Brazil	India	US		
Predicted Class	Brazil	141	0	1	Predicted Class	
	India	0	129	0		
	US	1	0	66		

(c)

Figure 1.10: Confusion matrix of LDA (A) PNIR (B) BNIR and (C) LC-e-nose.

1.4.4.2 LDA for LC-enose

The LDA results for e-nose showed lower overall F1 score ($> 99\%$) (Figure 1.10). There was one misclassification for both American and Brazilian tea samples. These results could be related to collinearity issues (EGGER; YU, 2022), however the lower misclassification level might be related to the type of data. When compared to a high correlated spectra e-nose data tend to be less evident when performing LDA models. All parameters sensitivity, selectivity, accuracy, and error rate are presented in Table 1.2. For e-nose systems LDA has been used to discriminate smell and monitor fermentation during the manufacture of oolong tea leaves. They used their e-nose to ran an online experiment at a tea factory to evaluate the e-nose’s capabilities further. Monitoring the changes in scent that take place during the fermentation process was the main objective for real-time scent monitoring in industrial settings, particularly where the strength of particular aromas may vary dramatically. The grassy smell they observed that comes from freshly cut grass is a common odor caused by green leaf volatiles (TSENG et al., 2021). This grassy smell comes from green leaf volatiles Z-3-hexenal into its isomer, E-2-hexenal Z-3-hexenal and E-2-hexenal, Z-3-hexenol may also have contributed to the discrimination of black tea towards e-nose sensors specially MQ3 and MQ135. It has been shown that LDA performs well for e-nose systems. The most impressive and consistent classification performance over time was achieved by utilizing Linear Discrimination Analysis (LDA) on the normalized conductance data from the sensing layer of the MOS gas sensors. Through this supervised LDA analysis, we successfully mitigated the impact of sensor drift during a three-month evaluation period. This improved robustness can be attributed to the adoption of independent Gaussian mixture models, which effectively characterized the two clusters of calibration data. As a result, our approach demonstrates the potential for reliable and stable gas sensor classification in long-term monitoring applications, ensuring accurate and consistent results even in the face of sensor drift (PALACÍN; RUBIES; CLOTET, 2022).

1.4.5 Classification model using PLS-DA

1.4.5.1 PLS-DA for NIR Systems

The confusion matrix of PLS-DA models for tea samples for both PNIR and BNIR

spectra is shown in Figure 7.12, while sensitivity, selectivity, accuracy, F1-scores and error rate are presented in Table 2. The transformations performed in the data were mean center, with 1st S-G derivative (o 2, w 9), since they showed the best results. The best model for PLS-DA using PNIR spectra, showed overall F1-score >99%.

Compared to LDA, PLS-DA can handle multicollinearity better. By taking into account latent variables that account for the variance in both the predictor and response variables, PLS-DA can still function well in scenarios where there are highly linked predictor variables (features). On the other hand, because LDA makes the assumption that the predictors are independent, it may be vulnerable to multicollinearity. When the predictors and class labels have a moderate association, PLS-DA frequently offers superior prediction accuracy. It takes into account the relationship between predictors and response variables' covariance structure, improving discrimination (Lasalvia, Capozzi, and Perna 2022).

Application of PLS-DA models for black tea dianhong variety for tea quality has been reported and their achieved prediction ability was based on multiple manipulation of latent variables (LV) and pre-treatments algorithm. The authors also mention the corresponding chemical bonds of the above four feature wavelengths (1169, 1211, 1260, and 1482 nm) (Ren, Ning, and Zhang 2021), where CH-CH second overtone, C-H first overtone, the first overtone of C-H combinations, and C-H first overtone respectively, and their nutrients related to these chemical bonds were free amino acids and tea polyphenol (Chen et al. 2018). These wavelengths are similar to the ones found for black tea in this work and show the importance of understanding the overtones and differences in absorption bands from other datasets and tea varieties to obtain a holistic understanding of the present findings. Discrimination of the geographical origin of Oolong tea using NIR-infrared spectroscopy. Standard normal variate (SNV) was applied to raw data spectra, so that PLS-DA models were created. The training set was randomly split into a secondary training set (50%) and a secondary predicting set (50%) for 20 times in order to estimate the number of PLS-DA latent variables. The minimum misclassification rate was calculated using the number of latent variables that was chosen. The sensitivity and specificity of the PLS-DA model were therefore calculated using the items in the prediction class. The specificity and sensitivity reached was 100% and 93% respectively (Yan et al. 2014). The device presented in this paper was able to overcome this for BNIR and LC-enose in both parameters.

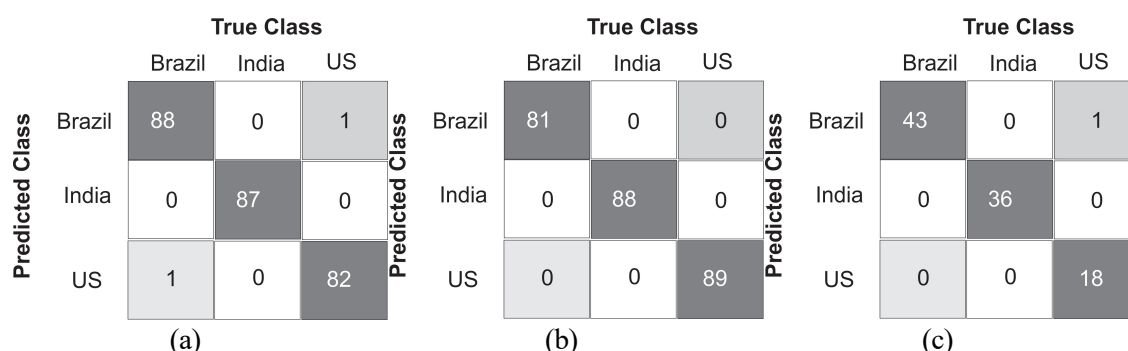


Figure 1.11: Confusion matrix of PLS-DA (a) PNIR (b) BNIR and (c) LC-e-nose.

* For PLS-DA calibration (70% cal) set and validation (30% test).

1.4.5.2 PLS-DA for LC-enose

The confusion matrix of PLS-DA models for tea samples for LC-e-nose is shown in (Figure 1.12), while sensitivity, selectivity, accuracy, F1-scores and error rate are presented in Table 2.

The transformations performed in the data were autoscaling. Regarding the best model for PLS-DA using PNIR spectra, showed overall F1-score >99%. The only misclassification was spot for USA samples. Similar good results were also demonstrated in previous use of e-nose for black tea classification and according to the findings, combined sensor response may categorize tea samples more accurately (classification rate of 99.75%). The suggested method is better suitable for discriminating between different tea quality levels when the performance of the extracted features is compared to that of various established techniques, two simple explanations for these include the ability of PLS-DA to deal with small dataset and reduce multicollinearity (Banerjee et al. 2019). Green Tea has been evaluated using PLS-DA models this time to analyze the aroma characteristics during drying process. The most important compounds found were Octanal, 5-Methyl-5-hepten-2-one, Benzene acetaldehyde, (Z)-3-hexen-1-ol, Pentan-1-ol, 3-Methylbutanal, Isopropyl alcohol. Additionally, PLS-DA scores of tea samples were 93.7 % (Yang et al. 2022) following the average performance found in the literature for e-nose devices (Chen et al. 2018; Yan et al. 2014; Yang et al. 2022). The performance of the model found in this work excel the ones found in the literature for both black and green tea.

1.5 Conclusions

The application of smart sensors technologies (e.g, NIR and e-nose) is indispensable in ensuring the production of high-quality food to meet the demands of a growing population. Our study focused on the test of Near-Infrared Spectroscopy (NIRS) using both portable and benchtop equipment, along with the innovative LC-e-Nose, and its power to identify black tea samples from different countries and processing methods. From the perspective of NIR spectroscopy, both PNIR and BNIR exhibited outstanding response when classifying tea based on its origin. Given the complexity of tea composition, which involves crucial components such as theaflavins, catechins, and caffeine, our study acknowledges the significant challenge posed to the tested equipment. The primary aim of this research was to demonstrate the feasibility of utilizing the LC-e-Nose device (at a cost of USD 200-300) for identification of tea origin. Therefore, our study establishes that low-cost NIR spectroscopy, in combination with novel and affordable customized LC-e-nose devices, can significantly contribute to the food industry's efforts in authenticating tea origin from different countries (Brazil, India, and USA). Embracing these cost-effective smart technologies, integrated with chemometrics, holds great promise for advancing tea quality control and ensuring consumer satisfaction in an increasingly dynamic and competitive market.

1.6 Acknowledgments

This study was financed in part by the Coordenação de Aperfeiçoamento de Pessoal de Nível Superior - Brasil (CAPES) - Finance Code 001, São Paulo Research Foundation (FAPESP) (project number 2015/24351-2) and Carlos Chagas Filho Foundation for Research Support of Rio de Janeiro State (FAPERJ) (project number E-26/210.631/2019). Marcus V S Ferreira acknowledges scholarship funding from CNPq, grant number 142568/2020-1. Prof. Douglas Fernandes Barbin is CNPq research fellow (308260/2021-0).

1.7 References

- BANERJEE, M. B. et al. Black tea classification employing feature fusion of E-Nose and E-Tongue responses. **Journal of Food Engineering**, Elsevier, v. 244, p. 55–63, 2019.
- BARNES, R. J.; DHANOA, M. S.; LISTER, S. J. Standard normal variate transformation and

- de-trending of near-infrared diffuse reflectance spectra. **Applied Spectroscopy**, SAGE Publications, London, England, v. 43, n. 5, p. 772–777, 1989.
- CHEN, Q. et al. Application of FT-NIR spectroscopy for simultaneous estimation of taste quality and taste-related compounds content of black tea. **Journal of Food Science and Technology**, Springer, v. 55, p. 4363–4368, 2018.
- EGGER, R.; YU, J. A Topic Modeling Comparison Between LDA, NMF, Top2Vec, and BERTopic to Demystify Twitter Posts. **Frontiers in Sociology**, Frontiers Media SA, v. 7, p. 886498, 2022.
- GHOSH, S. et al. A recurrent Elman network in conjunction with an electronic nose for fast prediction of optimum fermentation time of black tea. **Neural Computing and Applications**, Springer, v. 31, p. 1165–1171, 2019.
- HASTUTI, A. A. M. B.; ROHMAN, A. Application of elemental fingerprinting for the authentication of tea: A review. **Journal of Applied Pharmaceutical Science**, v. 12, n. 3, p. 045–054, 2022.
- LASALVIA, M.; CAPOZZI, V.; PERNA, G. A comparison of PCA-LDA and PLS-DA techniques for classification of vibrational spectra. **Applied Sciences**, MDPI, v. 12, n. 11, p. 5345, 2022.
- LI, S. et al. Black tea: chemical analysis and stability. **Food & Function**, Royal Society of Chemistry, v. 4, n. 1, p. 10–18, 2013.
- LIN, X.; SUN, D.-W. Recent developments in vibrational spectroscopic techniques for tea quality and safety analyses. **Trends in Food Science & Technology**, Elsevier, v. 104, p. 163–176, 2020.
- LIU, Z. et al. Dynamic changes of volatile and phenolic components during the whole manufacturing process of Wuyi Rock tea (Rougui). **Food Chemistry**, Elsevier, v. 367, p. 130624, 2022.
- LOUTFI, A. et al. Electronic noses for food quality: A review. **Journal of Food Engineering**, Elsevier, v. 144, p. 103–111, 2015.
- MAGWAZA, L. S. et al. NIR spectroscopy applications for internal and external quality analysis of citrus fruit—a review. **Food and Bioprocess Technology**, Springer, v. 5, p. 425–444, 2012.
- MARTENS, J. H. S.; GELADI, P. Multivariate Linearity Transformations for Near-Infrared Reflectance Spectrometry. In: PROCEEDINGS of Nordic Symposium for Applied Statistics. [S.l.: s.n.], 1983. p. 205–234.
- NI, K. et al. Multi-element composition and isotopic signatures for the geographical origin discrimination of green tea in China: A case study of Xihu Longjing. **Journal of Food Composition and Analysis**, Elsevier, v. 67, p. 104–109, 2018.
- OSBORNE, B. G. Theory of Near Infrared Spectrophotometry. In: [s.l.]: John Wiley & Sons, Ltd Chichester, UK, 1986. p. 212.
- PALACÍN, J.; RUBIES, E.; CLOTET, E. Application of a Single-Type eNose to Discriminate the Brewed Aroma of One Caffeinated and Decaffeinated Encapsulated Espresso Coffee Type. **Chemosensors**, MDPI, v. 10, n. 10, p. 421, 2022.
- PEARCE, T. C. et al. **Handbook of Machine Olfaction: Electronic Nose Technology**. [S.l.]: John Wiley & Sons, 2003.

- POREP, J. U.; KAMMERER, D. R.; CARLE, R. On-line application of near infrared (NIR) spectroscopy in food production. **Trends in Food Science & Technology**, Elsevier, v. 46, n. 2, p. 211–230, 2015.
- REN, G.; NING, J.; ZHANG, Z. Multi-variable selection strategy based on near-infrared spectra for the rapid description of dianhong black tea quality. **Spectrochimica Acta Part A: Molecular and Biomolecular Spectroscopy**, Elsevier, v. 245, p. 118918, 2021.
- REN, G. et al. Rapid characterization of black tea taste quality using miniature NIR spectroscopy and electronic tongue sensors. **Biosensors**, MDPI, v. 13, n. 1, p. 92, 2023.
- SCALA, A. et al. Green leaf volatiles: a plant's multifunctional weapon against herbivores and pathogens. **International Journal of Molecular Sciences**, MDPI, v. 14, n. 9, p. 17781–17811, 2013.
- SEETOHUL, L. N. et al. Discrimination of Sri Lankan black teas using fluorescence spectroscopy and linear discriminant analysis. **Journal of the Science of Food and Agriculture**, Wiley Online Library, v. 93, n. 9, p. 2308–2314, 2013.
- TSENG, T.-S. et al. Utilization of a gas-sensing system to discriminate smell and to monitor fermentation during the manufacture of oolong tea leaves. **Micromachines**, MDPI, v. 12, n. 1, p. 93, 2021.
- VISCARRA ROSSEL, R. A. ParLeS: Software for chemometric analysis of spectroscopic data. **Chemometrics and intelligent laboratory systems**, Elsevier, v. 90, n. 1, p. 72–83, 2008.
- WANG, J. et al. Enhanced cross-category models for predicting the total polyphenols, caffeine and free amino acids contents in Chinese tea using NIR spectroscopy. **LWT**, Elsevier, v. 96, p. 90–97, 2018.
- WEYER, L. G.; LO, S.-C. Spectra–structure correlations in the near-infrared. In: **HANDBOOK of Vibrational Spectroscopy**. [S.l.]: Wiley Online Library, 2006.
- XU, Y.-m.; QIAO, F.-b.; HUANG, J.-k. Black tea markets worldwide: Are they integrated? **Journal of Integrative Agriculture**, Elsevier, v. 21, n. 2, p. 552–565, 2022.
- YAN, S.-M. et al. Rapid discrimination of the geographical origins of an Oolong tea (Anxi-Tieguanyin) by near-infrared spectroscopy and partial least squares discriminant analysis. **Journal of Analytical Methods in Chemistry**, Hindawi, v. 2014, 2014.
- YANG, Y. et al. Aroma dynamic characteristics during the drying process of green tea by gas phase electronic nose and gas chromatography-ion mobility spectrometry. **LWT**, Elsevier, v. 154, p. 112691, 2022.
- ZHANG, B. et al. Discrimination of black tea fermentation degree based on multi-data fusion of near-infrared spectroscopy and machine vision. **Journal of Food Measurement and Characterization**, Springer, p. 1–12, 2023.
- ZHU, M.-Z. et al. The quality control of tea by near-infrared reflectance (NIR) spectroscopy and chemometrics. **Journal of Spectroscopy**, Hindawi, v. 2019, 2019.

CONCLUSÕES GERAIS

Ambos os equipamentos low-cost-e-nose mostraram ser uma ferramenta confiável para testar a qualidade em alimentos, o primeiro desenvolvido no Brasil foi capaz de classificar corretamente a pitaya com precisão superior a 90% e apresentou bons modelos de predição para TA e pH com os mesmos padrões como sensores NIR. Este último apresentou grande capacidade de classificar e prever a pitaya para controle de qualidade, apresentando excelente poder de classificação e predição para o índice de vida de prateleira proposto para LDA, PLS-DA e PLSR. O segundo Low-cost-e-nose também foi aplicado de forma eficiente, desta vez para o chá preto mostrando novamente excelentes resultados, onde desta vez alguns recursos como limitação de headspace, fatores de convecção e controle de umidade e temperatura foram abordados. O poder de classificação do LC-e-nose foi semelhante aos dois sensores ópticos comparados PNIR e BNIR mostrando classificação de 99% para F1-scores para equipamentos LC-e-nose. No geral, os dois dispositivos LC-e-nose foram capazes de serem usados para controle de qualidade de frutas e commodities vegetais (chá preto), portanto, podem ser usados em nível industrial para aprimorar o monitoramento como uma técnica de detecção inteligente semelhante às tarefas já atribuídas aos sensores NIR. Para estudos futuros alguns recursos devem ser realizados, como seleção de sensores e sensibilidade, o uso de uma variedade de tipos de sensores para aumentar a sensibilidade e seletividade. Diferentes sensores podem ser mais adequados para detectar tipos específicos de odores. Também, como a combinação de várias tecnologias de sensores (por exemplo, polímeros condutores, sensores de óxido metálico, microbalanças de cristal de quartzo) que podem melhorar o desempenho geral do sistema. Para calibração e processamento de dados, desenvolvemos técnicas de calibração robustas para levar em consideração o desvio do sensor, o envelhecimento e as mudanças ambientais. Algoritmos avançados de processamento de dados, como aprendizado de máquina e inteligência artificial, podem ajudar no reconhecimento de padrões e na melhor identificação de odores.

PERSPECTIVAS FUTURAS

Com base nos resultados apresentados nesta tese, as perspectivas futuras para o desenvolvimento e aprimoramento de dispositivos LC-e-nose são promissoras. Para estudos subsequentes, é crucial explorar a seleção criteriosa de sensores e sensibilidades, incorporando uma variedade de tipos de sensores para potencializar a sensibilidade e seletividade do sistema. A avaliação de diferentes sensores, como polímeros condutores, sensores de óxido metálico e microbalanças de cristal de quartzo, pode oferecer uma abordagem mais refinada na detecção de odores específicos. Além disso, a combinação sinérgica de diversas tecnologias de sensores pode elevar o desempenho global do sistema LC-e-nose. A calibração e o processamento de dados demandarão atenção contínua, com o desenvolvimento de técnicas robustas para lidar com desvios de sensores, envelhecimento e variações ambientais. A aplicação de algoritmos avançados de processamento de dados, incluindo aprendizado de máquina e inteligência artificial, surge como uma área promissora para otimizar o reconhecimento de padrões e a identificação precisa de odores, consolidando assim a LC-e-nose como uma ferramenta inteligente e eficaz para o monitoramento e controle de qualidade de alimentos em ambientes industriais.

APÊNDICE

APÊNDICE 1: Leitura com E-nose 1 utilizando a pitaya Capítulo II

1.1 Esquema do Enose-1 e NIR usados no artigo do Capítulo II.....	94
1.2.Acidez titulável.....	95
1.3.pH.....	95
1.4. Fenólicos totais – curva padrão	96
1.5. Umidade	96
1.6. Solidos totais	96

APÊNDICE 2: Tabelas suplementares utilizadas no Capítulo II

2. Tabelas suplementares utilizadas no Capítulo II	
2.1 Tabela 1.9 Correlação de Pearson.....	98
2.2 Tabela 1.10 LDA parametros usando NIR.....	98
2.3 Tabela 1.11 LDA parametros usando NIR.....	98
2.4 Tabela 1.12 LDA parametros usando Enose1	98
2.5 Tabela 1.13 LDA parametros usando Enose1	98
2.6 Tabela 1.14 PLSR parametros usando Enose1.....	100

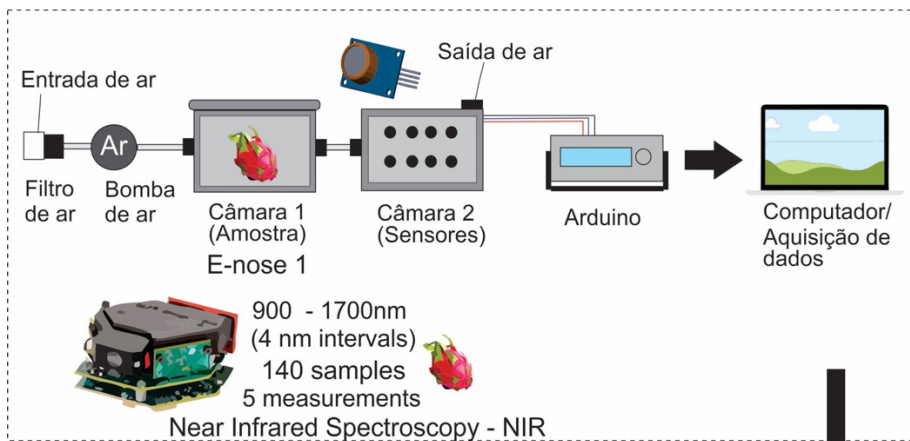
APÊNDICE 3: Metodologias detalhadas utilizadas no Capítulo III

3. Metodologias detalhadas utilizadas no Capítulo III.....	101
3.1. Aplicação do Enose 2 em chás.....	102
3.2. Procedimento – análise dos chás com NIR.....	103
3.3. Procedimento HPLC.....	104
3.3. Procedimento Curva padrão HPLC.....	105

APÊNDICE 4: Fotos de equipamento utilizados nos capítulos II e III

4.1. E-nose 1.....	106
4.2. Protótipo e-nose 2.....	107
4.3. Prototipo e-nose 2 e câmaras.....	110

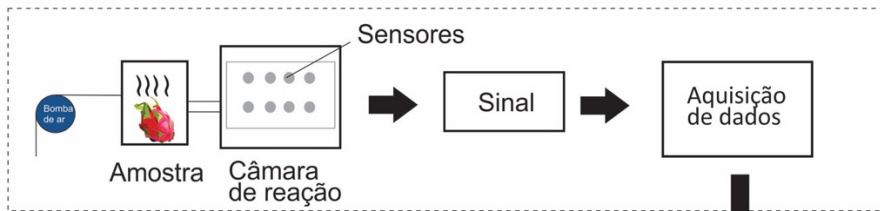
APÊNDICE 5: Artigo adicional Computer vision.....	111
---	-----



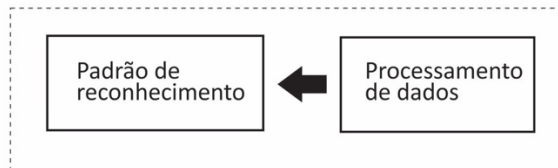
Parte Lógica



Parte Física



Parte Lógica



1.1 Esquema do Enose-1 e NIR usados no artigo do Capítulo II

1- Acidez titulável

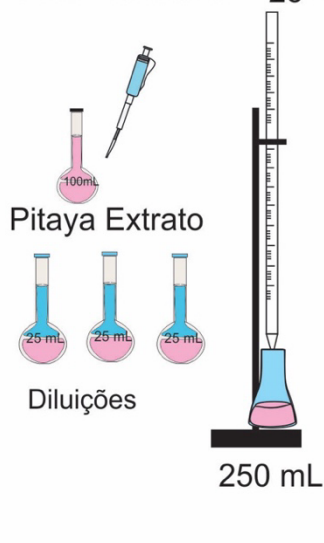
2- pH

3- Fenólicos Totais (curva padrão 3.1 e análise 3.2)

4- Umidade

5- Sólidos Totais.

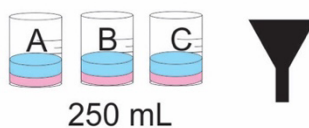
1- Acidez titulável 25 - 50 mL



O pH foi determinado utilizando-se um medidor de pH (modelo MB-10; Marte, São Paulo, Brasil), A acidez titulável foi medida a partir do suco da fruta (NIELSEN et al., 2003)

Suco de pitaya, 60 mL

- 3 Copos de 250 mL
- 2 Burets, 25 ou 50 mL
- 4 frascos Erlenmeyer, 250 mL
- Funil, pequeno, para caber topo de buret de 25 ou 50 mL
- Cilindro graduado, 50 mL
- 2 pipetas volumétricas, 10 ou 20 mL



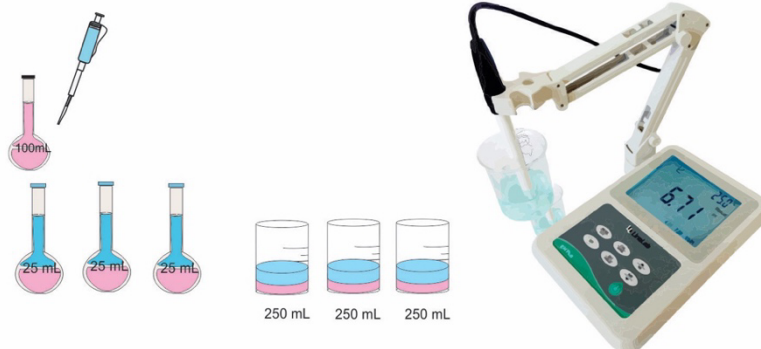
Em cada um dos três (A, B, C) 250- mL de béqueres, pipeta de 20 mL de suco de Pitaya.

Adicionar

cerca de 50 mL de água livre de CO₂ para cada um. Para a amostra C,

Adicione três gotas de uma solução de fenolftaleína a 1%. Usando dois burets preenchidos com a solução padronizada de NaOH (ca. 0.1N), titular as amostras B e C simultaneamente.


2- pH



Siga o pH durante titulação da amostra C contendo fenolftaleína.



3.1- Curva Padrão Fenólicos

1 Solução de Folin Ciocalteu (1:3)
Diluir 12,5 mL do Reativo Folin Ciocalteu (p/ fenol) para 37,5 mL de água destilada, homogeneizar e transferir para um frasco de vidro âmbar devidamente etiquetado. Armazenar em temperatura ambiente por até um mês.



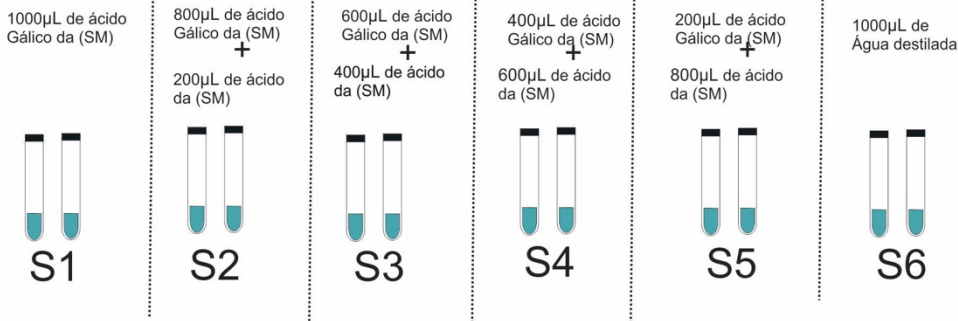
2 Dissolver 10 g de carbonato de sódio (Na_2CO_3) para cada 100 mL de água destilada.

3 Solução de Ácido Gálico
Dissolver 5 mg de Ácido Gálico (PM = 170,12) em água destilada e completar para 100 mL em um balão volumétrico âmbar (Solução Mãe -SM) e homogeneizar. Preparar e usar apenas no dia da análise.

CURVA-PADRÃO DO ÁCIDO GÁLICO

4 A partir da solução inicial de 100 mL de Ácido Gálico 50 μg (Solução Mãe) prepara no item 3. Utilizando diluições sucessivas, preparar as demais soluções variando de 0 a 40 μg



Vide Tabela 1.

5 Em seguida acrescentar 1 mL do folin ciocalteu (1:10), 1 mL do carbonato de sódio 10% e 1 mL de água destilada (Obanda & Owor, 1997- adaptado). Homogeneizar a amostra e deixar em repouso à temperatura ambiente e protegido da luz por 2 horas

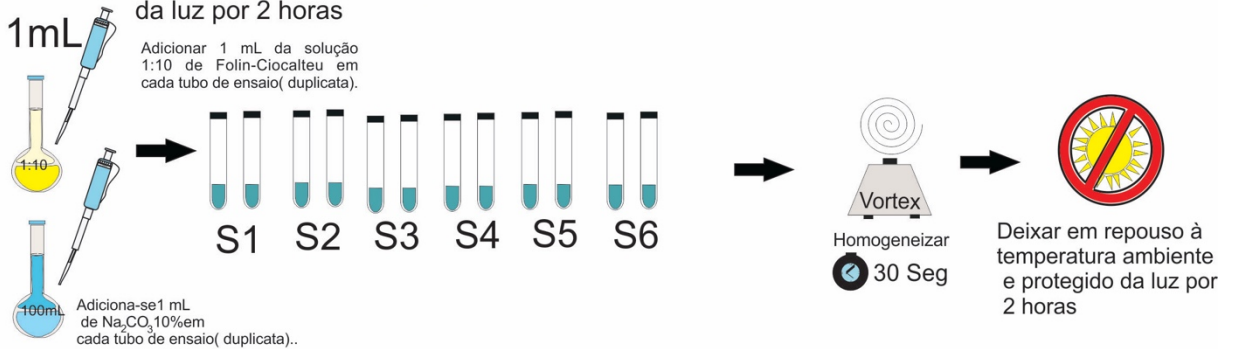
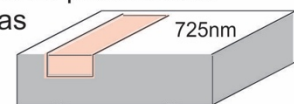


Tabela 1. Preparo das soluções para curva-padrão.

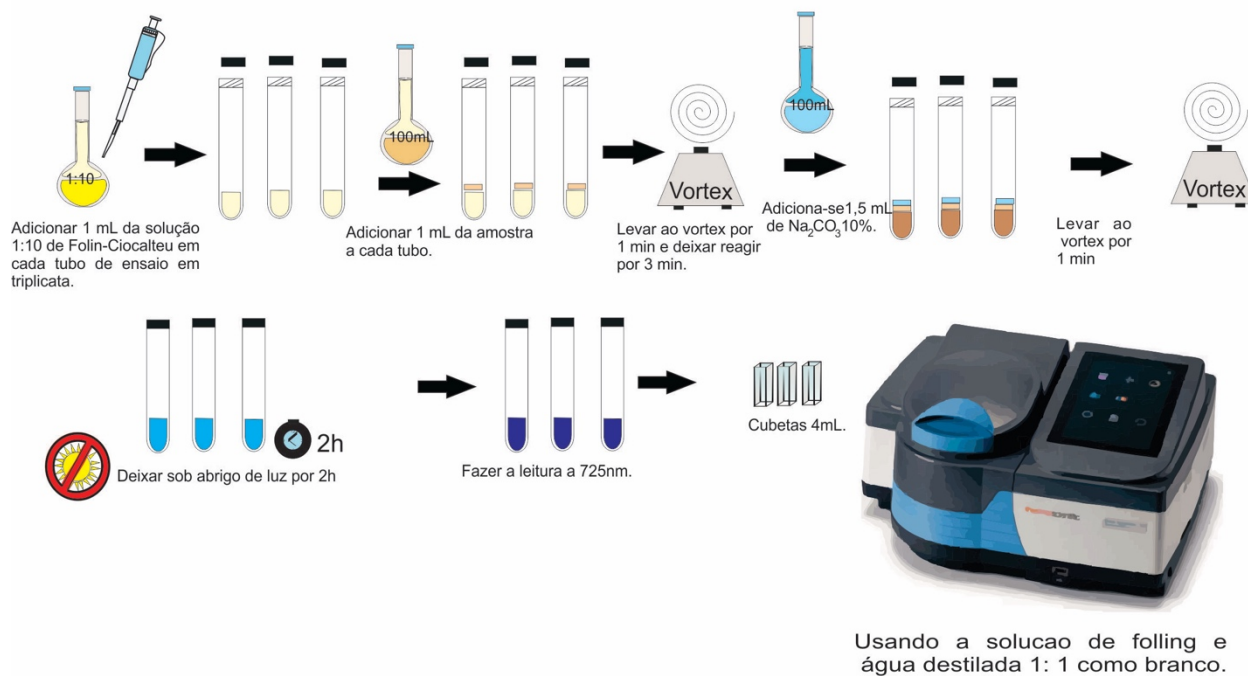
[Ácido Gálico] (μg)	Padrão (μL)	Água destilada (μL)
S6 - 0	0	1000
S5 - 10	200	800
S4 - 20	400	600
S3 - 30	600	400
S2 - 40	800	200
S1 - 50	1000	0

6 Em ambiente escuro, transferir as concentrações para as cubetas de poliestireno. As leituras, em espectrofotômetro a 725 nm, devem ser realizadas após 2 horas. O espectrofotômetro deve ser zerado com a solução S6.

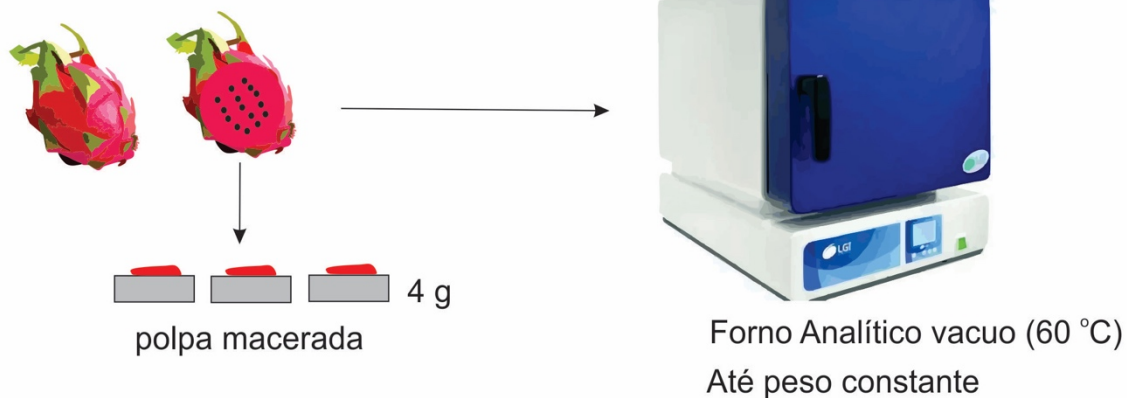


Usando a solução S6 como branco.

3.2- Fenólicos Totais



4- Umidade



5- Sólidos Totais

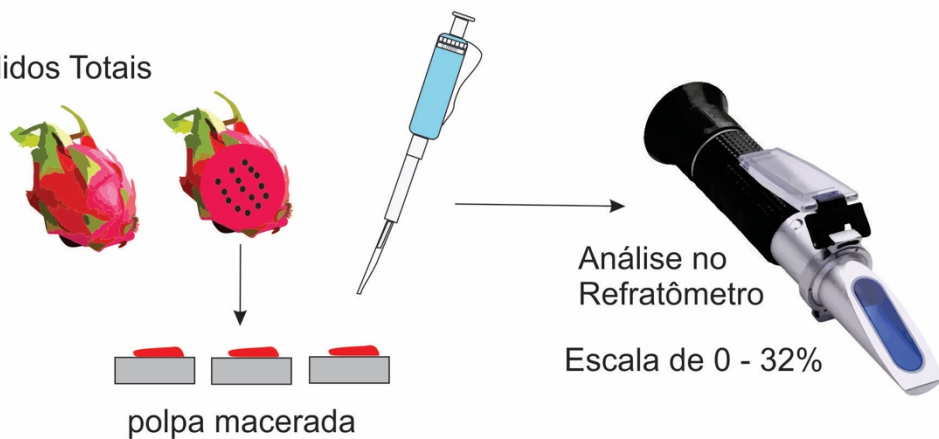


Table 1.10: Sensitivity, specificity, accuracy, and error rate values for LDA classification for two temperatures 15 °C and 25 °C for of Pitaya fruit using NIR.

	15 °C				25 °C			
	Sensitivity	Specificity	Accuracy	Error rate	Sensitivity	Specificity	Accuracy	Error rate
Day 0	0.97	1.00	0.99	0.01	0.97	1.00	0.99	0.01
Day 7	0.60	0.98	0.92	0.08	0.93	0.91	0.91	0.09
Day 14	0.73	0.89	0.86	0.14	0.83	0.98	0.93	0.07
Day 21	0.75	0.93	0.74	0.11	-	-	-	-
Day 25	0.75	0.97	0.77	0.08	-	-	-	-

* (-) No data.

Table 1.11: Sensitivity, specificity, accuracy, and error rate values for LDA classification for combined temperatures for Pitaya fruit using NIR.

15 °C and 25 °C using NIR				
	%			
	Sensitivity	Specificity	Accuracy	Error rate
Day 0	0.93	1.00	0.80	0.01
Day 7	0.66	0.94	0.88	0.12
Day 14	0.68	0.88	0.82	0.18
Day 21	0.75	0.93	0.79	0.10
Day 25	0.80	0.95	0.81	0.07

Table 1.12: Sensitivity, specificity, accuracy, and error rate values for LDA classification for two temperatures 15 °C and 25 °C for of Pitaya fruit using e-nose system.

	15 °C				25 °C			
	Sensitivity	Specificity	Accuracy	Error rate	Sensitivity	Specificity	Accuracy	Error rate
Day 0	1.00	1.00	1.00	0.00	1.00	1.00	1.00	0.00
Day 7	1.00	0.97	0.97	0.02	1.00	1.00	1.00	0.00
Day 14	1.00	1.00	1.00	0.00	1.00	1.00	1.00	0.00
Day 21	1.00	1.00	1.00	0.00	-	-	-	-
Day 25	1.00	0.97	0.97	0.03	-	-	-	-

* (-) No data.

Table 1.13: Sensitivity, specificity, accuracy, and error rate values for LDA classification for combined temperatures for of Pitaya fruit using e-nose system.

15 °C and 25 °C using e-nose				
	%			
	Sensitivity	Specificity	Accuracy	Error rate
Day 0	1.00	0.98	0.98	0.01
Day 7	0.90	0.91	0.90	0.09
Day 14	0.91	0.94	0.93	0.06
Day 21	1.00	1.00	1.00	0.00
Day 25	0.89	0.99	0.98	0.02

Table 1.14 Parameters for the calibration and prediction sets for reference analysis in pitaya using portable NIR and e-nose with PLSR.

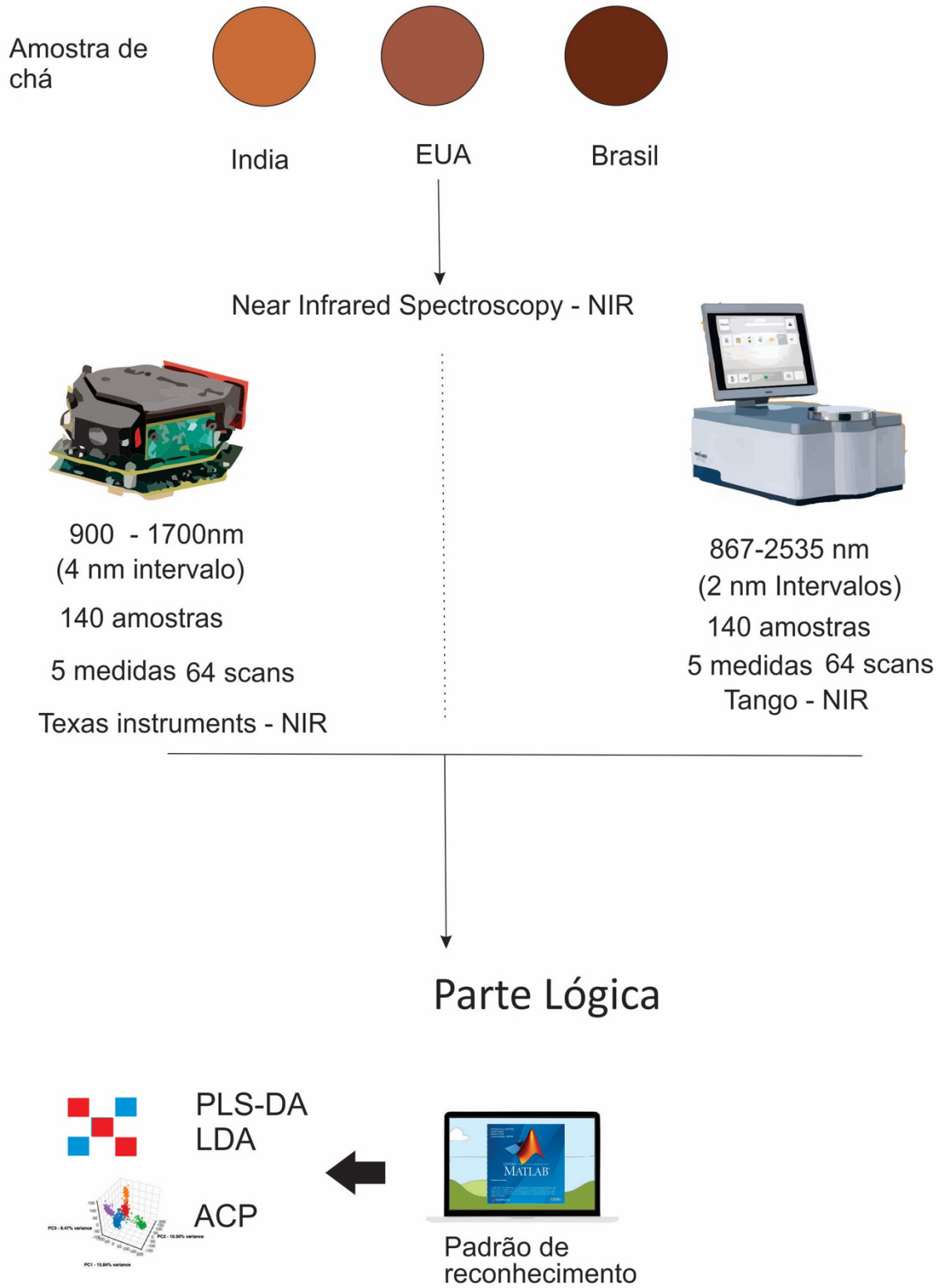
Reference Analyses	Equipment	Pre-Processing	LV	R ² C	RMSEC	R ² C _v	RMSECV	R ² P	RMSEP	RPD	RER
TSS	NIR spectrometer	MC. SM S-G (o) 0 (w) 11. 1st S-G (o)2. (w) 9. SNV	9	0.55	0.69	0.35	0.86	0.50	0.70	1.73	8.94
	e-nose	autoscaling	4	0.55	0.83	0.04	1.48	0.00	1.23	0.98	5.04
pH	NIR spectrometer	MC. SM S-G (o) 0 (w) 11. 1st S-G (o)2. (w) 9 2 nd (o) 2 (w) 9.SNV	6	0.83	0.22	0.79	0.25	0.83	0.23	2.40	8.81
	e-nose	autoscaling. smoothing S-G o (0) (w) 9	7	0.89	0.19	0.81	0.25	0.86	0.22	2.50	8.71
TA	NIR spectrometer	MC. SM S-G (o) 0 (w) 11. 1st S-G (o)2. (w) 9 2 nd (o)2. (w) 9.SNV	5	0.88	0.04	0.84	0.03	0.89	0.03	2.78	11.57
	e-nose	AS.	7	0.84	0.04	0.76	0.04	0.85	0.04	2.6	9.54

		SM S-G (o) 0 (w) 9									
Moisture	NIR	MC. SM S-G (o) 0 (w) 11. 1st S-G (o)2. (w) 9 2 nd (o)2. (w) 9.SNV	8	0.58	0.96	0.49	1.14	0.35	0.98	1.98	8.82
	e-nose	autoscaling	5	0.37	2.06	0.19	2.46	0.00	2.46	0.96	5.86
Phenolics	NIR	MC. SM S-G (o) 0 (w) 11. 1st S-G (o)2. (w) 9 2 nd (o)2. (w) 9.SNV	9	0.60	0.05	0.43	0.07	0.41	0.05	1.55	7.41
	e-nose	autoscaling smoothing S-G (o) 0 (w) 9	20	0.78	0.04	0.04	0.14	0.37	0.07	1.02	5.86

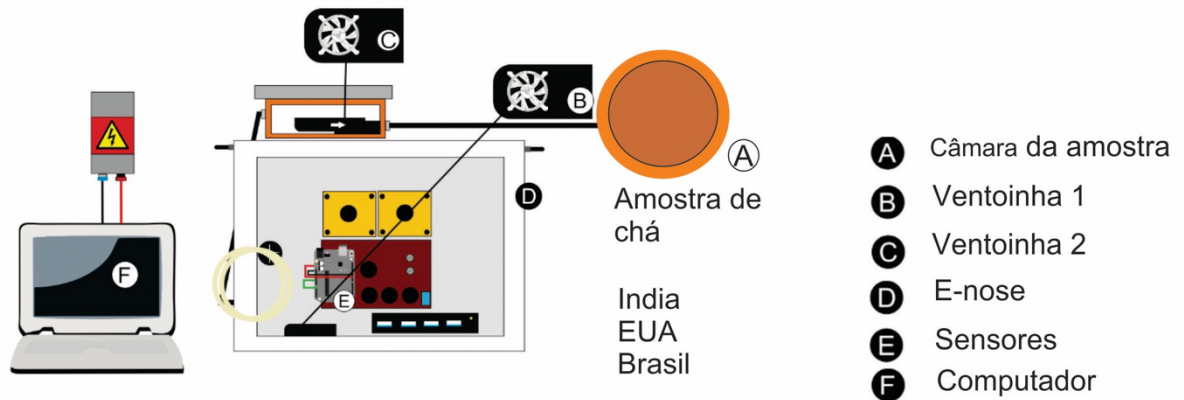
*All models were built using full spectra and maximum variable number NIR (228) and e-nose (928).

APÊNDICE 3: Metodologias detalhadas utilizadas no Capítulo III

Near-Infrared spectroscopy



E-nose 2



Parte Lógica



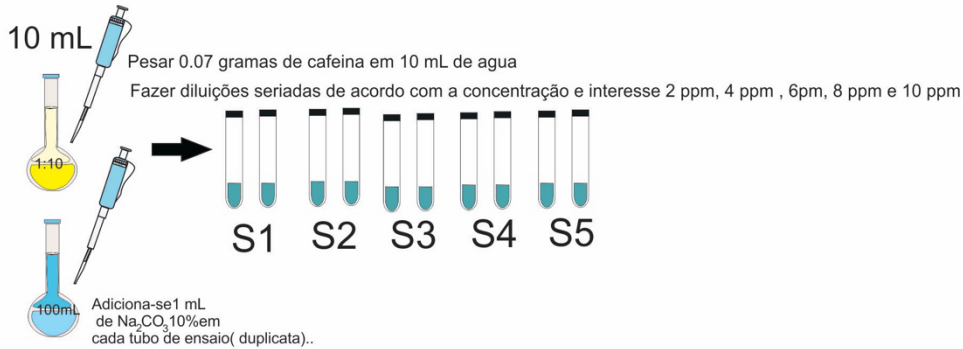
Análise Complementar

HPLC - High performance liquid chromatography

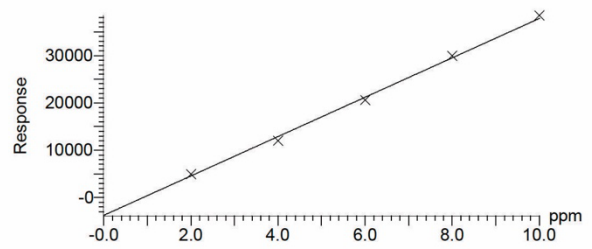
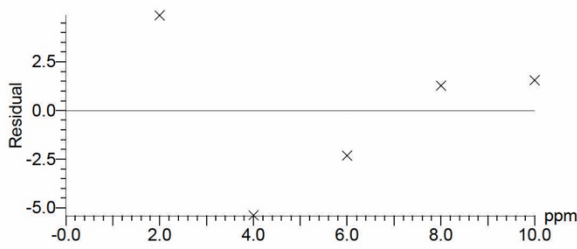
Validação qualitativa

3.3. Procedimento HPLC

Curva Padrão

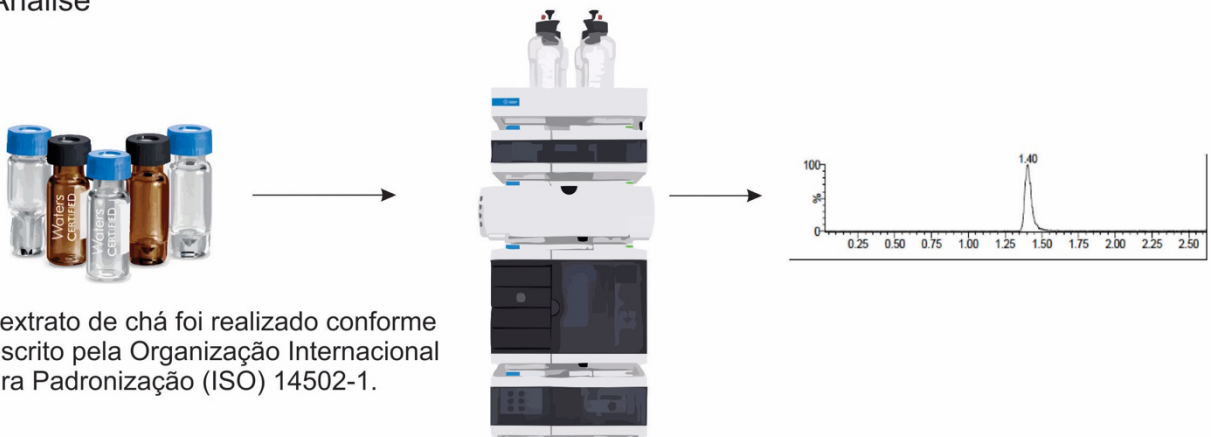


#	Name	Type	Std. Conc	RT	Area	IS Area	Response	Primar...	ppm	%Dev
1	1 Synapt2_29777b	Standard	2.000	1.41	4986.916		4986.916	bb	2.1	4.9
2	2 Synapt2_29778a	Standard	4.000	1.41	11994.654		11994.654	bb	3.8	-5.4
3	3 Synapt2_29779a	Standard	6.000	1.40	20617.873		20617.873	bb	5.9	-2.3
4	4 Synapt2_29780a	Standard	8.000	1.40	29927.418		29927.418	bb	8.1	1.3
5	5 Synapt2_29781a	Standard	10.000	1.40	38458.359		38458.359	bb	10.2	1.6



HPLC - High performance liquid chromatography

Análise



O extrato de chá foi realizado conforme descrito pela Organização Internacional para Padronização (ISO) 14502-1.

Uma quantidade de 0,20 gramas de cada amostra foi pesada e colhida em balão volumétrico. Em seguida, 5 mL de metanol a 70% a 70 °C foram adicionados e o extrato foi misturado e aquecido com um vórtice a 70 °C durante 10 minutos, seguido de arrefecimento à temperatura ambiente

3.3. Procedimento Curva padrão HPLC

Dataset: Untitled

Last Altered: Monday, October 30, 2023 11:18:58 Central Daylight Time

Printed: Monday, October 30, 2023 11:19:07 Central Daylight Time

Method: D:\Synapt2_2023.PRO\MethDB\caffeine.mdb 30 Oct 2023 11:17:46

Calibration: 30 Oct 2023 11:18:58

Compound name: Coffeine

Correlation coefficient: $r = 0.998565$, $r^2 = 0.997131$

Calibration curve: $4153.93 * x + -3726.51$

Response type: External Std, Area

Curve type: Linear, Origin: Exclude, Weighting: 1/x, Axis trans: None

	#	Name	Type	Std. Conc	RT	Area	IS Area	Response	Primar...	ppm	%Dev
1	1	Synapt2_29777b	Standard	2.000	1.41	4986.916		4986.916	bb	2.1	4.9
2	2	Synapt2_29778a	Standard	4.000	1.41	11994.654		11994.654	bb	3.8	-5.4
3	3	Synapt2_29779a	Standard	6.000	1.40	20617.873		20617.873	bb	5.9	-2.3
4	4	Synapt2_29780a	Standard	8.000	1.40	29927.418		29927.418	bb	8.1	1.3
5	5	Synapt2_29781a	Standard	10.000	1.40	38458.359		38458.359	bb	10.2	1.6

Dataset: Untitled

Last Altered: Monday, October 30, 2023 11:18:58 Central Daylight Time
 Printed: Monday, October 30, 2023 11:19:07 Central Daylight Time

Method: D:\Synapt2_2023.PRO\MethDB\caffeine.mdb 30 Oct 2023 11:17:46
 Calibration: 30 Oct 2023 11:18:58

Name: Synapt2_29777b, Date: 30-Oct-2023, Time: 10:32:00, ID: Caffeine 2 ppm, Description:

#	Name	Trace	RT	Area	IS Area	Response	Primar...	ppm	%Dev
1	1 Caffeine	195.088	1.41	4986.916		4986.916	bb	2.1	4.9

Name: Synapt2_29778a, Date: 30-Oct-2023, Time: 10:40:41, ID: Caffeine 4 ppm, Description:

#	Name	Trace	RT	Area	IS Area	Response	Primar...	ppm	%Dev
1	1 Caffeine	195.088	1.41	11994.654		11994.654	bb	3.8	-5.4

Name: Synapt2_29779a, Date: 30-Oct-2023, Time: 10:49:57, ID: Caffeine 6 ppm, Description:

#	Name	Trace	RT	Area	IS Area	Response	Primar...	ppm	%Dev
1	1 Caffeine	195.088	1.40	20617.873		20617.873	bb	5.9	-2.3

Name: Synapt2_29780a, Date: 30-Oct-2023, Time: 10:58:36, ID: Caffeine 8 ppm, Description:

#	Name	Trace	RT	Area	IS Area	Response	Primar...	ppm	%Dev
1	1 Caffeine	195.088	1.40	29927.418		29927.418	bb	8.1	1.3

Name: Synapt2_29781a, Date: 30-Oct-2023, Time: 11:07:44, ID: Caffeine 10 ppm, Description:

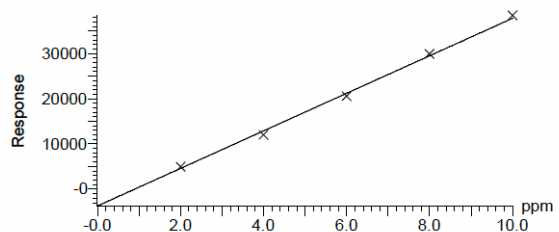
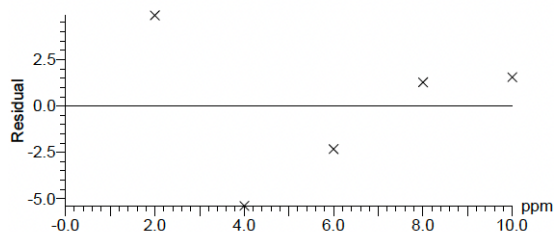
#	Name	Trace	RT	Area	IS Area	Response	Primar...	ppm	%Dev
1	1 Caffeine	195.088	1.40	38458.359		38458.359	bb	10.2	1.6

Dataset: Untitled

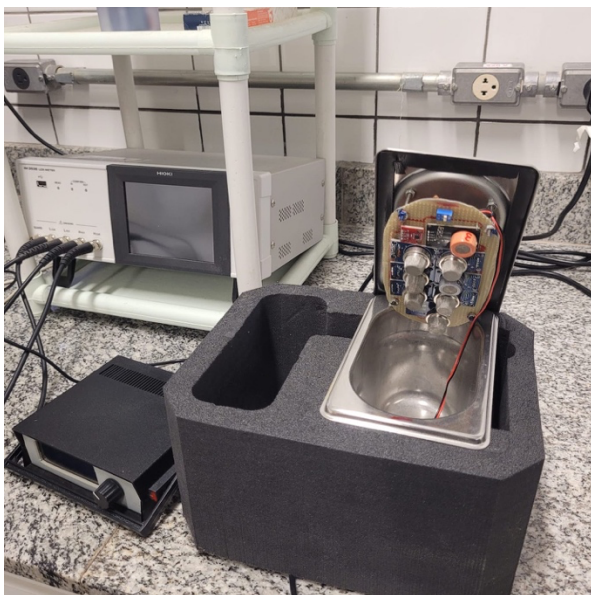
Last Altered: Monday, October 30, 2023 11:18:58 Central Daylight Time
 Printed: Monday, October 30, 2023 11:19:07 Central Daylight Time

Method: D:\Synapt2_2023.PRO\MethDB\caffeine.mdb 30 Oct 2023 11:17:46
 Calibration: 30 Oct 2023 11:18:58

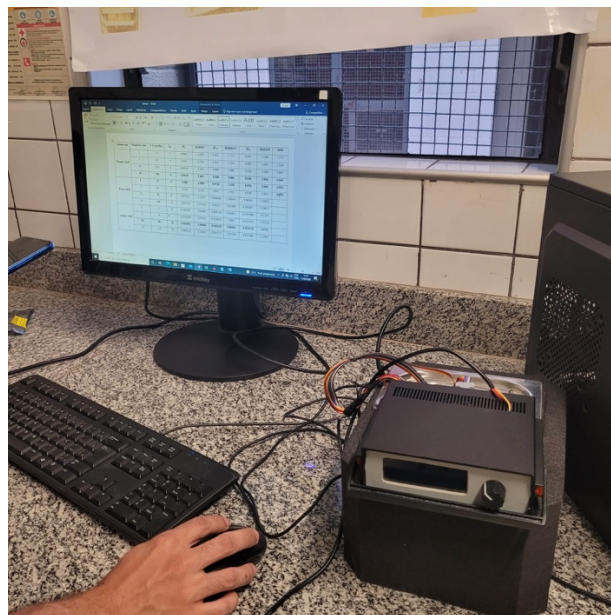
Compound name: Caffeine
 Correlation coefficient: $r = 0.998565$, $r^2 = 0.997131$
 Calibration curve: $4153.93 * x + -3726.51$
 Response type: External Std, Area
 Curve type: Linear, Origin: Exclude, Weighting: 1/x, Axis trans: None



APÊNDICE 4: Fotos de equipamento utilizados nos capítulos II e III



E-nose 1 Camara dos sensores



E-nose 1 Computador e Placa mãe (controladora)



E-nose 1 - Sistema de sucção com suporte duplo (1) amostra (2) headspace de sucção.

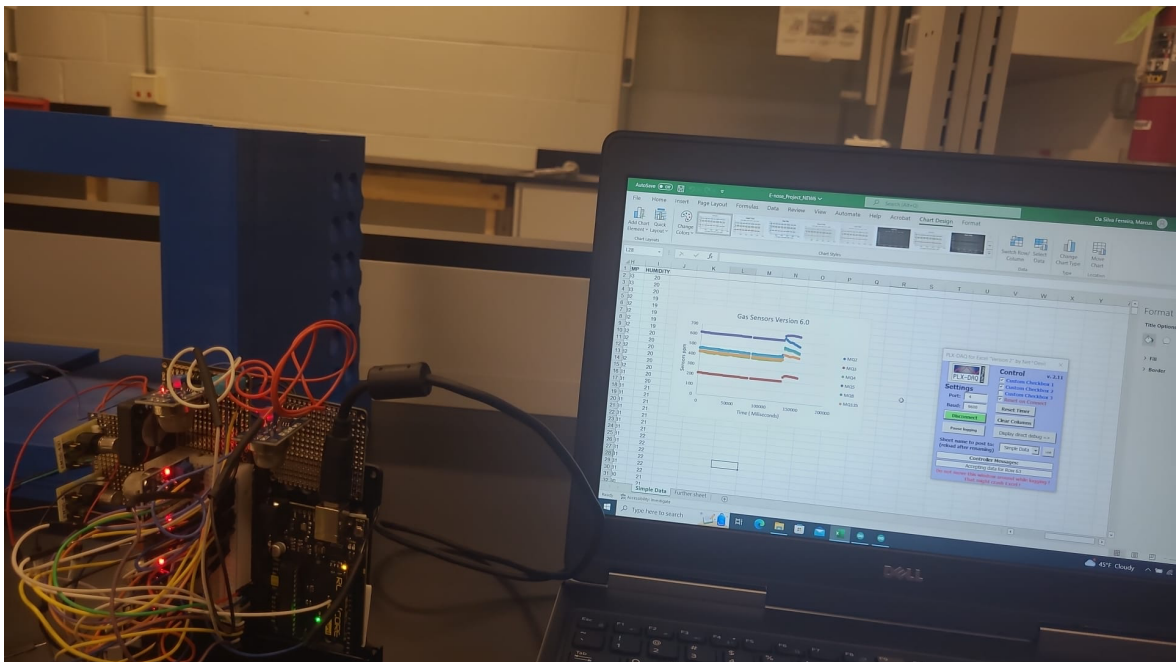
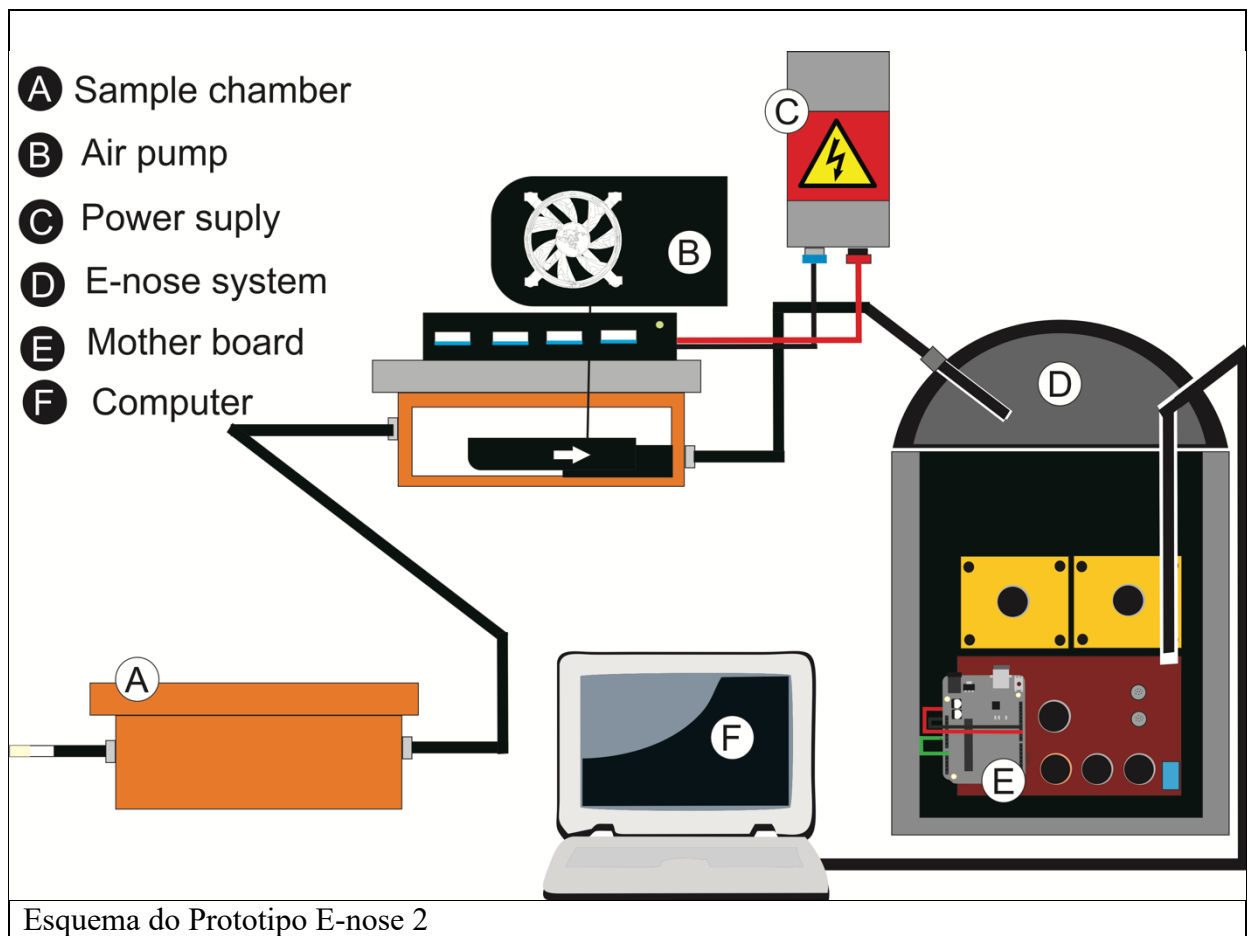


E-nose 1 Camara de sensores para amostras maiores (exemplo melão)



E-nose 1 Camara de sensores para amostras maiores (exemplo melão) com a tampa contendo os sensores

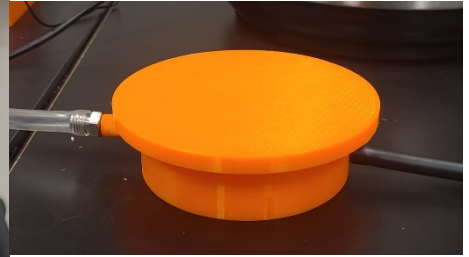
4.2. Prototipo e-nose 2



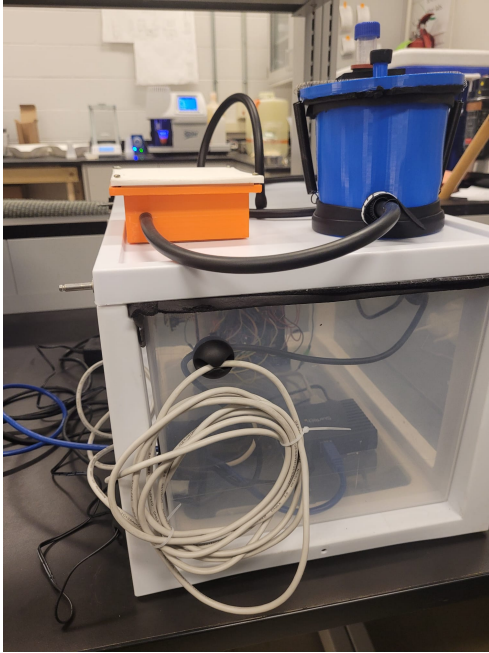
Sistema de hardware E-nose 2 e sistema de aquisição de dados



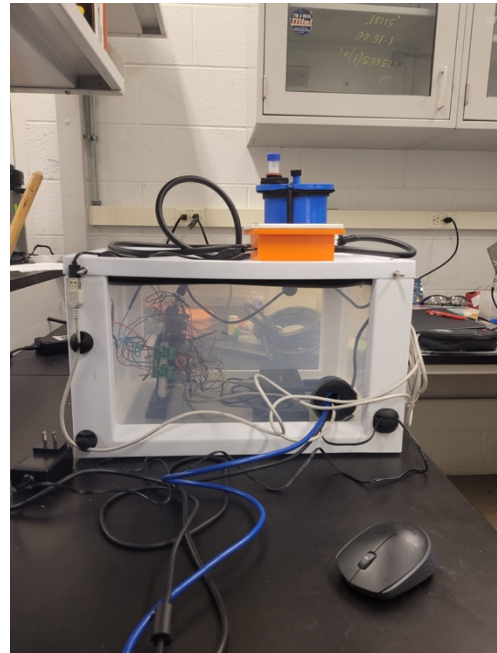
E-nose 2 – Prototipo Panela de pressao usada para camara hermeticamente fechada



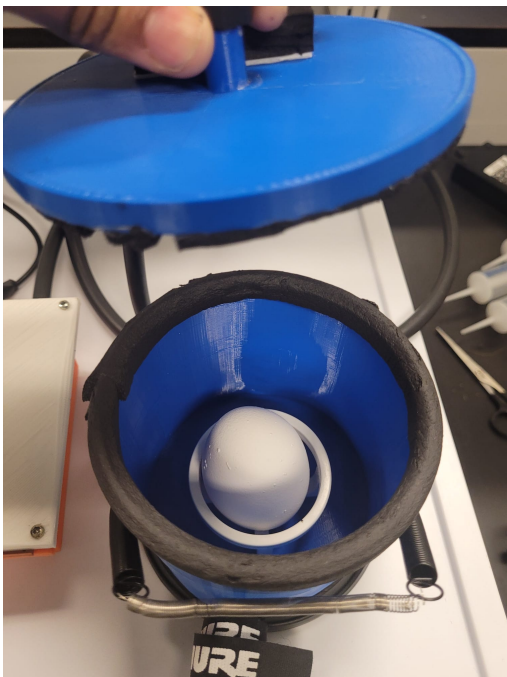
Camara para amostra desenvolvida para chás.



E-nose 2 camara de sensores



E-nose 2 camara de sensores – vista lateral



E-nose 2 camara da amostra para diferent produtos



E-nose 2 camara da amostra para produtos em pó/grãos

Deep computer vision system and image explanation for *dragon fruit* post-harvest classification

Marcus Vinicius da Silva Ferreira¹ - Sylvio Barbon Junior^{4,*} - Victor G. Turrisi da Costa² - Douglas Fernandes Barbin³ - Jose Lucena Barbosa Jr¹

¹Federal Rural University of Rio de Janeiro (UFRRJ), Department of Food Technology, Seropédica, RJ, Brazil

²University of Trento, Trento, Italy

³Department of Food Engineering and Technology, School of Food Engineering, University of Campinas, Campinas, SP, Brazil

⁴University of Trieste, Trieste, Italy

* Correspondence e-mail: sylvio.barbonjunior@units.it

1.5 Abstract

Dragon fruit (*Selenicereus undatus*) is a fruit that has gained popularity in the Brazilian market, evaluating its quality presents a significant challenge to the industry due to its unique morphological features. Image analysis, combined with Deep Learning (DL) techniques, offers a promising solution for visually discriminating dragon fruit. However, DL architecture such as ResNet and ViT transformer are challenging to train especially for new objects, such as exotic fruit. In this work, we compare two Deep Learning Computer Vision System (DCVS) architecture Res-Net and ViT transformer in the direction of Explainable Artificial Intelligence (XAI) support for understanding of black-box models operations such as Grad-CAM method that enhance co-arse regions in the image boosting classification outcome. This paper comprises substantial information on the computer vision field employing machine learning for the classification of dragon fruit in 4 shelf-life stages (SLI: 30, 50, 80, and 100). DCVS showed a good predictive model with ResNet and ViT as the literature suggests. DCVS map reveals the potential to use the morphological aspects of dragon fruit and predict its respective classes. ViT Small outperformed the other models (ViT Tiny and ResNet 18 and 50), achieving an overall accuracy of 91.00%, with an accuracy of up to 97.00% for SLI30 classification. This approach has promising potential for directing dragon fruit to the right product segment in the fruit industry and could be further implemented for other agricultural products.

Keywords: Artificial Intelligence. Machine Learning. pitaya. pitahaya. RGB imagery. shelf-life.

1.6 Introduction

Brazil is the largest producer of tropical fruit in the world (PINTO; JACOMINO, 2013). Dragon fruit (*Selenicereus undatus*) is one of the fruit whose consumption has increased in the Brazilian market (LOUREIRO et al., 2020). This fruit, also known as pitaya or pitahaya, has been consumed on a large scale due to the presence of anthocyanins, which have antioxidant properties that have been proven to minimize the oxidation process in the human body, and also because of the fruit's potential to control the growth of microorganisms in food (preservatives), making it a good alternative to artificial bactericides (JIMENEZ-GARCIA et al., 2022).

Evaluating the ripeness of fruit can be a challenging task as it often relies on subjective human assessments, involving senses such as smell, vision, and touch (ISMAIL; MALIK, 2022). Dragon fruit presents its best harvest period of around 35 d and it is commercialized in this period. However, after this time the fruit continues to ripen and after 40 d there is a loss in physical quality with the degradation of pigments and the limp of the spikes, although it may still be suitable for consumption (MAGALHES et al., 2019). Since quality control is an important step in the food industry, having an automated system to correctly determine the right shelf-life index (SLI) stages would significantly benefit fruit producers not relying on subjective techniques (VILLAMIEL; MNDEZ-ALBIANA, 2022). Therefore, finding alternative techniques such as Computer vision (RGB imagery) to identify the stages in the post-harvest is crucial to guarantee accuracy in the destination of the fruit.

Recently several methods have been used to evaluate freshness, ripening or shelf-life stage and other quality aspects in fruit such as vis-NIR spectroscopy, hyperspectral imaging, Raman spectroscopy, and RGB imaging (PATHMANABAN; GNANAVEL; ANANDAN, 2019; TRIEU; THINH, 2022). Except for NIR spectroscopy (NIRS) and RGB imaging, the other techniques are still expensive to be purchased by local farmers and small producers. RGB imaging stands out as an affordable technique compared to the others that are costly and laborious. This equipment in tandem with object detection is a common and widely used technique available in computer vision (CV) that is used as an excellent method to interpret images and videos. However, this approach is one of the biggest challenges in the CV field (OKSUZ et al., 2021), which sparked the development of machine learning algorithms to help improving some of these drawbacks, such as misclassification.

Computer vision techniques were used to spot defects in fruit that are related to the ripening process in melon (VIJAYAKUMAR; R., 2020) palm fruit (WONG; CHEW; PHANG, 2020) and dragon fruit (PATIL et al., 2021). There are some emerging methods for image analysis, such as very convolutional network (VGGNet), You Only Look Once (YOLO), Residual Neural Network (Resnet) (YUE; FU; LIANG, 2018; LOPES et al., 2022) and Vision Transformer (ViT) (XAVIER et al., 2022). A VGGNet is a type of convolutional neural network (CNN) that has achieved great success in image classification and recognition tasks. YOLO is another CNN, very useful for object detection in images and videos in real-time. Unlike traditional object detection algorithms, YOLO performs object detection and classification in a single stage, making it much faster and more efficient. Resnet is a deep learning architecture that introduces skip connections, or shortcuts, allowing the network to bypass one or more layers. These skip connections help to address the vanishing gradient problem, which can occur in very deep neural networks and make it difficult for the network to learn effectively. ViT uses the same principles as the Transformer model, which was initially proposed for natural language processing by replacing the convolutional layers used in traditional image recognition models with a series of self-attention layers. This allows the model to attend to different parts of the image to extract features, without relying on convolutional kernels.

Therefore, the main contribution of this paper is to be able to classify dragon fruit into 4 classes according to its SLI using visual information from image analysis and artificial vision. The implementation of image visualisation with the use of explainable AI (XAI) might shed a light to help new classification strategies to the ones that have already been used (WU, 2022; SHINDE; SHAH, 2018). Since previous studies using AI and machine learning to classify dragon fruit did not use the architecture proposed in this work nor the 4 stages of classification (TRIEU; THINH, 2022; PATIL et al., 2021), this work proposes the visualisation of dragon fruit and the comparison of two versions of vision architectures (ResNet 18 and

50 and the state-of-the-art ViT small and tiny transformers) to understand of the performance of these methods in action while classifying fruit samples. Likewise, our dragon fruit database will provide relevant information on the use of DL for classification to assist the industry in the decision of dragon fruit destinations. Comparing GradCAM from ResNet and Attention Maps from ViT can provide insights into the differences in the way these two architectures perform visual recognition. ResNet uses residual blocks to learn more complex features and deeper representations, while ViT employs self-attention mechanisms to extract contextual information from the image. By comparing the visualisation generated by GradCAM and Attention Maps, we can understand which regions of the image are being attended to by each model and how they differ in their focus. This comparison can help us understand the strengths and weaknesses of each architecture and provide guidance for future improvements. The following objectives were pursued in this research:

- Proposing a Deep Learning Computer Vision System (DCVS) to classify dragon fruit according to their SLI stages.
- Designing a solution based on Explainable Artificial Intelligence (XAI) principles to facilitate interpretation and gain insights into classification outcomes.
- Providing a comprehensive comparison between two key visualisation techniques, GradCAM and Attention Maps.

This work has been structured as follows: Section 2 - Material and Methods, Background of the Techniques used, Section 3 Results and discussion, and finally Section 4 with the conclusion.

1.7 Material and Methods

1.7.1 Deep Computer Vision System

Deep Computer Vision System (DCVS) is a recent denomination used to designate Deep Learning models embedded in Computer Vision Systems, that has been applied for food quality evaluation (LOPES et al., 2022). In particular, the agricultural sector has increased the application of DL solutions to improve product inspection by avoiding some data processing steps, such as image pre-processing and feature extraction, traditionally part of computer vision systems. Additionally, DCVS solutions surpass the predictive accuracy of traditional methods in addition to reducing data processing steps (OLIVEIRA et al., 2021).

Deep learning methods used to induce classification models aim at learning feature hierarchies from different levels of details formed by the composition of lower-level features, emphasizing the visual information from pixel colours to complex image structures (GLOROT; BENGIO, 2010). Among the several methods available, Residual Network (ResNet) presents important advantages regarding its training, particularly in reducing the computational effort and addressing vanishing gradients (HANIF; BILAL, 2020). We can represent a ResNet block as in Figure 7.1, in which the output of the function $F(x)$ is added with x , where $F(x)$ can be any function such as $z^{(l)} = a(W^{(l)}x^{(l)} + b^{(l)})$. Using identity mapping to skip some connections, the ResNet architecture allows the network to ignore an entire convolutional layer when necessary, making the network reuse useful abstract representations (WIGHTMAN; TOUVRON; JGOU, 2021). To predict the outcome as a multinomial probability distribution, the softmax function is used as the activation function in the output layer for classification problems.

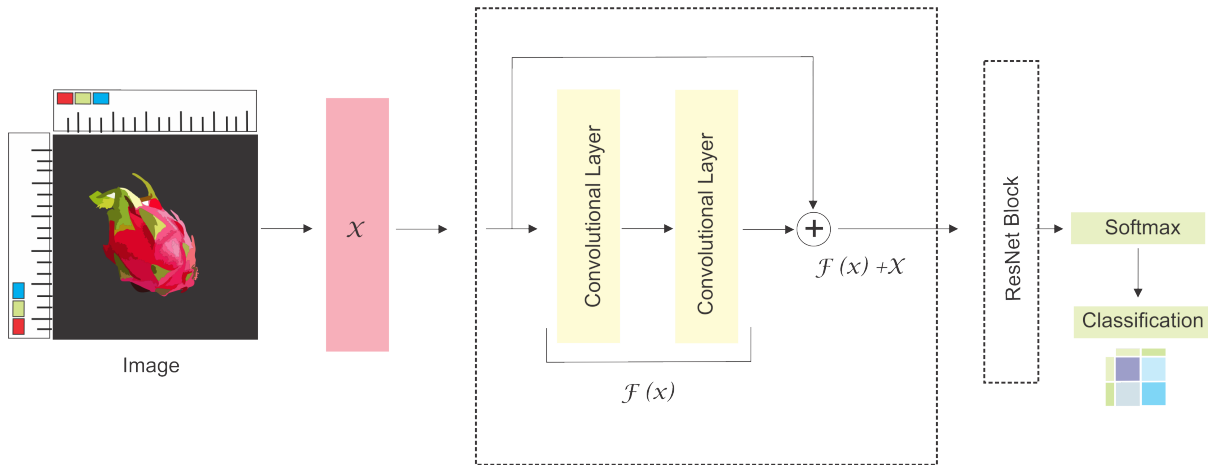


Figure 7.1: Residual Network (ResNet) scheme overview

More recently, Visual Transformers (ViT), introduced by (DOSOVITSKIY et al., 2020), have been used in multiple works with comparable or even superior results in comparison to ResNet architecture or traditional Convolutional Neural Networks (CNN) (ROSSO et al., 2023). ViT replaces the convolutional layers used in traditional image recognition models with a series of self-attention layers by splitting an image into patches towards creating an embedding used as an input to a Transformer Encoder (TE). TE were proposed by (VASWANI et al., 2017) for machine translation and have since become the state-of-the-art method for many natural language process tasks. As shown in Figure 7.2, an image is converted to flattened regions of the same size. The number of regions is a hyperparameter that fixed the size, D , of patch embedding, preserving their sequence and positional information. The encoded vector elements, called tokens, are combined with the image class (i.e., image label) to be used as the input of Transformer Encoders. Transformer Encoders are organised as layers, using constant latent vectors of D size to map D linear projections as the patch embeddings. Multiheaded self-attention and multilayer perception blocks alternate in the TE, towards delivering a final encoded vector used in the final predictor, a multilayer perception that outcomes the final classification.

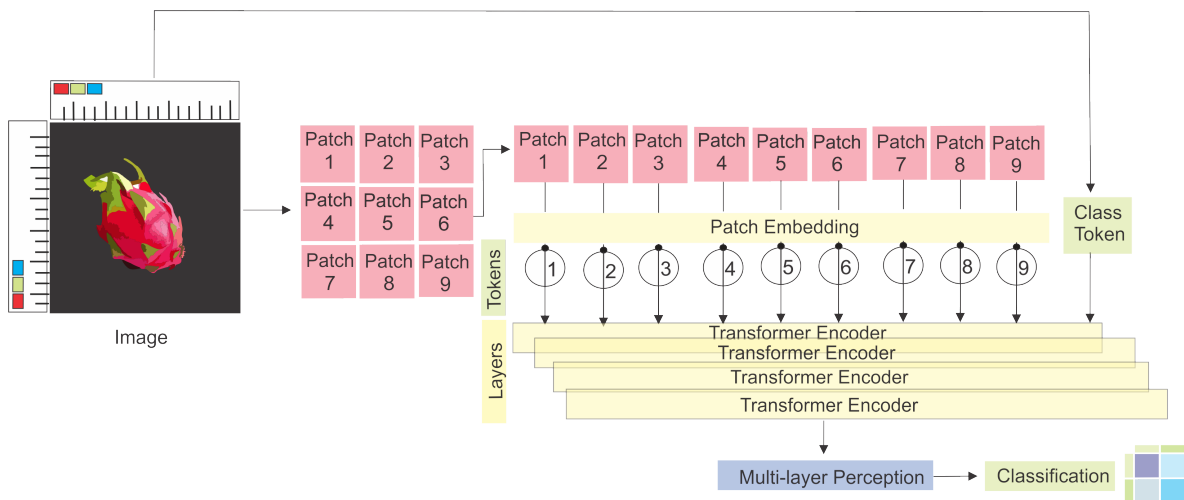


Figure 7.2: Vision Transform (ViT) overview

1.7.2 Explainable Deep Computer Vision

DCVS has increased the complexity of its models in a sense of allowing better predictive models, precisely, using deep learning it is possible to reach highly accurate predictions (LOPES et al., 2022). Although researchers and practitioners have rapidly adopted the usage of these complex models, understanding the intricate rationale of learning models could contribute to model improvement, validation, and even phenomena interpretation.

Explainable Artificial Intelligence (XAI) techniques allow to comprehend the black-box model operations, how they provide decisions, the presence of bias, and other shortcomings in data-sets and model performance. In which the term Explainability refers to the notion of explanation as an interface between humans and decision-makers that is both accurate and easily understandable (KAKOGEORGIOU; KARANTZALOS, 2021). DCVS models that use RGB images may include an explanation of pixel maps that contribute to their output, emphasizing the most important regions in the original image (LOPES et al., 2022). A heat map or coloured regions projected over the RGB sample can represent the most significant image area used by the models. These important regions could be computed or obtained during the training step or in the final trained model, e.g., using the average gradient of each layer of the model to highlight coarse regions of the image that have a positive contribution in the final classification.

ResNet and ViT have been used (KUMAR; SHIVANI, 2022), to address the problem of image classification with potential XAI contribution based on visual mechanisms that represent the contribution in the classification. The obtained classification can be explained by ResNet using a Grad-CAM method.

The Grad-CAM method (SELVARAJU et al., 2017) obtains the gradients of the output named feature map activation of a given layer. At that point, the gradients are averaged for each layer to obtain the importance weights. Therefore, the average gradients for each channel are multiplied by layer activation, and the results are summed. Grad-CAM output is upsampled using bilinear interpolation and then a Rectified Linear Unit (ReLU) is applied, returning only non-negative attributions. Grad-CAM emphasises coarse regions in the image that contribute positively to the result.

In ViT, an encoder is built using a self-attention map mechanism. Unlike ResNet, ViT does not involve any convolutional layer. Instead, input images are split into patches and fed into the network. Through the encoded global information, the self-attention structure mechanism can capture interactions between image patches. In the context of vision transformers, the cls token refers to a special token that is added to the input sequence of the transformer, representing the image as a whole, and is typically used to obtain a global representation of the image. In addition, the transformer can also attend to other tokens in the input sequence that correspond to specific regions of the image, allowing the model to focus on particular areas of the image that are most relevant for a given classification task. The final attention map, organised in patches, could be visualised and projected over the original image.

In our work, we aim to identify the morphological aspects that purposes. The common aspects to be evaluated in fruit comprise the change in colour and the presence of mould or other indications of spoilage and fruit senescence. Dealing with dragon fruit is difficult due to the variability presented in the crop from a morphological and colour perspective. Previous work with this tropical fruit focused on scaly spikes and tail Figure 1.3, as these morphological aspects contribute to the classification of the fruit into three commercial destinations (level 1, 2, and 3) as they are associated with defects present in it(MINH TRIEU; THINH, 2021). Some morphological quality parameters suggested for dragon fruit include bracts length, soluble solid content (Brix), seed size, and fruit colour (BETANCUR G; MURIEL R; GONZÁ- LEZ J, 2020). The proposed SLI represents the Brix and ultimately color, which is correlated to acidity changes within the fruit and therefore can be a good predictive measure to rightfully select the fruit into desired classes. Thus, the proposed morphological ROI was set as the spikes senescence and the deformation (damage) to dragon fruit’s red skin colour Figure 7.3.

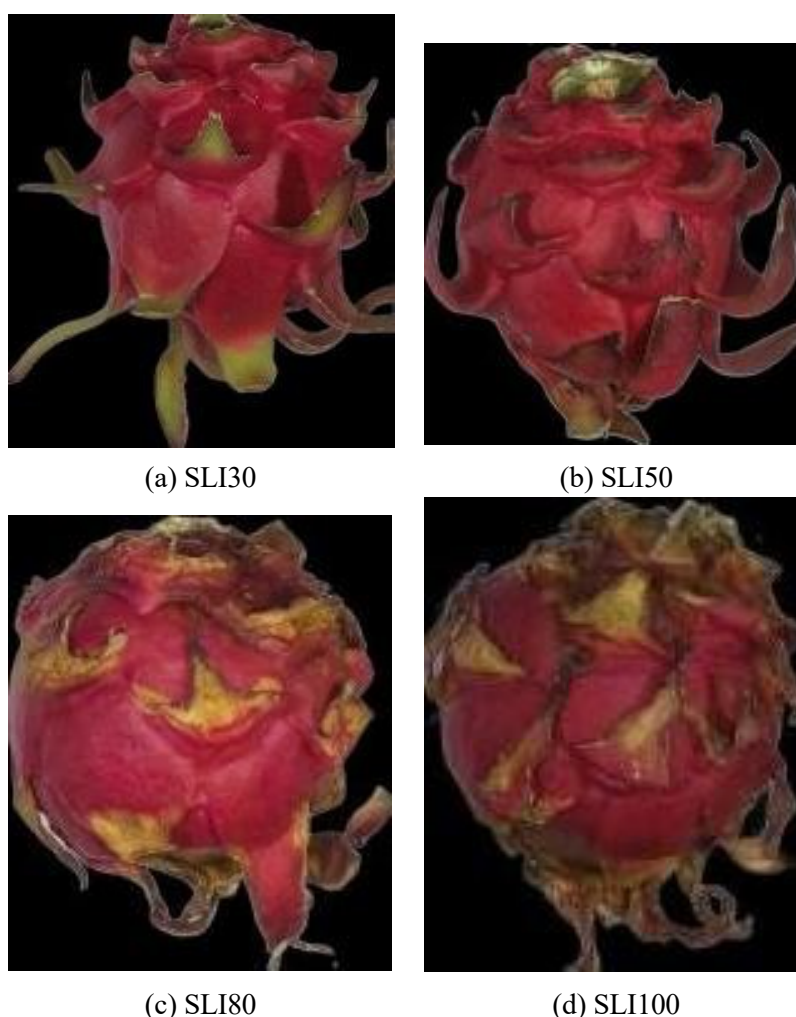


Figure 7.3: Different SLI indexes (A) 30, (B) 50, (C) 80 and (D) 100.

1.7.3 Fruit acquisition and RGB imaging setup

A total of 150 dragon fruit (red-fleshed variety) were obtained immediately after harvest from a local producer. The images were acquired using a camera (f/1.2/1X optical zoom) with a resolution of 12 megapixels (4096 x 3072 pixels/cm). Thirty photos (one for each sample) were immediately taken on day 0. The remaining samples were stored at two temperatures (15 °C and 25 °C), and additional photos were taken on days 7, 14, 21, and 25 of storage (approx. 60/d).

Then, the days were classified into a proposed shelf-life index (SLI) (WU, 2022) based on the ratio between total soluble solids (TSS) and titratable acid (TA) to identify the sample conditions regardless of the storage temperature. The fruit were then labeled as SLI 30 (day 0), 50 (day 7), 80 (days 14 and 21), and 100 (day 25), respectively and SLI indexes were carried out throughout the work. The apparatus used to capture the photos based on RGB imaging is shown in Figure 7.4. The images were taken from 3 angles so that information about the quality of the whole fruit was obtained. Many images were part of the data set, and each one of them had different size ratios.

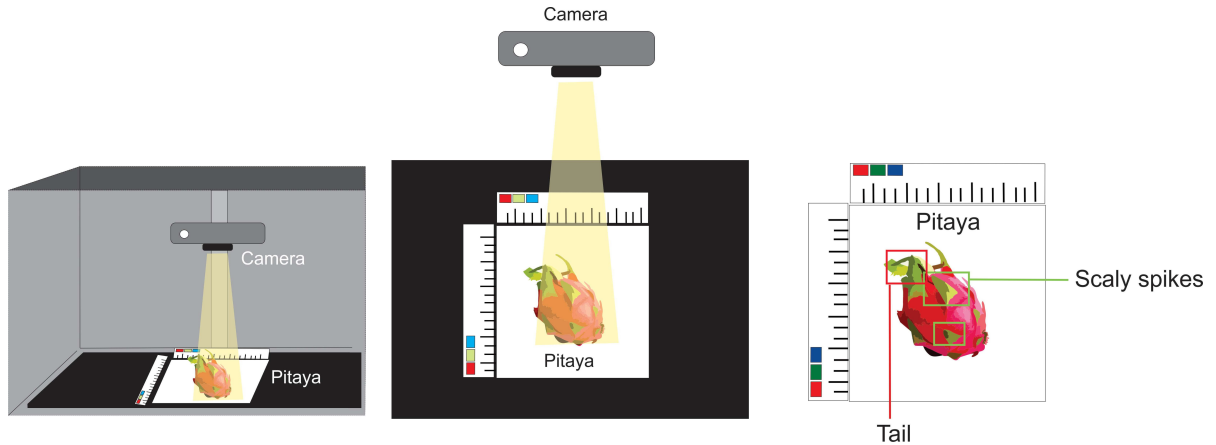


Figure 7.4: RGB imaging chamber set up showing the chamber (A) and the position for the acquisition of each fruit and (B) the focused features in dragon fruit.

We resized the fruit images to 256×256 and cropped the centre to 224×224 to fit the pretrained deep learning models. Moreover, a training and validation sub-samples were randomly generated, in which the training was augmented twice by using a horizontal flip.

1.7.4 Deep Learning and Explainable Methods

In our experiments, we compared the performance of four classifiers: ResNet 18, ResNet 50, ViT Tiny, and ViT Small using transfer learning. Grad-Cam was used for visualising the regions of an image that are important for a neural network's classification decision. The ResNet models have 18 and 50 layers, while ViT Tiny and Small have different embedding sizes of 192 and 384, respectively. These models were chosen for their balance between parameters (i.e., size) and performance, and have been successfully used to classify the quality of food such as beet, parsley, and spinach (REEDHA et al., 2022). We used pre-trained ResNet and ViT models from the Pytorch torch-vision library ¹ and experimented with various hyperparameters as shown in Table 7.1.

We opted to use small deep learning methods over larger ones, such as ResNet 128 with 128 layers, as our data did not contain much abstract information. ViT Tiny and ResNet 18 had similar sizes, as did ViT Small and ResNet 50 in terms of the number of neurons used in the learning process. We observed that ResNet 18 performed better than ResNet 50, possibly due to the relatively easy nature of the classification task, which involved only four classes. Not having to deal with a large number of classes or continuous parameters may have favored ResNet 18 over 50. (ZHAN; CAO, 2019)

¹ <https://pytorch.org/vision>

Table 7.1: Hyperparameters evaluated for training the DCVS models

Hyperparameter	Values
learning rate	[2e-4, 3e-4, 4e-4,]
weight decay	[1e-3, 1e-4, 1e-5, 1e-6]
optimiser	[Adam, Adam(W)]
batch size	[32, 64, 128]
epochs	[50, 100, 120, 150]

It is worth noting that the best classification results were achieved using Adam(W) optimizer, with a batch size of 64 and 120 epochs. The values reported in the results section were obtained with these fixed hyperparameters. However, the learning rate and weight decay were discussed separately.

All models were designed to classify input images into one of four categories, using a fully connected layer for multi-class classification. A linear layer with a Softmax activation function was used to generate output predictions for the four categories.

We compared the visualisation of each DCVS using the Grad-CAM method and the attention map. Grad-CAM was implemented and projected as an additional layer that shows a heat map on top of the original input image using *pytorch - grad - cam* package (GILDENBLAT, 2021). Colours on the heat map indicate (from blue to red) the most important regions for classifying a given sample. To visualise the ViT attention map, it was implemented the rollout-based attention visualisation method using the ViT-pytorch github repository ².

1.7.5 Model Performance Criteria

For the DCVS performances (ResNet 18, 50, ViT Small and Tiny) comparison the training set was randomly divided as (x: y) for calibration and test respectively. The comparison was derived from the predictive performance by using a confusion matrix Figure 7.6 that allows models to be compared into pre-defined parameters, such as precision and F1 ,which is the weighted precision and recall value (Equations (1), (2), and (3), respectively).

$$Precision = \frac{TP}{TP + FP} \quad (6.1)$$

$$Recall = \frac{TP}{TP + FN} \quad (6.2)$$

$$F1 = \frac{Precision \times Recall}{Precision + Recall} \quad (6.3)$$

1.8.1 Overall accuracy

Overall, the DCVS method performed well for the four classifiers (ResNet 18, ResNet 50, ViT Tiny, and ViT Small) using transfer learning, as evidenced by the results obtained with the Adam(W) optimiser, batch size, and epochs set as described in Table 1.1. The boxplot (Figure 1.4) provides descriptive statistics for the accuracy of the four models and shows the distribution of the results and their iterations, which relates to the learning capability. Dragon fruit presents interesting features, such as signs of dehydration and brownish color in their spike's areas, similar to pineapple fruit, which Sirichaoen et al. (SIRICHAROEN; YOMSATIEAN- KUL; BUNSRI, 2023) evaluated using a variety of model architectures to assess the stage of sweetness and sourness. This similarity suggests that deep learning models may identify and deal with morphological characteristics in a similar way. For dragon fruit, the proposed SLI index measured these features in the fruit and was related to TSS and TA. Further investigation could explore the relationship between the different regions of the fruit and their sweet and sour characteristics.

Regarding the performance of the two architecture models, they showed similar results with some differences in terms of computational efficiency, as the ViT models were faster. However, a challenge arises from this, which is the gradient descent algorithm used in deep learning optimisation. This algorithm is a first-order iterative optimisation technique used to find a local minimum of a differentiable function. In addition, transformers, which are a type of deep learning model, have been used to identify kiwifruit diseases in complex natural environments. The results of this study showed that ViT outperformed ResNet by 10.00% by reducing the number of parameters and increasing accuracy by 4.50%. However, a convolution block had to be used to account for inaccurately located regions in the fruit. In the case of dragon fruit, ViT also performed slightly better, but the ROIs, which included spikes similar to kiwi leaves, suffered from darkened dehydration colour, making it a more complex training process according to Li et al. (2022).

The intention is to iterate in several steps assuming the inverted position of the function at a current point for this direction by minimising a general nonlinear function (BUHRMESTER; MNCH; ARENS, 2021). Therefore, there is a need to find the minimum error, though if the learning rate is too high there might be misleading information (YOU et al., 2019). Finding the perfect combination of learning rates to optimise the final solution without compromising the result is a challenge. The variables that were modified were learning rate ($2e-4$, $3e-4$, and $4e-4$) and weight decay ($1e-3$, $1e-4$, $1e-5$, and $1e-6$) for the binary search had a variation of 3.00-4.00%, which may be considered a little big. However, from the literature, common learning rates are from $1e-3$ order (MACALUSO; SHIH, 2018). Therefore, the values used in this work were lower compared to the literature. The weight decay works as a factor to avoid over fitting. It is used to check the direction of the learning method and consequently, reduce the possibility of overfit. Taking two variables will only have a correlation with the learning method in the exact place where the error is being reduced. So, what happens is an error reduction attempt.

Overall, the median accuracy of the models were similar, with ViT Tiny and ResNet 18 showing slightly lower standard deviation. However, both methods have an outlier that could explain the difference. Although ViT transformers performed slightly better than ResNet, statistically speaking, there is no significant difference, indicating that the only distinguishing factor is the learning process. This finding favours ViT Tiny over other models since they are easier to train. As a result, choosing between ViT Tiny and Small would have little impact as you

only need to train the model once.

The confusion matrix for the four models using one selected model previously assigned having weight decay of $1e-4$ and rate of $4e-05$ is presented in Figure 1.6. Augmentation was used to reduce the unbalanced data as well as to better train the model. The results showed that from the 4 models, SLI80 had the highest number of samples since based on this SLI, days 14 and 21 were merged. This approach is a good indication that the data was not overfit as the performance for this class does not differ much from the other SLI indexes Table 1.2. It can also be seen from Table 1.2 that F1, Precision, and Recall show that overall ViT small had the best values for all the indexes. F1 was chosen over accuracy to balance out the unbalanced data issue, however, it is evaluated by classes, in which each class has its performance. It gives a better measure of the incorrectly classified cases than the accuracy metric. SLI100 contributed to diminishing the performance of ResNet 50. ResNet 18, which uses a convolutional neural network of 18 layers based on a pre-trained network, classified better than the 50 layers deep.

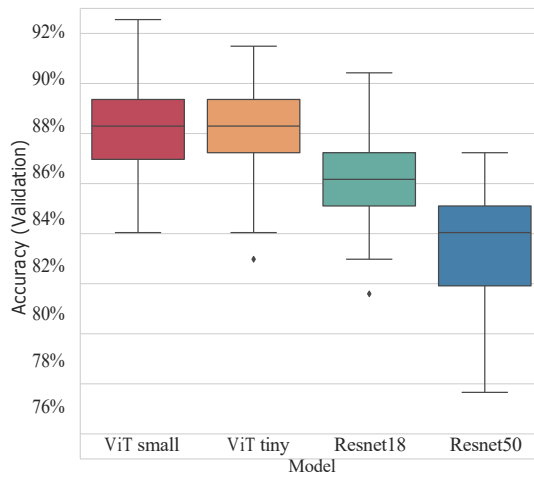


Figure 7.5: Boxplot of deep learning methods sorted by average F1 after 10 repetitions of each combination with different learning rate ($2e-4$, $3e-4$, and $4e-4$) and weight decay ($1e-3$, $1e-4$, $1e-5$, and $1e-6$).

This evidence may be due to the classes being easily distinguishable, which represents their easy identification. That makes ResNet 18 faster, smaller to process, and therefore, much more suitable with better F1 scores compared to the 50-layer model. The results may also indicate that these models are prone to overfitting and can be challenging to train. Notably, SLI30 and SLI80, which had more samples in the dataset, outperformed SLI50 and SLI100, which had fewer images, making this observation quite intuitive. In a previous study on deep learning for shiitake mushroom sorting, ViT models were found to be superior to CNN, leading to recommendations for their use in crop classification in the industry (DENG; LIU; XIAO, 2022).

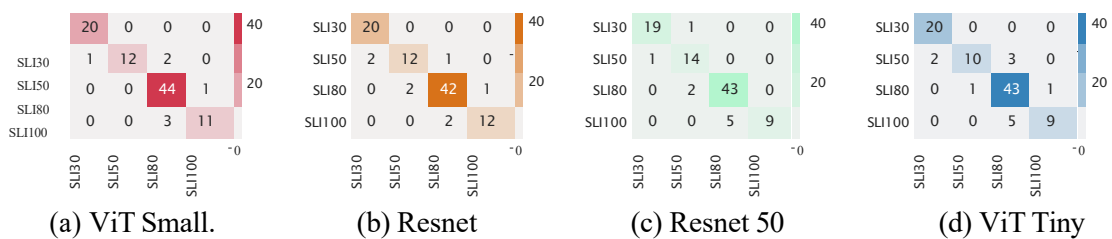


Figure 7.4: Confusion Matrix of deep learning model using weight decay of $1e-4$ and learning

rate of 4e-05

Both ViT transformers showed to deliver the same outcome achieving similar F1 average scores of 90.50, 94.25, and 89.25% for ViT small compared to 89.50, 89.75, and 90.50% for the Tiny model. Some authors have found a better efficacy of 86.5% of ViT Tiny with 21M parameters over the tested ViT ones that scored approximately 78.00% in random data (WU et al., 2022). However, the data set size may have influenced the poor difference in the model scale-down, which tends to have a better transfer ability over other models in many downstream assignments. Optimised small and medium-sized ViTs creating more efficient ViT systems has already been proposed by (GRAHAM et al., 2021). Other conducted essays using dragon fruit and CNN to identify characteristics in the fruit (i.e., scaly spikes and tail) managed to obtain 97.38% accuracy (MINH TRIEU; THINH, 2021). The unbalanced data of the models is a good indication that the performance of each class architecture can increase. Yet the proposed classification model has not mistaken more than one degree of classification, therefore showing good efficacy.

	ViT Small			ViT Tiny			ResNet 18			ResNet 50		
	F1	Prec	Rec	F1	Prec	Rec	F1	Prec	Rec	F1	Prec	Rec
SLI30	0.97	0.95	1.00	0.95	1.00	0.91	0.95	0.91	1.00	0.95	0.95	0.95
SLI50	0.88	1.00	0.80	0.82	0.80	0.86	0.76	0.91	0.67	0.87	0.93	0.82
SLI80	0.93	0.90	0.98	0.93	0.93	0.93	0.89	0.84	0.96	0.92	0.96	0.90
SLI100	0.84	0.92	0.79	0.88	0.86	0.92	0.75	0.90	0.64	0.78	0.64	1.00

Table 7.2: Predictive performance (F1, Precision, and Recall) of all deep learning models (ViT Small, Vit Tiny, ResNet18, and ResNet50) with fixed hyperparameters across all classes (SLI30, SLI50, SLI80, and SLI100)

1.8.2 Visualisation methods performance

The Grad-CAM method showed its power in the identification of important features from relevant regions of the dragon fruit images, thus classifying the original image. The data (sample images) were taken from the previously shown confusion matrix Figure 7.4. As can be seen from Figure 7.5 from *g* to *l*, SLI30 dragon fruit with tiny and small classification and their respective Grad-CAM view. Predominantly, the points of importance from the sample images were the tail and scaly spikes represented from blue (less important) to red (very important) as reported by other computer vision work that also dealt with dragon fruit (MINH TRIEU; THINH, 2021). Post-harvest of dragon fruit has been proposed by a state-of-the-art computer-based robot embedded in AI, to select the ripened fruit from the dragon fruit tree with an accuracy of 95.00% using YOLO V3-Tiny. The challenge they faced was to distinguish the immature green fruit from the rest of the plant due to the colour similarity (HUANG et al., 2022). YOLO was intended to leverage ViT models, however, it has been seen from our findings the performance for object detection was as good as YOLO's while classifying dragon fruit based on colour and other morphological characteristics (spikes and tail changes). The transformer's images from *m* to *r* focus the attention maps on the absence of pixels to make its decision. Therefore, the borders are the ROI for the SLI30 class, since it looks for spikes in the dragon fruit images (yellow and orange pixels), rather than centred.

Figure 7.6 exposes the SLI50 that represents the fruit after 7 days and the spikes and tail remain as the main point of importance, which has driven the heat map to a more centred-oriented configuration. ViT uses CNN with self-attention when splitting the image in patches through a transformer encoder using a self-attention map for further classification. The former basically split the image into visual tokens instead of a pixels array as the latter. ViT differs from ResNet by not relying on convolutional layers (ZHOU et al., 2021). All the encoded global information as well as the self-attention structure and the iterations that visualised and project the patches into the original image enhance the features of the fruit images and grant categorically to the classification methods. This class is a transition to a centred-focused heat g to l and attention maps from m to r Figure 7.6 The attention mechanism is a fundamental component and a prominent area in the field of deep learning. Essentially, it allows networks to selectively focus on relevant information (features) within a specific context. For instance, the morphology of dragon fruit fruit changes over time during storage, and so does the high attention frequency, or “redness” (MINH TRIEU; THINH, 2021). Similarly, deep learning techniques applied to apples in orchard environments have shown impressive efficiency, accuracy, and robustness in detecting green fruit in complex settings. This accomplishment suggests that such implementation can avoid the need for complex and slow state-of-the-art segmentation algorithms (JIA et al., 2021).

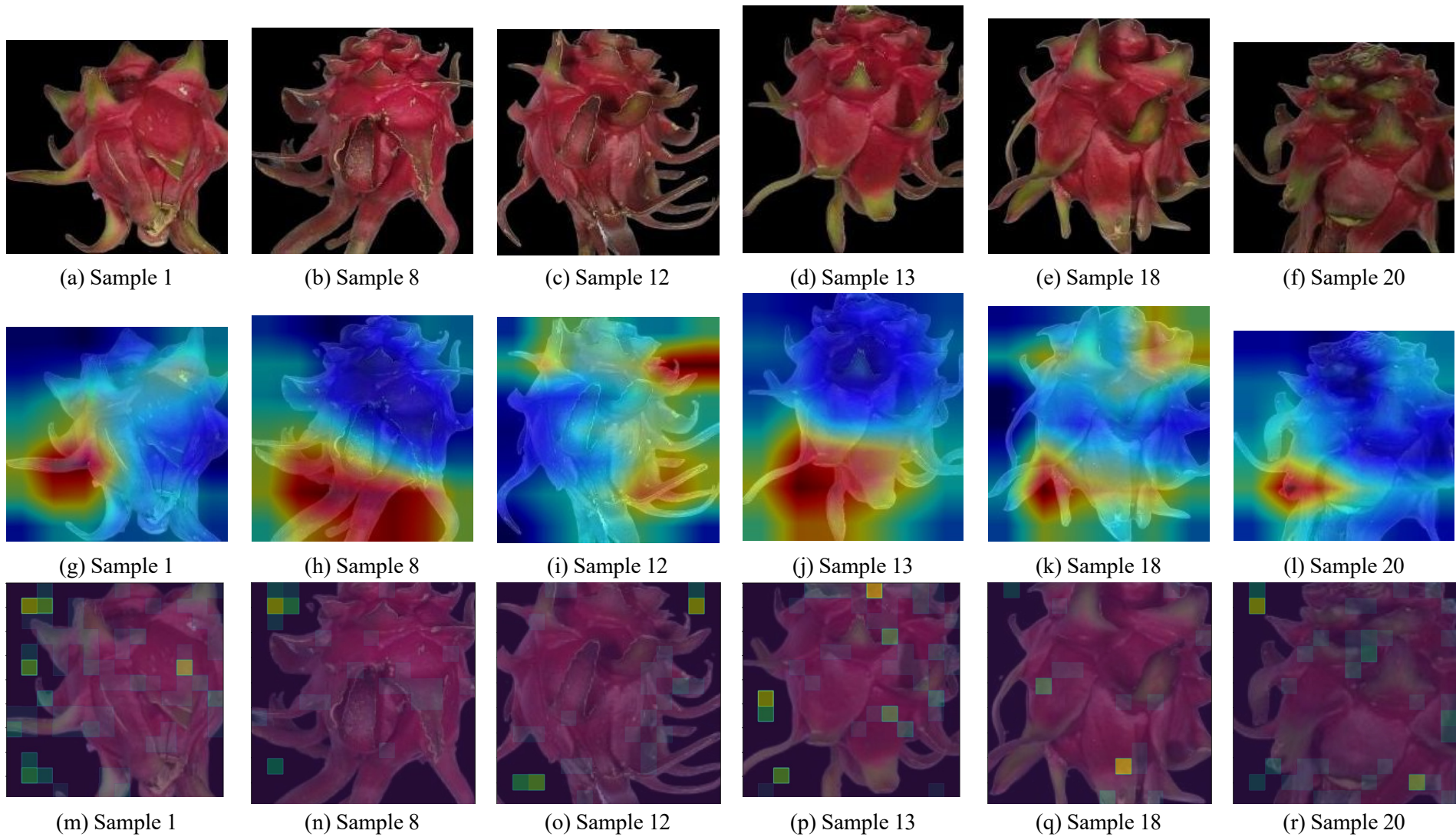


Figure 7.5: SLI30 image samples.

* From A to F the RGB images after background removal. From G to L GradCAM layer over the former images. From M to R the over the images of the first row: A, B, C, D, E, and F, respectively.

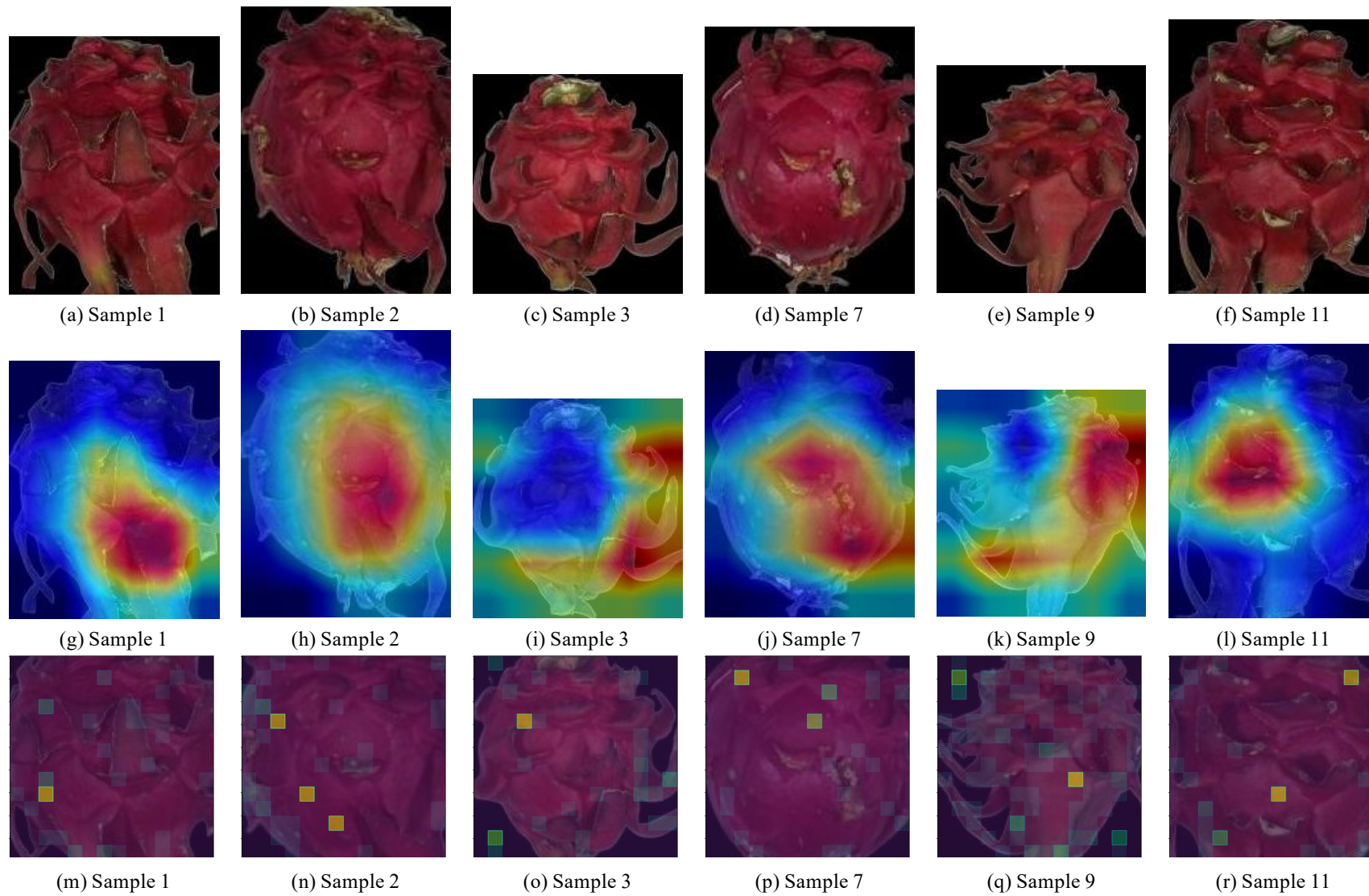


Figure 7.6: SLI50 image samples.

* From A to F the RGB images after background removal. From G to L GradCAM layer over the former images. From M to R the over the images of the first row: A, B, C, D, E, and F, respectively.

Figure 7.7 shows SLI80 class, which showed the same trend of centering the region of interest (ROI). This index combines two days of storage days 14 and 20 that started showing either severe dehydration or contamination by a fungus, which is commonly seen in dragon fruit at the latest maturation stages (DY et al., 2022), and may explain the center-oriented ROI observed in the attention maps. These centered-neurons weights were also observed in Figure 7.7 from *g* to *l*. However, this time some edges were selected as ROI since the dehydration and injuries started being prominent in the borders and scaly spikes as well. One of the reasons why sample 23 did not have the darkened and injured skin was due to this pattern being a standard for other SLI classes, which makes the algorithm avoid the same weighted neuron regions. Another research group in computer vision used an image segmentation based on the algorithms that use the maximum inter-class variance method to identify dragon fruit diseases, where they claimed to enhance the accuracy compared to other image segmentation methods even though no values but images were shown to validate their statement (DONG; XIA; LIU, 2020). The transformers models for this class are now more centred-distributed as well as diffused within the samples. When the spikes are not present, there is a comprehensive mapping trying to find these image features (spikes and tails), making increase the ROI in these regions to correctly classify the images, and sometimes end up making wrong assumptions. Also, when the image is filled with the information the attention points decrease significantly, which shows this pattern of the algorithm in finding these areas, once they do not find them, only a few attention points are needed to classify such as a darkened area or injury.

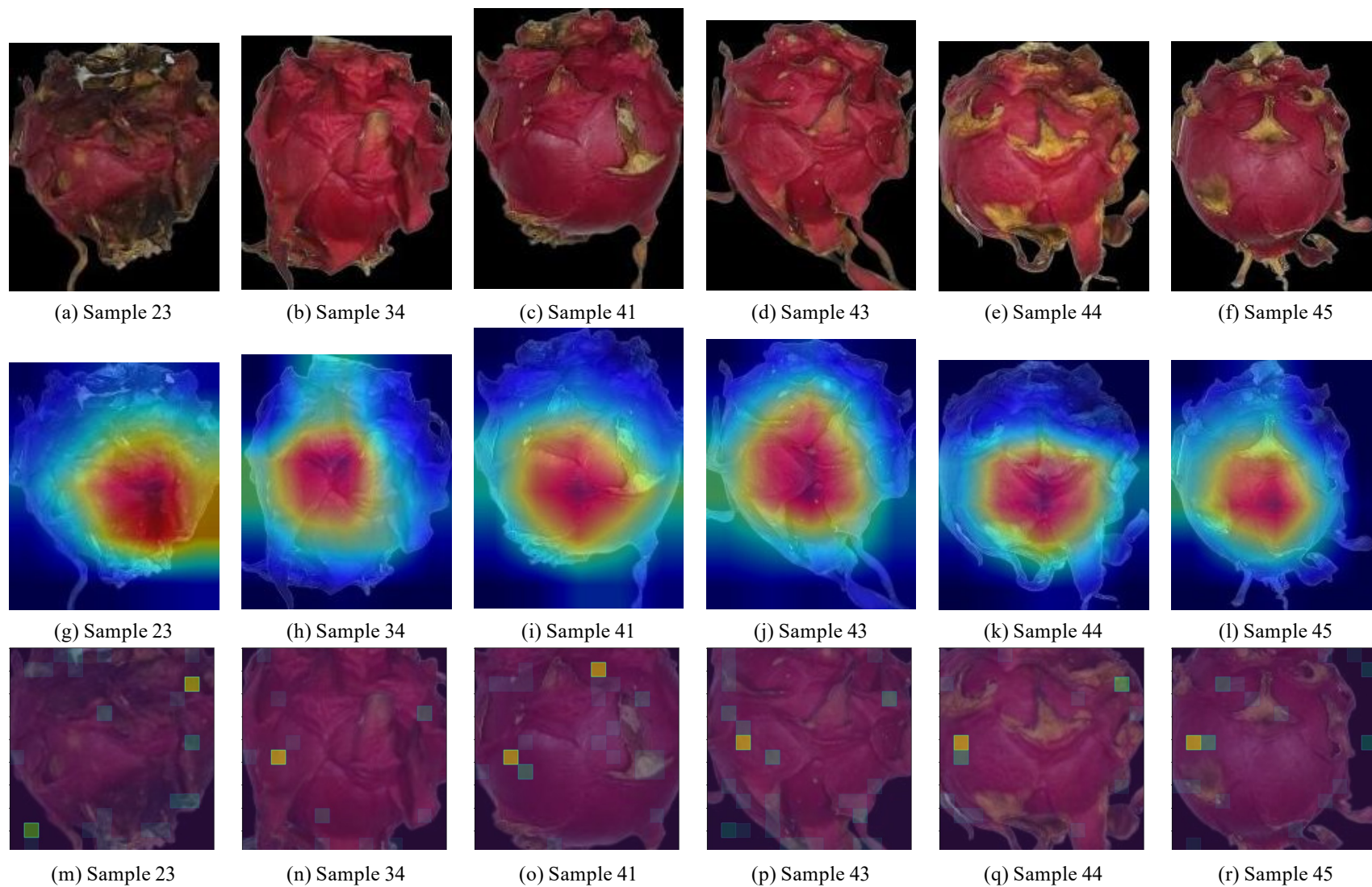


Figure 7.7 SLI80 image samples.

* From A to F the RGB images after background removal. From G to L GradCAM layer over the former images. From M to R the over the images of the first row: A, B, C, D, E, and F, respectively.

1.8.3 Approach Limitations

Some misleading samples, as shown in Figure 7.7 were in general driving the class to their neighbors, in which *a* to *d* SLI 100, SLI50, SLI50, and SLI80 assigned as SLI80, SLI30, SLI80, and SLI50 respectively. They were sample 11(f), 3(c), 7(d) 34 (b) from Figures 6.7 6.8 6.9 6.10 . This fact suggests the efficacy of the model in classifying extreme classes such as SLI30 from SLI100. Even though the unbalanced data may have benefited SLI80 over other classes due to the fusion of day 14 and 21 data. The data set augmentation that was used in dragon fruit images has shown very efficient in reducing over-fitting, in which the model works well on the training set as opposed to the test set (JOSEPH; KUMAR; MATHEW, 2021).

1.8.4 Explainability remarks

The grad-CAM method made possible to identify the important regions so that the classification of dragon fruit is achievable. These regions were spotted using attention maps which led to an extensive interpretation of important features in the fruit. The use of explainability enhanced the data interpretation, and therefore increased the reliability of the presented data. This result can then be shared to help and add to other computer vision dragon fruit's research database (DONG; XIA; LIU, 2020) (HUANG et al., 2022) and other ongoing investigations, as well as to dragon fruit and general fruit industry. Even though it is a natural product with low cost and wide availability, without proper treatment, it may oppose great loss to the industry. When taking into consideration the fruit industry the robustness and maintainability and computational efficiency from the end customer perspective it is quite difficult to handle the black box paradigm. There is why XAI is an extremely important alternative to overcome these limitations (ROFFILLI, 2021). From this research, it was able to spot the importance of spikes as main ROIs and the relevance of the TSS and TA in the features captured by the RGB camera. Deeply understanding the morphological aspects of dragon fruit is a big challenge since it presents many variations (colour transformation) that were somehow diminished by the physical characteristics (i.e., scaly spikes) that shrank and darkened over time. Having this variability depicted in a complex system is not an easy job to accomplish. Since colour was not relevant to classify dragon fruit, having multiple phases where colour can be assigned as not the only indicator, XAI can be helpful and well applied to benefit this hard yet common scenario when classifying these fruit (EL-ASSADY et al., 2019).

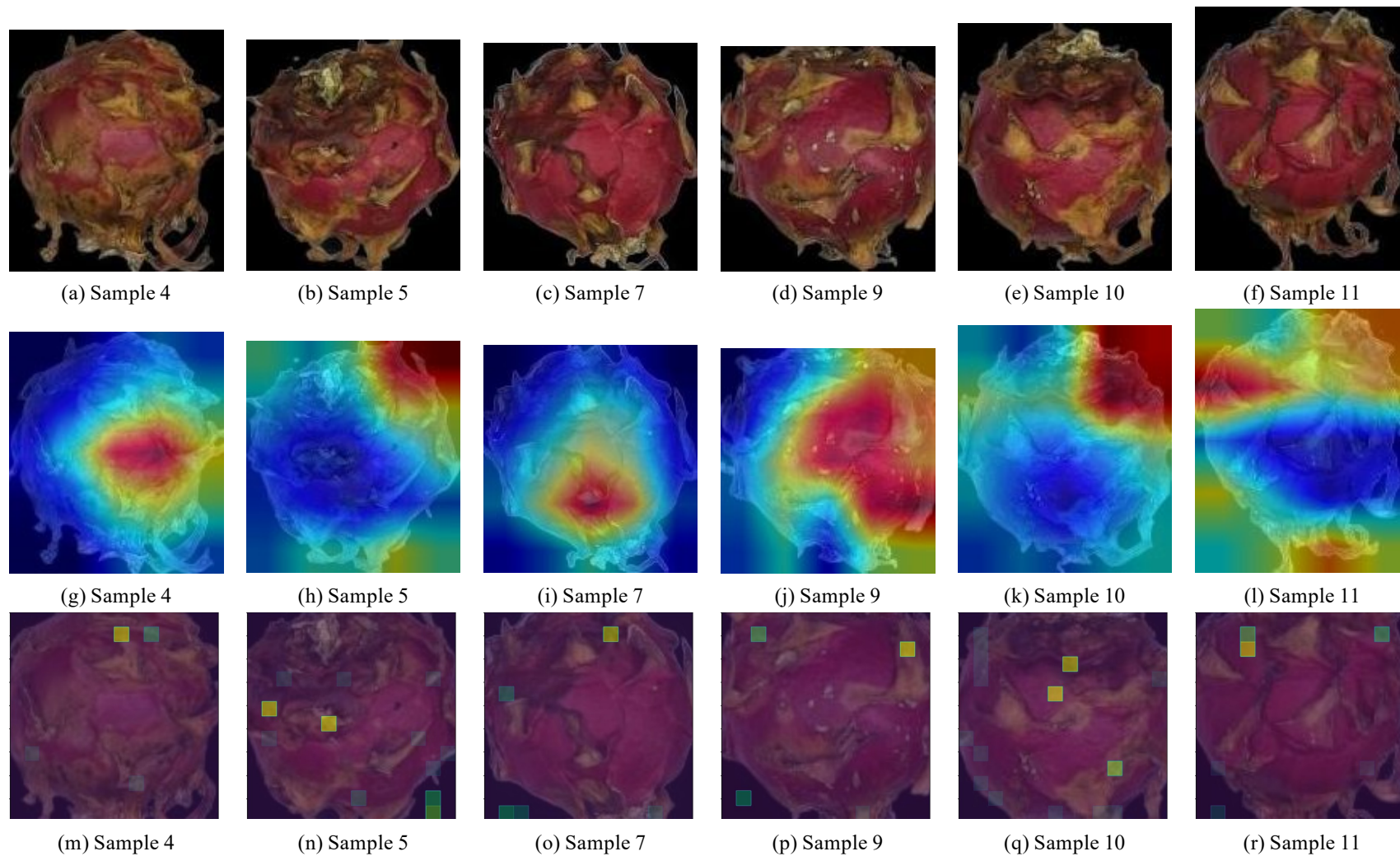


Figure 7.8: SLI100 image samples.

* From A to F the RGB images after background removal. From G to L GradCAM layer over the former images. From M to R the over the images of the first row: A, B, C, D, E, and F, respectively.



(a) SLI100 as SLI80 (b) SLI50 as SLI30 (c) SLI50 as SLI80 (d) SLI80 as SLI50

Figure 7.11: Example of misclassified samples by ViT Small model.

* (A) is a SLI100 sample predicted as SLI80, (B) is a SLI50 predicted as SLI30, (C) is a SLI50 predicted as SLI80 and (D) is a SLI80 predicted as SLI50.

1.9 Conclusion

The DCVS method has demonstrated a strong predictive model for dragon fruit classification using ResNet and ViT architectures, in line with the literature. Among the models tested, ViT Small showed the best performance, with an overall accuracy of 91.00% and up to 97.00% for SLI 30 classification. The heat map and attention maps generated by the model showed a tendency to move from the edges to the centre of the fruit, taking into account the presence of spikes and tails, which contributed strongly to the classification process. The methods proposed in this work have the potential to benefit the food industry and fruit producers by enabling accurate and efficient classification of fruit, which is much faster than traditional observational methods. This could enhance productivity and aid in the accurate selection of fruit for a pre-determined production line.

1.10 Acknowledgement

This study was financed in part by the Coordenação de Aperfeiçoamento de Pessoal de Nível Superior - Brasil (CAPES) - Finance Code 001, São Paulo Research Foundation (FAPESP) (project number 2015/24351-2) and Carlos Chagas Filho Foundation for Research Support of Rio de Janeiro State (FAPERJ) (project number E-26/210.631/2019). Marcus V S Ferreira acknowledges scholarship funding from CNPq, grant number 142568/2020-1 and 140914/2021-8. Prof. Douglas Fernandes Barbin is CNPq research fellow (308260/2021-0).

1.11 Declaration of Interest

None.

1.10 References

- EL-ASSADY, M. et al. Towards XAI: Structuring the Processes of Explanations. **ResearchGate**, 2019. Disponível em: <<https://www.researchgate.net/publication/332802468_Towards_XAI_Structuring_the_Processes_of_Explanations>>.
- BETANCUR G, J. A.; MURIEL R, S. B.; GONZÁLEZ J, E. P. Morphological characterization of the red dragon fruit - *Selenicereus undatus* (Haw.) DR Hunt - under growing conditions in the municipality of San Jerónimo (Antioquia, Colombia). **Revista Facultad Nacional de Agronomía Medellín**, Facultad de Ciencias Agrarias-Universidad Nacional de Colombia, v. 73, n. 1, p. 9019–9027, 2020.
- BUHRMESTER, V.; MNCH, D.; ARENS, M. Analysis of Explainers of Black Box Deep Neural Networks for Computer Vision: A Survey. **Mach. Learn. Knowl. Extr.**, Multidisciplinary Digital Publishing Institute, v. 3, n. 4, p. 966–989, 2021. ISSN 2504-4990. DOI: <10.3390/make3040048>.
- DENG, J.; LIU, Y.; XIAO, X. Deep-Learning-Based Wireless Visual Sensor System for Shiitake Mushroom Sorting. **Sensors**, v. 22, 2022. DOI: <10.3390/s22124606>.
- DONG, W.; XIA, Y.; LIU, Y. Dragon Fruit Disease Image Segmentation Based on FCM Algorithm and Two-Dimensional OTSU Algorithm. In: 2020 IEEE INTERNATIONAL CONFERENCE ON POWER, INTELLIGENT COMPUTING AND SYSTEMS (ICPICS). [S.l.]: IEEE, 2020. p. 969–973. DOI: <10.1109/ICPICS50287.2020.9202083>.
- DOSOVITSKIY, A. et al. An image is worth 16x16 words: Transformers for image recognition at scale. **arXiv preprint arXiv:2010.11929**, 2020.
- DY, K. S. et al. Morphological, Molecular Identification and Pathogenicity of *Neoscytalidium dimidiatum* Causing Stem Canker of *Hylocereus polyrhizus* in Southern Thailand. **Plants**, Multidisciplinary Digital Publishing Institute (MDPI), v. 11, n. 4, 2022. DOI: <10.3390/plants11040504>.
- GILDENBLAT, J. **contributors. Pytorch library for cam methods**. [S.l.: s.n.], 2021.
- GLOROT, X.; BENGIO, Y. Understanding the difficulty of training deep feedforward neural networks. In: JMLR WORKSHOP e CONFERENCE PROCEEDINGS. PROCEEDINGS of the thirteenth international conference on artificial intelligence and statistics. [S.l.: s.n.], 2010. p. 249–256.
- GRAHAM, B. et al. **LeViT: A Vision Transformer in ConvNet's Clothing for Faster Inference**. [S.l.: s.n.], 2021. p. 12259–12269. [Online; accessed 10. Nov. 2022]. Disponível em: <<https://openaccess.thecvf.com/content/ICCV2021/html/Graham_LeViT_A_Vision_Transformer_in_ConvNets_Clothing_for_Faster_Inference_ICCV_2021_paper.html>>.
- HANIF, M. S.; BILAL, M. Competitive residual neural network for image classification. **ICT Express**, Elsevier, v. 6, n. 1, p. 28–37, 2020. ISSN 2405-9595. DOI: <10.1016/j.icte.2019.06.001>.
- HUANG, X.-R. et al. An AI Edge Computing-Based Robotic Arm Automated Guided Vehicle System for Harvesting Pitaya. In: 2022 IEEE INTERNATIONAL CONFERENCE ON CONSUMER ELECTRONICS (ICCE). [S.l.]: IEEE, 2022. p. 1–2. DOI: <10.1109/ICCE53296.2022.9730442>.
- ISMAIL, N.; MALIK, O. A. Real-time visual inspection system for grading fruits using

- computer vision and deep learning techniques. **Information Processing in Agriculture**, Elsevier, v. 9, n. 1, p. 24–37, 2022. ISSN 2214-3173. DOI: <10.1016/j.inpa.2021.01.005>.
- JAMIL, S.; PIRAN, M. J.; KWON, O.-J. A Comprehensive Survey of Transformers for Computer Vision. **arXiv**, 2022. DOI: <10.48550/arXiv.2211.06004>. eprint: <2211.06004>.
- JIA, W. et al. FoveaMask: A fast and accurate deep learning model for green fruit instance segmentation. **Comput. Electron. Agric.**, Elsevier, v. 191, p. 106488, 2021. ISSN 0168-1699. DOI: <10.1016/j.compag.2021.106488>.
- JIMENEZ-GARCIA, S. N. et al. Pitahaya Peel: A By-Product with Great Phytochemical Potential, Biological Activity, and Functional Application. **Molecules**, Multidisciplinary Digital Publishing Institute (MDPI), v. 27, n. 16, 2022. DOI: <10.3390/molecules27165339>.
- JOSEPH, J. L.; KUMAR, V. A.; MATHEW, S. P. Fruit Classification Using Deep Learning. In: **INNOVATIONS IN ELECTRICAL AND ELECTRONIC ENGINEERING**. Singapore: Springer, 2021. p. 807–817. DOI: <10.1007/978-981-16-0749-3_62>.
- KAKOGEORGIOU, I.; KARANTZALOS, K. Evaluating explainable artificial intelligence methods for multi-label deep learning classification tasks in remote sensing. **International Journal of Applied Earth Observation and Geoinformation**, Elsevier, v. 103, p. 102520, 2021.
- KHOO, H. E. et al. Betacyanins and Anthocyanins in Pulp and Peel of Red Pitaya (*Hylocereus polyrhizus* cv. Jindu), Inhibition of Oxidative Stress, Lipid Reducing, and Cytotoxic Effects. **Front. Nutr.**, Frontiers Media SA, v. 9, 2022. DOI: <10.3389/fnut.2022.894438>.
- KUMAR, T.; SHIVANI, R. **Vision Transformer based System for Fruit Quality Evaluation**. [S.l.: s.n.], 2022. [Online; accessed 28. Nov. 2022]. DOI: <10.21203/rs.3.rs-1526586/v1>.
- LI, X. et al. Transformer helps identify kiwifruit diseases in complex natural environments. **Comput. Electron. Agric.**, Elsevier, v. 200, p. 107258, 2022. ISSN 0168-1699. DOI: <10.1016/j.compag.2022.107258>.
- LOPES, J. F. et al. Deep computer vision system for cocoa classification. **Multimedia Tools and Applications**, Springer, v. 81, n. 28, p. 41059–41077, 2022. ISSN 1573-7721. DOI: <10.1007/s11042-022-13097-3>.

- LOUREIRO, J. P. B. de et al. Economic viability of pitaya (*Hylocereus* sp.) Cultivation in Tom-A Municipality, Par State, Brazil. **Journal of Agricultural Studies**, v. 8, n. 2, p. 704–715, 2020. ISSN 2166-0379. DOI: <10.5296/jas.v8i2.16949>.
- MACALUSO, S.; SHIH, D. Pulling out all the tops with computer vision and deep learning. **J. High Energy Phys.**, Springer Berlin Heidelberg, v. 2018, n. 10, p. 1–27, 2018. ISSN 1029-8479. DOI: <10.1007/JHEP10(2018)121>.
- MAGALHES, D. S. et al. Physical and physicochemical modifications of white-fleshed pitaya throughout its development. **Sci. Hortic.**, Elsevier, v. 243, p. 537–543, 2019. ISSN 0304-4238. DOI: <10.1016/j.scienta.2018.08.029>.
- MINH TRIEU, N.; THINH, N. T. Quality Classification of Dragon Fruits Based on External Performance Using a Convolutional Neural Network. **Appl. Sci.**, Multidisciplinary Digital Publishing Institute, v. 11, n. 22, p. 10558, 2021. ISSN 2076-3417. DOI: <10.3390/app112210558>.
- OKSUZ, K. et al. Imbalance Problems in Object Detection: A Review. **IEEE Trans. Pattern Anal. Mach. Intell.**, IEEE Computer Society, v. 43, n. 10, p. 3388–3415, 2021. ISSN 0162-8828. DOI: <10.1109/TPAMI.2020.2981890>.
- OLIVEIRA, M. M. et al. Classification of fermented cocoa beans (cut test) using computer vision. **Journal of Food Composition and Analysis**, v. 97, p. 103771, 2021. ISSN 0889-1575. DOI: <https://doi.org/10.1016/j.jfca.2020.103771>. Disponível em: <<https://www.sciencedirect.com/science/article/pii/S0889157520314769>>.
- PATHMANABAN, P.; GNANAVEL, B. K.; ANANDAN, S. S. Recent application of imaging techniques for fruit quality assessment. **Trends Food Sci. Technol.**, Elsevier, v. 94, p. 32–42, 2019. ISSN 0924-2244. DOI: <10.1016/j.tifs.2019.10.004>.
- PATIL, P. U. et al. Grading and sorting technique of dragon fruits using machine learning algorithms. **J. Agric. Food Res.**, Elsevier, v. 4, p. 100118, 2021. ISSN 2666-1543. DOI: <10.1016/j.jafr.2021.100118>.
- PINTO, P. M.; JACOMINO, A. P. The Postharvest of Tropical Fruits in Brazil. In: **FOOD QUALITY, SAFETY AND TECHNOLOGY**. Wien, Austria: Springer, Vienna, 2013. p. 77–87. DOI: <10.1007/978-3-7091-1640-1_6>.
- REEDHA, R. et al. Transformer Neural Network for Weed and Crop Classification of High Resolution UAV Images. **Remote Sens.**, MDPI, v. 14, n. 3, 2022. ISSN 2072-4292. DOI: <10.3390/rs14030592>.
- ROFFILLI, M. On how to develop machine learning algorithms for the control of industrial-grade fruit sorting machines. **PROCEEDINGS OF SIMAI 2020+ 21**, 2021.
- ROSSO, M. M. et al. Convolutional networks and transformers for intelligent road tunnel investigations. **Comput. & Structures**, Pergamon, v. 275, p. 106918, 2023. ISSN 0045-7949. DOI: <10.1016/j.compstruc.2022.106918>.
- SELVARAJU, R. R. et al. Grad-cam: Visual explanations from deep networks via gradient-based localization. In: **PROCEEDINGS of the IEEE international conference on computer vision**. [S.l.: s.n.], 2017. p. 618–626.
- SHINDE, P. P.; SHAH, S. A Review of Machine Learning and Deep Learning Applications. In: **2018 FOURTH INTERNATIONAL CONFERENCE ON COMPUTING COMMUNICATION CONTROL AND AUTOMATION (ICCUBEA)**. [S.l.]: IEEE, 2018. p. 1–6. DOI: <10.1109/ICCUBEA.2018.8697857>.

- SIRICHAROEN, P.; YOMSATIEANKUL, W.; BUNSRI, T. Recognizing the sweet and sour taste of pineapple fruits using residual networks and green-relative color transformation attached with Mask R-CNN. **Postharvest Biol. Technol.**, Elsevier, v. 196, p. 112174, 2023. ISSN 0925-5214. DOI: <10.1016/j.postharvbio.2022.112174>.
- TRIEU, N. M.; THINH, N. T. Development of Grading System Based on Machine Learning for Dragon Fruit. In: THE AUN/SEED-NET JOINT REGIONAL CONFERENCE IN TRANSPORTATION, ENERGY, AND MECHANICAL MANUFACTURING ENGINEERING. Singapore: Springer, 2022. p. 230–243. DOI: <10.1007/978-981-19-1968-8_19>.
- VASWANI, A. et al. Attention is all you need. **Advances in neural information processing systems**, v. 30, 2017.
- VIJAYAKUMAR, T.; R., M. Mellowness Detection of Dragon Fruit Using Deep Learning Strategy. **Journal of Innovative Image Processing**, v. 2, p. 35–43, 2020. DOI: <10.36548/jiip.2020.1.004>.
- VILLAMIEL, M.; MNDEZ-ALBIANA, P. Update of challenges for food quality and safety management. **J. Agric. Food Res.**, Elsevier, v. 10, p. 100393, 2022. ISSN 2666-1543. DOI: <10.1016/j.jafr.2022.100393>.
- WIGHTMAN, R.; TOUVRON, H.; JGOU, H. ResNet strikes back: An improved training procedure in timm. **arXiv**, 2021. DOI: <10.48550/arXiv.2110.00476>. eprint: <2110.00476>.
- WONG, Z. Y.; CHEW, W. J.; PHANG, S. K. Computer vision algorithm development for classification of palm fruit ripeness. **AIP Conf. Proc.**, American Institute of Physics, v. 2233, n. 1, p. 030012, 2020. ISSN 0094-243X. DOI: <10.1063/5.0002188>.
- WU, C.-T. **Pitaya Fruit Maturity Index Implementation**. [S.l.: s.n.], 2022. [Online; accessed 2. Nov. 2022]. Disponível em: <<<https://apec-flows.ntu.edu.tw/category-detail.aspx?seq=37>>>.
- WU, K. et al. Tinyvit: Fast pretraining distillation for small vision transformers. In: SPRINGER. EUROPEAN Conference on Computer Vision. [S.l.: s.n.], 2022. p. 68–85.
- XAVIER, A. I. et al. Object Detection via Gradient-Based Mask R-CNN Using Machine Learning Algorithms. **Machines**, Multidisciplinary Digital Publishing Institute, v. 10, n. 5, p. 340, 2022. ISSN 2075-1702. DOI: <10.3390/machines10050340>.
- YIN, J.-z. et al. Apple appearance quality classification method based on double branch feature fusion network. **Cognit. Comput. Syst.**, The Institution of Engineering e Technology, v. 4, n. 3, p. 284–293, 2022. ISSN 2517-7567. DOI: <10.1049/ccs2.12059>.
- YOU, K. et al. How Does Learning Rate Decay Help Modern Neural Networks? **arXiv**, 2019. DOI: <10.48550/arXiv.1908.01878>. eprint: <1908.01878>.
- YUE, B.; FU, J.; LIANG, J. Residual Recurrent Neural Networks for Learning Sequential Representations. **Information**, Multidisciplinary Digital Publishing Institute, v. 9, n. 3, p. 56, 2018. ISSN 2078-2489. DOI: <10.3390/info9030056>.
- ZHAN, H.; CAO, Y. Deep Model Compression via Deep Reinforcement Learning. **ResearchGate**, 2019. Disponível em: <<https://www.researchgate.net/publication/337781610_Deep_Model_Compression_via_Deep_Reinforcement_Learning>>.
- ZHOU, D. et al. Refiner: Refining Self-attention for Vision Transformers. **arXiv**, 2021. DOI: <10.48550/arXiv.2106.03714>. eprint: <2106.03714>.